# The terrestrial carbon cycle in transition: tracking changes using novel tracers on multiple timescales

**A thesis**

**submitted in fulfilment**

**of the requirements of the degree**

**of**

**Doctor of Philosophy**

**in the Faculty of Science and Engineering**

**at**

**The University of Waikato**

**by**

**Andrew R. Pearson**


THE UNIVERSITY OF
WAIKATO
*Te Whare Wānanga o Waikato*

**2020**

# Abstract

Soils store more carbon than the atmosphere and terrestrial vegetation combined, therefore, changes in soil carbon storage can affect the global carbon budget. One of the forms in which carbon is exported from soil is as dissolved organic carbon (DOC). Upon release from soil, components of DOC can be oxidised to $CO_2$, thus potentially contributing to the global climate crisis. In freshwater systems, DOC is considered a pollutant because of its detrimental impact on freshwater ecology and biodiversity (by blocking light and reducing photosynthesis and altering thermal-mixing regimes in lakes), increasing freshwater acidity, transporting nutrients (particularly N and P) and trace metal pollutants. Further, during the water treatment process (for human consumption), DOC can form toxic by-products.

This project aimed to shed new light on terrestrial carbon dynamics by testing the hypothesis that climate can drive increases in soil DOC export. This research focused on past soil DOC exports in New Zealand, an archipelago located in the mid-latitudes of the Southern Hemisphere. New Zealand's palaeo-environmental archives (e.g. speleothems and lake sediments) provide a unique opportunity to reconstruct the concentrations and characteristics of DOC under changing climate conditions over centennial/millennial timescales. New Zealand was uninhabited by humans until the 13$^{th}$ century. Palaeo-environmental records that extend beyond the 13$^{th}$ century, therefore, exclude interference from anthropogenic factors, thus enabling the climate hypothesis to be assessed.

**Using lake sediment archives to reconstruct DOC concentrations and characteristics through the past 14,000 years**

This study explored the use of 3D EEM (excitation-emission matrix spectroscopy) fluorescence of water extractable dissolved organic matter (WEDOM) from lake

sediments in reconstructing both past soil export of DOM and past trophic status. DOM and water quality are linked because DOM can contain nutrients (N, and P), provide an energy source to heterotrophs and algae, can reduce light penetration, and lead to reduced dissolved oxygen concentrations.

Mean trophic level index (TLI) monitoring data of the lake water columns were compared against protein-like fluorescence from contemporary sedimentary WEDOM from ten lakes, producing strong positive correlations with total phosphorous ($R^2$= 0.81), and TLI scores ($R^2$= 0.74 ), and weak positive correlations with total nitrogen ($R^2$= 0.5) and chlorophyll a ($R^2$= 0.44). The equation produced from the correlation between TLI scores and protein-like fluorescence of WEDOM was used to reconstruct TLI scores through the past 13,700 years at Adelaide Tarn (a climatically sensitive, sub-alpine lake located in the north west of the South Island), indicating predominantly oligotrophic conditions throughout the record.

Humic-like DOM fluxes in Adelaide Tarn responded to known climate shifts over the course of the Holocene, indicating a climatic control on soil DOM production and/or export. The results indicate that WEDOM fluorescence can be used as a reliable indicator of past soil export of DOM as well as past trophic status.

To examine total organic carbon concentration; a partial-least square regression (PLSR) model was produced using Fourier transform infrared spectroscopy (FTIRS) data vs conventionally measured TOC of 141 sediment samples from 13 lakes, resulting in strong positive correlation ($R^2$ =0.88). The equation from this correlation was then used to reconstruct past TOC concentrations from sediments in Adelaide Tarn. The FTIRS-TOC and humic-like DOM records showed a clear relationship with known temperature changes over the past ~14,000 years BP.

**Testing the reliability of calcite to record DOC concentrations from its parent solution**

Natural carbonates (such as speleothems) are known to contain DOM. Speleothems accumulate for hundreds of thousands of years, thus potentially containing long-term records of DOM export from their overlying soil. However, the ability of carbonates to reliably record DOM concentrations from their parent solutions is unknown. A calcite precipitation experiment was undertaken in growth solutions (diluted peat water) of differing $[DOC]_{aq}$ (0, 5, 10, 15 ppm) with the aim of testing the reliability of calcite to record $[DOC]_{aq}$, and the potential of 3D excitation emission (EEM) analysis to assess the DOC concentration in dissolved calcite samples. A case study of flowstones and dripwaters from three New Zealand caves was also conducted. In the case study, 3D EEM fluorescence-inferred DOC concentrations were measured in the dripwaters and speleothems, thus enabling calculation of DOC partition coefficients between dripwaters and their associated flowstones. Overall, the study demonstrated that calcite [DOC] is controlled by aqueous [DOC] from the parent solution, in natural and experimental environments.

Further, $[DOC]_{aq}$ within the experimental range did not alter the calcium carbonate polymorph (calcite), yet heavily influenced calcite crystal structure; smooth-faced, rhombohedral crystals formed in growth solutions with low $[DOC]_{aq}$ (0–5 ppm), whereas prismatic, 'impure' crystals were produced at high $[DOC]_{aq}$ (10 and 15 ppm).

**Using speleothem archives to test the impact of climate on aquatic DOC concentrations in a pre-human continent**

3D EEM fluorescence was used to measure humic-like DOC concentrations in modern dripwaters and within three flowstones (secondary carbonate deposits)

from three caves distributed along a 7° latitudinal gradient. Calculated DOC concentrations from recently deposited flowstone calcite and dripwater monitoring were used to calculate empirical distribution coefficient ($K_d$) values, enabling an estimate of dripwater DOC concentrations through the past ~14,000 years BP.

Correspondence between heightened aquatic DOC concentrations during periods of known temperature increases (especially the Holocene climatic optimum) was observed at Hodges Creek (north-west South Island) and Dave's Cave (south-west South Island), whilst climatic cooling (during the mid-Holocene) yielded lower DOC values. This occurrence was not clear at Waipuna Cave (western North Island), perhaps owing to its relatively low altitude and lack of climatic sensitivity compared to the other sites.

Ratios of Mg to Ca in the flowstone showed a strong correspondence between periods of drier climate and increases in DOC dripwater concentration at each site. The findings of this study show that DOC concentrations have been higher in the past at the high-altitude sites, and that climate (in the absence of anthropogenic impacts) plays a pivotal role in soil DOC export in sub-alpine and alpine environments.

**Summary**

The thesis produced several outcomes. Chapter 3 demonstrated that protein-like fluorescence of sedimentary WEDOM is associated with trophic level index score and can be used as an indicator of past trophic level (i.e. productivity). Further, the Adelaide Tarn palaeo-environmental reconstruction demonstrated that humic-like fluorescence responded to climate shifts through the Holocene, indicating a temperature control on soil C production and/or export. At large, the DOC

concentration over the ~10 kyr period approximately halved with a decrease in temperature of 1.2 °C.

The project also demonstrated (in Chapter 4) that speleothems can reliably record DOC from their parent solutions, showing a linear response between dissolved and solid phase organic concentration. This finding formed the foundation of Chapter 5, which demonstrated that high humic-like DOC concentrations in flowstones were associated with drier conditions at Waipuna Cave (lower-altitude North Island site), however there was no clear correspondence between temperature and [DOC] in the Waipuna record.

At the high altitude, South Island sites (Hodges Creek cave, Adelaide Tarn and Dave's Cave), DOC concentrations were higher during periods with relatively low precipitation and high temperature. Hodges Creek Cave (940 m a.s.l.) is situated at a similar altitude to Adelaide Tarn (1,250 m a.s.l.) the two sites being only 32 km apart. Adelaide Tarn's WEDOM and FTIR-TOC records show strikingly similar patterns of humic-like fluorescence and TOC concentrations to the Hodge's Creek fluorescence record, providing support for a regionally coherent signal. The relationship between climate and soil DOC export was most clear during the Holocene climatic optimum. At this time, temperatures were approximately 1.5-2.5 °C warmer than present, whilst humic-like DOC values (relative to modern) were 57 % higher at Hodge's Creek, 36 % higher at Adelaide Tarn and 40 % higher at Dave's Cave. The HCO was also drier than most of the Holocene at these sites. Following the HCO, temperature declined, and wetness increased, corresponding with a notable decline in DOC concentrations at these sites.

These findings imply that in the absence of human interference, higher temperatures and aridity were important drivers of elevated soil DOC export

through the past 14,000 years BP was controlled by temperature and wetness at the high-altitude sites, whilst only wetness was important at low altitude.

*Education is the path from cocky ignorance to miserable uncertainty.*

-Mark Twain

# Acknowledgements

Firstly, an enormous thank you to my chief supervisor, Dr Adam Hartland. I am hugely grateful for the opportunities, support, guidance, and patience you have given me throughout the PhD process. The field campaign of 2016 was one of the highlights of my life so far, and I count myself as extremely lucky to have had you as my chief supervisor. Your optimism and passion for science is inspiring and infectious, and I have thoroughly enjoyed working with you. I look forward to having many more beers and science discussions in the future.

Secondly, I would like to thank my supervisor, Dr Bethany R.S. Fox. You have put an immeasurable amount of time and effort into editing and co-writing parts of my manuscripts, providing feedback, encouragement, and insight, and pushing me to produce work of a higher standard. The completion of this thesis would have been several orders of magnitude more difficult without you as my supervisor, and for that, I am very grateful.

I would also like to thank my co-supervisor, Dr Marcus J. Vandergoes. I am very grateful for your hospitality and generosity, and for making my trips to GNS so fun and interesting. Thank you for providing me with the sediment core from Adelaide Tarn, and for your vital inputs into my thesis.

I would also like to thank several collaborators in this research project. An enormous thanks to Dr John C. Hellstrom for helping with speleothem core collection, sub-sampling advice, fascinating insights and for your amazing generosity in providing speleothem dates and for hosting me at the University of Melbourne in 2016. Thanks to Associate Professor Silvia Frisia for your supportive words and vital input into my calcite precipitation manuscript. I would also like to thank Dr Sebastian Breitenbach for your guidance and advice on speleothem sub-

sampling, COPRA modelling, inspirational levels of energy and enthusiasm, and kind words of encouragement. I would also like to thank Dr Russell N. Drysdale for hosting me and analysing one of our samples at the University of Melbourne. A huge thanks to Dr Rebecca Bartlett for providing me with the fantastic opportunity to work under her supervision as a short-term research assistant at the University of Birmingham.

Research would be impossible without great technical support. I would like to thank Annie Barker for your help with FAAS, your generosity and for always giving me a good laugh in the lab. I am very grateful to Steve Newcombe; thank you for being cutting the speleothem slabs and preparing glassware for the calcite precipitation experiment. Thanks to Kirsty Vincent for being so helpful with XRD analysis, and to Helen Turner for assistance with SEM analysis. I would also like to thank Cheryl Ward for help with thesis formatting.

I want to thank my mum and dad. I am the first person in our family to have studied at university. I know that my BSc, MSc and now PhD would have been completely impossible without your years of love, generosity, hard work and support. For having you as my parents, I must be the luckiest person in the world. Words alone cannot express my gratitude to you. I would also like to thank my sister, Louise for her love, support and encouraging words.

When I first arrived as a graduate student in New Zealand, I was excited, but also daunted by the prospect of being more than 18,000 km away from home, in a hemisphere of the planet in which I did not know a single person. However, I have never felt alone in New Zealand. For that, I would like to give a huge thanks to my friends Joss Ratcliffe, Lara Heppenstall, John Mering, Claire Newton, Morkel Zaayman, Huma Saeed, Lena Schallenberg, Nicola Manghi, Kohji Muraoka,

Dorisel Torres-Rojas, Ben Norris and Francesca Spinardi. I feel very lucky to have met you and have a catalogue of fantastic memories and laughs with each of you.

A big thanks to my friends in the Waikato Environmental Geochemistry (WEG) group, especially my fellow ‘speople’ Brittany Ward, Seb Hoepker and Cinthya Nava. It was a pleasure to work with you all and I look forward to continuing our friendships.

Finally, I would like to thank Steph Mangan (aka Mango). You are my best friend; without you, I would never have been able to finish this PhD. I am incredibly lucky to have you in my life, and now look forward to our future adventures and to helping you finish your PhD too.

Funding for this PhD research was provided by the Royal Society of New Zealand’s Marsden Fund grant UOW1403. I would like to thank the Department of Conservation for allowing us to access and sample from Dave’s Cave and Hodges Creek Cave (Research and Collection Permit 37934-GEO), and Pete and Libby Chandler for allowing us to access and sample from dripwaters and flowstones within Waipuna Cave and supporting our ongoing monitoring campaigns. A big thanks to Travis Cross for his help in sample collection.

# Table of Contents

# List of Figures

# List of Tables

# List of Abbreviations

| | |
|---|---|
| 3D EEMs | three-dimensional excitation-emission matrix |
| ACR | Antarctic cold reversal |
| BP | before present |
| CCD | Charge-coupled device |
| CE | Common Era |
| Chl-a | Chlorophyll a |
| COPRA | Constructing Proxy Records from Age models |
| DOC | dissolved organic carbon |
| DOM | dissolved organic matter |
| FA | fulvic acid |
| FAAS | flame atomic absorption spectroscopy |
| FDOM | fluorescent dissolved organic matter |
| FTIRS | Fourier transform infrared spectroscopy |
| HA | humic acid |
| HCO | Holocene climatic optimum |
| $K_d$ values | dissociation constant value |
| LA-ICP-MS | laser ablation inductively coupled plasma mass spectrometry |
| LAWA | Land Air Water Aotearoa |
| MAT | mean annual temperature |
| MC-ICP-MS | multi collector inductively coupled plasma mass spectrometry |
| NIST | National Institute of Standards and Technology |
| NPOC | non-purgable organic carbon |
| PARAFAC | parallel factor analysis of components |
| POM | particulate organic matter |
| SEM | scanning electron microscope |
| SOM | soil organic matter |
| SST | sea-surface temperature |
| TLI | trophic level index |
| TN | total nitrogen |
| TP | total phosphorus |
| WEDOM | water-extractable dissolved organic matter |
| XRD | x-ray diffraction |

# 1 Chapter 1

# Introduction

## 1.1 Thesis structure and outline

This thesis is divided into six chapters including: Introduction (Chapter 1), Literature Review (Chapter 2), Research components (Chapters 3–5) and Conclusion (Chapter 6).

**Chapter 1** is a general introduction describing the background and significance of this research, and how palaeo-climatic archives in New Zealand may help to enhance our understanding of the impacts of climate on soil DOC export.

**Chapter 2** is a literature review which begins by describing dissolved organic carbon in detail. The review then introduces lake sediment and speleothem archives alongside their associated organic carbon proxies and relevant methods of organic carbon analysis. Finally, the merits of utilising the palaeo-environmental archives and associated methods in New Zealand are discussed.

**Chapter 3** is titled *Evaluating past lake water quality and carbon fluxes using sediment fluorescence.* This chapter has been written as a thesis chapter and will be re-adapted for publication in future.

**Chapter 4** is titled *Formation of calcite in the presence of dissolved organic matter: partitioning, fabrics and fluorescence*. This chapter has been published in *Chemical Geology*.

**Chapter 5** is titled *Climate controls soil DOM export in the absence of human impacts.* This chapter was written as a thesis chapter and will be re-adapted for publication in the future.

**Chapter 6** is a general thesis conclusion which provides a brief summary of the PhD research and some proposals for future research.

## 1.2 Background and significance of research

Soils contain more than double the amount of carbon stored in the Earth's vegetation or atmosphere (Batjes, 1996). Temperature is expected to increase by > 2 °C by 2100 (Raftery *et al*., 2017), with unknown consequences for soil DOC export. DOC has numerous environmental impacts (Ask *et al.*, 2009; Karlsson *et al.*, 2009 Yang *et al.*, 2013) and may also provide a positive feedback to global climate change (through release of $CO_2$). Improving our understanding of climate change on soil DOM export is therefore imperative.

This PhD research sought targeted geochemical proxies within flowstone (cave carbonate) and lake sediment archives spanning the length of the Holocene in New Zealand. Due to the late arrival of humans in New Zealand ($13^{th}$ century CE) (McWethy *et al.*, 2010), palaeo-environmental archives provide a unique opportunity to test climate impacts on soil DOC export (in the absence of human impacts).

During their growth, speleothems can incorporate DOC transported from the soil overlying the cave (Blyth *et al*., 2008; Blyth *et al*., 2016). Speleothems can grow for millennia, potentially storing information on past soil DOC export trends. However, the reliability of speleothem archives to reliably record DOC concentrations and characteristics from their parent dripwaters is largely untested. This study aimed to use fluorescence methods to test the ability of carbonates (via a calcite precipitation experiment) to record DOC concentrations and characteristics. This approach allowed the utilisation of speleothem archives to reconstruct DOC export at pristine sites with similar hydroclimates, but different

mean annual temperatures (due to latitude and latitudinal differences between sites) over the past 14,000 years BP. The findings from the speleothem DOC reconstructions were complimented by an alkenone-based SST trace-element record from the Tasman Sea (west of New Zealand's South Island) (Barrows *et al*,, 2007) and speleothem (Mg/Ca) trace-element based reconstructions of wetness overlying the cave (as applied in previous studies (e.g. Cruz *et al.,* 2007). The speleothem-based DOC reconstructions were supported by a lake sediment reconstruction of TOC and humic-like DOM inputs over the past 14,000 years BP.

## 1.3 Overall aim of research:

This project aimed to determine whether atmospheric warming is capable of driving increases in DOC concentrations in inland waters in the absence of human interference. To achieve this aim, experimental process-based research was integrated with the analysis of speleothem and lake sediment archives in New Zealand.

## 1.4 Research objectives

- To determine whether atmospheric warming is capable of driving increases in DOC concentrations in inland waters in the absence of acidification at sites with different temperature regimes and climate sensitivities (due to altitude).
- To build an understanding of climate effects (temperature and precipitation) and controls on DOC loss from soil over long (centennial/millennial) time scales) in the absence of human interference in New Zealand.
- To validate the use of speleothems as reliable recorders of DOC concentration and characteristics.

## 1.5 References


Ask, J., Karlsson, J., Persson, L., Ask, P., Byström, P., & Jansson, M. (2009). Terrestrial organic matter and light penetration: Effects on bacterial and primary production in lakes. *Limnology and Oceanography, 54*(6), 2034-2040.

Barrows, T. T., Lehman, S. J., Fifield, L. K., & De Deckker, P. (2007). Absence of cooling in New Zealand and the adjacent ocean during the Younger Dryas chronozone. *Science, 318*(5847), 86-89.

Batjes, N. H. (1996). Total carbon and nitrogen in the soils of the world. *European Journal of Soil Science, 47*(2), 151-163.

Blyth, A. J., Baker, A., Collins, M. J., Penkman, K. E. H., Gilmour, M. A., Moss, J. S., Genty, D., & Drysdale, R. N. (2008). Molecular organic matter in speleothems and its potential as an environmental proxy. *Quaternary Science Reviews, 27*(9), 905-921.

Blyth, A. J., Hartland, A., & Baker, A. (2016). Organic proxies in speleothems – New developments, advantages and limitations. *Quaternary Science Reviews, 149*, 1-17.

Cruz, F. W., Burns, S. J., Jercinovic, M., Karmann, I., Sharp, W. D., & Vuille, M. (2007). Evidence of rainfall variations in Southern Brazil from trace element ratios (Mg/Ca and Sr/Ca) in a Late Pleistocene stalagmite. *Geochimica et Cosmochimica Acta, 71*(9), 2250-2263.

Karlsson, J., Byström, P., Ask, J., Ask, P., Persson, L., & Jansson, M. (2009). Light limitation of nutrient-poor lake ecosystems. *Nature, 460*(7254), 506.

McWethy, D. B., Whitlock, C., Wilmshurst, J. M., McGlone, M. S., Fromont, M., Li, X., Dieffenbacher-Krall, A., Hobbs, W. O., Fritz, S. C., & Cook, E. R. (2010). Rapid landscape transformation in South Island, New Zealand, following initial Polynesian settlement. *Proceedings of the National Academy of Sciences, 107*(50), 21343-21348.

Raftery, A. E., Zimmer, A., Frierson, D. M. W., Startz, R., & Liu, P. (2017). Less than 2 °C warming by 2100 unlikely. *Nature Climate Change, 7*, 637.

Yang, Y., He, Z., Wang, Y., Fan, J., Liang, Z., & Stoffella, P. J. (2013). Dissolved organic matter in relation to nutrients (N and P) and heavy metals in surface runoff water as affected by temporal variation and land uses – A case study from Indian River Area, south Florida, USA. *Agricultural Water Management, 118*, 38-49.

# 2 Chapter 2

# Literature review

## 2.1 Soils in a global context

The global soil carbon pool of 2,500 Gt includes 1,550 Gt of organic carbon (Lal, 2004). Soil contains more carbon than the Earth's vegetation and atmosphere combined (Lehmann & Kleber, 2015). The temperature sensitivity of soil respiration may partly determine the amount of carbon transferred to the atmosphere as a result of anthropogenic global warming (Davidson *et al.*, 2000; Kirschbaum, 2000). Global temperatures are expected to exceed 2 °C above pre-industrial levels by 2100 (Raftery *et al.*, 2017), with unquantified impacts on C export from soil. Indeed, the release of even a small fraction of soil carbon as $CO_2$ or $CH_4$ (from permafrost) could cause substantial increases of these gases in the atmosphere (Lehmann & Kleber, 2015), and further exacerbate the rate of global warming (Friedlingstein *et al.*, 2013). Currently, the uncertainty surrounding soil carbon stability is creating uncertainty in the forecasting of future climate change (Evans *et al.*, 2007). Although carbon-cycle climate feedbacks are included in climate projections, they are commonly represented in models by outdated knowledge of soil carbon turnover (Bradford *et al.*, 2016). Thus, direct measurements of warming-induced changes in soil C stocks will be pivotal in increasing confidence in future climate projections (Bradford *et al.*, 2016).

## 2.2 The soil carbon continuum

Biological, physical, and chemical transformation processes convert dead plant material into simpler organic products. These products can form relationships with soil minerals, and, this interaction complicates the study of the nature of soil organic

matter (SOM) (Lehmann & Kleber, 2015). The number of compounds that may constitute OM is effectively limitless, and therefore a specific chemical description cannot be given (Evans *et al.*, 2005). However, the proportion of unidentifiable compounds is quite small, and the traditional view of the existence of a novel set of complex (high molecular weight) compounds termed 'humic substances' has been superseded thanks to modern analytical organic methods (Kelleher & Simpson, 2006). The complex mixture of identifiable biopolymers that make up the "humic" fraction of soils account for some 60 % of total SOM (Trevisan *et al.*, 2010). This fraction has a broad spectrum of physiochemical properties and thus can form water-soluble (hydrophilic) and water-insoluble (hydrophobic) complexes with inorganic ions and other organic compounds, as well as coatings on oxides, hydroxides and other minerals (Trevisan *et al.*, 2010). The soluble fraction of SOM is therefore extremely important in soils and can promote dissolution, mobilisation, and transportation of metals in soil and water, as well as accumulation of trace elements within soil horizons (Trevisan *et al.*, 2010; Hartland, 2011). Lehmann & Kleber (2015) described the emergent view of SOM as a continuum of progressively decomposing organic compounds, ranging from intact plant material to highly oxidised carboxylic acids (Lehmann & Kleber, 2015). These and numerous authors, hence, posit that available evidence does not support the long-held view of formation of large molecular size, or persistent humic substances in soil.

Dissolved organic matter (DOM) is an important component of SOM and plays an important role in cycling and the distribution of carbon and nutrients between ecosystems. DOM plays an integral role in the soil forming process (Kalbitz *et al.*, 2000), and primarily originates from plant litter, soil humus, microbial biomass and root exudates (Kalbitz *et al.*, 2000). DOM is an amalgam of heterogeneous

compounds that are influenced by microbial and physicochemical reactivity, which in turn influences DOM processing and composition (Kellerman *et al.*, 2014). DOM is generally considered to be representative of total SOM, because the soluble phase is very often in equilibrium with the solid phase of SOM.

DOM is operationally defined as the fraction of molecules possessing dimensions <0.45 μm in size (Thurman, 1985). Therefore, DOM is not necessarily dissolved and may include colloidal matter. Colloidal material has been observed at multiple scales, from globular nanoparticles 0.5-4 nm in size (Stolpe & Hassellöv, 2007; Baalousha *et al.*, 2011; Hartland *et al.*, 2011), up to aggregates in the hundreds of nm (Lead & Wilkinson, 2006). This size continuum is influenced by aquatic chemistry and particle-particle interactions (Buffle *et al.*, 1998). The mixture of aromatic and aliphatic compounds, i.e. those containing oxygen, nitrogen and sulphur functional groups (e.g. carboxyl, phenol, enol, alcohol, carbonyl, amine and thiol) (Chen *et al.*, 2003), in DOM dictate its pH-dependent solubility. Hence, DOM composition is a determining factor in its physicochemical behaviour.

Organic compounds can range in size from relatively small molecules to highly complex structures containing thousands of atoms (Ashman & Puri, 2013). One could argue that this heterogeneity means that the most meaningful insights about DOM cycling across environmental gradients or long timescales are to be gained by considering the broader, functional properties of DOM mixtures (and changes therein) rather than the specific molecular character of any given sample. Because SOM must first be solvated to be accessed by microorganisms, DOM is the most bioavailable fraction of SOM (Marschner & Kalbitz, 2003). Extending the concept of bioavailability further, DOM also controls other important nutrients (e.g. organic N and P), and trace micronutrients (e.g. Co, Ni, Cu, Zn) (Welikala *et al.*, 2018), and

therefore DOM dynamics are important for understanding nutrient dynamics in soils more generally (Kalbitz *et al.*, 2000; Kaiser *et al.*, 2001).

## 2.3 DOM in aquatic systems

Soils (including wetlands, permafrost and peatlands) are vital sources of organic carbon to aquatic ecosystems, with implications for biogeochemical processes in rivers, lakes and estuaries (Jaffé *et al.*, 2008; Marín-Spiotta *et al.*, 2014). Soil carbon content is dependent on the rates of addition from plant growth versus rates of removal via decomposition, leaching and other soil processes. Each of these processes is influenced by climate, land-use (Zsolnay, 1996), soil pH (Schimel *et al.*, 2001; Smith *et al.*, 2003), soil structure and soil composition.

The active fraction of soil carbon can be oxidised to $CO_2$ or leached and exported to the surrounding environment as DOM. The movement of carbon (including DOM) occurs via an aquatic continuum, whereby carbon is laterally transported from upland soils to the open sea via lakes, rivers, streams and estuaries (Regnier *et al.*, 2013). During passage through the aquatic continuum, carbon can be 'filtered' (i.e. processed geochemically, exported to the atmosphere as $CO_2$ or $CH_4$, or stored within sediments). Streams and rivers are usually net emitters of $CO_2$ to the atmosphere, much of which is derived primarily from microbial metabolism and respiration of allochtonous C (including particulate and DOM).

DOM has several important environmental impacts and is a vital modulator of the structure and function of lake ecosystems (Sobek *et al.*, 2007). DOM can impact light-penetration (Williamson *et al.*, 1999; Rae *et al.*, 2001; Ask *et al.*, 2009; Karlsson *et al.*, 2009), thus impeding photosynthesis and altering thermal structure and the mixing depths of lakes (Fee *et al.*, 1996). DOM can strongly influence the acidity of terrestrial waterbodies. For example, heightened seasonal inputs of DOM

has been shown to increase the acidity of freshwater (by up to two pH units) in boreal Swedish lakes (Laudon *et al*., 2001). DOM can also transport metals (e.g. Al in the UK) (Evans *et al*., 2005), and nutrients (particularly N and P) (Yang *et al.*, 2013). The presence of DOM even reduces the quality of drinking water, through the production of toxic by-products during the water decontamination processes (Diehl *et al.*, 2000).

The aforementioned roles of DOM demonstrate that organic matter research necessarily transcends disciplinary and ecosystem boundaries (Marín-Spiotta *et al.*, 2014). Understanding the drivers of the recent increase in DOM export is of clear importance for climate modellers, soil scientists, and those in the wider aquatic sciences. This literature review aims to summarise and discuss the commonly proposed drivers of the recently observed increase in aquatic DOM. The review will also explore the contribution of long-term (centennial to millennial scale) limnological and speleothem-based reconstructions of DOM concentrations and the methods used. Finally, the review will suggest how historical studies of these archives in New Zealand can inform this modern debate and disentangle the array of overlapping proposed drivers that prevent firm conclusions being drawn from studies based solely on recent decadal-scale datasets.

## 2.4 Analytical approaches for analysing DOM concentrations and characteristics

This section will describe two geochemical methods used in palaeo-environmental reconstructions of DOM export. DOM is a complex mix of high weight molecules, (Kalbitz *et al.*, 2000), not all of which are identifiable, e.g. humic and fulvic fractions, sugars, amino acids and other biomolecules are chemically identifiable, depending on the technique applied (Herbert, 1995). A range of spectroscopic

techniques have been used to measure DOM concentration and molecular characteristics. These include, but are not limited to; NMR (nuclear magnetic resonance), FTIRS (Fourier transform infrared) spectroscopy (Rosén & Persson, 2006; Tranvik *et al.*, 2009; Rosén *et al.*, 2010; Rosén *et al.*, 2011; Meyer-Jacob *et al.*, 2014; Meyer-Jacob *et al.*, 2015); fluorescence spectroscopy (Coble, 1996; Baker, 2001; Baker & Inverarity, 2004). The latter two techniques require relatively small sample sizes, no manipulative sample preparation, and provide quantitative or qualitative data on molecular structure and chemical or functional properties of DOM. However, interpreting the resulting data and disentangling the components measured by this family of techniques can be challenging due to the over-lapping of spectra and broad peaks obtained (Chen *et al.*, 2002). Fluorescence methods have been widely utilised to characterise the components of organic matter in water (Baker, 2001; Stedmon *et al.*, 2003; Baker & Inverarity, 2004; Baker *et al.*, 2004; Hudson *et al.*, 2007; Fellman *et al.*, 2010) and soil (Chen *et al.*, 2003; Tranvik *et al.*, 2009) and will be the main focus of this review, alongside FTIRS, which has been routinely used to characterise and quantify organic carbon in soil and lacustrine sediments.

### 2.4.1 3D EEM (excitation-emission matrix) fluorescence

Fluorescence occurs when light energy (photons) excite loosely held electrons in the outer orbitals of a molecule, to a higher energy level (Fairchild & Baker, 2012). As the electron returns (relaxes) to its original ground state, energy is lost as fluorescence (emission of photons). Some energy is also lost by collision, non-radiative decay and other processes prior to emission, so the energy of the emitted photon is lower than the excitation energy (i.e. at a longer wavelength). This phenomenon is known as Stokes shift. Figure 2.1 shows the energy transfer of the fluorescence process (Hudson *et al.*, 2007) from excitation to fluorescence

(emission). Organic compounds that adsorb light are generically known as chromophores and molecules that re-emit light are described as fluorophores (Mopper *et al.*, 1996). Humic and fulvic substances typically contain functional groups with loosely held electrons, mostly in their aromatic carbon ring structures (Senesi *et al.*, 1989; Senesi, 1990). Broadly, the fluorescence intensity of organic molecules should be proportional to their concentration, whilst the wavelengths at which fluorescence occurs relates to their specific molecular structures and/or sources (Hudson *et al.*, 2007; Fellman *et al.*, 2010; Fairchild & Baker, 2012). However, when large compositional changes occur, the intensity: concentration relationship can break down.

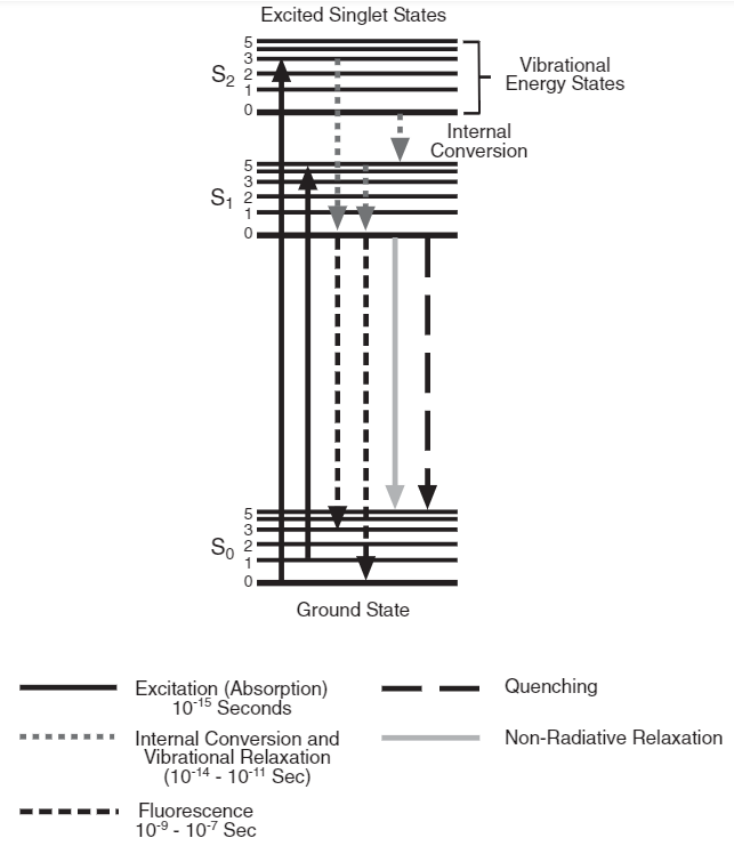


**Figure 2.1**- Jablonski diagram. Figure from Hudson *et al.*, (2007).

A common approach to fluorescence characterisation of DOM is three-dimensional excitation-emission matrix (EEM) analysis. 3D EEM analysis has been utilised in

a range of aquatic ecosystems to characterise DOM, including marine environments (Coble *et al.*, 1990; Coble, 1996; Para *et al.*, 2010), terrestrial waterbodies (Baker, 2001; Baker & Inverarity, 2004; Baker *et al.*, 2004), and caves (Hartland *et al.*, 2012b; Rutlidge *et al.*, 2014; Rutlidge *et al.*, 2015), and has very commonly been utilised to assess OM properties through water treatment stages (Shutova *et al.*, 2014). Because the biochemical characteristics of DOM are related to its optical properties, fluorescence can provide information about DOM composition (Stedmon *et al.*, 2003), and may also provide information about the redox state, source, and biological activity of DOM (Mladenov *et al.*, 2008; Fellman *et al.*, 2010). Compounds with humic-like fluorescence (including lignin, tannins, polyphenols and quinone moieties (Cory & McKnight, 2005)) are known to account for a large fraction of the chromophoric DOM pool in natural waters. Compounds with protein-like fluorescence are dominated by constituent amino acids (tryptophan and tyrosine) and this type of fluorescence has frequently been attributed to biological productivity or nutrient pollution in aquatic systems (Baker & Inverarity, 2004; Baker *et al.*, 2004).

3D EEMs are typically analysed statistically using PARAFAC (parallel factor analysis of components) (Bro, 1997; Stedmon & Bro, 2008). PARAFAC is a multivariate modelling technique that can statistically distinguish individual fluorescent signatures as statistical components (Fellman *et al.*, 2010). Each component represents a group of fluorophores, such as humic-like, fulvic-like, or protein-like, which display fluorescence characteristics that are similar to reference standards (Fellman *et al.*, 2010). An example of a 3D EEM spectrum is shown in Figure 2.2. The different wavelengths at which fluorescence occur are related to the molecular structure of the compounds, whilst the intensity of fluorescence increases

with concentration. For example, Peaks C and A correspond to humic-like fluorescence, whilst peak T represents protein-like material (Coble, 1996).

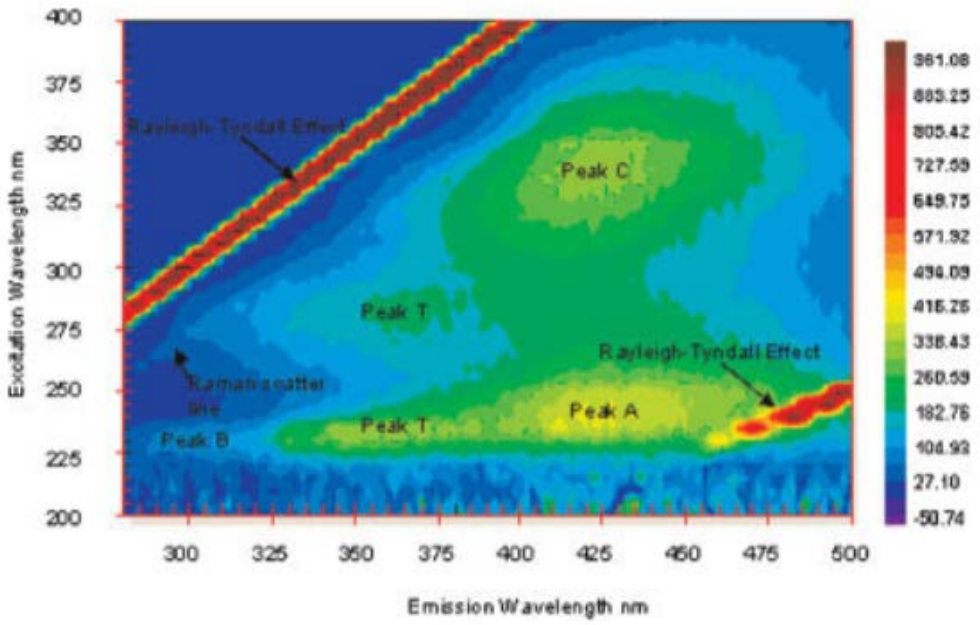


**Figure 2.2-** 3D excitation-emission matrix (EEM) features as named by Coble (1996) (Peaks C, A, T and B). Figure from Hudson *et al.,* (2007).

### 2.4.2 **Fourier transform infrared spectroscopy (FTIRS)**

FTIRS (Fourier transform infrared spectroscopy) allows rapid determination of organic matter composition and has been utilised to assess organic matter quality and quantity in peatlands (Niemeyer *et al.,* 1992; Artz *et al.*, 2008; Beer *et al.*, 2008) and lake sediments (Meyer-Jacob *et al.*, 2014; Meyer-Jacob *et al.*, 2015; Meyer-Jacob *et al.*, 2017).

FTIRS has also been applied in several environments to assess sedimentary silica and other minerals (Mecozzi *et al.*, 2001; Rosén *et al.*, 2010). Compared to many other techniques, FTIRS has the advantage of requiring only a small amount of ground, dried sediment (10 mg) (Rosén *et al.,* 2010) which is mixed with KBr (potassium bromide) (at a ratio of 2% sediment to KBr) before being pressed into translucent sample discs, which can then be analysed for their

reflectance/transmission of light at a wide range of wavelengths (typically 3,750 and 400 $cm^{-1}$ [wavenumbers] for analysis of organic carbon). The basic principle of FTIRS is that infrared light (as photons) causes vibrations of covalent chemical bonds, forcing a change in dipole moment, which leads to the absorption of infrared energy at specific frequencies, which are in-turn representative of specific chemical bonds or functional groups (Liu *et al.*, 2013) (Figure 2.3). The small sample size and minimal preparation required for FTIRS mean that it is a useful technique for high-resolution sedimentary studies.

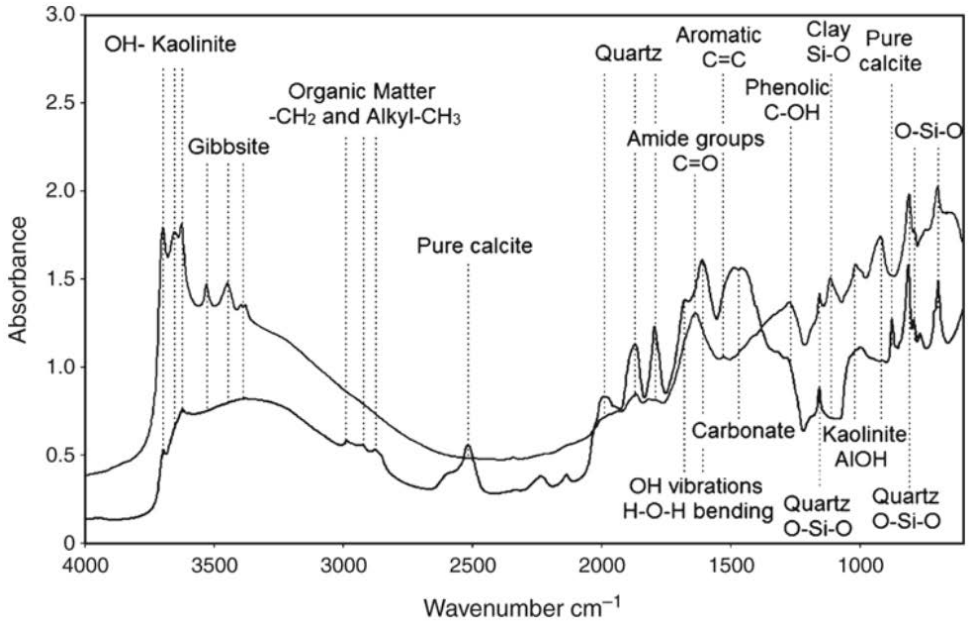


**Figure 2.3-** Infrared spectrum of absorption peaks related to mineral and organic composition of soil. Figure from (Guillou *et al.*, 2015).

## 2.5 Palaeo-environmental archives of DOM export

### 2.5.1 Lake sediments as archives of DOM export

Lakes act as sediment sinks, accumulating ecological, physical, biological, and chemical information that can inform us about environmental change of the past (Lowe & Walker, 2014). Lake sediments comprise both allochtonous and autochtonous material and are therefore derived either from organic production

within the lake, or from the in-wash of organic and inorganic material from the lake catchment (Aaby & Berglund, 1986). Of the organic carbon that is deposited into the sediments, a certain proportion will be remineralised as $CO_2$, and the remainder will be incorporated and buried over geological timescales (Gudasz *et al.*, 2010). Cole *et al.*, (2007) estimated that inland waters annually receive on the order of 1.9 Pg $y^{-1}$ of carbon from the terrestrial landscape globally, of which, about 0.2 Pg $y^{-1}$ is buried in the sediments, 0.8 Pg $y^{-1}$ is transferred back to the atmosphere, and the remaining 0.9 Pg $y^{-1}$ is deposited in the oceans. Despite the relatively small area of coverage, inland waters play a key role in regulating climate on local and regional scales (Cole *et al.*, 2007; Raymond *et al.*, 2013).

Sediments from individual lakes can be used to infer both natural and anthropogenic changes on local scales, whilst the study of multiple lakes can produce an understanding of regional-scale dynamics (Filella & Rodríguez-Murillo, 2014). Organic carbon is one of many proxies 'archived' by lake sediments and thus allows the reconstruction of past soil carbon export (if sediment DOM characteristics and source can be distinguished, e.g. via the utilisation of fluorescence methods). Lakes are particularly valuable as archives of organic carbon dynamics because of their sensitivity to change, though this can be somewhat complicated because allochtonous DOM input can also be altered by anthropogenic change (e.g. land-use) and by diagenesis within the sediments. Lakes are also subject to hydrological and geomorphological influence, and therefore correlations between changes in lake sediment properties and climate may be non-linear, and may vary between individual lakes (Fritz, 2008). FTIRS has also been applied to palaeolimnological records (Rosén & Persson, 2006; Rosén *et al.*, 2010; Rosén *et al.*, 2011; Meyer-Jacob *et al.*, 2014) to reconstruct inputs of TOC. Rosén *et al.*, (2006) showed that FTIRS models of total organic carbon concentration based on analysis of surface

sediment samples can be applied to sediment cores for retrospective analysis. Meyer-Jacob *et al.*, (2014) applied FTIRS measurements to quantitatively reconstruct TOC, TIC and biological silica (BSi) concentrations in sediments that accumulated over the past 3.6 million years in Lake El'gygytgyn, East Arctic Russia (Meyer-Jacob *et al.*, 2014). That study found a strong, positive correlation between FTIRS-inferred and conventionally measured data for Bsi, TOC and TIC respectively (Figure 2.4), thus validating this technique.

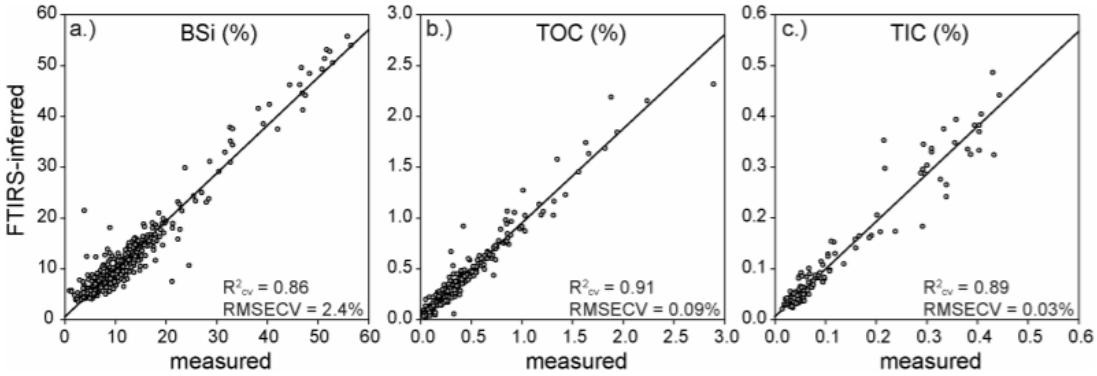


**Figure 2.4**- Conventionally measured versus FTIRS-inferred concentrations of (a) biogenic silica (BSi), (b) total organic carbon (TOC), and (c) total inorganic carbon (TIC) with the cross-validated coefficient of determination ($R^2$ CV) and root mean square error of cross-validation (RMSECV) resulting from the internal validation of the calibration models. Figure from Meyer-Jacob *et al.*, (2014).

Because FTIRS only requires a relatively small sample size, it is particularly useful in high-resolution studies where sample size may act as a limitation for analysis using other techniques (Rosén *et al.*, 2010; Meyer-Jacob *et al.*, 2014). As with all palaeo-environmental archives, lake sediments as archives of organic matter have some limitations (particularly diagenesis, which is difficult to quantify in palaeo reconstructions).

### 2.5.2 Speleothems- a brief introduction and their use as palaeo-environmental archives

Speleothems (Figure 2.5) are carbonate mineral deposits typical of limestone caves (Gunn, 2004), and are globally widespread. The word "speleothem" is derived from

Greek; spelaion means "cave" and thema means "deposit". In geological terms, speleothems are more commonly designated by their morphology as stalagmites, stalactites or flowstones. Speleothem formation is controlled by surface geomorphology, the quantity and chemical properties of water, cave geometry, aquifer properties and the surface microclimate (Fairchild *et al.*, 2006). Speleothem growth is a part of the meteoric water cycle and is influenced by environmental processes above the cave (Lauritzen & Lundberg, 1999). Pioneering research in the 1960's and 1970's discovered that speleothems incorporate climate signals during their growth and can therefore be utilised as palaeo-environmental archives (Hendy & Wilson, 1968; Hendy, 1971). Speleothems have some major advantages over other palaeo-environmental archives, as they are more physically and chemically stable than sediments at the Earth's surface (Wigley & Brown, 1976), and can be dated to a higher degree of accuracy than other archives (due to the accuracy and precision of U/Th dating techniques).

Speleothems are formed when waters enter a cave system and via degassing of excess carbon dioxide (Fairchild & Treble, 2009), become supersaturated with respect to $CaCO_3$. Before entering the cave, dripwater is in equilibrium with $CO_2$ at elevated partial pressure ($pCO_2$) within the soil percolation zone. The lower $pCO_2$ of cave air leads to the degassing of $CO_2$ from the water upon entry to the cave. This degassing causes calcite to be deposited as a speleothem (Lauritzen & Lundberg, 1999) in the reaction described by the overall equation:

$$Ca^{2+}{}_{(aq)} + 2HCO_3^-{}_{(aq)} \rightarrow CaCO_{3(s)} + H_2O_{(aq)} + CO_{2(g)} \qquad (2\text{-}1)$$

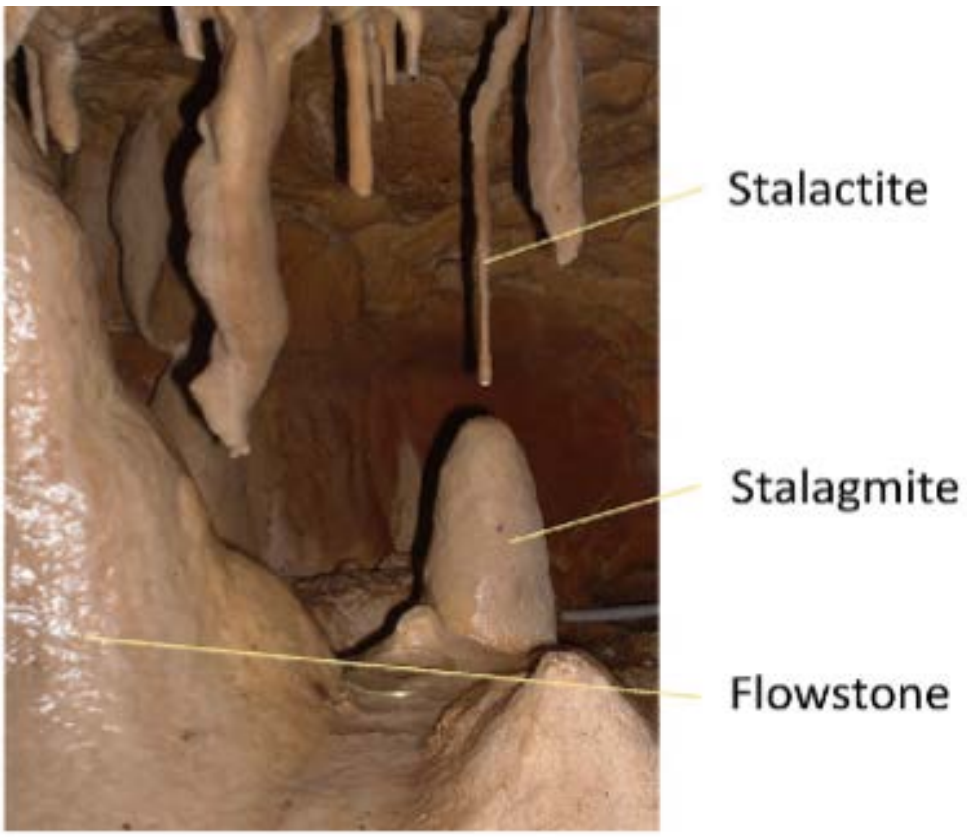


**Figure 2.5**- Three of the most commonly observed sub-types of speleothems. Image from Blyth *et al.*, (2016).

### 2.5.3 Speleothems as archives of organic carbon

Speleothems have most commonly been used to reconstruct climate and/or vegetation (Hendy & Wilson, 1968; Hendy, 1971; Hellstrom *et al.*, 1998; Wang *et al.*, 2001; McDermott, 2004; Yuan *et al.*, 2004; Mattey *et al.*, 2008), predominantly focusing on isotopic ratios of oxygen ($^{18}O/^{16}O$) and carbon ($^{13}C/^{12}C$). Carbon isotope ratios in speleothems have been well-studied (Spötl *et al.*, 2005; Atsawawaranunt *et al.*, 2018). However, few studies have examined speleothem organic matter (Blyth *et al.*, 2007; Blyth *et al.*, 2016) despite the several advantages of speleothems for organic geochemical analysis (e.g. speleothems are typically closed systems and not subject to post-depositional disturbance). Indeed, speleothems have long been known to contain organic material including lipids (Xie et al., 2003), lignin (Blyth *et al.*, 2010; Blyth et al., 2016; Heidke *et al.*, 2018) and

pollen (Festi *et al.*, 2016; Sniderman *et al.*, 2019). Thus, speleothems have potential as archives of SOM fluxes.

Early studies of organic material in speleothems focussed on organic matter as an important component of $\delta^{13}C$ records, or as a determinant of speleothem colour (Caldwell *et al.*, 1982; Van Beynen *et al.*, 2001). UV fluorescence of speleothems has long been known to be caused by the presence of organic matter (White, 1981), whilst Van Beynen *et al.*, (2001) utilised fluorescence to conclusively determine that speleothem colour is determined by organic matter content, and not by the presence of trace metals. Pioneering studies by Baker *et al.*, (1993) and Shopov *et al.*, (1994) found that speleothem fluorescence is caused by the presence of humic-like and fulvic-like material, and that this material exhibits annual to sub-annual banding in some samples. Baker *et al.*, (1993) determined that the intensity changes of fluorescence-bands in speleothems corresponded to annual-growth bands (determined to be annual by TIMS (thermal ionisation mass spectrometry) $^{230}Th$ dating)), meaning that speleothem fluorescence could be used for annually-resolved palaeo-environmental reconstructions (Baker *et al.*, 1993).

Several studies have employed fluorescence to study the mobility of DOM into caves, with many using DOM as a hydrological tracer of infiltration. For example, 3D EEM (excitation-emission matrix) fluorescence has been used to characterise fluorescence components in dripwater samples (Rutlidge *et al.*, 2014). The two dominant fluorophores were considered to be derived from soil (unprocessed, fresh humic-like DOM) and limestone bedrock (processed humic-like DOM), whilst the third component was tryptophan-like and therefore indicative of microbial activity (Hudson *et al.*, 2007). Speleothems are fed by dripwaters, which contain organic material derived from the soil zone (e.g. plant litter) which may be further processed within the vadose zone, and/or or from microbial and faunal activity within the cave

(Blyth *et al.*, 2016) (Figure 2.6). Speleothems may contain organic matter from the distant past, for example, organic materials have been identified in a stalagmite that was dated to 2.9 Ma (Blyth *et al.*, 2010).

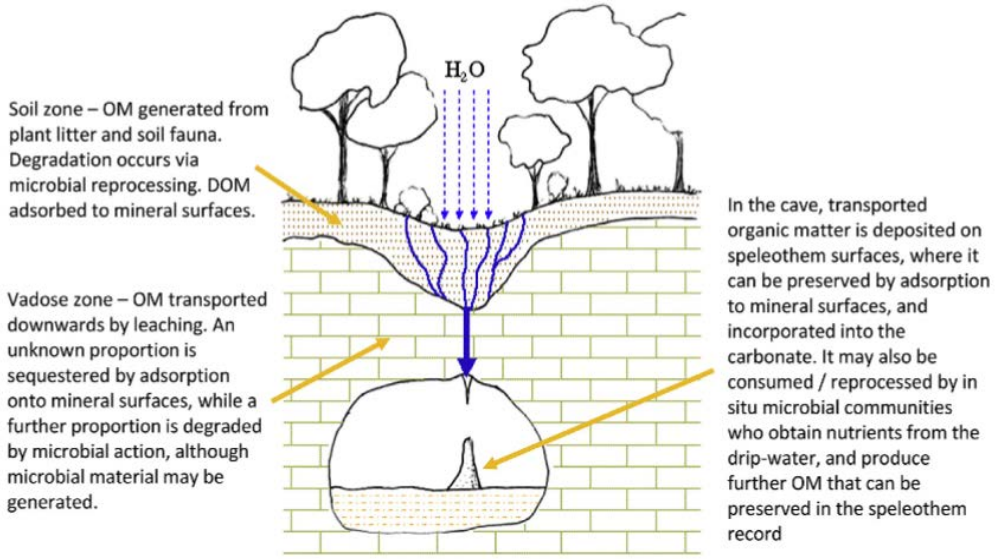


**Figure 2.6** - A schematic of the potential sources of DOM. Image and annotations from Blyth *et al.*, (2016).

In New Zealand, speleothem-based palaeo-climatic studies have typically focused on records of either $\delta^{13}C$ or $\delta^{18}O$ (Hellstrom *et al.*, 1998; Williams *et al.*, 1999; Williams *et al.*, 2005; Lorrey *et al.*, 2008; Whittaker *et al.*, 2011). An indicator of the scarcity of speleothem data in New Zealand is the fact that trace element records have only been published for one speleothem in New Zealand thus far (Hellstrom & McCulloch, 2000), and there are currently no speleothem-based reconstructions of soil DOM export in New Zealand.

The use of speleothems as archives of soil DOM has certain limitations. Notably, there is a poor understanding of potential alterations to and/or removal of DOM during transport from soil to cave (Fairchild & Baker, 2012). The degree of vadose zone processing is typically unconstrained, but there is growing evidence for the

commonality of soil, dripwater and speleothem OM signals (Blyth *et al.*, 2016) indicating the likely suitability of speleothems as archives of soil processes.

### 2.5.4 Mechanisms of incorporation of DOM into speleothems and impact on speleothem fabrics

Organic carbon is a well-known trace constituent of carbonate minerals (Ramseyer *et al.*, 1997; Dean & Gorham, 1998; Blyth *et al.*, 2008; Blyth *et al.*, 2013). Dissolved organic matter is known to act as an inhibitor in nucleation and calcium carbonate crystal growth, yet it is not well-known which chemical and physical processes are involved (Falini *et al.*, 2009). Two main processes have been proposed for organic matter incorporation into calcareous minerals; primarily ionic adsorption of organic molecules, particularly bridging reactions between $Ca^{2+}$ and carboxyl groups ($COO^-$) (Fairchild & Baker, 2012); and incorporation of organic matter as fluid inclusions (Ramseyer *et al.*, 1997). Adsorption of humic substances onto calcite crystals is an important geochemical process that occurs at the mineral-water interface (Chalmin *et al.*, 2012). Organic matter in carbonates is often analysed for environmental studies; however, incorporation mechanisms and types of interaction remain poorly understood (Chalmin *et al.*, 2012). Because of the multitude and complexities of the variables involved in speleothem growth, laboratory-based calcite growth experiments are helpful in understanding associated processes. Several laboratory studies have tested the incorporation of organic carbon (or humic acids) in calcite during growth, although these studies have predominantly utilised laboratory grade-humic acids, as opposed to 'natural' organic matter (Falini *et al.*, 2009; Chalmin *et al.*, 2012).

Gruzensky (1967) developed a basic method of calcite crystal growth, which has been used in several studies (Paquette & Reeder, 1995; Barker & Cox, 2011; Chalmin *et al.*, 2012) (Figure 2.7), and is based on solid ammonium carbonate as a

source of $CO_3^{2-}$ ions. In this method, $CO_{3(g)}$ diffuses into the aqueous calcium and ammonium chloride solution (Gruzensky, 1967). The vapour pressure of $(NH_4)_2CO_3$ enables vapour- phase diffusion to the solution, where a reaction takes place with $CaCl_{2(aq)}$ as described by the equation:

$$\mathbf{CaCl_{2\ (aq)} + (NH_4)_2CO_{3\ (aq)} = CaCO_{3\ (s)} + 2NH_4Cl_{\ (aq)}} \qquad (2\text{-}2)$$

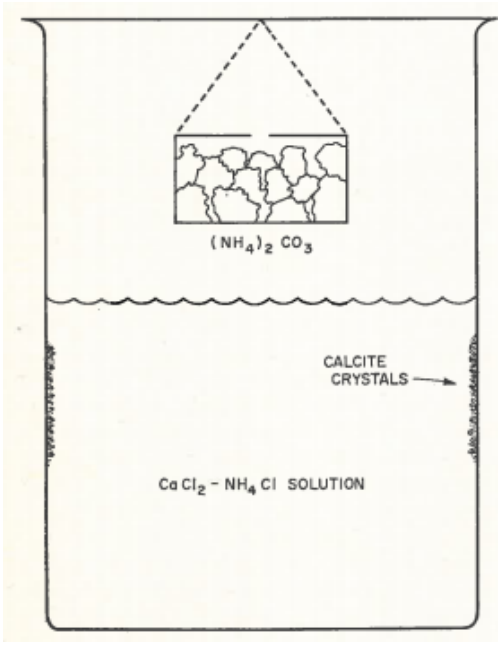


**Figure 2.7** - Apparatus for growing synthetic calcite crystals Figure from Gruzensky (1967).

Chalmin *et al.*, (2012) conducted a crystal precipitation experiment based on the Gruzensky method, to investigate interactions between OM and the calcite matrix during crystallisation processes with humic acid (HA) entrapment. This experimental approach illustrated that HA can be adsorbed onto the calcite surface and incorporated or adsorbed during crystallisation.

Most speleothem studies have focused on applying classic nucleation theories to determine the processes that cause the wide range of speleothem fabrics (Frisia *et al.*, 2018), yet non-classical growth theory may explain several unusual crystal growth pathways. Frisia *et al.*, (2018) undertook a precipitation experiment to

investigate initial speleothem crystallisation in the presence of natural organic matter in two caves (Antro del Corchia, Italy, and Yarrangobilly caves, Australia) with cave passages of similar temperatures (8–11 °C). (Frisia *et al.*, 2018). This study found unusual speleothem fabrics which incorporated colloids and adsorbed ions. Understanding the effects of organic matter incorporation on crystal morphology is vital, because physical properties (nano-crystal aggregation, open vs. compact columnar fabrics, defect-ridden fabrics and presence of nano-domains) have been routinely used to determine environmental parameters at the time of crystal formation (Frisia *et al.*, 2000; Nielsen *et al.*, 2014).

### 2.5.5 Speleothem age-dating using U/Th decay

Speleothem analysis for environmental reconstructions remains relatively novel compared to other terrestrial archives. The field of speleothem science has received heightened interest recently, partly due to its potential to provide high-resolution (seasonal/annual to decadal) terrestrial climate records with accurate and precise chronologies (Fairchild & Treble, 2009), which may extend for hundreds of thousands of years (Geyh & Thiedig, 2008; Vaks *et al.*, 2013). The accuracy and reliability of speleothem dating is not typically matched in other terrestrial environmental archives (e.g. lake sediments, peatlands, tree-rings), which are also limited by the comparatively short half-life of the primary chronometer ($^{14}C$ $t_{1/2}$ = 5700 ± 30 years).

Research on speleothems has been ongoing since the 1960's, though progress was initially hindered by the need for relatively large samples (approximately 10g) for alpha-spectrometric U-series dating (McDermott, 2004). Technological progress in speleothem dating in the late 1980s led to a revitalisation of interest in the topic, as TIMS (thermal ionisation mass-spectrometry) was able to provide $^{230}Th/U$ (U-Th) dates that were almost 10 times more precise than conventional alpha-spectrometry,

requiring a sample mass of 1 g (McDermott, 2004). Speleothems have come further to the forefront of terrestrial environmental reconstructions, due to the recent advancements in techniques such as MC-ICP-MS (Multi-collector inductively coupled plasma mass-spectrometry) (Hoffmann *et al.*, 2009), which typically require around ~100 mg of calcite, depending on U concentrations.

U-Th dating of speleothem calcite is an exceptionally useful technique for providing a chronology for Quaternary palaeo-environmental records and is arguably the most robust geochronometer available over much of this period (Hellstrom, 2006). U-Th dating is based on the decay of $^{238}U$ and $^{234}U$ to $^{230}Th$. The technique provides ages in calendar years, thus circumventing the radiocarbon calibration problems encountered in radiocarbon dating (McDermott, 2004). Due to advances in TIMS dating and MC-ICP-MS, the relative age uncertainties within speleothems are small and commonly range between 0.5 and -2% of the absolute age, depending on the U content (generally 0.05–0.5 ppm) (Fleitmann *et al.*, 2008). Nevertheless, U-Th dating has some notable issues: there are large age uncertainties associated with the presence of "initial" $^{230}Th$, which may have been incorporated during speleothem formation, and may cause over-estimates of age (Fleitmann *et al.*, 2008). However, speleothems usually act as closed systems with respect to U-series isotopes (Hellstrom, 2006). There are greater uncertainties surrounding 'young' (< 2000 year) speleothems with low U content, with errors ranging from 5 to -10% (Fleitmann *et al.*, 2008). Therefore, it can be difficult to make precise correlations between speleothem-based time series and alternative records, such as instrumental data (Fleitmann *et al.*, 2008).

The problem of age uncertainties for recent speleothems can be somewhat mitigated by the detection of the $^{14}C$ bomb-peak caused by the nuclear bomb tests of the 1960's, which is resolvable in some stalagmites (Genty & Massault, 1999).

Detection may be difficult if the $^{14}C$ activity of the speleothem is buffered and unclear (Genty & Massault, 1999), but if annual laminae are identified then this may be better constrained. As with any environmental archives, it is vital that any hiatuses are identified, and the chronology is constrained accordingly.

The advent of MC-ICP-MS instrumentation has provided an alternative to TIMS for high-precision dating of speleothems. In comparison with TIMS, MC-ICP-MS achieves a more efficient ionisation of Th (up to a factor of 100) using 8000 K plasma, which reduces the need for stringent sample preparation (Hoffmann *et al.*, 2009). MC-ICP-MS is a particularly valuable technique because the sample size requirements are more than an order of magnitude lower than thermal ionisation mass spectrometry (TIMS) (Hellstrom, 2003), and thus there is potential to analyse at much higher resolutions (where lack of sample mass may inhibit TIMS high-resolution analysis). It is important that U-Th dates are corrected for the any input of detrital Th (Th transported via groundwater) which can cause overestimation of age (Fairchild & Baker, 2012). Speleothems are not always closed systems, and some may not be suitable for U-Th dating.

### 2.5.6 Trace elements as recorders of environmental change and their relationship with DOM

Atmospheric deposition, superficial deposits and bedrock are all sources of the individual trace elements found in speleothems (Fairchild & Treble, 2009). However, primary trace elements may also be altered via soil processes prior to being transported to the cave. Trace elements can vary spatially within laminae and annual geochemical patterns can be observed even when laminae are not visible (Fairchild *et al.*, 2000). Trace elements can be useful proxies of environmental conditions or events (Fairchild & Treble, 2009). For example, variations in trace elements that show affinities for DOM may provide information on the timing and

magnitude of soil infiltration events (Hartland *et al.*, 2012b), volcanic eruptions (Badertscher *et al.*, 2014; Jamieson *et al.*, 2015) and atmospheric sulphate deposition (Frisia *et al.*, 2005). Trace element records have also been utilised in palaeo-climatic reconstructions, including studies of monsoons (Johnson *et al.*, 2006; Bernal *et al.*, 2016), glacial/interglacial cycles (Belli *et al.*, 2017; Weber *et al.*, 2018) and seasonal variations in precipitation (Warken *et al.*, 2018).

Trace element ratios of alkaline earth metals such as Mg/Ca and Sr/Ca have been used as proxies for rainfall changes. Following initial host-rock dissolution, the amount of Mg and Sr (relative to Ca) in dripwater is primarily controlled by prior calcite precipitation (PCP), whereby under drier environmental conditions, calcite precipitates along the aquifer flow path (due to longer mean residence times), prior to entering the cave (Fairchild & Baker, 2012), thus causing heightened concentrations of Mg and Sr compared to Ca. This approach has been tested and frequently applied to speleothem-based environmental reconstructions (Fairchild *et al.*, 2000; Sinclair *et al.*, 2012).

In natural waters, particulate organic matter, DOM and colloids compete to bind trace metals (Warnken *et al.*, 2007; Hartland *et al.*, 2012b).Several trace elements are strongly associated with organic matter fluorescence signals in speleothems, particularly because fluorescent colloids may bind trace elements that are transported from soil and into the karst system (Borsato *et al.*, 2007; Hartland *et al.*, 2012b). Thus, trace elements in dripwaters and which become incorporated in speleothems are affected by numerous processes. One important process is metal-organic matter binding (Hartland *et al.*, 2012a; Rutlidge *et al.*, 2014; Hartland & Zitoun, 2018), which in turn responds to geochemical changes along the flow-path (e.g. PCP). As with visible/fluorescent laminae, trace metals may vary annually (Borsato *et al.*, 2007). For example, in speleothems from Grotta di Ernesto cave in

NE Italy, there is a peak in trace element concentration which is believed to be deposited following the annual autumn recharge event. Borsato *et al.,* (2007) proposed that this event brings fine particles and colloids into the cave, which act as agents of transport of Cu, Pb, Zn, and Y (Borsato *et al.*, 2007). This inference was in part supported by subsequent monitoring by Hartland *et al.,* (2012).

Speleothem trace metal concentrations are most commonly measured using LA-ICP-MS (laser ablation inductively coupled plasma mass spectrometry), although other techniques including X-ray fluorescence (XRF) are also increasingly used LA-ICP-MS is a particularly useful technique because highly detailed geochemical data (at ppm levels) can be acquired rapidly and at fine resolution, enabling selective sampling of speleothem layers. This has led to several major advances in the field of speleothem research. For example, Smith *et al.,* (2009) found that trace elements produce seasonal patterns within speleothems and created a trace-element dating tool based on elemental layer counting using a speleothem with well-defined laminae which provided an independent chronology (Smith *et al.,* 2009). A similar approach has been utilised to date speleothems from the Mediterranean (Nagra *et al.*, 2017).

## 2.6 New Zealand: a natural laboratory with uniquely pre-human archives of soil DOM export through the Holocene

New Zealand (approximately 34.4 to 46.6 °S) provides a unique opportunity to study the effects of climate on soil processes due to its location in the southern mid-latitudes, where it receives atmospheric inputs from the tropical Pacific to the north, and the extra-tropical Southern Ocean to the south (Kidson & Renwick, 2002). Mainland New Zealand has a large latitudinal gradient (~12 °), and a geographically

diverse climate, which can be split into heterogenous regions via synoptic-climatological classification (Kidson, 2000). New Zealand also lies on a tectonic plate boundary, and therefore has high topographical relief (e.g. the Southern Alps), which, combined with the dominance of prevailing westerly air masses causes relatively high precipitation (>4,000 mm per year) in high-altitude areas of the west coast (Figure 2.8 b).

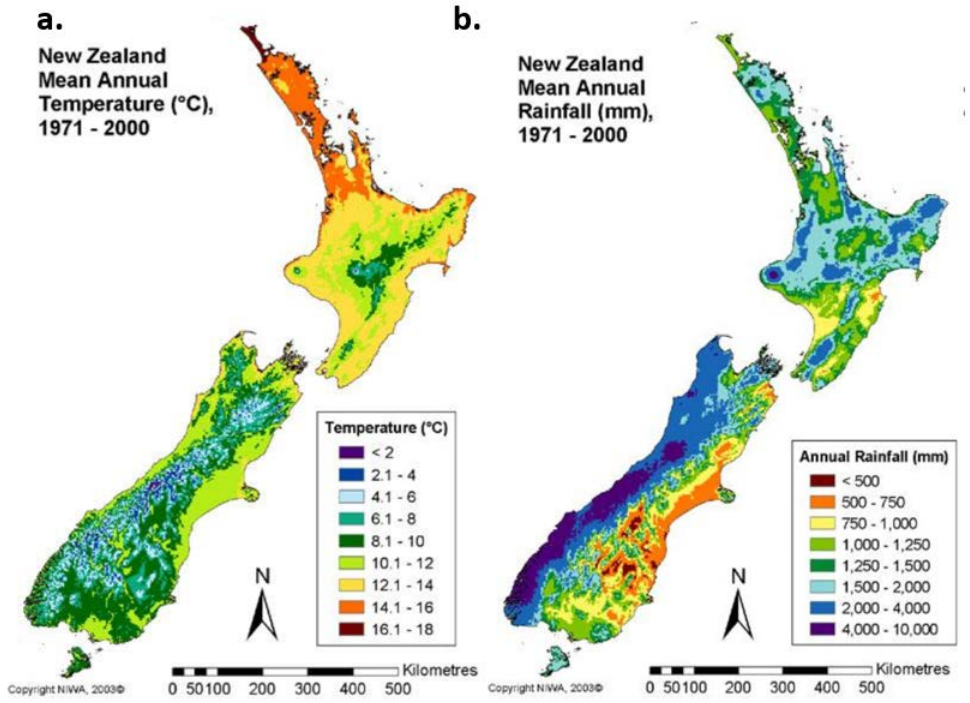


**Figure 2.8- (a.)** New Zealand mean annual temperature (°C) (1971–2000). **(b.)** New Zealand mean annual rainfall (mm) (1971–2000). Figure from NIWA (2016).

### 2.6.1 A short history of anthropogenic impacts on New Zealand landscapes

New Zealand has only inhabited by humans relatively recently (since the thirteenth century AD) (Wilmshurst & Higham, 2004; McWethy *et al.*, 2014), when Māori arrived from the Pacific Islands. Within 200 years of Māori arrival, widespread burning converted nearly half of the South Island's native forests to open vegetation. This burning is evidenced by pollen, charcoal and biochemical signals recorded in coeval lacustrine sediments (McWethy *et al.*, 2010; McWethy *et al.*,

2014). This period is known as the Initial Burning Period (McWethy *et al.*, 2010), and marks the first large-scale anthropogenic impact in New Zealand. In the mid-19th century, New Zealand's landscape underwent widespread change (primarily deforestation for agriculture) after the arrival of European settlers (King, 2003). Over recent decades, industrial-scale agriculture has caused increasing nutrient loads in New Zealand's inland waters (Snelder *et al.*, 2018). Indeed, intensively managed pastoral land covers approximately one-third of New Zealand's total landmass (Abell *et al.*, 2011).

New Zealand's short human history provides a unique opportunity to assess the impacts of climatic and natural processes and fluctuations on soil DOM export in a pre-human continent (prior to Māori arrival in the 13th century).

### 2.6.2 The Holocene climate of New Zealand

The Holocene is an inter-glacial epoch which spans 11,700 years BP to present and is the most studied interval within the entire geological record globally (Walker *et al.*, 2019). Although the Holocene is an entirely interglacial period, and is more stable than previous epochs, notable Holocene climatic variability has been reconstructed for New Zealand. Quaternary scientists have used a variety of archives in terrestrial environments, including speleothems (Hellstrom *et al.*, 1998; Williams *et al.*, 2005), lake sediments (Vandergoes *et al.*, 2008; Augustinus *et al.*, 2012; Stephens *et al.*, 2012a; Jara *et al.*, 2015; Zink *et al.*, 2016), peat bogs (McGlone & Wilmshurst, 1999; Wilmshurst *et al.*, 2003), glacial deposits (Putnam *et al.*, 2012; Kaplan *et al.*, 2013; Doughty *et al.*, 2017) and marine sediment cores (Barrows *et al.*, 2007; Pedro *et al.*, 2015) to reconstruct palaeo-environmental change in New Zealand. Many of New Zealand's terrestrial environmental reconstructions are produced from pollen-based evidence and are spatially or temporally fragmentary. The evidence for and timing of events in New Zealand

may be greatly improved by utilising well-dated speleothem-based proxies (such as trace element reconstructions of precipitation and/or temperature). The following section provides a brief overview of reconstructions of Holocene climate in New Zealand.

#### 2.6.2.1 The glacial transition (pre-Holocene) and early Holocene climatic optimum (HCO)

Prior to the onset of the Holocene, and after the last glacial maximum (LGM), New Zealand's late-glacial transition (from ca. 18–12,000 years BP) (Hodgson & Sime, 2010), was disrupted by the Antarctic cold reversal (ACR), a period of cooling from 14,500–12,900 years BP (Kaplan *et al.*, 2010; Stephens *et al.*, 2012b), reaching its coolest point at approximately 13,000 years BP (Vandergoes *et al.*, 2008; Putnam *et al.*, 2010). A chironomid-based temperature record from Boundary Stream Tarn (Mackenzie basin, Canterbury, South Island), showed that during the ACR summer temperatures were approximately 2.9 °C lower than modern summer temperatures (Vandergoes *et al.*, 2008). The ACR was followed by an increase in temperature, from 11,500 to 10,000 years BP (Pahnke & Sachs, 2006; Vandergoes *et al.*, 2008) in a period known as the Holocene climatic optimum (HCO). Pollen-based temperature records show that temperature may have been >1.5 °C warmer than today during the HCO in the northern South Island (Wilmshurst *et al.*, 2007; Jara *et al.*, 2015).

Jara *et al.*, (2015) found an increase in podocarp (*Dacrydium cupressinum*) (conifer tree) pollen percentages at Adelaide Tarn, a high-altitude lake in Kahurangi National Park, Nelson (NW South Island). They interpreted this as indicating an increase in treeline altitude due to a sustained period of warming, reaching a climax at ~10,000 years BP. This record is reaffirmed by the reconstruction of an increasing Dacyrdium-dominated podocarp forest on the west coast of the South

Island from ~12,000–10,000 years BP, which has been attributed to substantial warming (Alloway *et al.*, 2007). Similarly, pollen evidence has shown forest expansion and compositional changes (Newnham & Lowe, 2000) in the central North Island between 11,400 and 11,000 years BP. These compositional changes marked the onset of vegetation assemblages similar to present, thus indicating a transition to full interglacial conditions at the site. Elsewhere in the South Island, a pollen-based climate reconstruction showed that mean annual temperatures were at least 1.5 °C warmer than today in Canterbury during the HCO, yet treelines were lower than today (McGlone *et al.*, 2010). The same study postulated that this could be explained by reduced temperature seasonality (i.e. cooler summers and warmer winters), combined with lower annual precipitation (McGlone *et al.*, 2010). Further north, a reconstruction from Lake Pupuke (Auckland, North Island) showed that temperatures were warm and stable during the early Holocene (Augustinus *et al.*, 2012).

The HCO has also been observed in Antarctica, where a comparison of water isotope records from ice cores located at eleven sites on the central plateau showed a warm period from 11.5–9,000 years BP (Masson *et al.*, 2000). During the same time-period, a marine sediment record from the west coast of Antarctica showed that SST may have been approximately 3.5 °C warmer than present (Shevenell *et al.*, 2011). Jara *et al.*, (2015) suggested that there may have been a teleconnection between high and mid-latitudes (including NZ and South America) of the Southern Hemisphere and Antarctica during the late glacial period and early Holocene, perhaps due to relatively weak westerly circulation.

#### 2.6.2.2 Mid-Holocene (8–4,000 years BP)

After the HCO, there is thought to have been a general reduction in temperatures, as shown by speleothem isotope records from northwest Nelson (Hellstrom *et al.*,

1998). However, this is not entirely consistent with the pollen temperature proxy record produced by Jara *et al.*, (2015), which showed high magnitude temperature oscillations from 6,000–3,000 years BP.

#### 2.6.2.3 Late Holocene (4,000 years BP) to present

Pollen records from several peatland sites across New Zealand, suggest that a cooling and drying occurred from 4,000–3,000 years BP (Li *et al.*, 2008). Meanwhile from Adelaide Tarn (NW Nelson), a pollen-temperature proxy record showed that a prolonged cooling occurred from 3,000 years BP to present, despite increasing atmospheric $CO_2$ levels (Jara *et al.*, 2015). These findings are inconsistent with Antarctic temperature reconstructions, which show oscillations with no clear sustained trend (EPICA_Community_Members, 2004).

## 2.7 Summary of literature review

By utilising palaeo-environmental archives that pre-dates human arrival, the effects of natural variability on DOM export can be assessed using palaeo-environmental archives. Speleothems and lake sediments are both used to reconstruct environmental conditions of the past. Lake sediments have been used to reconstruct total organic carbon concentrations in sites around the world, yet there are relatively few studies of long-term (i.e. palaeo) soil carbon export. A range of natural (climate, vegetation change, soil type) and anthropogenic factors (agricultural practices, atmospheric S deposition) are known to impact organic carbon production, removal from soil and export into terrestrial waterbodies. The use of speleothems as climatic archives has typically focused on isotopic values (especially in New Zealand), yet other geochemical methods are becoming more common place. The use of speleothems for reconstructions of DOM dynamics is novel, benefitting from robust chronologies and the application of new high-resolution techniques for measuring

trace element geochemistry (LA-ICP-MS), in conjunction with conventional TOC analysis and fluorescence methods.

New Zealand provides an ideal ‘natural laboratory’, allowing natural processes underlying DOM trends to be addressed by using analysis of environmental archives, such as speleothems and lake sediments. Long-term reconstructions of soil DOM export provided by New Zealand speleothems and lake sediments can test the importance of natural (i.e. pre-human) environmental change on soil carbon export over long time scales, and set a ‘natural’ baseline and range of variability against which current soil carbon export (which is subject to anthropogenic impacts) can be compared.

## 2.8 References


Aaby, B., & Berglund, B. (1986). Characterization of peat and lake deposits. *Handbook of Holocene Palaeoecology and Palaeohydrology, 1*, 645-666.

Abell, J. M., Özkundakci, D., Hamilton, D. P., & Miller, S. D. (2011). Relationships between land use and nitrogen and phosphorus in New Zealand lakes. *Marine and Freshwater Research, 62*(2), 162.

Alloway, B. V., Lowe, D. J., Barrell, D. J. A., Newnham, R. M., Almond, P. C., Augustinus, P. C., Bertler, N. A. N., Carter, L., Litchfield, N. J., McGlone, M. S., Shulmeister, J., Vandergoes, M. J., Williams, P. W., & members, N.-I. (2007). Towards a climate event stratigraphy for New Zealand over the past 30 000 years (NZ-INTIMATE project). *Journal of Quaternary Science, 22*(1), 9-35.

Artz, R. R., Chapman, S. J., Robertson, A. J., Potts, J. M., Laggoun-Défarge, F., Gogo, S., Comont, L., Disnar, J.-R., & Francez, A.-J. (2008). FTIR spectroscopy can be used as a screening tool for organic matter quality in regenerating cutover peatlands. *Soil Biology and Biochemistry, 40*(2), 515-527.

Ashman, M., & Puri, G. (2013). *Essential soil science: a clear and concise introduction to soil science*. John Wiley & Sons.

Ask, J., Karlsson, J., Persson, L., Ask, P., Byström, P., & Jansson, M. (2009). Terrestrial organic matter and light penetration: Effects on bacterial and primary production in lakes. *Limnology and Oceanography, 54*(6), 2034-2040.

Atsawawaranunt, K., Comas-Bru, L., Amirnezhad Mozhdehi, S., Deininger, M., Harrison, S.P., Baker, A., Boyd, M., Kaushal, N., Ahmad, S.M., Ait Brahim, Y. (2018). The SISAL database: a global resource to document oxygen and carbon isotope records from speleothems. *Earth System Science Data.*

Augustinus, P., Cochran, U., Kattel, G., D'Costa, D., & Shane, P. (2012). Late Quaternary paleolimnology of Onepoto maar, Auckland, New Zealand: implications for the drivers of regional paleoclimate. *Quaternary International, 253*, 18-31.

Baalousha, M., Stolpe, B., & Lead, J. R. (2011). Flow field-flow fractionation for the analysis and characterization of natural colloids and manufactured nanoparticles in environmental systems: A critical review. *Journal of Chromatography A, 1218*(27), 4078-4103.

Badertscher, S., Borsato, A., Frisia, S., Cheng, H., Edwards, R., Tüysüz, O., & Fleitmann, D. (2014). Speleothems as sensitive recorders of volcanic eruptions–the Bronze Age Minoan eruption recorded in a stalagmite from Turkey. *Earth and Planetary Science Letters, 392*, 58-66.

Baker, A. (2001). Fluorescence excitation− emission matrix characterization of some sewage-impacted rivers. *Environmental Science & Technology, 35*(5), 948-953.

Baker, A., & Inverarity, R. (2004). Protein-like fluorescence intensity as a possible tool for determining river water quality. *Hydrological Processes, 18*(15), 2927-2945.

Baker, A., Smart, P. L., Edwards, R. L., & Richards, D. A. (1993). Annual growth banding in a cave stalagmite. *Nature, 364*, 518.

Baker, A., Ward, D., Lieten, S. H., Periera, R., Simpson, E. C., & Slater, M. (2004). Measurement of protein-like fluorescence in river and waste water using a handheld spectrophotometer. *Water Research, 38*(12), 2934-2938.

Barker, S. L. L., & Cox, S. F. (2011). Oscillatory zoning and trace element incorporation in hydrothermal minerals: insights from calcite growth experiments. *Geofluids, 11*(1), 48-56.

Barrows, T. T., Lehman, S. J., Fifield, L. K., & De Deckker, P. (2007). Absence of cooling in New Zealand and the adjacent ocean during the Younger Dryas chronozone. *Science, 318*(5847), 86-89.

Beer, J., Lee, K., Whiticar, M., & Blodau, C. (2008). Geochemical controls on anaerobic organic matter decomposition in a northern peatland. *Limnology and Oceanography, 53*(4), 1393-1407.

Belli, R., Borsato, A., Frisia, S., Drysdale, R., Maas, R., & Greig, A. (2017). Investigating the hydrological significance of stalagmite geochemistry (Mg, Sr) using Sr isotope and particulate element records across the Late Glacial-to-Holocene transition. *Geochimica et Cosmochimica Acta, 199*, 247-263.

Bernal, J., Cruz, F. W., Stríkis, N. M., Wang, X., Deininger, M., Catunda, M. C. A., Ortega-Obregón, C., Cheng, H., Edwards, R. L., & Auler, A. S. (2016). High-resolution Holocene South American monsoon history recorded by a speleothem from Botuverá Cave, Brazil. *Earth and Planetary Science Letters, 450*, 186-196.

Billett, M. F., Garnett, M. H., & Harvey, F. (2007). UK peatland streams release old carbon dioxide to the atmosphere and young dissolved organic carbon to rivers. *Geophysical Research Letters, 34*(23).

Blyth, A., Baker, A., Collins, M., Penkman, K., Gilmour, M., S. Moss, J., Genty, D., & Drysdale, R. (2008). Molecular organic matter in speleothems and its potential as an environmental proxy. *Quaternary Science Reviews, 27*(9-10), 905-921.

Blyth, A. J., Asrat, A., Baker, A., Gulliver, P., Leng, M. J., & Genty, D. (2007). A new approach to detecting vegetation and land-use change using high-resolution lipid biomarker records in stalagmites. *Quaternary Research, 68*(3), 314-324.

Blyth, A. J., Hartland, A., & Baker, A. (2016). Organic proxies in speleothems – New developments, advantages and limitations. *Quaternary Science Reviews, 149*, 1-17.

Blyth, A. J., Shutova, Y., & Smith, C. (2013). δ13C analysis of bulk organic matter in speleothems using liquid chromatography–isotope ratio mass spectrometry. *Organic Geochemistry, 55*, 22-25.

Blyth, A. J., Watson, J. S., Woodhead, J., & Hellstrom, J. (2010). Organic compounds preserved in a 2.9million year old stalagmite from the Nullarbor Plain, Australia. *Chemical Geology, 279*(3), 101-105.

Borsato, A., Frisia, S., Fairchild, I. J., Somogyi, A., & Susini, J. (2007). Trace element distribution in annual stalagmite laminae mapped by micrometer-resolution X-ray fluorescence: implications for incorporation of environmentally significant species. *Geochimica et Cosmochimica Acta, 71*(6), 1494-1512.

Bradford, M. A., Wieder, W. R., Bonan, G. B., Fierer, N., Raymond, P. A., & Crowther, T. W. (2016). Managing uncertainty in soil carbon feedbacks to climate change. *Nature Climate Change, 6*(8), 751.

Bro, R. (1997). PARAFAC. Tutorial and applications. *Chemometrics and Intelligent Laboratory Systems, 38*(2), 149-171.

Buffle, J., Wilkinson, K. J., Stoll, S., Filella, M., & Zhang, J. (1998). A Generalized Description of Aquatic Colloidal Interactions: The Three-colloidal Component Approach. *Environmental Science & Technology, 32*(19), 2887-2899.

Caldwell, J., Davey, A., Jennings, G., & Spate, A. (1982). Colour in some Nullarbor Plain speleothems. *Helictite, 20*(1), 3-10.

Chalmin, E., Perrette, Y., Fanget, B., & Susini, J. (2013). Investigation of organic matter entrapped in synthetic carbonates—A multimethod approach. *Microscopy and Microanalysis, 19*(1), 132-144.

Chantigny, M. H. (2003). Dissolved and water-extractable organic matter in soils: a review on the influence of land use and management practices. *Geoderma, 113*(3), 357-380.

Chen, J., Gu, B., LeBoeuf, E. J., Pan, H., & Dai, S. (2002). Spectroscopic characterization of the structural and functional properties of natural organic matter fractions. *Chemosphere, 48*(1), 59-68.

Chen, W., Westerhoff, P., Leenheer, J. A., & Booksh, K. (2003). Fluorescence Excitation−Emission Matrix Regional Integration to Quantify Spectra for Dissolved Organic Matter. *Environmental Science & Technology, 37*(24), 5701-5710.

Coble, P. G. (1996). Characterization of marine and terrestrial DOM in seawater using excitation-emission matrix spectroscopy. *Marine Chemistry, 51*(4), 325-346.

Coble, P. G., Green, S. A., Blough, N. V., & Gagosian, R. B. (1990). Characterization of dissolved organic matter in the Black Sea by fluorescence spectroscopy. *Nature, 348*, 432.

Cole, J. J., Prairie, Y. T., Caraco, N. F., McDowell, W. H., Tranvik, L. J., Striegl, R. G., Duarte, C. M., Kortelainen, P., Downing, J. A., Middelburg, J. J., & Melack, J. (2007). Plumbing the global carbon cycle: Integrating inland waters into the terrestrial carbon budget. *Ecosystems, 10*(1), 172-185.

Cory, R. M., & McKnight, D. M. (2005). Fluorescence spectroscopy reveals ubiquitous presence of oxidized and reduced quinones in dissolved organic matter. *Environmental Science & Technology, 39*(21), 8142-8149.

Davidson, E. A., Trumbore, S. E., & Amundson, R. (2000). Soil warming and organic carbon content. *Nature, 408*, 789.

Dean, W. E., & Gorham, E. (1998). Magnitude and significance of carbon burial in lakes, reservoirs, and peatlands. *Geology, 26*(6), 535-538.

Diehl, A. C., Speitel Jr, G. E., Symons, J. M., Krasner, S. W., Hwang, C. J., & Barrett, S. E. (2000). DBP formation during chloramination. *Journal-American Water Works Association, 92*(6), 76-90.

Doughty, A. M., Mackintosh, A. N., Anderson, B. M., Dadic, R., Putnam, A. E., Barrell, D. J., Denton, G. H., Chinn, T. J., & Schaefer, J. M. (2017). An exercise in glacier length modeling: Interannual climatic variability alone cannot explain Holocene glacier fluctuations in New Zealand. *Earth and Planetary Science Letters, 470*, 48-53.

EPICA_Community_Members, Augustin, L., Barbante, C., Barnes, P. R., Barnola, J. M., Bigler, M., Castellano, E., Cattani, O., Chappellaz, J., Dahl-Jensen, D., & Delmonte, B. (2004). Eight glacial cycles from an Antarctic ice core. *Nature, 429*, 623-628.

Evans, C. D., Freeman, C., Cork, L. G., Thomas, D. N., Reynolds, B., Billett, M. F., Garnett, M. H., & Norris, D. (2007). Evidence against recent climate-induced destabilisation of soil carbon from 14C analysis of riverine dissolved organic matter. *Geophysical Research Letters, 34*(7).

Evans, C. D., Monteith, D. T., & Cooper, D. M. (2005). Long-term increases in surface water dissolved organic carbon: Observations, possible causes and environmental impacts. *Environmental Pollution, 137*(1), 55-71.

Fairchild, I. J., & Baker, A. (2012). *Speleothem science: from process to past environments*. (Vol. 3). John Wiley & Sons.

Fairchild, I. J., Borsato, A., Tooth, A. F., Frisia, S., Hawkesworth, C. J., Huang, Y., McDermott, F., & Spiro, B. (2000). Controls on trace element (Sr–Mg) compositions of carbonate cave waters: implications for speleothem climatic records. *Chemical Geology, 166*(3-4), 255-269.

Fairchild, I. J., Smith, C. L., Baker, A., Fuller, L., Spötl, C., Mattey, D., & McDermott, F. (2006). Modification and preservation of environmental signals in speleothems. *Earth-Science Reviews, 75*(1-4), 105-153.

Fairchild, I. J., & Treble, P. C. (2009). Trace elements in speleothems as recorders of environmental change. *Quaternary Science Reviews, 28*(5-6), 449-468.

Falini, G., Fermani, S., Tosi, G., & Dinelli, E. (2009). Calcium Carbonate Morphology and Structure in the Presence of Seawater Ions and Humic Acids. *Crystal Growth & Design, 9*(5), 2065-2072.

Fee, E., Hecky, R., Kasian, S., & Cruikshank, D. (1996). Effects of lake size, water clarity, and climatic variability on mixing depths in Canadian Shield lakes. *Limnology and Oceanography, 41*(5), 912-920.

Fellman, J. B., Hood, E., & Spencer, R. G. M. (2010). Fluorescence spectroscopy opens new windows into dissolved organic matter dynamics in freshwater ecosystems: A review. *Limnology and Oceanography, 55*(6), 2452-2462.

Fenner, N., Freeman, C., & Reynolds, B. (2005). Observations of a seasonally shifting thermal optimum in peatland carbon-cycling processes; implications for the global carbon cycle and soil enzyme methodologies. *Soil Biology and Biochemistry, 37*(10), 1814-1821.

Festi, D., Hoffmann, D. L., & Luetscher, M. (2016). Pollen from accurately dated speleothems supports alpine glacier low-stands during the early Holocene. *Quaternary Research, 86*(1), 45-53.

Filella, M., & Rodríguez-Murillo, J. C. (2014). Long-term trends of organic carbon concentrations in freshwaters: Strengths and weaknesses of existing evidence. *Water, 6*(5), 1360-1418.

Fleitmann, D., Treble, P., Cruz Jr, F., Cole, J., & Cobb, K. (2008). White paper on Speleothem-based climate proxy records. *Paleoclimate Uncertainties Workshop Report*. http://ftp.pages-osm.org/download/docs/meeting-products/other/2008-trieste-ws-whitepaper-speleothems.pdf

Forbes, B. C., Fauria, M. M., & Zetterberg, P. (2010). Russian Arctic warming and 'greening' are closely tracked by tundra shrub willows. *Global Change Biology, 16*(5), 1542-1554.

Freeman, C., Fenner, N., Ostle, N., Kang, H., Dowrick, D., Reynolds, B., Lock, M., Sleep, D., Hughes, S., & Hudson, J. (2004). Export of dissolved organic carbon from peatlands under elevated carbon dioxide levels. *Nature, 430*(6996), 195.

Friedlingstein, P., Meinshausen, M., Arora, V. K., Jones, C. D., Anav, A., Liddicoat, S. K., & Knutti, R. (2013). Uncertainties in CMIP5 climate projections due to carbon cycle feedbacks. *Journal of Climate, 27*(2), 511-526.

Frisia, S., Borsato, A., Fairchild, I. J., & McDermott, F. (2000). Calcite fabrics, growth mechanisms, and environments of formation in speleothems from the Italian Alps and southwestern Ireland. *Journal of Sedimentary Research, 70*(5), 1183-1196.

Frisia, S., Borsato, A., Fairchild, I. J., & Susini, J. (2005). Variations in atmospheric sulphate recorded in stalagmites by synchrotron micro-XRF and XANES analyses. *Earth and Planetary Science Letters, 235*(3-4), 729-740.

Frisia, S., Borsato, A., & Hellstrom, J. (2018). High spatial resolution investigation of nucleation, growth and early diagenesis in speleothems as exemplar for sedimentary carbonates. *Earth-Science Reviews, 178*, 68-91.

Fritz, S. C. (2008). Deciphering climatic history from lake sediments. *Journal of Paleolimnology*, *39*(1), 5-16.

Genty, D., & Massault, M. (1999). Carbon transfer dynamics from bomb-14C and δ13C time series of a laminated stalagmite from SW France—modelling and comparison with other stalagmite records. *Geochimica et Cosmochimica Acta*, *63*(10), 1537-1548.

Geyh, M. A., & Thiedig, F. (2008). The Middle Pleistocene Al Mahrúqah Formation in the Murzuq Basin, northern Sahara, Libya evidence for orbitally-forced humid episodes during the last 500,000 years. *Palaeogeography, Palaeoclimatology, Palaeoecology*, *257*(1-2), 1-21.

Gruzensky, P. (1967). Growth of calcite crystals. *Crystal Growth*, 365-367.

Gudasz, C., Bastviken, D., Steger, K., Premke, K., Sobek, S., & Tranvik, L. J. (2010). Temperature-controlled organic carbon mineralization in lake sediments. *Nature*, *466*, 478.

Gunn, J. (2004). *Encyclopedia of caves and karst science*. Taylor & Francis.

Hartland, A. (2011). *Colloidal geochemistry of speleothem-forming groundwaters*. PhD thesis, University of Birmingham, U.K..

Hartland, A., Baker, A., Timms, W., Shutova, Y., & Yu, D. (2012a). Measuring dissolved organic carbon δ 13 C in freshwaters using total organic carbon cavity ring-down spectroscopy (TOC-CRDS). *Environmental Chemistry Letters*, *10*(3), 309-315.

Hartland, A., Fairchild, I. J., Lead, J. R., Borsato, A., Baker, A., Frisia, S., & Baalousha, M. (2012b). From soil to cave: transport of trace metals by natural organic matter in karst dripwaters. *Chemical Geology*, *304*, 68-82.

Hartland, A., Fairchild, I. J., Lead, J. R., Zhang, H., & Baalousha, M. (2011). Size, speciation and lability of NOM–metal complexes in hyperalkaline cave dripwater. *Geochimica et Cosmochimica Acta*, *75*(23), 7533-7551.

Hartland, A., & Zitoun, R. (2018). Transition metal availability to speleothems controlled by organic binding ligands. *Geochemical Perspectives Letters*, *8*, 22–25

Heidke, I., Scholz, D., & Hoffmann, T. (2018). Quantification of lignin oxidation products as vegetation biomarkers in speleothems and cave drip water. *Biogeosciences*, *15*(19), 5831-5845.

Hellstrom, J. (2003). Rapid and accurate U/Th dating using parallel ion-counting multi-collector ICP-MS. *Journal of Analytical Atomic Spectrometry*, *18*(11), 1346-1351.

Hellstrom, J. (2006). U–Th dating of speleothems with high initial 230Th using stratigraphical constraint. *Quaternary Geochronology, 1*(4), 289-295.

Hellstrom, J., & McCulloch, M. (2000). Multi-proxy constraints on the climatic significance of trace element records from a New Zealand speleothem. *Earth and Planetary Science Letters, 179*(2), 287-297.

Hellstrom, J., McCulloch, M., & Stone, J. (1998). A detailed 31,000-year record of climate and vegetation change, from the isotope geochemistry of two New Zealand speleothems. *Quaternary Research, 50*(2), 167-178.

Hendy, C., & Wilson, A. (1968). Palaeoclimatic data from speleothems. *Nature, 219*(5149), 48.

Hendy, C. H. (1971). The isotopic geochemistry of speleothems—I. The calculation of the effects of different modes of formation on the isotopic composition of speleothems and their applicability as palaeoclimatic indicators. *Geochimica et Cosmochimica Acta, 35*(8), 801-824.

Herbert, B. E. (1995). Characterization of dissolved and colloidal organic matter in soil solution: a review. *Carbon Forms and Functions in Forest Soils*, 63-88.

Hodgson, D. A., & Sime, L. C. (2010). Southern westerlies and CO2. *Nature Geoscience, 3*, 666.

Hoffmann, D. L., Spötl, C., & Mangini, A. (2009). Micromill and in situ laser ablation sampling techniques for high spatial resolution MC-ICPMS U-Th dating of carbonates. *Chemical Geology, 259*(3-4), 253-261.

Hudson, N., Baker, A., & Reynolds, D. (2007). Fluorescence analysis of dissolved organic matter in natural, waste and polluted waters—a review. *River Research and Applications, 23*(6), 631-649.

Jaffé, R., McKnight, D., Maie, N., Cory, R., McDowell, W. H., & Campbell, J. L. (2008). Spatial and temporal variations in DOM composition in ecosystems: The importance of long-term monitoring of optical properties. *Journal of Geophysical Research: Biogeosciences, 113*(G4), n/a-n/a.

Jamieson, R. A., Baldini, J. U., Frappier, A. B., & Müller, W. (2015). Volcanic ash fall events identified using principal component analysis of a high-resolution speleothem trace element dataset. *Earth and Planetary Science Letters, 426*, 36-45.

Jara, I. A., Newnham, R. M., Vandergoes, M. J., Foster, C. R., Lowe, D. J., Wilmshurst, J. M., Moreno, P. I., Renwick, J. A., & Homes, A. M. (2015). Pollen–climate reconstruction from northern South Island, New Zealand (41°S), reveals varying high- and low-latitude teleconnections over the last 16 000 years. *Journal of Quaternary Science, 30*(8), 817-829.

Johnson, K. R., Hu, C., Belshaw, N. S., & Henderson, G. M. (2006). Seasonal trace-element and stable-isotope variations in a Chinese speleothem: The potential for high-resolution paleomonsoon reconstruction. *Earth and Planetary Science Letters, 244*(1-2), 394-407.

Kaiser, K., Guggenberger, G., & Zech, W. (2001). Organically bound nutrients in dissolved organic matter fractions in seepage and pore water of weakly developed forest soils. *Acta Hydrochimica et Hydrobiologica, 28*(7), 411-419.

Kalbitz, K., Solinger, S., Park, J.-H., Michalzik, B., & Matzner, E. (2000). Controls on the dynamics of dissolved organic matter in soils: a review. *Soil Science, 165*(4), 277-304.

Kaplan, M. R., Schaefer, J. M., Denton, G. H., Barrell, D. J. A., Chinn, T. J. H., Putnam, A. E., Andersen, B. G., Finkel, R. C., Schwartz, R., & Doughty, A. M. (2010). Glacier retreat in New Zealand during the Younger Dryas stadial. *Nature, 467,* 194.

Kaplan, M. R., Schaefer, J. M., Denton, G. H., Doughty, A. M., Barrell, D. J., Chinn, T. J., Putnam, A. E., Andersen, B. G., Mackintosh, A., & Finkel, R. C. (2013). The anatomy of long-term warming since 15 ka in New Zealand based on net glacier snowline rise. *Geology, 41*(8), 887-890.

Karlsson, J., Byström, P., Ask, J., Ask, P., Persson, L., & Jansson, M. (2009). Light limitation of nutrient-poor lake ecosystems. *Nature, 460*(7254), 506.

Kelleher, B. P., & Simpson, A. J. (2006). Humic Substances in Soils: Are They Really Chemically Distinct? *Environmental Science & Technology, 40*(15), 4605-4611.

Kellerman, A. M., Dittmar, T., Kothawala, D. N., & Tranvik, L. J. (2014). Chemodiversity of dissolved organic matter in lakes driven by climate and hydrology. *Nature Communications, 5*(1), 3804.

Kidson, J. W. (2000). An analysis of New Zealand synoptic types and their use in defining weather regimes. *International Journal of Climatology, 20*(3), 299-316.

Kidson, J. W., & Renwick, J. A. (2002). Patterns of convection in the tropical Pacific and their influence on New Zealand weather. *International Journal of Climatology, 22*(2), 151-174.

King, M. (2003). *The Penguin history of New Zealand*. History of New Zealand. Auckland, N.Z.: Penguin.

Kirschbaum, M. U. (2000). Will changes in soil organic carbon act as a positive or negative feedback on global warming? *Biogeochemistry, 48*(1), 21-51.

Lal, R. (2004). Soil Carbon Sequestration Impacts on Global Climate Change and Food Security. *Science, 304*, 1623-1627.

Laudon, H., Westling, O., Löfgren, S., & Bishop, K. (2001). Modeling preindustrial ANC and pH during the spring flood in northern Sweden. *Biogeochemistry, 54*(2), 171-195.

Lauritzen, S.-E., & Lundberg, J. (1999). Speleothems and climate: a special issue of The Holocene. *The Holocene, 9*(6), 643-647.

Lead, J. R., & Wilkinson, K. J. (2006). Aquatic colloids and nanoparticles: current knowledge and future trends. *Environmental Chemistry, 3*(3), 159-171.

Lehmann, J., & Kleber, M. (2015). The contentious nature of soil organic matter. *Nature, 528*(7580), 60-68.

Li, X., Rapson, G. L., & Flenley, J. R. (2008). Holocene vegetational and climatic history, Sponge Swamp, Haast, south-western New Zealand. *Quaternary International, 184*(1), 129-138.

Liu, X., Colman, S. M., Brown, E. T., Minor, E. C., & Li, H. (2013). Estimation of carbonate, total organic carbon, and biogenic silica content by FTIR and XRF techniques in lacustrine sediments. *Journal of Paleolimnology, 50*(3), 387-398.

Lorrey, A., Williams, P., Salinger, J., Martin, T., Palmer, J., Fowler, A., Zhao, J.-x., & Neil, H. (2008). Speleothem stable isotope records interpreted within a multi-proxy framework and implications for New Zealand palaeoclimate reconstruction. *Quaternary International, 187*(1), 52-75.

Lowe, J. J., & Walker, M. J. (2014). *Reconstructing quaternary environments*. Routledge.

Marín-Spiotta, E., Gruley, K. E., Crawford, J., Atkinson, E. E., Miesel, J. R., Greene, S., Cardona-Correa, C., & Spencer, R. G. M. (2014). Paradigm shifts in soil organic matter research affect interpretations of aquatic carbon cycling: transcending disciplinary and ecosystem boundaries. *Biogeochemistry, 117*(2), 279-297.

Marschner, B., & Kalbitz, K. (2003). Controls of bioavailability and biodegradability of dissolved organic matter in soils. *Geoderma, 113*(3), 211-235.

Masson, V., Vimeux, F., Jouzel, J., Morgan, V., Delmotte, M., Ciais, P., Hammer, C., Johnsen, S., Lipenkov, V. Y., Mosley-Thompson, E., Petit, J.-R., Steig, E. J., Stievenard, M., & Vaikmae, R. (2000). Holocene Climate Variability in Antarctica Based on 11 Ice-Core Isotopic Records. *Quaternary Research, 54*(3), 348-358.

Mattey, D., Lowry, D., Duffet, J., Fisher, R., Hodge, E., & Frisia, S. (2008). A 53 year seasonally resolved oxygen and carbon isotope record from a modern Gibraltar speleothem: reconstructed drip water and relationship to local precipitation. *Earth and Planetary Science Letters, 269*(1-2), 80-95.

McDermott, F. (2004). Palaeo-climate reconstruction from stable isotope variations in speleothems: a review. *Quaternary Science Reviews, 23*(7), 901-918.

McGlone, M. S., Hall, G. M. J., & Wilmshurst, J. M. (2010). Seasonality in the early Holocene: Extending fossil-based estimates with a forest ecosystem process model. *The Holocene, 21*(4), 517-526.

McGlone, M. S., & Wilmshurst, J. M. (1999). A Holocene record of climate, vegetation change and peat bog development, east Otago, South Island, New Zealand. *Journal of Quaternary Science, 14*(3), 239-254.

McWethy, D. B., Whitlock, C., Wilmshurst, J. M., McGlone, M. S., Fromont, M., Li, X., Dieffenbacher-Krall, A., Hobbs, W. O., Fritz, S. C., & Cook, E. R. (2010). Rapid landscape transformation in South Island, New Zealand, following initial Polynesian settlement. *Proceedings of the National Academy of Sciences, 107*(50), 21343-21348.

McWethy, D. B., Wilmshurst, J. M., Whitlock, C., Wood, J. R., & McGlone, M. S. (2014). A high-resolution chronology of rapid forest transitions following Polynesian arrival in New Zealand. *PLoS One, 9*(11), e111328.

Mecozzi, M., Pietrantonio, E., Amici, M., & Romanelli, G. (2001). Determination of carbonate in marine solid samples by FTIR-ATR spectroscopy. *Analyst, 126*(2), 144-146.

Meyer-Jacob, C., Michelutti, N., Paterson, A. M., Monteith, D., Yang, H., Weckström, J., Smol, J. P., & Bindler, R. (2017). inferring past trends in lake water organic carbon concentrations in northern lakes using sediment spectroscopy. *Environmental Science & Technology*.

Meyer-Jacob, C., Tolu, J., Bigler, C., Yang, H., & Bindler, R. (2015). Early land use and centennial scale changes in lake-water organic carbon prior to contemporary monitoring. *Proceedings of the National Academy of Sciences, 112*(21), 6579-6584.

Meyer-Jacob, C., Vogel, H., Gebhardt, A., Wennrich, V., Melles, M., & Rosén, P. (2014). Biogeochemical variability during the past 3.6 million years recorded by FTIR spectroscopy in the sediment record of Lake El'gygytgyn, Far East Russian Arctic. *Climate of the Past, 10*(1), 209-220.

Mopper, K., Feng, Z., Bentjen, S. B., & Chen, R. F. (1996). Effects of cross-flow filtration on the absorption and fluorescence properties of seawater. *Marine Chemistry, 55*(1-2), 53-74.

Nagra, G., Treble, P. C., Andersen, M. S., Bajo, P., Hellstrom, J., & Baker, A. (2017). Dating stalagmites in Mediterranean climates using annual trace element cycles. *Scientific Reports, 7*(1), 621-621.

Newnham, R. M., & Lowe, D. J. (2000). Fine-resolution pollen record of late-glacial climate reversal from New Zealand. *Geology, 28*(8), 759-762.

Nielsen, M. H., Aloni, S., & De Yoreo, J. J. (2014). In situ TEM imaging of $CaCO_3$ nucleation reveals coexistence of direct and indirect pathways. *Science, 345*(6201), 1158-1162.

Niemeyer, J., Chen, Y., & Bollag, J.-M. (1992). Characterization of humic acids, composts, and peat by diffuse reflectance Fourier-transform infrared spectroscopy. *Soil Science Society of America Journal, 56*(1), 135-140.

NIWA - National Institute of Water and Atmospheric Research. (2016). *Overview of New Zealand's Climate*. Retrieved January, 2019, from https://niwa.co.nz/education-and-training/schools/resources/climate/overview.

Pahnke, K., & Sachs, J. P. (2006). Sea surface temperatures of southern midlatitudes 0–160 kyr BP. *Paleoceanography, 21*(2), PA2003.

Paquette, J., & Reeder, R. J. (1995). Relationship between surface structure, growth mechanism, and trace element incorporation in calcite. *Geochimica et Cosmochimica Acta, 59*(4), 735-749.

Pastor, J., Solin, J., Bridgham, S. D., Updegraff, K., Harth, C., Weishampel, P., & Dewey, B. (2003). Global warming and the export of dissolved organic carbon from boreal peatlands. *Oikos, 100*(2), 380-386.

Pedro, J. B., Bostock, H. C., Bitz, C. M., He, F., Vandergoes, M. J., Steig, E. J., Chase, B. M., Krause, C. E., Rasmussen, S. O., Markle, B. R., & Cortese, G. (2015). The spatial extent and dynamics of the Antarctic Cold Reversal. *Nature Geoscience, 9*, 51-55.

Putnam, A. E., Denton, G. H., Schaefer, J. M., Barrell, D. J. A., Andersen, B. G., Finkel, R. C., Schwartz, R., Doughty, A. M., Kaplan, M. R., & Schlüchter, C. (2010). Glacier advance in southern middle-latitudes during the Antarctic Cold Reversal. *Nature Geoscience, 3*, 700.

Putnam, A. E., Schaefer, J. M., Denton, G. H., Barrell, D. J. A., Finkel, R. C., Andersen, B. G., Schwartz, R., Chinn, T. J. H., & Doughty, A. M. (2012). Regional climate control of glaciers in New Zealand and Europe during the pre-industrial Holocene. *Nature Geoscience, 5*, 627-630.

Rae, R., Howard-Williams, C., Hawes, I., Schwarz, A.-M., & Vincent, W. F. (2001). Penetration of solar ultraviolet radiation into New Zealand lakes: Influence of dissolved organic carbon and catchment vegetation. *Limnology, 2*(2), 79-89.

Raftery, A. E., Zimmer, A., Frierson, D. M. W., Startz, R., & Liu, P. (2017). Less than 2 °C warming by 2100 unlikely. *Nature Climate Change, 7*, 637.

Ramseyer, K., Miano, T. M., D'orazio, V., Wildberger, A., Wagner, T., & Geister, J. (1997). Nature and origin of organic matter in carbonates from speleothems, marine cements and coral skeletons. *Organic Geochemistry, 26*(5-6), 361-378.

Raymond, P. A., Hartmann, J., Lauerwald, R., Sobek, S., McDonald, C., Hoover, M., Butman, D., Striegl, R., Mayorga, E., Humborg, C., Kortelainen, P., Durr, H., Meybeck, M., Ciais, P., & Guth, P. (2013). Global carbon dioxide emissions from inland waters. *Nature, 503*(7476), 355-359.

Regnier, P., Friedlingstein, P., Ciais, P., Mackenzie, F. T., Gruber, N., Janssens, I. A., Laruelle, G. G., Lauerwald, R., Luyssaert, S., & Andersson, A. J. (2013). Anthropogenic perturbation of the carbon fluxes from land to ocean. *Nature Geoscience, 6*(8), 597-607.

Rosén, P., & Persson, P. (2006). Fourier-transform Infrared Spectroscopy (FTIRS), a new method to infer past changes in tree-line position and TOC using lake sediment. *Journal of Paleolimnology, 35*(4), 913-923.

Rosén, P., Vogel, H., Cunningham, L., Hahn, A., Hausmann, S., Pienitz, R., Zolitschka, B., Wagner, B., & Persson, P. (2011). Universally applicable model for the quantitative determination of lake sediment composition using Fourier transform infrared spectroscopy. *Environmental Science & Technology, 45*(20), 8858-8865.

Rosén, P., Vogel, H., Cunningham, L., Reuss, N., Conley, D. J., & Persson, P. (2010). Fourier transform infrared spectroscopy, a new method for rapid determination of total organic and inorganic carbon and biogenic silica concentration in lake sediments. *Journal of Paleolimnology, 43*(2), 247-259.

Rutlidge, H., Andersen, M. S., Baker, A., Chinu, K. J., Cuthbert, M. O., Jex, C. N., Marjo, C. E., Markowska, M., & Rau, G. C. (2015). Organic characterisation of cave drip water by LC-OCD and fluorescence analysis. *Geochimica et Cosmochimica Acta, 166*, 15-28.

Rutlidge, H., Baker, A., Marjo, C. E., Andersen, M. S., Graham, P. W., Cuthbert, M. O., Rau, G. C., Roshan, H., Markowska, M., Mariethoz, G., & Jex, C. N. (2014). Dripwater organic matter and trace element geochemistry in a semi-arid karst environment: Implications for speleothem paleoclimatology. *Geochimica et Cosmochimica Acta, 135*, 217-230.

Schimel, D. S., House, J. I., Hibbard, K. A., Bousquet, P., Ciais, P., Peylin, P., Braswell, B. H., Apps, M. J., Baker, D., & Bondeau, A. (2001). Recent patterns and mechanisms of carbon exchange by terrestrial ecosystems. *Nature, 414*(6860), 169-172.

Schmidt, M. W. I., Torn, M. S., Abiven, S., Dittmar, T., Guggenberger, G., Janssens, I. A., Kleber, M., Kögel-Knabner, I., Lehmann, J., Manning, D. A. C., Nannipieri, P., Rasse, D. P., Weiner, S., & Trumbore, S. E. (2011). Persistence of soil organic matter as an ecosystem property. *Nature, 478*, 49-56.

Senesi, N. (1990). Molecular and quantitative aspects of the chemistry of fulvic acid and its interactions with metal ions and organic chemicals: Part II. The fluorescence spectroscopy approach. *Analytica Chimica Acta, 232*, 77-106.

Senesi, N., Miano, T., Provenzano, M., & Brunetti, G. (1989). Spectroscopic and compositional comparative characterization of IHSS reference and standard fulvic and humic acids of various origin. *Science of the Total Environment, 81*, 143-156.

Shevenell, A., Ingalls, A., Domack, E., & Kelly, C. (2011). Holocene Southern Ocean surface temperature variability west of the Antarctic Peninsula. *Nature, 470*(7333), 250-254.

Shutova, Y., Baker, A., Bridgeman, J., & Henderson, R. K. (2014). Spectroscopic characterisation of dissolved organic matter changes in drinking water treatment: From PARAFAC analysis to online monitoring wavelengths. *Water Research, 54*, 159-169.

Sinclair, D. J., Banner, J. L., Taylor, F. W., Partin, J., Jenson, J., Mylroie, J., Goddard, E., Quinn, T., Jocson, J., & Miklavič, B. (2012). Magnesium and

strontium systematics in tropical speleothems from the Western Pacific. *Chemical Geology, 294-295*, 1-17.

Smith, C. L., Fairchild, I. J., Spötl, C., Frisia, S., Borsato, A., Moreton, S. G., & Wynn, P. M. (2009). Chronology building using objective identification of annual signals in trace element profiles of stalagmites. *Quaternary Geochronology, 4*(1), 11-21.

Smith, K., Ball, T., Conen, F., Dobbie, K., Massheder, J., & Rey, A. (2003). Exchange of greenhouse gases between soil and atmosphere: interactions of soil physical factors and biological processes. *European Journal of Soil Science, 54*(4), 779-791.

Snelder, T. H., Larned, S. T., & McDowell, R. W. (2018). Anthropogenic increases of catchment nitrogen and phosphorus loads in New Zealand. *New Zealand Journal of Marine and. Freshwater Research., 52*(3), 336-361.

Sniderman, J., Hellstrom, J., Woodhead, J., Drysdale, R., Bajo, P., Archer, M., Hatcher, L. (2019). Vegetation and climate change in southwestern Australia during the Last Glacial Maximum. *Geophysical Research Letters, 46*, 1709-1720.

Sobek, S., Tranvik, L. J., Prairie, Y. T., Kortelainen, P., & Cole, J. J. (2007). Patterns and regulation of dissolved organic carbon: An analysis of 7,500 widely distributed lakes. *Limnology and Oceanography, 52*(3), 1208-1219.

Spötl, C., Fairchild, I. J., & Tooth, A. F. (2005). Cave air control on dripwater geochemistry, Obir Caves (Austria): Implications for speleothem deposition in dynamically ventilated caves. *Geochimica et Cosmochimica Acta, 69*(10), 2451-2468.

Stedmon, C. A., & Bro, R. (2008). Characterizing dissolved organic matter fluorescence with parallel factor analysis: a tutorial. *Limnology and Oceanography: Methods, 6*(11), 572-579.

Stedmon, C. A., Markager, S., & Bro, R. (2003). Tracing dissolved organic matter in aquatic environments using a new approach to fluorescence spectroscopy. *Marine Chemistry, 82*(3), 239-254.

Stephens, T., Atkin, D., Augustinus, P., Shane, P., Lorrey, A., Street-Perrott, A., Nilsson, A., & Snowball, I. (2012a). A late glacial Antarctic climate teleconnection and variable Holocene seasonality at Lake Pupuke, Auckland, New Zealand. *Journal of Paleolimnology, 48*(4), 785-800.

Stephens, T., Atkin, D., Cochran, U., Augustinus, P., Reid, M., Lorrey, A., Shane, P., & Street-Perrott, A. (2012b). A diatom-inferred record of reduced effective precipitation during the Last Glacial Coldest Phase (28.8–18.0 cal kyr BP) and increasing Holocene seasonality at Lake Pupuke, Auckland, New Zealand. *Journal of Paleolimnology, 48*(4), 801-817.

Stolpe, B., & Hassellöv, M. (2007). Changes in size distribution of fresh water nanoscale colloidal matter and associated elements on mixing with seawater. *Geochimica et Cosmochimica Acta, 71*(13), 3292-3301.

Thurman, E. (1985). Amount of organic carbon in natural waters. In *Organic geochemistry of natural waters* (pp. 7-65). Springer.

Tranvik, L. J., Downing, J. A., Cotner, J. B., Loiselle, S. A., Striegl, R. G., Ballatore, T. J., Dillon, P., Finlay, K., Fortino, K., Knoll, L. B., Kortelainen, P. L., Kutser, T., Larsen, S., Laurion, I., Leech, D. M., Leigh McCallister, S., McKnight, D. M., Melack, J. M., Overholt, E., Porter, J. A., Prairie, Y., Renwick, W. H., Roland, F., Sherman, B. S., Schindler, D. W., Sobek, S., Tremblay, A., Vanni, M. J., Verschoor, A. M., Von Wachenfeldt, E., & Weyhenmeyer, G. A. (2009). Lakes and reservoirs as regulators of carbon cycling and climate. *Limnology and Oceanography, 54*(6 PART 2), 2298-2314.

Trevisan, S., Francioso, O., Quaggiotti, S., & Nardi, S. (2010). Humic substances biological activity at the plant-soil interface: from environmental aspects to molecular factors. *Plant Signaling & Behavior, 5*(6), 635-643.

Vaks, A., Gutareva, O. S., Breitenbach, S. F., Avirmed, E., Mason, A. J., Thomas, A. L., Osinzev, A. V., Kononov, A. M., & Henderson, G. M. (2013). Speleothems reveal 500,000-year history of Siberian permafrost. *Science, 340*(6129), 183-186.

Van Beynen, P., Bourbonniere, R., Ford, D., & Schwarcz, H. (2001). Causes of colour and fluorescence in speleothems. *Chemical Geology, 175*(3-4), 319-341.

Vandergoes, M. J., Dieffenbacher-Krall, A. C., Newnham, R. M., Denton, G. H., & Blaauw, M. (2008). Cooling and changing seasonality in the Southern Alps, New Zealand during the Antarctic Cold Reversal. *Quaternary Science Reviews, 27*(5), 589-601.

Wang, Y.-J., Cheng, H., Edwards, R. L., An, Z., Wu, J., Shen, C.-C., & Dorale, J. A. (2001). A high-resolution absolute-dated late Pleistocene monsoon record from Hulu Cave, China. *Science, 294*(5550), 2345-2348.

Warken, S. F., Fohlmeister, J., Schröder-Ritzrau, A., Constantin, S., Spötl, C., Gerdes, A., Esper, J., Frank, N., Arps, J., & Terente, M. (2018). Reconstruction of late Holocene autumn/winter precipitation variability in SW Romania from a high-resolution speleothem trace element record. *Earth and Planetary Science Letters, 499*, 122-133.

Warnken, K. W., Davison, W., Zhang, H., Galceran, J., & Puy, J. (2007). In situ measurements of metal complex exchange kinetics in freshwater. *Environmental Science & Technology, 41*(9), 3179-3185.

Weber, M., Scholz, D., Schröder-Ritzrau, A., Deininger, M., Spötl, C., Lugli, F., Mertz-Kraus, R., Jochum, K. P., Fohlmeister, J., & Stumpf, C. F. (2018). Evidence of warm and humid interstadials in central Europe during early MIS 3 revealed by a multi-proxy speleothem record. *Quaternary Science Reviews, 200*, 276-286.

Welikala, D., Hucker, C., Hartland, A., Robinson, B. H., & Lehto, N. J. (2018). Trace metal mobilization by organic soil amendments: insights gained from

analyses of solid and solution phase complexation of cadmium, nickel and zinc. *Chemosphere, 199*, 684-693.

White, W. (1981). Reflectance spectra and colour in speleothems. *National Speleological Society Bulletin, 43*(1), 20-6.

Whittaker, T. E., Hendy, C. H., & Hellstrom, J. C. (2011). Abrupt millennial-scale changes in intensity of Southern Hemisphere westerly winds during marine isotope stages 2–4. *Geology, 39*(5), 455-458.

Wigley, T., & Brown, M. (1976). The physics of caves. *The Science of Speleology, 3*(3), 329-347.

Williams, P., Marshall, A., Ford, D., & Jenkinson, A. (1999). Palaeoclimatic interpretation of stable isotope data from Holocene speleothems of the Waitomo district, North Island, New Zealand. *The Holocene, 9*(6), 649-657.

Williams, P. W., King, D., Zhao, J.-X., & Collerson, K. (2005). Late Pleistocene to Holocene composite speleothem 18 O and 13 C chronologies from South Island, New Zealand—did a global Younger Dryas really exist? *Earth and Planetary Science Letters, 230*(3), 301-317.

Williamson, C. E., Morris, D. P., Pace, M. L., & Olson, O. G. (1999). Dissolved organic carbon and nutrients as regulators of lake ecosystems: resurrection of a more integrated paradigm. *Limnology and Oceanography, 44*(3part2), 795-803.

Wilmshurst, J. M., McGlone, M. S., Leathwick, J. R., & Newnham, R. M. (2007). A pre-deforestation pollen-climate calibration model for New Zealand and quantitative temperature reconstructions for the past 18 000 years BP. *Journal of Quaternary Science, 22*(5), 535-547.

Wilmshurst, J. M., Wiser, S. K., & Charman, D. J. (2003). Reconstructing Holocene water tables in New Zealand using testate amoebae: differential preservation of tests and implications for the use of transfer functions. *The Holocene, 13*(1), 61-72.

Wilmshurst, J. M., & Higham, T. F. G. (2004). Using rat-gnawed seeds to independently date the arrival of Pacific rats and humans in New Zealand. *The Holocene, 14*(6), 801-806.

Xie, S., Yi, Y., Huang, J., Hu, C., Cai, Y., Collins, M., Baker, A. (2003). Lipid distribution in a subtropical southern China stalagmite as a record of soil ecosystem response to paleoclimate change. *Quaternary Research*, 60, 340-347.

Yang, Y., He, Z., Wang, Y., Fan, J., Liang, Z., & Stoffella, P. J. (2013). Dissolved organic matter in relation to nutrients (N and P) and heavy metals in surface runoff water as affected by temporal variation and land uses – A case study from Indian River Area, south Florida, USA. *Agricultural Water Management, 118*, 38-49.

Yuan, D., Cheng, H., Edwards, R. L., Dykoski, C. A., Kelly, M. J., Zhang, M., Qing, J., Lin, Y., Wang, Y., & Wu, J. (2004). Timing, duration, and

transitions of the last interglacial Asian monsoon. *Science, 304*(5670), 575-578.

Zink, K. G., Vandergoes, M. J., Bauersachs, T., Newnham, R. M., Rees, A. B. H., & Schwark, L. (2016). A refined paleotemperature calibration for New Zealand limnic environments using differentiation of branched glycerol dialkyl glycerol tetraether (brGDGT) sources. *Journal of Quaternary Science, 31*(7), 823-835.

Zsolnay, A. (1996). Dissolved humus in soil waters. In *Humic substances in terrestrial ecosystems* (pp. 171-223). Elsevier.

# 3 Chapter 3

# Evaluating past lake water quality and carbon fluxes using sediment fluorescence

Andrew R. Pearson[a,*]; Adam Hartland[a]; Marcus J. Vandergoes[b]; Bethany R.S. Fox[c,a].

[a]Environmental Research Institute, School of Science, Faculty of Science and Engineering, University of Waikato, Hamilton, 3240, New Zealand.

[b]GNS Science, Lower Hutt, 5040, New Zealand.

[c]Department of Biological and Geographical Sciences, University of Huddersfield, Huddersfield, HD1 3DH, United Kingdom.

*apearson181@gmail.com

**Keywords:** Dissolved organic matter (DOM)**;** Fourier transform infrared (FTIRS), 3D Excitation emission matrices (EEMs), Fluorescence, Water quality, Eutrophication, Holocene, climate change

## 3.1 Abstract

Lake sediments retain information on past C fluxes and thus have the potential to illuminate the mechanisms of past terrestrial C cycling. However, lakes also contain an overprint of autochthonous DOM produced by within-lake primary production, which may limit their utility for reconstructing past soil C export trends. This study explores the use of 3D EEM fluorescence (excitation-emission spectroscopy) of water extractable dissolved organic matter (WEDOM) from lake sediments as a method for reconstructing both past soil export of DOM and past trophic status. Using contemporary lake sediments from ten New Zealand lakes with different characteristics, we demonstrate that this method provides a robust and inexpensive means to characterise the allochthonous and autochthonous components of lake organic matter.

A comparison of WEDOM fluorescence measurements and water-quality data from the water columns of ten lakes revealed positive correlations between protein-like fluorescence and nutrients/trophic level index, indicating that protein-like fluorescence in sedimentary WEDOM can be used as an indicator of trophic status. The same methods were also applied to a 13,770-year sedimentary record from Adelaide Tarn, northern South Island, New Zealand, a pristine, sub-alpine lake with a simple catchment. Protein-like fluorescence indicated a consistently microtrophic to oligotrophic status. Humic-like DOM fluxes in Adelaide Tarn responded to known climate shifts over the course of the Holocene, indicating a climatic control on soil C production and/or export. Our results indicate that WEDOM fluorescence can be used as a reliable indicator of past soil export of DOM as well as past trophic status.

## 3.2 Introduction

### 3.2.1 Increases in soil export of dissolved organic matter (DOM)

Dissolved organic matter (DOM) is a ubiquitous component of natural waters and constitutes the most dynamic component of the terrestrial carbon cycle. Lakes are active sites for storage, transport and transformation of DOM (Tranvik *et al.*, 2009), which constitutes the most common form of OM in most lakes (Tranvik *et al.*, 2018). The movement of carbon (including DOM) is described via an aquatic continuum, whereby carbon is laterally transported from upland soils to open sea, via lakes, rivers, streams and estuaries (Regnier *et al.*, 2013). During passage through the aquatic continuum, carbon can be 'filtered' (i.e. processed geochemically, exported to the atmosphere as $CO_2$ or $CH_4$ or stored within sediments). DOM is also a vital modulator of the structure and function of lake ecosystems (Sobek *et al.*, 2007), impacting light penetration (Ask *et al.*, 2009), thermal structure and the mixing depths of lakes (Fee *et al.*, 1996), and can serve as a substrate for heterotrophs (Tranvik, 1988).

Eutrophication of terrestrial water bodies has also become a major ecological issue over recent decades (Smith, 2003). In many parts of the world, nutrient loading associated with anthropogenic pollution exceeds natural nitrogen and phosphorus loads (Smith, 2003), and climate change is expected to amplify the risk of eutrophication in terrestrial waterbodies (O'Neil *et al.*, 2012; Charlton *et al.*, 2018).

Global temperatures are expected to increase by 2.0–4.9 °C by the year 2100 (Raftery *et al.*, 2017), thus, it is of key importance to assess the relationship between increased temperatures (and associated landscape response), DOM export and eutrophication. Despite the numerous monitoring studies of DOM concentrations in inland waters, the response of soil carbon stocks to long-term temperature shifts

remains unknown (Bradford *et al.*, 2008) and is difficult to establish. Clearly, palaeo-environmental research has a role to play in delivering a long-term perspective on the impact of temperature on DOM export.

### 3.2.2 New Zealand as a natural laboratory for baseline water quality and DOM inputs

New Zealand is a geographically isolated archipelago, located in the west Pacific Ocean in the southern mid-latitudes (~46.5 to 32.5 °S). New Zealand has undergone climate change through the Holocene, but its short human history (as the last major landmass to be colonised by humans) (13$^{th}$ century CE (McWethy *et al.*, 2010)), provides a unique opportunity to study the impacts of natural changes in the absence of human interference. New Zealand's natural 'reference state' has been regarded as prior to the onset of widespread land-use in the 18$^{th}$ century CE (Abell *et al.*, 2019). In recent decades, water quality has declined further, predominantly due to increased nutrient loads from agricultural intensification (Foote *et al.*, 2015).

In New Zealand, rivers have been estimated to export around twice the global average of DOM (4 ± 1 mg C km$^{-2}$ yr$^{-1}$, 1994–2006) (due to high levels of localised erosion, particularly in catchments predominantly used for pastoral agriculture), which is equivalent to approximately 40 % of New Zealand's fossil fuel emissions (Scott *et al.*, 2006). There is no existing programme that regularly monitors DOM concentrations in New Zealand's lakes, and as elsewhere, New Zealand's water quality monitoring programme is limited both spatially and temporally. New Zealand's lake monitoring programme only began in the 1990's (Verburg *et al.*, 2010), and although New Zealand has 3820 lakes greater than 1 ha. in surface area (Leathwick *et al.*, 2010) (representing 1.3 % of New Zealand's total land area), only 3 % of these lakes are monitored regularly (Verburg et al., 2010). In New Zealand, lake water quality is assessed by the trophic level index (TLI), which was

specifically developed for New Zealand lakes (Burns et al., 2000). TLI scores are calculated from log-transformed measurements of total nitrogen (TN), total phosphorus (TP) and chlorophyll a (Chl-a) and Secchi disc depth (SDD). In New Zealand, poor water quality (eutrophic or hypertrophic) is associated with higher temperatures and high percentages of pastoral land cover, whilst higher water quality (oligotrophic) is found in low-temperature alpine lakes with predominantly native land cover (Verburg *et al*., 2010). Climate change is expected to increase the vulnerability of lakes to eutrophication in New Zealand (Verburg *et al.*, 2010) and across the globe (Sinha *et al.*, 2017).

Determining the reference (i.e. pre-human) conditions of lakes can aid development of contemporary monitoring and management policies (Swetnam *et al.*, 1999). The European Commission recommends that analysis of historical data from sites prior to disturbance can be used (alongside other approaches, such as analysis of data in contemporary pristine sites) to establish natural reference conditions in lakes (European Commission, 2003). Quaternary scientists have developed quantitative and qualitative methods to reconstruct past lacustrine organic carbon fluxes (such as FTIRS-TOC) (Rosén *et al.*, 2010; Meyer-Jacob *et al.*, 2017) and water quality (diatoms and stable isotopes) (Kinder *et al.*, 2019; Makri *et al.*, 2019). Diatom counting has been widely used to reconstruct palaeo-water quality; however, this approach is time-consuming and can be limited by secondary variables such as alkalinity and lake depth (Juggins *et al.*, 2013).

### 3.2.3 Fluorescence as a method for characterising dissolved organic matter (DOM)

Lakes are an important sink for carbon exported from soils (Cole *et al.*, 2007), and the recalcitrance of this allochtonous OM typically enables efficient burial and preservation (von Wachenfeldt *et al.*, 2008). Once deposited on a lakebed, OM may

undergo numerous physical, chemical and biological changes, be re-mineralised, or stored and archived within the sediments under anaerobic/anoxic conditions (Cole *et al.*, 2007) (Figure 3.1). Sedimentary OM is derived from both autochthonous (produced within lakes by algae, macrophytes or bacteria) and allochthonous (terrigenous, usually from higher plants or soil) sources (Chen & Hur, 2015) (Figure 3.1). Autochthonous and allochthonous DOM have different molecular characteristics; for example, autochthonous DOM is lower in molecular weight and less aromatic than allochthonous DOM (McKnight *et al.*, 2001). A proportion of DOM is fluorescent (known as FDOM), i.e. it absorbs and emits light at characteristic wavelengths, meaning that different fractions (and therefore OM sources) can be distinguished and quantified. 3D excitation-emission matrices (3D EEMs), are a well-established method in environmental monitoring (Fellman *et al.*, 2010) but this method has generally been used to characterise DOM in the water column, rather than the sediments.

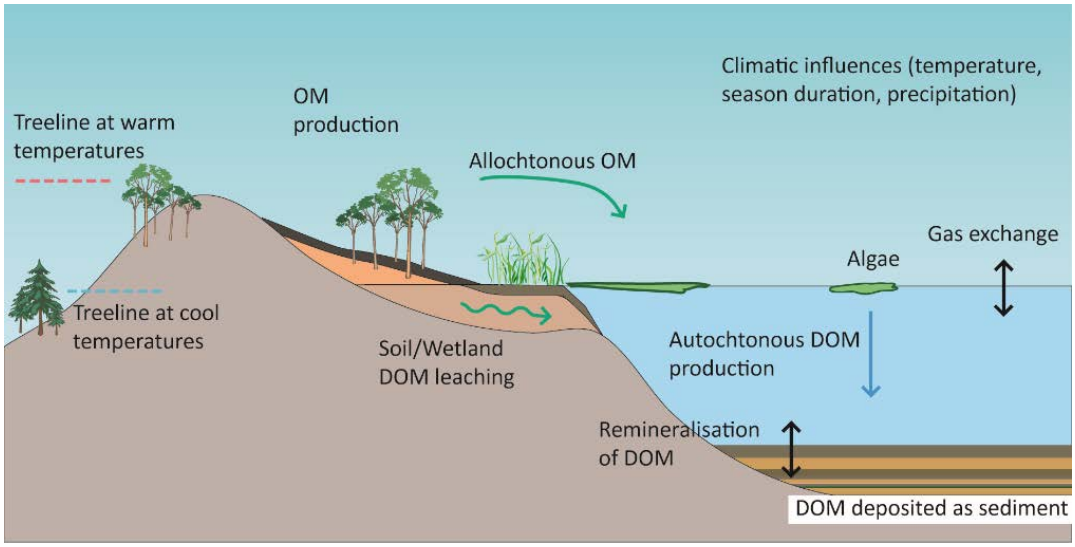


**Figure 3.1**-Conceptual lacustrine DOM deposition in a pristine alpine environment, such as Adelaide Tarn.

This study establishes a transfer function to relate fluorescence of sedimentary water extractable DOM (WEDOM) to water quality parameters from contemporary

monitoring data from 10 lakes in New Zealand. This transfer function is used to reconstruct trophic level index scores for Adelaide Tarn (a pristine, sub-alpine lake with a simple catchment) through the past 13,770 cal. years BP.

We also present a NZ-specific calibration for the determination of total organic carbon (TOC) by FTIRS (Fourier-transform infrared spectroscopy) using a large dataset (n= 141) of conventionally measured non-purgable organic carbon (NPOC) concentrations from modern sediments in 13 lakes. FTIRS has been successfully deployed in several previous studies to reconstruct past lacustrine TOC (Rosén *et al.*, 2010; Meyer-Jacob *et al.*, 2014) and was used in this reconstruction of environmental change at Adelaide Tarn.

## 3.3 Study sites and field methods

### 3.3.1 Modern lake sediment WEDOM training set

Sediments (from 4 cm depth or higher) were sampled from ten New Zealand lakes to build a fluorescence training dataset (Figure 3.2; Figure 3.A1). All lakes in the training set are monitored by LAWA (Land Air Water Aotearoa). These lakes cover a latitudinal gradient spanning approximately 7 ° and are characterised by varying climate, land-use regimes and trophic levels. A survey of New Zealand lake water quality (Verburg *et al.*, 2010) found that most New Zealand lakes are mesotrophic and that the highest water quality is found in alpine lakes in catchments with high native vegetation cover, whilst poor water quality (eutrophic) is associated with warmer lakes in catchments dominated by pastoral land use (Verburg *et al.*, 2010). To capture the widest possible trophic range, we have included lakes of each type in our training dataset.

Lakes Rotoiti, Rotorua, Rotoehu, Rotomahana, Taupo and Tarawera are in the Central Volcanic Plateau of the North Island (Figure 3.2). These lakes (most

notably Rotomahana) are of volcanic origin, and several are influenced by geothermal inflows (Mazot *et al.*, 2014). Anthropogenic activities (predominantly urbanisation and agriculture) also affect several of these lakes, especially Rotorua and Rotoehu. Lake Rotorua's catchment land use includes 39 % forest, 52 % pasture, and 8 % urban and the catchment also includes the city of Rotorua (Verburg *et al.*, 2014). The nearby catchments of Rotoehu, Rotoiti, Tarawera, Rotomahana and Taupo are mainly dominated by native vegetation (Verburg *et al.*, 2010). Lakes Aviemore and Benmore (oligotrophic lakes) are man-made reservoirs created in the 1960s in Canterbury, South Island and their catchment land-use is principally pastoral (Verburg *et al.*, 2010). Lake Benmore is upstream from Aviemore, and forms part of the Waitaki hydroelectric scheme. Lake Ohau is a microtrophic glacial lake, located in the South Island, which is fed by rivers with sources located on the Southern Alps mountain range. Lake Pearson's catchment is dominated by native vegetation, its trophic status varied between mesotrophic and oligotrophic in the years prior to sample collection (2011). Sediments from Aviemore, Benmore, Ohau and Pearson (South Island, New Zealand) were collected in the deepest part of each lake using a gravity corer in November 2011. Core samples from Lakes Rotorua and Rotoehu (North Island, New Zealand) were collected using a gravity corer in 2016. Sediments from Lake Okataina, Rotomahana, Tarawera and Taupo were collected using a gravity corer in multiple years between 2006 and 2011. All samples were freeze-dried and stored for subsequent analysis.

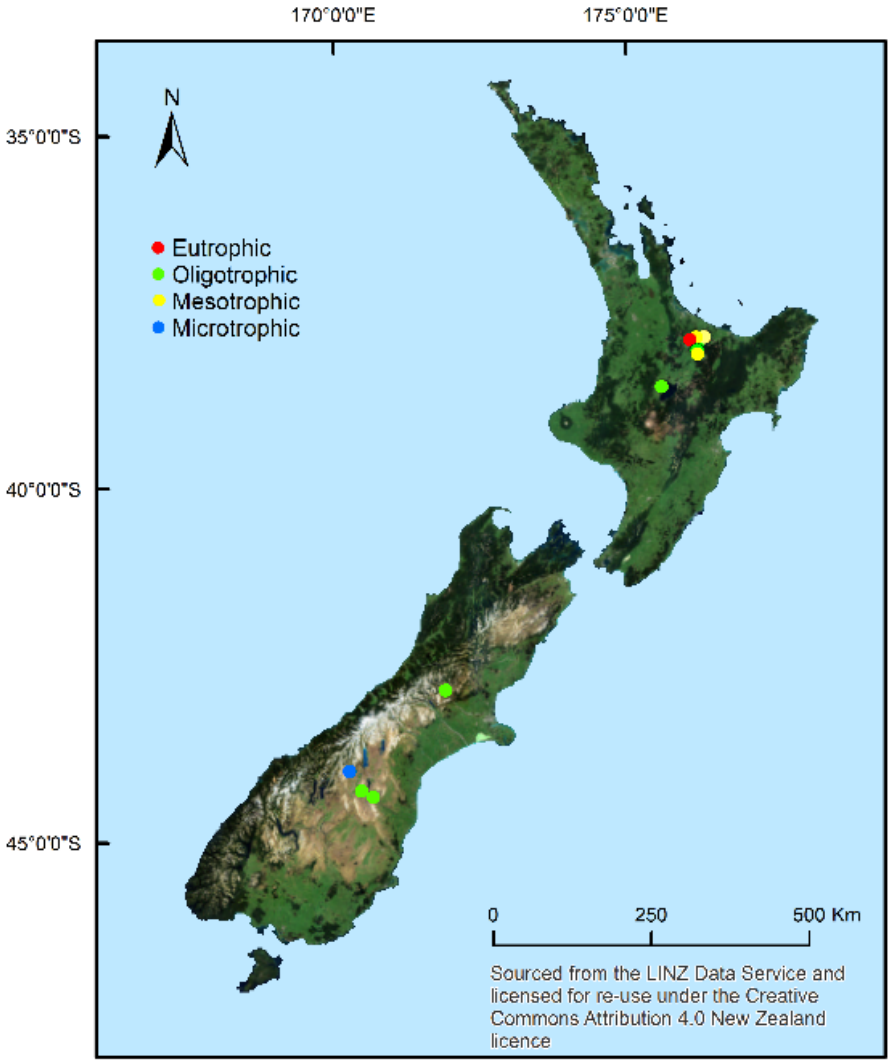


**Figure 3.2** Locations of training set lakes used to calibrate 3D EEM fluorescence signals against TLI monitoring data.

### 3.3.2 Adelaide Tarn's sedimentary archive and pristine catchment

Adelaide Tarn (Lat: -40.941; Long: 172.544) is a small (0.06 $km^2$, maximum depth 7.6 m) low-alpine lake (1250 m altitude) with one inlet and one outlet, located in the Douglas Range of the Tasman Mountains, NW Nelson Region, in the northwest of New Zealand's South Island (Figure 3.3 a, b) (Jara *et al.*, 2015). The lake is situated in a glacial cirque (3.8 $km^2$) with steep slopes and thin soil and was formed when permanent ice retreated from the catchment around ~16,100 cal. years BP (Jara *et al.*, 2015). Adelaide Tarn is currently located above the treeline (Figure 3.3

a). Nearby forest is dominated by mountain beech (*Fuscospora cliffortioides)* with low-shrub species including *Coprosma* and *Griselinia spp.* forming the sub-canopy. The low alpine ground cover is dominated by herbaceous flora including *Astelia*, *Uncinia*, *Apiaceae*, *Plantaginaceae*, and *Asteraceae spp*. Since ~1850 AD, grazing animals have altered the alpine vegetation of some parts of NW Nelson (Jara *et al.*, 2015), although it is unknown whether Adelaide Tarn's vegetation has been affected. Adelaide Tarn has an estimated mean annual temperature of 6.2 °C and annual precipitation of 2,500 mm (Leathwick *et al.*, 2010).

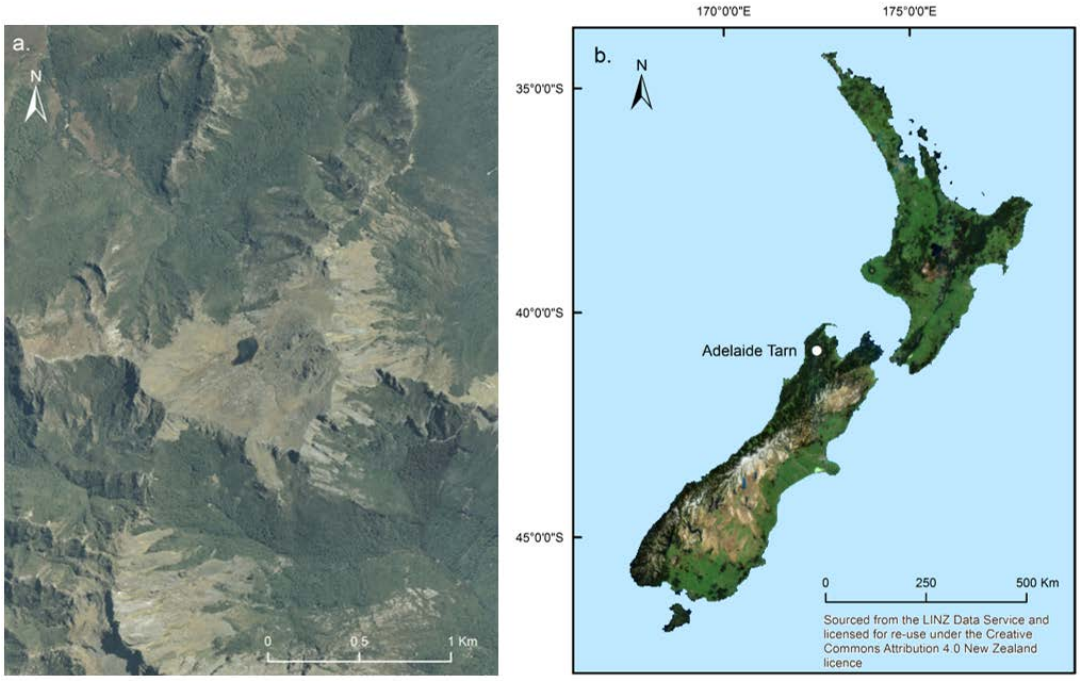


**Figure 3.3- (a.)** Aerial view of Adelaide Tarn within a glacial cirque, currently above the treeline within the Douglas Range in Kahurangi National Park, Nelson region. **(b.)** Location of Adelaide Tarn in the north west of New Zealand's South Island.

Two overlapping sediment cores (AT 1115 and AT 1116) were collected from an anchored platform using a 5 cm diameter square-rod piston corer (Wright, 1967) from the deepest part (7.6 m) of the tarn. Both cores consist of multiple overlapping 1 m length core sections. A gravity core was taken to collect the water-sediment interface. A single composite succession was constructed by cross correlating

common stratigraphic units (Jara *et al.*, 2015). The age model has been reported previously by Jara *et al.,* (2015) and is reproduced for convenience in Figure 3.A4. The sedimentary chronology was constructed from 16 accelerator mass spectrometer (AMS) radiocarbon dates and calibrated using the SH Cal13 dataset (Hogg *et al.,* 2013). There are no visible stratigraphic disturbances in the sedimentary sequence above a gravel layer deposited at 12,500 cal. years BP, and the age-depth model indicates that the sediment accumulation rate has been relatively stable up to present (Jara *et al.*, 2015), with a range of 0.1–1.1 mm $yr^{-1}$ and an average of 0.36 mm $yr^{-1}$.

## 3.4 Analytical methods

### 3.4.1 Monitoring data

Monitoring data were collected by respective regional councils and compiled by LAWA (Land Air Water Aotearoa (LAWA, 2014). The TLI score can be calculated via two different techniques, either as TLI3 or TLI4. TLI4 is calculated from log-transformed values of four variables: total phosphorous (TP), total nitrogen (TN), chlorophyll a (Chl-a) and Secchi disc depth (SDD) (a measure of water clarity), whilst TLI3 ignores SDD. TLI measurements in New Zealand differ from Carlson's Trophic State Index (Carlson, 1977), which excludes TN measurements. Each lake is assigned a TLI score between 1 and 7, where the lower the number, the higher the water quality. This study used the TLI3 method, as SDD data are not available for every lake in the training set. Total nitrogen (TN), total phosphorous (TP) and chlorophyll a (Chl-a) were measured for each lake. Secchi depth (as a proxy of water clarity) was not measured regularly, nor at every lake, and was therefore excluded from the analysis reported here.

To characterise each lake, mean TN, TP, Chl-a and TLI values for the three years prior to core extraction were calculated from the LAWA database for each lake. The number of measurements, the number of within lake sampling sites and the number of years of measurements used in this study are listed in the Appendix (Table 3.A1). Total nitrogen is the sum of all inorganic and organic forms ($NO_3$, $NO_2$, $NH_4$ and amino acids and plant tissues). Total phosphorus includes dissolved reactive phosphorus, orthophosphate and organic P bound to sediments. Chlorophyll a is measured to estimate the biomass of phytoplankton suspended in the water column. Our selected lakes cover a range of trophic statuses, catchment land-uses and formation processes. Nevertheless, our training set is somewhat biased towards oligotrophic lakes, primarily because we intended to relate these data to Adelaide Tarn, which was expected to be oligotrophic. No monitoring data for Adelaide Tarn existed prior to this study.

### 3.4.2 Water extraction of sedimentary organic matter

To build a link between past DOM concentrations and sedimentary OM recovered from lake sediments, a water extraction protocol was used to produce DOM (referred to as water extractable dissolved organic matter (WEDOM)) aliquots for fluorescence analysis. Sediment DOM was extracted using a water extraction method commonly used in soil analysis (Guigue *et al.*, 2014). 10 mg of freeze-dried, homogenised sediment was added to 7 mL of distilled-deionised (18 MΩ) water in a polypropylene tube and shaken vigorously for 60 minutes, before being centrifuged for 30 minutes at 3600 rpm. Traditionally, assessments of water extractable organic matter are limited to alkaline extractions from sediments (Corvasce *et al.*, 2006). However, Lehmann and Kleber (2015) suggested that analysis should focus on water-soluble (and therefore bioavailable) OM. For example, an alkaline treatment at pH 13 ionises compounds that would never

dissolve in the natural soil pH range (pH 3.5 to pH 8.5) (Lehmann & Kleber, 2015). Thus, extraction in pure water was considered the most representative measure of DOM.

Freeze-drying prior to WEDOM extraction for fluorescence analysis has rarely been reported in the literature and is known to alter pore structure and to cause stress to the microbial community within the sample (Zsolnay, 2003). However, the effect of freeze-drying on pore structure is less relevant in poorly- consolidated lake sediments and is more relevant for evaluating soil properties. Furthermore, air drying can obliterate ecologically interesting differences in DOM quality and quantity (Zsolnay, 2003). For this reason, freeze-drying was undertaken in sample preparation.

### 3.4.3 3D EEM fluorescence measurements of water extractable dissolved organic matter (WEDOM)

3D EEM fluorescence is a routine approach to assessing water quality in lakes and rivers (Baker *et al.*, 2004; Hudson *et al.*, 2007). The wavelengths at which fluorescence excitation and emission occurs allow the biochemical characteristics and sources of DOM to be distinguished (Fellman *et al.*, 2010). Following water extraction, supernatants were filtered through 0.45 μm cellulose acetate syringe filters (Microanalytix Pty Ltd, Australia). The extracts were then analysed using a Horiba Jobin Yvon Aqualog® fluorescence spectrometer with a 0.5 sec integration time, a step-size of 3 nm, and a measurement range of 240–600 nm excitation and 245–800 nm emission. To correct for instrument specific biases (Stedmon & Bro, 2008), each matrix was corrected for inner-filter effects, scatter lines were Rayleigh masked, and spectra were then Raman normalised to the mean Raman intensity of distilled de-ionised water.

### 3.4.4 PARAFAC (parallel factor analysis of components) of WEDOM fluorescence

Fluorescence data in this study were processed using parallel factor analysis (PARAFAC) using the N-way toolbox (Andersson & Bro, 2000), a multivariate modelling technique developed in MATLAB® 2013. PARAFAC provides multi-way analysis through which fluorescence signals can be distinguished and separated into statistically valid independent components. PARAFAC thus provides estimates of the relative contribution of each component to the total fluorescence signal and can quantify common fluorophores present in natural OM samples as statistical components (Fellman *et al.*, 2010). The model was validated using the drEEM toolbox (Stedmon & Bro, 2008).

### 3.4.5 FTIRS (Fourier Transform Infrared spectroscopy)

FTIRS spectra from NZ lake sediments (Figure 3.A2, Figure 3.A3, Table 3.A2) were related to conventionally measured TOC using a PLSR (partial least square regression) approach (Rosén *et al.*, 2011). Many FTIRS-TOC studies have established local/regional calibrations, and these can differ substantially depending on local variations in sediment character (Meyer-Jacob *et al.*, 2014). For TOC measurement, samples first underwent acid pre-treatment to remove carbonates, followed by catalytic combustion (900 °C, $O_2$) and separation, before analysis in a thermal conductivity detector [Elementar Analyser]. The same samples were also analysed via FTIR spectroscopy using a Perkin-Elmer Spectrum 100 spectrometer. Prior to analysis, samples were freeze-dried overnight, ground and homogenised using a pestle and mortar. Aliquots of 2 mg (± 2.5 %) of each sub-sample were extracted, mixed and homogenised with 1 g of oven-dried (100°C) KBr, before being compressed under 10,000 kg of pressure, to form translucent discs. Discs were kept dry in desiccators prior to analysis. After recording a blank (no disc in

the cell), the discs were measured under controlled conditions, with blank measurements taken every 15 measurements to avoid possible spectral drift due to changes in temperature, humidity or laser strength. The absorbance of infrared (IR) light with wavenumbers of 3750–400 $cm^{-1}$ was recorded through 64 scans per sample.

### 3.4.6 Total carbon and total nitrogen measurements of Adelaide Tarn sediment core

Total carbon (TC) and total nitrogen (TN) measurements from selected Adelaide Tarn sediment samples are used in this study for comparison and cross checking against the fluorescence and FTIR data. Ten subsamples were taken from depths covering the uppermost 417 cm (13,777 cal. years BP) in the Adelaide Tarn core. These subsamples were freeze-dried and analysed for TC % and TN % using an Elementar Isoprime 100 (Isoprime Ltd, Cheadle, UK).

## 3.5 Results and Discussion

### 3.5.1 Fourier transform infrared spectroscopy –total organic carbon calibration

Partial least squares regression (PLSR) modelling of FTIRS data vs conventionally measured TOC resulted in a 5-component model, characterised by an $R^2$ value of 0.88 (Figure 3.A2). Higher TOC values (>10 %) are less accurately estimated by this model due to the underrepresentation of this sample type in the FTIRS-TOC training set. The regression line has the equation y= 0.9375x + 0.3774. In subsequent discussion and presentation of results we have used this equation to calculate TOC concentrations from FTIRS measurements.

### 3.5.2 3D EEM fluorescence of WEDOM

Figure 3.4 shows that most of the lake sediments exhibit peak C, A, and T fluorescence peaks (Coble, 1996), and that the intensities of each peak vary considerably between lakes (Figure 3.4 a). Peaks C and A are commonly associated with humic-like fluorescence from allochthonous sources (higher plant matter and soil) (Fellman *et al.*, 2010). Peak T is 'protein-like' (representing free and bound amino acids), may be produced or altered by autochtonous bacterial/microbial activity, but is also an important component of sewage and wastewater (Baker & Inverarity, 2004). Protein-like DOM represents a bioavailable or labile fraction of freshwater DOM (Baker & Inverarity, 2004; Fellman *et al.*, 2010).

The relatively low humic-like fluorescence peak in Ohau, Aviemore and Benmore suggests a very low input of terrestrial organic matter in these lakes, which also have a low overall EEM fluorescence signal compared to the other lakes (Figure 3.4 b–4d). Meanwhile lakes such as Rotorua, Okataina, and Pearson show strong inputs of both humic-like and protein-like DOM, suggesting both allochthonous and autochthonous inputs of DOM to the sediments (Figure 3.4 e, f, j). The uppermost sediments of Adelaide Tarn are clearly dominated by peak A fluorescence, and this lake overall displays a similar level of fluorescence to the oligotrophic lakes in the training set, except for lake Aviemore (i.e. Okataina, Pearson, and Taupo; Figure 3.4 e, f, l).

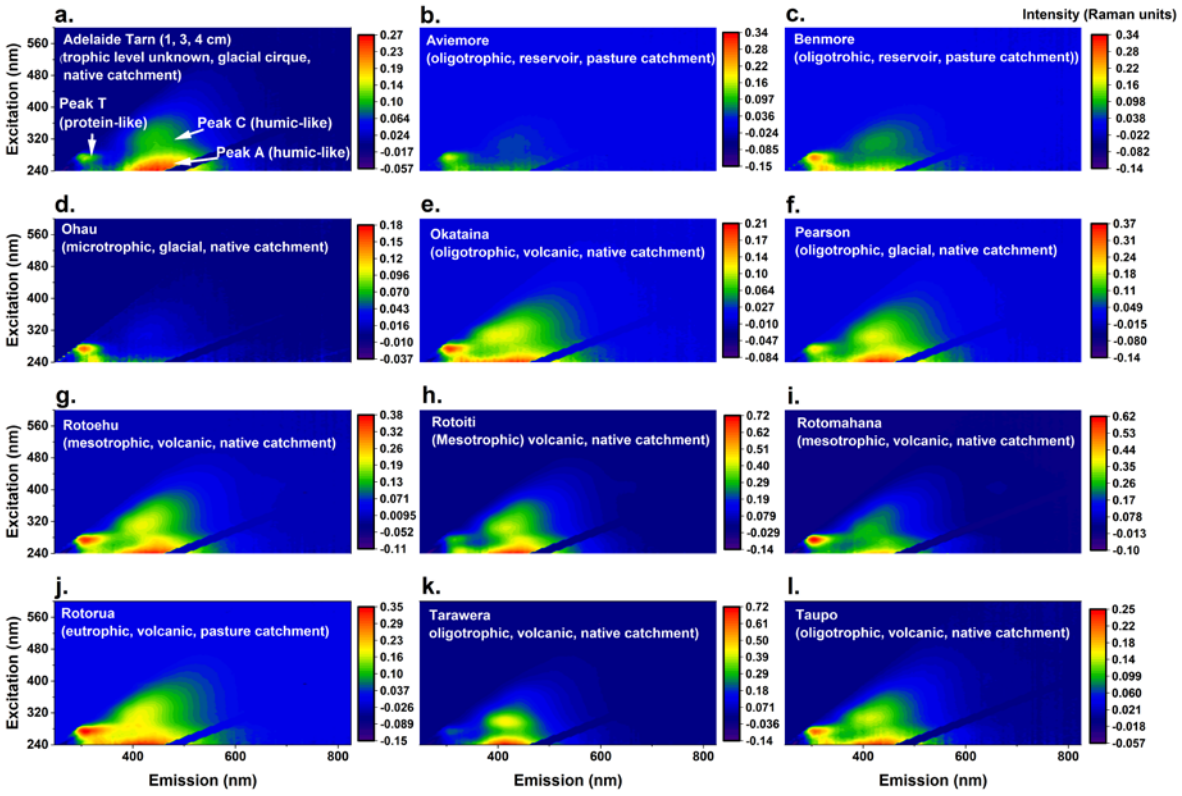


**Figure 3.4**- 3D EEM contour plots illustrate that FDOM characteristics and concentrations vary considerably across the dataset.

Figure 3.5 shows the first three components from a PARAFAC model that included all WEDOM samples (Adelaide Tarn and monitored training set lakes). Components 1 and 2 are both clearly humic-like. However, they are atypical in shape. There is a diverse range of fluorescence peak shapes at the different sites, explaining the generation of the atypical humic-like components. Given that the main focus of this study is the quantification of autochtonous vs allochtonous contributions in the lake carbon reservoir, and given that the physical meaning of the two humic-like peaks is not well understood, we henceforth consider humic-like components 1 and 2 together (described as “Total humic-like fluorescence”). If a two-component model was generated, then a protein-like peak was not produced. However, for the three-component model, the third component was clearly protein-like. This component spans a relatively wide range of emission

wavelengths. This may be due to the red shifting (exhibiting emission at long wavelengths) of this peak due to the variety of conjugated biomolecules found at different sites.

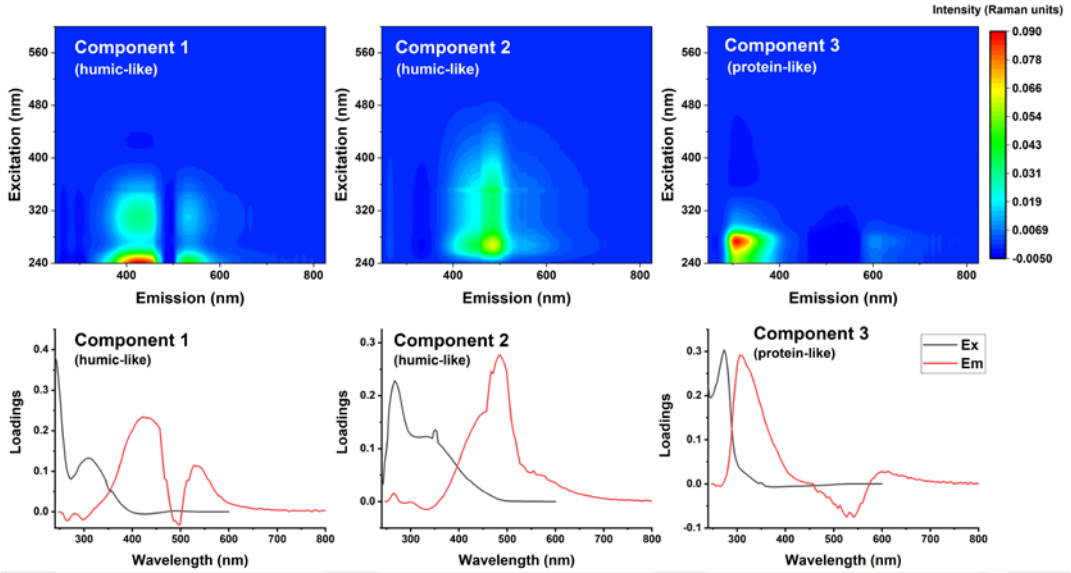


**Figure 3.5**- A three-component model combining Adelaide Tarn and New Zealand calibration data sets. Components 1 and 2 are atypical but clearly humic-like, whilst component 3 is a typical protein-like component.

### 3.5.3 Constructing a transfer function to predict trophic level from WEDOM fluorescence intensity

Figure 3.6 shows correlations between various measures of lake water quality, sedimentary FTIRS-TOC, and sedimentary WEDOM fluorescence. All fluorescence components are strongly positively correlated with each other and with FTIRS-TOC, indicating that increases in allochthonous input are not independent of increases in autochthonous production. This is to be expected; in fact, it is the export of soil organic matter (humic-like fluorescence) and dissolved nutrients to terrestrial water bodies that is assumed to be the cause of increases in trophic level and thus increased autochthonous productivity (protein-like fluorescence). Similarly, it is not surprising that all indicators of trophic level are positively correlated with the intensity of all fluorescence measurements. However,

of note here is that protein-like fluorescence (indicating autochthonous organic matter) is very strongly correlated with total nitrogen, total phosphorus and especially trophic level index, as well as strongly correlated with chlorophyll a (Figure 3.6). Conversely, humic-like fluorescence (indicating allochthonous organic matter) is significantly less correlated to indicators of trophic level. This indicates that the sedimentary protein-like fluorescence signal is indeed closely related to water-column productivity and lake trophic state (Figure 3.6).

Table 3.1 shows regression statistics for fluorescence components vs trophic level indicators. The relationship between humic-like fluorescence and Chl-a, TN and TP are not statistically significant at the $p < 0.05$ level. The relationship between humic-like fluorescence and TLI is statistically significant but explains a relatively low proportion of the variation. Protein-like fluorescence has a statistically significant relationship ($p < 0.05$) with all trophic level indicators, and particularly with TLI and TP, and a relatively high $R^2$ in all cases (again, especially TLI and TP). This indicates that TLI is the trophic level indicator that can be most usefully predicted by WEDOM fluorescence measurements. Although both humic-like and protein-like fluorescence have statistically significant relationships with TLI, these variables are highly collinear, and so we constructed our transfer function using protein-like fluorescence only. Regression values and statistics are reported in Table 3.2 and the regression is shown in Figure 3.7. Residuals passed the Shapiro-Wilk test (Shapiro & Wilk, 1965) for homoscedasticity with a p-value of 0.445.

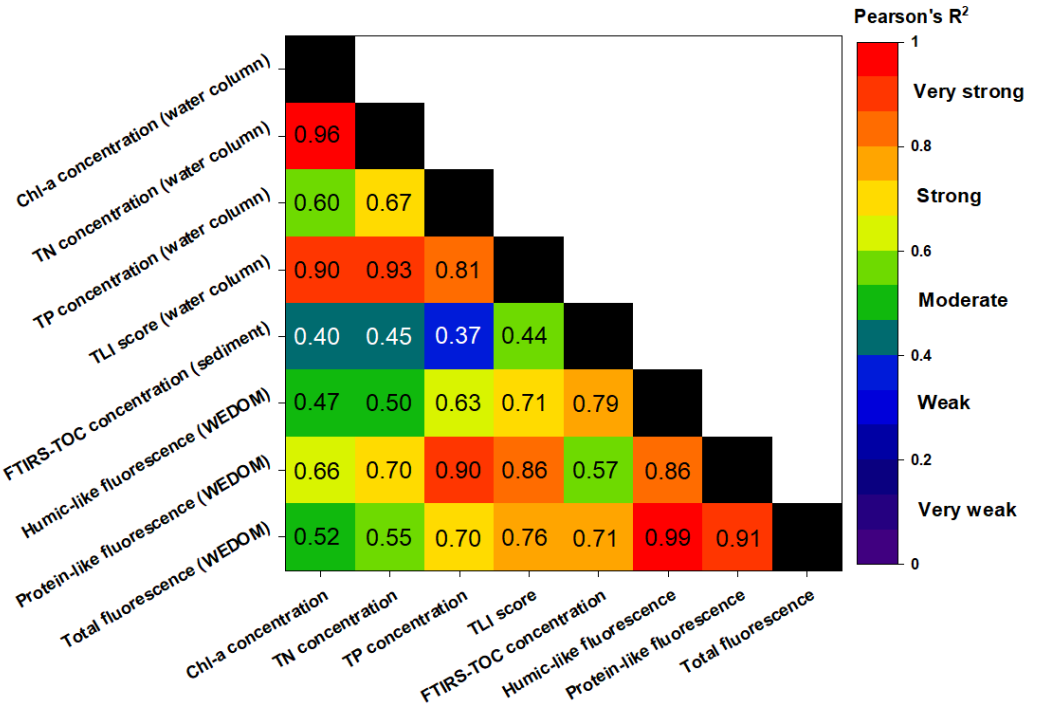


**Figure 3.6-** Pearson correlation matrix of averaged monitoring data from modern New Zealand lakes and fluorescence intensity for total humic-like fluorescence (C1 + C2), total protein-like fluorescence (C3) and total fluorescence (C1 + C2 + C3). Chl-a = chlorophyll a, TN = total nitrogen, TP = total phosphorous. Some results are white for clarity.

**Table 3.1**- Regression statistics for fluorescence components vs trophic level indicators.

| 3D EEM fluorescence components signal | Chl-a | | TN | | TP | | TLI | |
|---|---|---|---|---|---|---|---|---|
| | $R^2$ | p-value | $R^2$ | p-value | $R^2$ | p-value | $R^2$ | p-value |
| **Total humic-like** | 0.25 | 0.1209 | 0.25 | 0.1209 | 0.40 | 0.03829 | 0.50 | 0.01441 |
| **Protein-like** | 0.44 | 0.02734 | 0.50 | 0.01599 | 0.81 | 0.0001745 | 0.74 | 0.0007375 |

**Table 3.2**- Regression values and statistics for C3 (protein-like fluorescence component) coefficient used to reconstruct TLI scores in Adelaide Tarn.

| Intercept | C3 coefficient | $R^2$ | p-value |
|---|---|---|---|
| 1.2951 | 0.5423 | 0.74 | 0.0007375 |

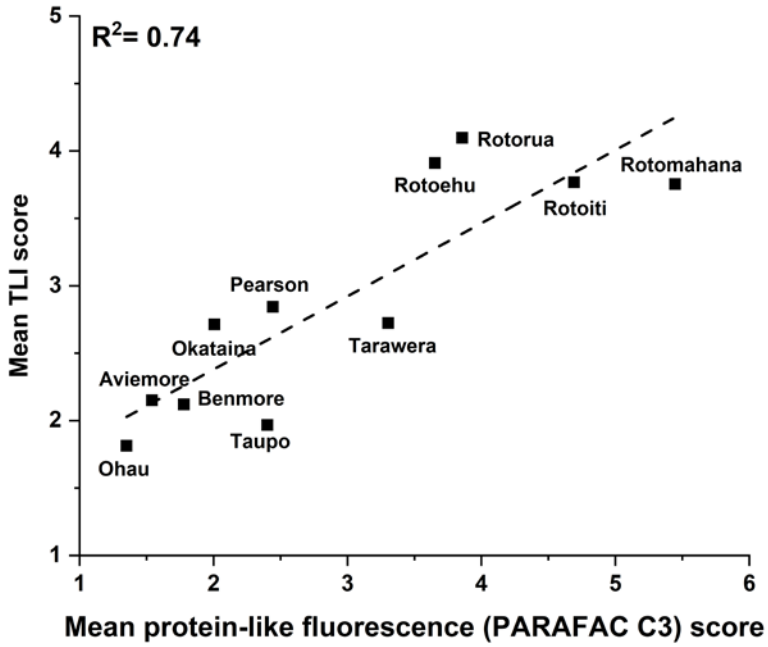


**Figure 3.7**- Regression of trophic-level index against protein-like fluorescence intensity for the 10 training-set New Zealand lakes. See Tables 3.1 and 3.2 for regression values and statistics.

### 3.5.4 Fluorescence and sedimentary organic matter in Adelaide Tarn

Table 3.3 gives the results of conventional and optical measurements of organic matter characteristics in the 10 subsamples from the Adelaide Tarn core. Figure 3.8 shows correlations between the conventional and optical measurements for these subsamples. As with the modern lakes, all fluorescence measures are correlated with measures of total carbon and total nitrogen (though it should be emphasised that the values reported here are of total *sedimentary* nitrogen, not of nitrogen in the water column). Again, this is not surprising, as allochthonous and autochthonous carbon inputs are not independent and would be expected to vary together. However, the proportions represented by the different components have a different relationship with sedimentary carbon and nitrogen. The proportion of humic-like components (allochthonous organic matter) is strongly positively correlated with sedimentary total carbon (TC) and sedimentary total nitrogen (TN) and weakly positively correlated with the sedimentary carbon-nitrogen ratio (C/N), while the

proportion of protein-like fluorescence naturally shows the exact opposite pattern. The correlations with TC and TN indicate that, although both types of organic matter contribute to increases in total carbon, the proportion of allochthonous organic matter increases with sedimentary carbon. This suggests that variability in organic matter in Adelaide Tarn was predominantly controlled by input from the catchment rather than changes in within-lake productivity. This is consistent with our observations of modern New Zealand lakes, where FTIRS-TOC is more strongly correlated with humic-like than protein-like fluorescence because humic-like allochtonous DOM typically constitutes the largest DOM fraction (Figure 3.8).

**Table 3.3**- Conventional measurements of sediment organic carbon and optical measurements of WEDOM from 10 subsamples from the Adelaide Tarn core.

| Depth (cm) | Age (Cal. years BP) | Sediment Total nitrogen (%) | Sediment Total carbon (%) | Sediment C:N ratio | Sediment FTIRS-inferred TOC (%) | WEDOM PARAFAC C1 score (humic-like) | WEDOM PARAFAC C2 score (humic-like) | WEDOM PARAFAC C3 score (protein-like) |
|---|---|---|---|---|---|---|---|---|
| **4** | **276** | 0.44 | 5.83 | 13.28 | 6.0 | 2.94 | 3.69 | 1.29 |
| **44** | **1,306** | 0.52 | 7.66 | 14.66 | 7.2 | 2.90 | 3.40 | 1.26 |
| **97** | **2,756** | 0.58 | 8.39 | 14.49 | 10.9 | 4.63 | 5.14 | 1.50 |
| **204** | **5,992** | 0.58 | 8.98 | 15.58 | 7.1 | 5.23 | 6.15 | 1.61 |
| **257** | **8,410** | 0.66 | 11.59 | 17.45 | 11.7 | 5.33 | 4.54 | 1.55 |
| **299** | **9,674** | 0.74 | 13.61 | 18.42 | 14.9 | 7.69 | 5.90 | 2.01 |
| **338** | **10,869** | 0.80 | 13.03 | 16.38 | 12.6 | 10.49 | 10.72 | 2.10 |
| **366** | **11,858** | 0.59 | 9.22 | 15.58 | 9.7 | 5.97 | 5.01 | 1.56 |
| **395** | **12,726** | 0.61 | 8.80 | 14.39 | 9.5 | 5.31 | 5.34 | 1.69 |
| **417** | **13,234** | 0.58 | 8.47 | 14.53 | 9.8 | 6.23 | 7.34 | 1.65 |

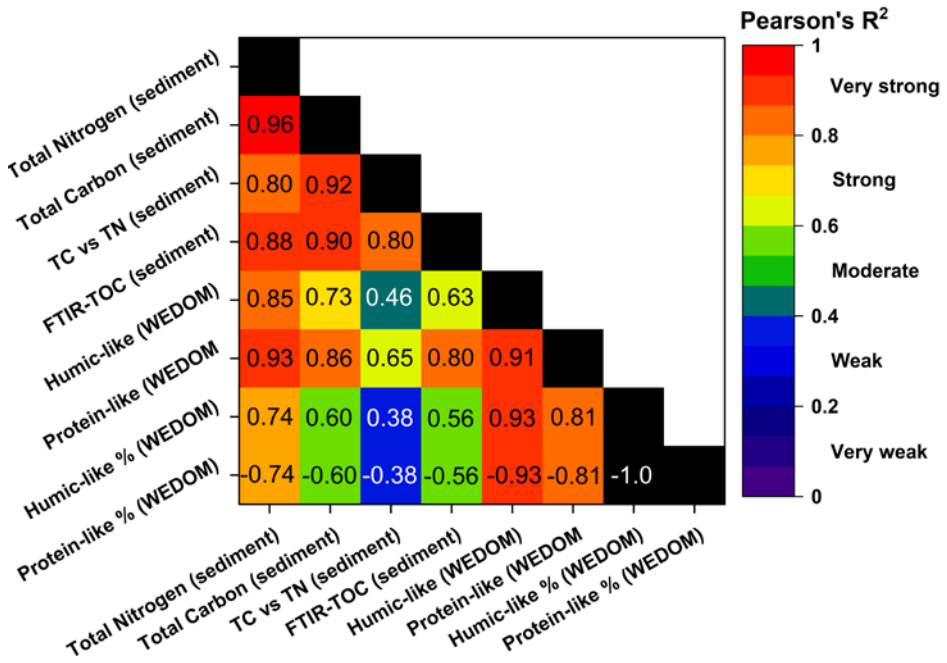


**Figure 3.8-** Pearson correlation matrix of conventional sediment measurements and optical WEDOM measurements from 10 Adelaide Tarn sediment sub-samples (Table 3.3). Some data are presented in white for clarity.

The pattern of correlation between fluorescence measurements and carbon-nitrogen ratio is important for validating our ability to apply modern interpretations of fluorescence intensity to ancient lake sediments. Fresh DOM from planktonic organisms has a C/N ratio of 6–9, whilst terrestrial plants show ratios greater than 15 (Meyers & Benson, 1988). We would therefore expect the proportion of protein-like fluorescence to be negatively correlated with C/N ratios, since the contributing fluorophores represent the optically active organic N fraction in sediments. Sobek *et al.*, (2009) argued that autochthonous material is predominantly mineralised rather than buried in sediments (Sobek *et al.*, 2009), nevertheless, the relationship between protein-like fluorescence and sedimentary TN suggests that protein-like fluorescence can be used as a reliable proxy for water quality at Adelaide Tarn. The fact that we observe this pattern in our Adelaide Tarn data indicates that our interpretation of the fluorescence measurements is consistent with other methods of analysing ancient lacustrine organic carbon.

Figure 3.9 a shows stable carbon and nitrogen isotope analyses of Adelaide Tarn organic matter, taken from Foster (2013). These values indicate that DOM in Adelaide Tarn is predominantly derived from terrestrial C3 plants (trees, shrubs, grasses) or emergent plants (aquatic or littoral plants). There are no data points that indicate high inputs from phytoplankton. These data are consistent with both the C/N ratios measured on the ten Adelaide Tarn subsamples (Table 3.3) and the fluorescence measurements, which indicate that DOM in Adelaide Tarn was consistently of predominantly (75–80 %) allochthonous origin (Figure 3.A5). Thus, our fluorescence measurements are consistent with stable isotope values in the Adelaide Tarn sediments.

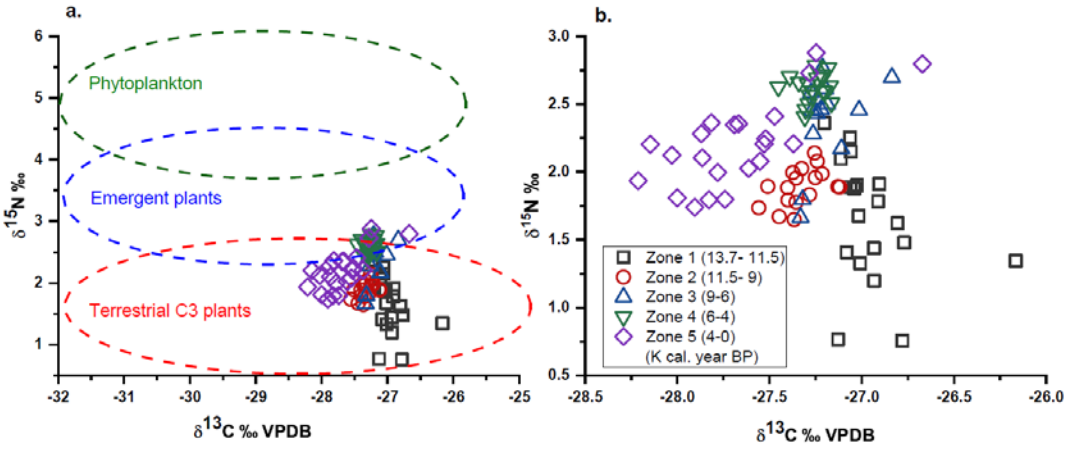


**Figure 3.9-** (a.) Adelaide Tarn $\delta^{13}C$ and $\delta^{15}N$ data organised by OM source based on the classifications of (Meyers & Lallier-vergés, 1999) and (Hamilton & Lewis, 1992) (note different axis scales for clarity). Stable isotope data has been published previously (Foster, 2013). (b.) $\delta^{13}C$ and $\delta^{15}N$ values appear to have varied depending on time-period of deposition.

Transfer functions were applied to the time-series of FTIRS and protein-like fluorescence in Adelaide Tarn to reconstruct TOC concentrations and TLI up to 13,770 cal. years BP. These reconstructed values and total humic-like fluorescence are shown in Figure 3.10, along with carbon and nitrogen stable isotope values (Foster, 2013), a pollen-based temperature proxy (Jara *et al.*, 2015), and a sea-surface temperature reconstruction from the Tasman Sea (Barrows *et al.*, 2007). These data are discussed below.

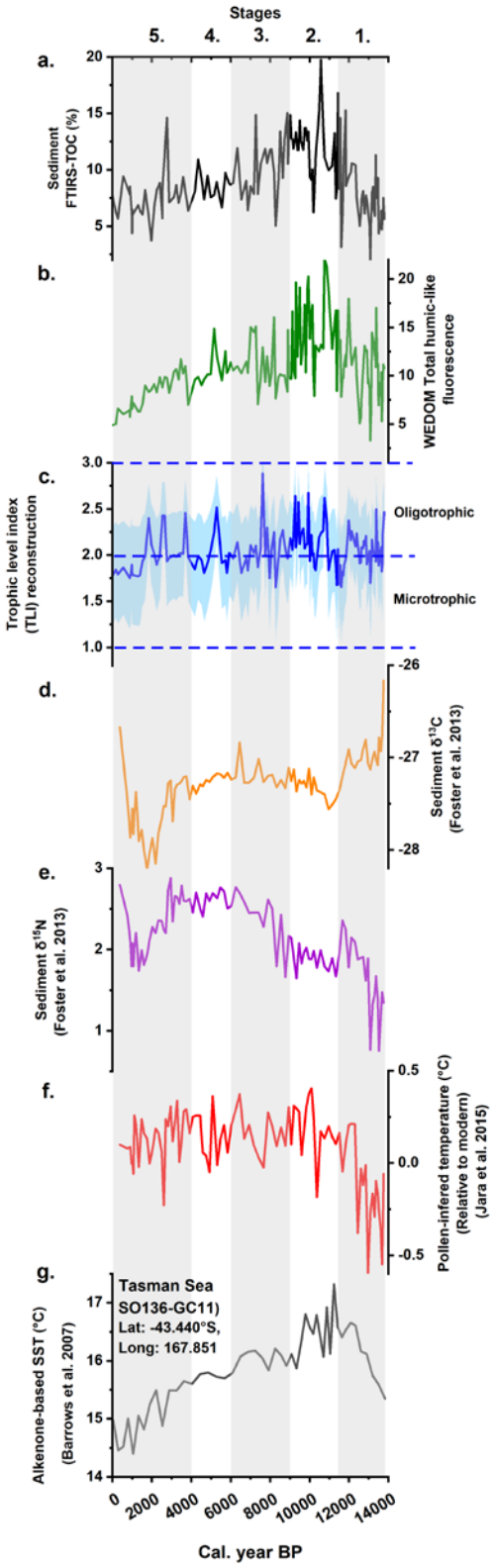


**Figure 3.10-** Time-series of organic matter components in Adelaide Tarn over the last 13,770 years.

## Sources of DOM in Adelaide Tarn

In Adelaide Tarn, a simple catchment with limited anthropogenic influence, changes in allochthonous inputs are likely to be associated with natural environmental change. Due to Adelaide Tarn's location in the southern mid-

latitudes, it has been subject to climate variability through the Holocene (Jara *et al.*, 2015). Changes in climate are likely to feed back into the decomposition of carbon substrates in soil (Davidson & Janssens, 2006; Melillo *et al.*, 2017), as well as vegetation and treeline shifts (Jara *et al.*, 2015). A study of 75,000 widely distributed lakes found that DOM concentration and characteristics are regulated via a hierarchical structure, whereby climate and topography regulate terrestrial vegetation, soils and hydrology on a regional scale (Sobek *et al.*, 2007). Locally, lake DOC is influenced by the proportion of wetlands and upstream lakes, as well as water retention time (Sobek *et al.*, 2007). Further, increases in temperature, terrestrial vegetation and run-off were found to be a significant factor in freshwater DOC concentration increases in 70 Norwegian lakes (including alpine lakes) between 1986 and 2013 (Finstad *et al.*, 2016). Indeed, the impacts of future climate change on lakes are expected to be most pronounced at high elevations (Bradley *et al.*, 2004), where treeline advancement and vegetation change has occurred due to temperature and precipitation changes (Roush *et al.*, 2007). The importance of treeline changes was demonstrated by Su *et al.*, (2015), who compared DOM properties of lake water from lakes above and below a treeline in southwest China and found that total DOM concentrations as well as protein-like and humic-like PARAFAC component scores of water in lakes below the treeline were substantially higher than those above the treeline (Su *et al.*, 2015). These studies imply that shifts in treeline and other vegetation changes (temperature driven or otherwise) in lake catchments are important determiners of DOM concentrations and molecular characteristics in lake water columns. Adelaide Tarn's catchment has undergone climate-driven vegetation change and treeline shifts (Jara *et al.*, 2015), and therefore concentrations and characteristics of DOM should have varied accordingly. WEDOM fluorescence in Adelaide Tarn is predominantly humic-like

(75–80 %), and therefore primarily of allochthonous origin. A positive correlation between allochtonous and autochtonous WEDOM fluorescence deposition may be expected in unproductive ecosystems, as nutrients associated with allochtonous DOM can stimulate autotroph productivity (Karlsson *et al.*, 2009). As noted above, FTIRS-TOC is (moderately) positively correlated with humic-like fluorescence and negatively correlated with protein-like fluorescence, and the variance of humic-like fluorescence is much higher than that of protein-like fluorescence. This indicates that changes in overall WEDOM fluorescence intensity and TOC are likely to be primarily influenced by changes in catchment vegetation (which in turn has been shown to be influenced by climate at Adelaide Tarn (Jara *et al.*, 2015)).

High altitude lakes are typically nutrient poor (Vincent & Quesada, 2012), and although Adelaide Tarn exhibits some variability in TOC, our TLI reconstruction suggests that it has remained microtrophic (very good water quality) to oligotrophic (good water quality) throughout most of the depositional period. These findings are unsurprising; contemporary monitoring data in New Zealand has demonstrated that TLI has a moderate negative correlation with percentage of native/alpine vegetation cover ($R^2$= -0.55) (Verburg *et al.*, 2010), and lakes in very cold climates had the lowest median TLI score (2.3: oligotrophic) compared to lakes from other climate regimes in New Zealand. Verburg *et al.*, (2010) extrapolated their findings to suggest that New Zealand lakes are mesotrophic on average, yet alpine lakes with native vegetation are typically microtrophic or oligotrophic (Verburg *et al.*, 2010). Further, a modelling study demonstrated that most lakes under pre-human conditions were oligotrophic in New Zealand (Abell *et al.*, 2019). In addition, New Zealand lakes with greater than 50 % catchment grass cover are known to contain less DOC, whilst lakes surrounded by high proportions of forest have higher DOC concentrations (Rae *et al.*, 2001). Given that Adelaide Tarn is an alpine lake in a

catchment characterised by native vegetation throughout its depositional history, we would expect it to exhibit consistently low TLI scores. Our TLI reconstructions for Adelaide Tarn are thus consistent with the known properties of modern New Zealand lakes.

### 3.5.6 Evolution of terrestrial carbon inputs and trophic level in Adelaide Tarn since 13,770 cal. years BP

In Adelaide Tarn, five stages of deposition can be distinguished based on the fluorescence values. These are discussed individually below.

#### 3.5.6.1 Stage 1- 13,770–11,500 cal. years BP

FTIRS-inferred TOC concentration was low during stage 1 (13,770–11,400 cal. years BP) but with a rising trend (Figure 3.10). The pattern of FTIRS-inferred TOC concentration very closely resembles that of the pollen temperature proxy until about 11,900 cal. years BP (Jara *et al.*, 2015), when the two diverge. Humic-like fluorescence was moderate and variable, bearing some resemblance to the pattern shown by FTIRS-TOC concentration. TLI scores were relatively high and variable, though with a drop towards the end of the interval, concomitant with high TOC. Other than this coincidence, there is no clear resemblance between TLI scores and TOC. The lithology of this interval was described by Jara *et al*., (2015) as brownish/black silty clay.

The early part of this interval (13,700–12,500 cal. years BP) coincides with the latter part of the Antarctic cold reversal (ACR) (Alloway *et al.*, 2007) (a period of cooling during New Zealand's late glacial transition from 14,700–12,000 cal. years BP) (Pedro *et al.*, 2015). In New Zealand, the ACR reached its coolest point at 13,000 cal. years BP (Vandergoes *et al.*, 2008). In our data, we see a sudden rise in FTIRS-TOC and pollen temperature coinciding with the end of the ACR (lagging somewhat behind the change in SST from the Tasman Sea), but there is no clear

evidence of any change in other aspects of the sedimentary organic matter. Towards the end of the interval, around 12,100–11,500 cal. years BP, there is a distinct drop in TLI score, coinciding with a fall in pollen temperature and humic-like fluorescence, and a shorter decline in TOC. Overall, this would seem to indicate that inputs of organic carbon to the lake decreased during the cool ACR, increased during the immediately following warm period, and then decreased again during a subsequent, less dramatic cooling. The resemblance between our humic-like fluorescence record and FTIRS-TOC seems to indicate that, as in the contemporary sediments of the training set lakes, the changes in carbon input are largely related to allochthonous carbon. This might be explained by changes in the tree line during this interval, indicating that the Adelaide Tarn site was surrounded by forests during warmer periods and grassland during cooler periods. However, relatively few macrofossils were found in the Adelaide Tarn sediments through this interval, with most being bryophytes (non-vascular plants such as mosses) and graminoids (herbaceous grasses, sedges and rush) (Jara *et al.*, 2015). We therefore interpret these changes in allochtonous input as related to increased terrestrial shrub and grass cover and productivity during warmer periods without major changes in the species assemblages. TLI scores during this interval do not seem to have been strongly affected by changes in terrestrial carbon input, remaining in the upper microtrophic to lower oligotrophic range throughout, dropping to very low levels at the end of the period along with a fall in pollen temperature (Jara *et al.*, 2015).

#### 3.5.6.2 Stage 2- The Holocene Climatic Optimum (HCO) (11,500–9,000 cal. years BP)

Because the Adelaide Tarn record covers an interval characterised by pristine catchment conditions (with no possible anthropogenic influences prior to ~750 cal. years BP (McWethy *et al.*, 2014)), the effects of natural environmental changes and

climate variation on organic matter input into the lake can be assessed. A key period of temperature (and therefore environmental) change is the Holocene climatic optimum (HCO) (ca. 11,500–9,000 cal. years BP). The pollen-derived temperature proxy from Adelaide Tarn ((Figure 3.10; (Jara *et al.*, 2015)), indicates that, during the HCO, terrestrial plant species normally found at low altitudes were present in the catchment. This was interpreted by Jara *et al.*, (2015) to indicate climatic warming at Adelaide Tarn and was supported by lipid palaeo-thermometry (Zink *et al.*, 2016). In New Zealand, the HCO is thought to have been characterised by mean annual temperatures between 1.5 and 3 °C warmer than today (Wilmshurst *et al.*, 2007), whilst a SST reconstruction from the Tasman Sea (Figure 3.10 g) (Barrows *et al.*, 2007) shows a peak temperature of 17.3 °C at 11,220 cal. years BP.

FTIRS-TOC concentration increased from 7 % at the start of the HCO to a maximum of 20 % at around 10,500 cal. years BP (Figure 3.10 a). Overall, the HCO had a higher average TOC concentration than the ACR. TOC concentration remained relatively high throughout the HCO then declined around 8,500 cal. years BP, though remaining higher than during the ACR. This pattern is broadly similar to that shown by humic-like fluorescence intensity. The high levels of TOC and humic-like fluorescence during this period may relate to increased catchment vegetation, due to warmer conditions. Advancing treelines during this interval have been inferred based on a large negative excursion in $\delta^{13}C$ in speleothems from Mt. Arthur (a high-altitude cave-site in NW Nelson) from 11,000–10,000 cal. years BP (Hellstrom *et al.*, 1998). The correlation between humic-like fluorescence and TOC % in this part of the Adelaide Tarn record is consistent with the relationship between these two measures observed in the calibration lakes. Thus, our data suggest an increase in terrestrial vegetation productivity in the catchment and/or erosion of organic-rich material into the lake during the HCO. According to Jara *et al.*, (2015)

the treeline is unlikely to have entered the catchment during this period, but between 10,500 and 10,000 cal. years BP, there was an increase in the proportion of shrubs and tree fern species in the catchment (Jara *et al.*, 2015) (Figure 3.A4). The macrofossil record indicates an increase in the proportion of tree ferns. New Zealand's indigenous tree ferns are prominent in early and mid-successional forest communities and are known to impact nutrient cycling and increase organic matter accumulation (Brock *et al.*, 2016).

Both humic-like fluorescence and TLI reconstructions show notable peaks around 11,000 cal. years BP followed by a two-step drop to minima around 10,500 cal. years BP (Figure 3.10 b, c, d). Interestingly, this pattern is the reverse of that shown by FTIRS-TOC over this period, where levels rise sharply from ~8 % around 10,900 cal. years BP to ~20 % around 10,500 cal. years BP before dropping back down to ~6 % around 10,100 cal. years BP. This could be due to either inputs of non-fluorescent organic compounds, or an increase of particulate organic matter that was not extracted during the water-extraction process. During the second half of the HCO, FTIRS-TOC, TLI and humic-like fluorescence are all relatively high with high variance. The high TLI across most of the HCO (Figure 3.10 c), suggests that bacterial and microbial growth within Adelaide Tarn responded to the warmer conditions, influx of terrestrial carbon, and/or potential changes in substrate availability. Macrofossil evidence suggests that peak treeline elevation may have occurred by 10,000 cal. years BP, as evidenced by the first appearance of tree (*Lophozonia* menziesii (silver beech)) macrofossils (Jara *et al.*, 2015).

#### 3.5.6.3 Stage 3- Cooling and DOM decrease (9,000–6,000 cal. years BP)

From 10,000 cal. years BP onwards, the pollen record indicates a local development of high-elevation southern beech forest[57]. This change in species assemblage is consistent with estimated SSTs from the Tasman Sea, which began falling around

10,000 cal. years BP (Barrows *et al.*, 2007). There is a decline in overall FTIRS-TOC as well as in TLI until about 7,300 cal. years BP, after which both FTIRS-TOC and TLI remained at relatively low but stable levels. Humic-like fluorescence declined earlier and more abruptly and was low for the entire interval. According to the palynological data, this cooling lacked the intensity to lower the treeline from the catchment (Jara *et al.*, 2015). However, there were substantial changes in forest vegetation, which became dominated by cold-preferring flora, including *Fuscospora cliffortioides* and *Lophozonia* forest (beech trees) (Jara *et al.*, 2015). Trees were located within the catchment from 9,000 cal. years BP, and interestingly this corresponds with a general downwards trend in TOC % and DOM.

The sediment core lithology changed from dark brown organic-rich silt/ clay to light brown clay/silt at 6,900 cal. years BP (Jara *et al.*, 2015). This corresponds with a local minimum in FTIRS-TOC concentration and TLI and a sharp drop in humic-like fluorescence (Figure 3.10 a, b). A SST reconstruction from the Tasman Sea also indicates a cooling after the HCO (Barrows *et al.*, 2007) (Figure 3.10 g), and this interpretation is consistent with the reduction in allochtonous input and autochtonous productivity during this period.

#### 3.5.6.4 Stage 4- (6,000–4,000 cal. years BP)

There is a period of variable TOC concentration through this period. TOC and total humic-like fluorescence declined, whilst $\delta^{13}C$ (Figure 3.10 d) values became more negative. There is one large peak (5,000 cal. years BP) in both total humic-like fluorescence and TLI, reaching a TLI score of 2.5, although this change is not clearly reflected in the other proxies. The percentage of tree pollen (presumably from both the catchment and surrounding area) reached its highest value for the whole record (> 80 %) during this period. The temperature remained relatively stable during this period.

#### 3.5.6.5 Stage 5- Late Holocene cooling (4,000 cal. years BP to present)

According to the Tasman Sea SST reconstruction, a distinct cooling occurred in the New Zealand region from 4,000 to 50 cal. years BP, declining from 15.6 °C to 15.0 °C (Figure 3.10 g). This is consistent with palynological evidence from several sites across New Zealand, which suggested a cooling and drying (Li *et al.*, 2008), whilst $\delta^{18}O$ records from a speleothem in Nettlebed cave (also in NW Nelson) indicate a drying from 3,000 cal. years BP (Hellstrom *et al.*, 1998). A marked reduction in tree macrofossils from 2,500 cal. years BP indicates cooling and a retreat of trees from the catchment, with an increased dominance of cold-tolerant *Poaceae* (grass) (Jara *et al.*, 2015), perhaps explaining the changes in organic carbon characteristics.

From 4,000 cal. years BP, TLI scores were quite variable, with three distinct peaks. During this period, there was a considerable decline in total humic-like fluorescence (from a score of 13 (4,000 cal. years BP) to 5 (0 cal. years BP)), as well as a slight overall decline in TOC concentration. There is a pronounced disparity between the steady reduction in humic-like fluorescence and the pattern of sharp peaks followed by an abrupt decline shown by the TLI signal. The first of these peaks in TLI score, at around 2,500 cal. years BP, coincides with a peak in TOC concentration, indicating an increase in lake productivity. However, the other two peaks do not correspond with any features in any of the other measures of sedimentary organic matter, and it is not clear at present what these peaks may represent.

The abrupt fall in TLI to low and relatively constant values which occurs around 2,000 cal. years BP coincides with a similar fall in $\delta^{13}C$ and $\delta^{15}N$ (Figure 3.10, d, e) However, values for both the latter rise again around 1,000 cal. years BP, while both humic-like fluorescence and TLI decline (Figure 3.10 b, c).

#### 3.5.6.6 TOC and humic-like DOM content broadly corresponded with temperature shifts

Adelaide Tarn's sedimentary record demonstrates that pre-human environmental change can impact soil carbon export in a small, simple sub-alpine catchment. Specifically, WEDOM humic-like fluorescence and sedimentary TOC concentrations both broadly corresponded with known periods of temperature change since 13,770 cal. years BP in Adelaide Tarn. During known periods of higher temperature in the region (such as the Holocene climatic optimum), TOC concentrations and humic-like fluorescence were at their highest level through the entire sedimentary record. Further, during periods of temperature decline (late Holocene), humic-like fluorescence and TOC concentrations both markedly declined.

Temperature was the principal determinant of the vegetation surrounding Adelaide Tarn (Jara *et al.*, 2015), and therefore temperature-induced vegetation change is likely to be the predominant driver of soil C production and export in the catchment. However, several other variables (changes in annual ice-cover duration, soil productivity, or increased soil OM solubility) may also have influenced soil processes within the cirque. Nevertheless, the interpretation of a relationship between temperature and humic-like DOM and TOC concentrations should be treated with caution. For instance, increased temperatures can alter burial efficiency (due to mineralisation) of organic material in lake sediments (Gudasz *et al.*, 2010), and this process is unquantified in Adelaide Tarn, although this process would reduce OC concentrations in sediment from higher temperature regimes, which is counter to the relationship observed here.

## 3.6 Limitations and recommendations of further research

TLI measurements are New Zealand-specific (because this measure includes TN). A future case study could test the relationship between fluorescence and Carlson's trophic state index (Carlson, 1977) elsewhere. Furthermore, the application of water quality indices in contemporary monitoring is somewhat flawed, as the indices are constructed using independent variables that may not co-vary (e.g. TN concentration may increase, but TP may decline), potentially resulting in similar TLI scores representing quite different ecosystem properties. Some studies have suggested defining lake trophic status using the nutrient-colour paradigm, which includes FDOM absorption (Williamson *et al.*, 1999; Webster *et al.*, 2008). Optical properties of DOM in lakes has previously been demonstrated to change with trophic level status (Zhang *et al.*, 2010; Zhang *et al.*, 2018). Indeed, DOM is one of the most important water colour parameters and is also known to be closely linked to nutrients.

This study reconstructed TLI scores through time in one (mostly pre-human) lake, using a calibration based on a training set of lakes with a range of characteristics (climate, geology, lake morphometry, residence times, catchment use and mixing regimes). Further, in the training set, TP (from modern agricultural intensification) was a strong influence on lake TLI scores (and had a strong positive correlation with protein-like fluorescence). However, at Adelaide Tarn, TP will not have strongly influenced TLI scores or protein-like fluorescence. The data could be improved further by increasing the number of lakes within the training set.

Further research should be undertaken to test the relationship between 3D EEM fluorescence in contemporary water samples and in recently deposited sediments and/or suspended sediments. Microbial reworking of organic matter during sinking

and early sedimentation may diminish the total organic matter concentration whilst replacing many primary organic compounds with secondary ones, and therefore the DOM contained in sediment may be degraded compared to DOM contained in the surface waters (Meyers & Ishiwatari, 1993). The effects of lake turnover time and stratification on chromophoric DOM deposition are also currently unknown and unexplored in our study, as are the effects of remineralisation. These are all fertile areas for further study.

Water extraction of DOM may also have limitations in its power to delineate stratigraphic differences. The extraction of DOM will always be incomplete. Indeed, even in NaOH extractions, 50–70 % of the organic matter is left unextracted, therefore extractable OM can never be fully representative of total OM (Lehmann & Kleber, 2015). Little is known about the possibility of DOM mobility and degradation once stored in the sediments. The vigorous shaking required to extract FDOM (after freeze-drying) indicates that the WEDOM in Adelaide Tarn was very strongly bound to the sediment particles, and perhaps unlikely to be mobile once deposited (Meyers & Ishiwatari, 1993). The fact that the proportions of humic-like to protein-like fluorescence and the overall WEDOM fluorescence were very similar in the uppermost sediments and in the sediments as a whole supports this assumption, as does our TLI reconstruction, which is consistent with what we know both about alpine lakes in catchments with native vegetation and with what we know about Holocene climatic and environmental variability in New Zealand and at Adelaide Tarn. However, although we have shown that WEDOM fluorescence can be used as a proxy for past carbon inputs into a lacustrine system, future work using this proxy must consider potential degradation of the signal through diagenetic alteration or mobilisation of sedimentary organic carbon.

## 3.7 Conclusions

Adelaide Tarn's sediments represent a geochemical archive through which Holocene climate and associated landscape response (in the absence of human presence) in New Zealand can be reconstructed providing a natural baseline for DOM concentrations and eutrophication in relatively small, pristine, high-altitude lakes. Establishing such baselines can enable comparison with and improved understanding of modern observations. Water extraction and fluorescence analysis of lake sediment DOM is an inexpensive and rapid method to characterise past changes in lake-water quality and to provide simple reconstructions. Our measurements of both modern and ancient lake sediments support the application of these optical measurements for reconstructing DOM sources and changes in biogeochemical cycling.

TOC and humic-like fluorescence in Adelaide Tarn were at their highest during the HCO, a warm period (with shorter summers) when catchment ecology was dominated by grasses, shrubs and herbs (Jara *et al.*, 2015). From 9–3 ka, humic-like fluorescence and TOC % showed a general decline, whilst plant macrofossil records indicate that beech (*Fuscospora cliffortioides*) forest was established in the catchment during this period (Jara *et al.,* 2015). Meanwhile, reconstructed TLI scores remained low throughout the depositional period, in the upper microtrophic to lower oligotrophic range. These findings suggest that temperature change and associated shifts in vegetation cover and composition within the catchment are the principal factors driving organic carbon dynamics in Adelaide Tarn.

Understanding the mechanisms that link climate change and carbon cycling remains a great challenge. Lakes are important reservoirs and regulators of the C cycle, yet the causes of soil carbon export to lakes as DOM are strongly contested. Adelaide

Tarn's small and simple catchment, climatically sensitive location and lack of anthropogenic disturbance means that it is of importance in understanding the impacts of climate changes on soil carbon export and eutrophication.

## 3.8 Acknowledgements

This study was made possible by Marsden Fund Grant UOW1403 and public research funding from the Government of New Zealand via contract C05X1702 to GNS Science. AH was also supported by a Rutherford Discovery Fellowship award (RDF-UOW1601). We thank Dr Carsten Meyer-Jacob (Paleoecological Environmental Assessment and Research Laboratory, Queen's University Canada/ Department of Ecology and Environmental Science, University of Umeå) for PLSR modelling of FTIRS-TOC. We would like to thank Jackson White for producing the artwork in Figure 3.1. We thank Dr Ignacio A. Jara and Courtney Foster for providing data and information from their publications/theses.

## 3.9 References


Abell, J. M., Özkundakci, D., Hamilton, D. P., van Dam-Bates, P., & McDowell, R. W. (2019). Quantifying the extent of anthropogenic eutrophication of lakes at a national scale in New Zealand. *Environmental Science & Technology*, 53(16), 9439-9452

Alloway, B. V., Lowe, D. J., Barrell, D. J. A., Newnham, R. M., Almond, P. C., Augustinus, P. C., Bertler, N. A. N., Carter, L., Litchfield, N. J., McGlone, M. S., Shulmeister, J., Vandergoes, M. J., Williams, P. W., & members, N.-I. (2007). Towards a climate event stratigraphy for New Zealand over the past 30 000 years (NZ-INTIMATE project). *Journal of Quaternary Science, 22*(1), 9-35.

Andersson, C. A., & Bro, R. (2000). The N-way toolbox for MATLAB. *Chemometrics and Intelligent Laboratory Systems, 52*(1), 1-4.

Ask, J., Karlsson, J., Persson, L., Ask, P., Byström, P., & Jansson, M. (2009). Terrestrial organic matter and light penetration: Effects on bacterial and primary production in lakes. *Limnology and Oceanography, 54*(6), 2034-2040.

Baker, A., & Inverarity, R. (2004). Protein-like fluorescence intensity as a possible tool for determining river water quality. *Hydrological Processes, 18*(15), 2927-2945.

Baker, A., Ward, D., Lieten, S. H., Periera, R., Simpson, E. C., & Slater, M. (2004). Measurement of protein-like fluorescence in river and waste water using a handheld spectrophotometer. *Water Research, 38*(12), 2934-2938.

Barrows, T. T., Lehman, S. J., Fifield, L. K., & De Deckker, P. (2007). Absence of cooling in New Zealand and the adjacent ocean during the Younger Dryas chronozone. *Science, 318*(5847), 86-89.

Blaauw, M., & Christen, J. A. (2011). Flexible paleoclimate age-depth models using an autoregressive gamma process. *Bayesian Analysis, 6*(3), 457-474.

Bradford, M. A., Davies, C. A., Frey, S. D., Maddox, T. R., Melillo, J. M., Mohan, J. E., Reynolds, J. F., Treseder, K. K., & Wallenstein, M. D. (2008). Thermal adaptation of soil microbial respiration to elevated temperature. *Ecology Letters, 11*(12), 1316-1327.

Bradley, R. S., Keimig, F. T., & Diaz, H. F. (2004). Projected temperature changes along the American cordillera and the planned GCOS network. *Geophysical Research Letters, 31*(16), L16210 .

Brock, J. M. R., Perry, G. L. W., Lee, W. G., & Burns, B. R. (2016). Tree fern ecology in New Zealand: A model for southern temperate rainforests. *Forest Ecology and Management, 375*, 112-126.

Carlson, R. E. (1977). A trophic state index for lakes 1. *Limnology and Oceanography, 22*(2), 361-369.

Charlton, M. B., Bowes, M. J., Hutchins, M. G., Orr, H. G., Soley, R., & Davison, P. (2018). Mapping eutrophication risk from climate change: Future phosphorus concentrations in English rivers. *Science of the Total Environment, 613-614*, 1510-1526.

Chen, M., & Hur, J. (2015). Pre-treatments, characteristics, and biogeochemical dynamics of dissolved organic matter in sediments: a review. *Water Research, 79*, 10-25.

Coble, P. G. (1996). Characterization of marine and terrestrial DOM in seawater using excitation-emission matrix spectroscopy. *Marine Chemistry, 51*(4), 325-346.

Cole, J. J., Prairie, Y. T., Caraco, N. F., McDowell, W. H., Tranvik, L. J., Striegl, R. G., Duarte, C. M., Kortelainen, P., Downing, J. A., Middelburg, J. J., & Melack, J. (2007). Plumbing the global carbon cycle: Integrating inland waters into the terrestrial carbon budget. *Ecosystems, 10*(1), 172-185.

Corvasce, M., Zsolnay, A., D'Orazio, V., Lopez, R., & Miano, T. M. (2006). Characterization of water extractable organic matter in a deep soil profile. *Chemosphere, 62*(10), 1583-1590.

Davidson, E. A., & Janssens, I. A. (2006). Temperature sensitivity of soil carbon decomposition and feedbacks to climate change. *Nature, 440*(7081), 165-173.

European Commission. (2003). *Common Implementation Strategy for the Water Framework Directive (2000/60/EC) Guidance Document No. 5 Transitionmal and Coastal Waters - Typology, Reference Conditions and Classification Systems*. Luxembourg (Vol. 5).

Fee, E., Hecky, R., Kasian, S., & Cruikshank, D. (1996). Effects of lake size, water clarity, and climatic variability on mixing depths in Canadian Shield lakes. *Limnology and Oceanography, 41*(5), 912-920.

Fellman, J. B., Hood, E., & Spencer, R. G. M. (2010). Fluorescence spectroscopy opens new windows into dissolved organic matter dynamics in freshwater ecosystems: A review. *Limnology and Oceanography, 55*(6), 2452-2462.

Finstad, A. G., Andersen, T., Larsen, S., Tominaga, K., Blumentrath, S., de Wit, H. A., Tømmervik, H., & Hessen, D. O. (2016). From greening to browning: Catchment vegetation development and reduced S-deposition promote organic carbon load on decadal time scales in Nordic lakes. *Scientific Reports, 6*, 31944.

Foote, K. J., Joy, M. K., & Death, R. G. (2015). New Zealand dairy farming: Milking our environment for all its worth. *Environmental Management, 56*(3), 709-720.

Foster, C. R. (2013). *Palaeolimnology of Adelaide Tarn, a ~14,000-year-old low-alpine glacial lake, northwestern South Island, New Zealand.* Masters thesis, University of Waikato, Hamilton, New Zealand.

Gudasz, C., Bastviken, D., Steger, K., Premke, K., Sobek, S., & Tranvik, L. J. (2010). Temperature-controlled organic carbon mineralization in lake sediments. *Nature, 466*, 478-481.

Guigue, J., Mathieu, O., Lévêque, J., Mounier, S., Laffont, R., Maron, P. A., Navarro, N., Chateau, C., Amiotte-Suchet, P., & Lucas, Y. (2014). A comparison of extraction procedures for water-extractable organic matter in soils. *European Journal of Soil Science, 65*(4), 520-530.

Hellstrom, J., McCulloch, M., & Stone, J. (1998). A detailed 31,000-year record of climate and vegetation change, from the isotope geochemistry of two New Zealand speleothems. *Quaternary Research, 50*(2), 167-178.

Hogg, A. G., Hua, Q., Blackwell, P. G., Niu, M., Buck, C. E., Guilderson, T. P., Heaton, T. J., Palmer, J. G., Reimer, P. J., & Reimer, R. W. (2013). SHCal13 Southern Hemisphere calibration, 0–50,000 years cal BP. *Radiocarbon, 55*(4), 1889-1903.

Hudson, N., Baker, A., & Reynolds, D. (2007). Fluorescence analysis of dissolved organic matter in natural, waste and polluted waters—a review. *River Research and Applications, 23*(6), 631-649.

Jara, I. A., Newnham, R. M., Vandergoes, M. J., Foster, C. R., Lowe, D. J., Wilmshurst, J. M., Moreno, P. I., Renwick, J. A., & Homes, A. M. (2015). Pollen–climate reconstruction from northern South Island, New Zealand (41°S), reveals varying high- and low-latitude teleconnections over the last 16 000 years. *Journal of Quaternary Science, 30*(8), 817-829.

Juggins, S., Anderson, N. J., Hobbs, J. M. R. R., & Heathcote, A. J. (2013). Reconstructing epilimnetic total phosphorus using diatoms: statistical and ecological constraints. *Journal of Paleolimnology, 49*(3), 373-390.

Karlsson, J., Byström, P., Ask, J., Ask, P., Persson, L., & Jansson, M. (2009). Light limitation of nutrient-poor lake ecosystems. *Nature, 460*(7254), 506-509.

Kinder, M., Tylmann, W., Bubak, I., Fiłoc, M., Gąsiorowski, M., Kupryjanowicz, M., Mayr, C., Sauer, L., Voellering, U., & Zolitschka, B. (2019). Holocene history of human impacts inferred from annually laminated sediments in Lake Szurpiły, northeast Poland. *Journal of Paleolimnology, 61*(4), 419-435.

LAWA. (2014). *Land Air Water Aotearoa website.* Retrieved 16 November 2017 from www.lawa.org.nz. Last Accessed: Sept 2019.

Leathwick, J., West, D., Gerbeaux, P., Kelly, D., Robertson, H., Brown, D., Chadderton, W., & Ausseil, A. (2010). *Freshwater ecosystems of New Zealand (FENZ) geodatabase.* Technical Report. Department of Conservation, New Zealand.

Lehmann, J., & Kleber, M. (2015). The contentious nature of soil organic matter. *Nature, 528*, 60-68.

Li, X., Rapson, G. L., & Flenley, J. R. (2008). Holocene vegetational and climatic history, Sponge Swamp, Haast, south-western New Zealand. *Quaternary International, 184*(1), 129-138.

Makri, S., Lami, A., Lods-Crozet, B., & Loizeau, J.-L. (2019). Reconstruction of trophic state shifts over the past 90 years in a eutrophicated lake in western Switzerland, inferred from the sedimentary record of photosynthetic pigments. *Journal of Paleolimnology, 61*(2), 129-145.

Mazot, A., Schwandner, F. M., Christenson, B., Ronde, C. E., Inguaggiato, S., Scott, B., Graham, D., Britten, K., Keeman, J., & Tan, K. (2014). CO2 discharge from the bottom of volcanic Lake Rotomahana, New Zealand. *Geochemistry, Geophysics, Geosystems, 15*(3), 577-588.

McKnight, D. M., Boyer, E. W., Westerhoff, P. K., Doran, P. T., Kulbe, T., & Andersen, D. T. (2001). Spectrofluorometric characterization of dissolved organic matter for indication of precursor organic material and aromaticity. *Limnology and Oceanography, 46*(1), 38-48.

McWethy, D. B., Whitlock, C., Wilmshurst, J. M., McGlone, M. S., Fromont, M., Li, X., Dieffenbacher-Krall, A., Hobbs, W. O., Fritz, S. C., & Cook, E. R. (2010). Rapid landscape transformation in South Island, New Zealand, following initial Polynesian settlement. *Proceedings of the National Academy of Sciences, 107*(50), 21343-21348.

McWethy, D. B., Wilmshurst, J. M., Whitlock, C., Wood, J. R., & McGlone, M. S. (2014). A high-resolution chronology of rapid forest transitions following Polynesian arrival in New Zealand. *PLoS One, 9*(11), e111328.

Melillo, J. M., Frey, S. D., DeAngelis, K. M., Werner, W. J., Bernard, M. J., Bowles, F. P., Pold, G., Knorr, M. A., & Grandy, A. S. (2017). Long-term pattern and magnitude of soil carbon feedback to the climate system in a warming world. *Science, 358*(6359), 101-105.

Meyer-Jacob, C., Vogel, H., Gebhardt, A., Wennrich, V., Melles, M., & Rosén, P. (2014). Biogeochemical variability during the past 3.6 million years recorded by FTIR spectroscopy in the sediment record of Lake El'gygytgyn, Far East Russian Arctic. *Climate of the Past, 10*(1), 209-220.

Meyers, P. A., & Benson, L. V. (1988). Sedimentary biomarker and isotopic indicators of the paleoclimatic history of the Walker Lake basin, western Nevada. *Organic Geochemistry, 13*(4-6), 807-813.

Meyers, P. A., & Ishiwatari, R. (1993). Lacustrine organic geochemistry—an overview of indicators of organic matter sources and diagenesis in lake sediments. *Organic Geochemistry, 20*(7), 867-900.

Meyers, P. A., & Lallier-vergés, E. (1999). Lacustrine sedimentary organic matter records of late Quaternary paleoclimates. *Journal of Paleolimnology, 21*(3), 345-372.

O'Neil, J. M., Davis, T. W., Burford, M. A., & Gobler, C. J. (2012). The rise of harmful cyanobacteria blooms: The potential roles of eutrophication and climate change. *Harmful Algae, 14*, 313-334.

Pedro, J. B., Bostock, H. C., Bitz, C. M., He, F., Vandergoes, M. J., Steig, E. J., Chase, B. M., Krause, C. E., Rasmussen, S. O., Markle, B. R., & Cortese, G. (2015). The spatial extent and dynamics of the Antarctic Cold Reversal. *Nature Geoscience, 9*, 51-55.

Rae, R., Howard-Williams, C., Hawes, I., Schwarz, A.-M., & Vincent, W. F. (2001). Penetration of solar ultraviolet radiation into New Zealand lakes: influence of dissolved organic carbon and catchment vegetation. *Limnology, 2*(2), 79-89.

Raftery, A. E., Zimmer, A., Frierson, D. M. W., Startz, R., & Liu, P. (2017). Less than 2 °C warming by 2100 unlikely. *Nature Climate Change, 7*, 637-641.

Regnier, P., Friedlingstein, P., Ciais, P., Mackenzie, F. T., Gruber, N., Janssens, I. A., Laruelle, G. G., Lauerwald, R., Luyssaert, S., & Andersson, A. J. (2013). Anthropogenic perturbation of the carbon fluxes from land to ocean. *Nature Geoscience, 6*(8), 597-607.

Rosén, P., Vogel, H., Cunningham, L., Hahn, A., Hausmann, S., Pienitz, R., Zolitschka, B., Wagner, B., & Persson, P. (2011). Universally applicable model for the quantitative determination of lake sediment composition using Fourier transform infrared spectroscopy. *Environmental Science & Technology, 45*(20), 8858-8865.

Rosén, P., Vogel, H., Cunningham, L., Reuss, N., Conley, D. J., & Persson, P. (2010). Fourier transform infrared spectroscopy, a new method for rapid determination of total organic and inorganic carbon and biogenic silica concentration in lake sediments. *Journal of Paleolimnology, 43*(2), 247-259.

Roush, W., Munroe, J. S., & Fagre, D. B. (2007). Development of a spatial analysis method using ground-based repeat photography to detect changes in the alpine treeline ecotone, Glacier National Park, Montana, USA. *Arctic, Antarctic, and Alpine Research, 39*(2), 297-308.

Scott, D. T., Baisden, W. T., Davies-Colley, R., Gomez, B., Hicks, D. M., Page, M. J., Preston, N. J., Trustrum, N. A., Tate, K. R., & Woods, R. A. (2006). Localized erosion affects national carbon budget. *Geophysical Research Letters, 33*(1), L01402.

Shapiro, S. S., & Wilk, M. B. (1965). An analysis of variance test for normality (complete samples). *Biometrika, 52*(3/4), 591-611.

Smith, V. H. (2003). Eutrophication of freshwater and coastal marine ecosystems a global problem. *Environmental Science and Pollution Research, 10*(2), 126-139.

Sobek, S., Durisch-Kaiser, E., Zurbrügg, R., Wongfun, N., Wessels, M., Pasche, N., & Wehrli, B. (2009). Organic carbon burial efficiency in lake sediments controlled by oxygen exposure time and sediment source. *Limnology and Oceanography, 54*(6), 2243-2254.

Sobek, S., Tranvik, L. J., Prairie, Y. T., Kortelainen, P., & Cole, J. J. (2007). Patterns and regulation of dissolved organic carbon: An analysis of 7,500 widely distributed lakes. *Limnology and Oceanography, 52*(3), 1208-1219.

Stedmon, C. A., & Bro, R. (2008). Characterizing dissolved organic matter fluorescence with parallel factor analysis: a tutorial. *Limnology and Oceanography: Methods, 6*(11), 572-579.

Stuiver, M., & Reimer, P. J. (1993). Extended 14 C data base and revised CALIB 3.0 14 C age calibration program. *Radiocarbon, 35*(1), 215-230.

Su, Y., Chen, F., & Liu, Z. (2015). Comparison of optical properties of chromophoric dissolved organic matter (CDOM) in alpine lakes above or below the tree line: insights into sources of CDOM. *Photochemical & Photobiological Sciences, 14*(5), 1047-1062.

Swetnam, T. W., Allen, C. D., & Betancourt, J. L. (1999). Applied historical ecology: using the past to manage for the future. *Ecological Applications, 9*(4), 1189-1206.

Tranvik, L. J. (1988). Availability of dissolved organic carbon for planktonic bacteria in oligotrophic lakes of differing humic content. *Microbial Ecology, 16*(3), 311-322.

Tranvik, L. J., Cole, J. J., & Prairie, Y. T. (2018). The study of carbon in inland waters—from isolated ecosystems to players in the global carbon cycle. *Limnology and Oceanography Letters, 3*(3), 41-48.

Tranvik, L. J., Downing, J. A., Cotner, J. B., Loiselle, S. A., Striegl, R. G., Ballatore, T. J., Dillon, P., Finlay, K., Fortino, K., Knoll, L. B., Kortelainen, P. L., Kutser, T., Larsen, S., Laurion, I., Leech, D. M., Leigh McCallister, S., McKnight, D. M., Melack, J. M., Overholt, E., Porter, J. A., Prairie, Y., Renwick, W. H., Roland, F., Sherman, B. S., Schindler, D. W., Sobek, S., Tremblay, A., Vanni, M. J., Verschoor, A. M., Von Wachenfeldt, E., & Weyhenmeyer, G. A. (2009). Lakes and reservoirs as regulators of carbon cycling and climate. *Limnology and Oceanography, 54*(6 PART 2), 2298-2314.

Vandergoes, M. J., Dieffenbacher-Krall, A. C., Newnham, R. M., Denton, G. H., & Blaauw, M. (2008). Cooling and changing seasonality in the Southern Alps, New Zealand during the Antarctic Cold Reversal. *Quaternary Science Reviews, 27*(5), 589-601.

Verburg, P., Hamill, K., Unwin, M., & Abell, J. (2010). *Lake water quality in New Zealand 2010: Status and trends.* National Institute of Water & Atmospheric Research Ltd, Hamilton, N.Z..

Verburg, P., Hickey, C. W., & Phillips, N. (2014). Mercury biomagnification in three geothermally-influenced lakes differing in chemistry and algal biomass. *Science of The Total Environment, 493*, 342-354.

Vincent, W. F., & Quesada, A. (2012). Cyanobacteria in high latitude lakes, rivers and seas. In *Ecology of cyanobacteria II* (pp. 371-385). Springer.

von Wachenfeldt, E., Sobek, S., Bastviken, D., & Tranvik, L. J. (2008). Linking allochthonous dissolved organic matter and boreal lake sediment carbon sequestration: The role of light-mediated flocculation. *Limnology and Oceanography*, *53*(6), 2416-2426.

Webster, K. E., Soranno, P. A., Cheruvelil, K. S., Bremigan, M. T., Downing, J. A., Vaux, P. D., Asplund, T. R., Bacon, L. C., & Connor, J. (2008). An empirical evaluation of the nutrient-color paradigm for lakes. *Limnology and Oceanography*, *53*(3), 1137-1148.

Williamson, C. E., Morris, D. P., Pace, M. L., & Olson, O. G. (1999). Dissolved organic carbon and nutrients as regulators of lake ecosystems: resurrection of a more integrated paradigm. *Limnology and Oceanography*, *44*(3part2), 795-803.

Wilmshurst, J. M., McGlone, M. S., Leathwick, J. R., & Newnham, R. M. (2007). A pre-deforestation pollen-climate calibration model for New Zealand and quantitative temperature reconstructions for the past 18 000 years BP. *Journal of Quaternary Science*, *22*(5), 535-547.

Wright, H. (1967). A square-rod piston sampler for lake sediments. *Journal of Sedimentary Research*, *37*(3), 975-976.

Zhang, Y., Zhang, E., Yin, Y., Van Dijk, M. A., Feng, L., Shi, Z., Liu, M., & Qina, B. (2010). Characteristics and sources of chromophoric dissolved organic matter in lakes of the Yungui Plateau, China, differing in trophic state and altitude. *Limnology and Oceanography*, *55*(6), 2645-2659.

Zhang, Y., Zhou, Y., Shi, K., Qin, B., Yao, X., & Zhang, Y. (2018). Optical properties and composition changes in chromophoric dissolved organic matter along trophic gradients: Implications for monitoring and assessing lake eutrophication. *Water Research*, *131*, 255-263.

Zink, K. G., Vandergoes, M. J., Bauersachs, T., Newnham, R. M., Rees, A. B. H., & Schwark, L. (2016). A refined paleotemperature calibration for New Zealand limnic environments using differentiation of branched glycerol dialkyl glycerol tetraether (brGDGT) sources. *Journal of Quaternary Science*, *31*(7), 823-835.

Zsolnay, Á. (2003). Dissolved organic matter: artefacts, definitions, and functions. *Geoderma*, *113*(3), 187-209.

## 3.10 **Appendix**

**Table 3.A1-** Information on lakes used in the training-set of fluorescence measurements of modern lake sediments.

| Lake | Trophic state (based on average of annual TLI scores 3-years prior to sampling) | Average TLI score [59] | TLI data years[59] | Lake size (ha.) | Max. water depth (m) | N. of modern samples (N. of cores) | Location | Altitude (m) | Co-ordinates | Geomorphic type | Dominant land cover[56] |
|---|---|---|---|---|---|---|---|---|---|---|---|
| Aviemore | Oligotrophic | 2.2 | 2010-2011 | 2900 | unknown | 2(1) | Canterbury, S. Island | 268 | Lat: -44.619; Long: 170.305 | reservoir | pasture |
| Benmore | Oligotrophic | 2.1 | 2009-2011 | 7585 | 120 | 1(1) | Canterbury, S. Island | 361 | Lat: -44.525; Long: 170.076 | reservoir | pasture |
| Ohau | Microtrophic | 1.8 | 2009-2011 | 5927 | 129 | 4(1) | Canterbury, S. Island | 410 | Lat: -44.235; Long: 169.850 | glacial | native |
| Okataina | Oligotrophic | 2.7 | 2009-2011 | 1080 | 78.5 | 4(2) | Bay of Plenty, N. Island | 284 | Lat: -38.134; Long: 176.407 | volcanic | native |
| Pearson | Oligotrophic | 2.8 | 2009-2011 | 202 | 17 | 2(1) | Canterbury, S. Island | 616 | Lat: -43.116; Long: 171.781 | glacial | native |

| Lake | Trophic state (based on average of annual TLI scores 3-years prior to sampling) | Average TLI score [59] | TLI data years[59] | Lake size (ha.) | Max. water depth (m) | N. of modern samples (N. of cores) | Location | Altitude (m) | Co-ordinates | Geomorphic type | Dominant land cover[56] |
|---|---|---|---|---|---|---|---|---|---|---|---|
| Rotoehu | Mesotrophic | 3.9 | 2013-2015 | 810 | 13.5 | 8(3) | Bay of Plenty, N. Island | 289 | Lat: -38.024; Long: 176.528 | volcanic | native |
| Rotoiti | Mesotrophic | 3.8 | 2009-2011 | 3400 | 126 | 3(3) | Bay of Plenty, N. Island | 277 | Lat: -38.029; Long: 176.384 | volcanic | native |
| Rotomahana | Mesotrophic | 3.8 | 2009-2011 | 900 | 125 | 5 (2) | Bay of Plenty, N. Island | 339 | Lat: -38.27028; Long: 176.42417 | volcanic | native |
| Rotorua | Eutrophic | 4.1 | 2013-2015 | 17980 | 45 | 11(4) | Bay of Plenty, N. Island | 386 | Lat: -38.068; Long: 176.273 | volcanic | pasture |
| Tarawera | Oligotrophic | 2.7 | 2009-2011 | 4130 | 87.5 | 4(3) | Bay of Plenty, N. Island | 282 | Lat: -38.21117; Long: 176.41093 | volcanic | native |
| Taupo | Oligotrophic | 2 (1.9-2) | 2009-2011 | 62200 | 162.8 | 5(5) | Waikato, N. Island | 360 | Lat: -38.751; Long: 175.793 | volcanic | native |

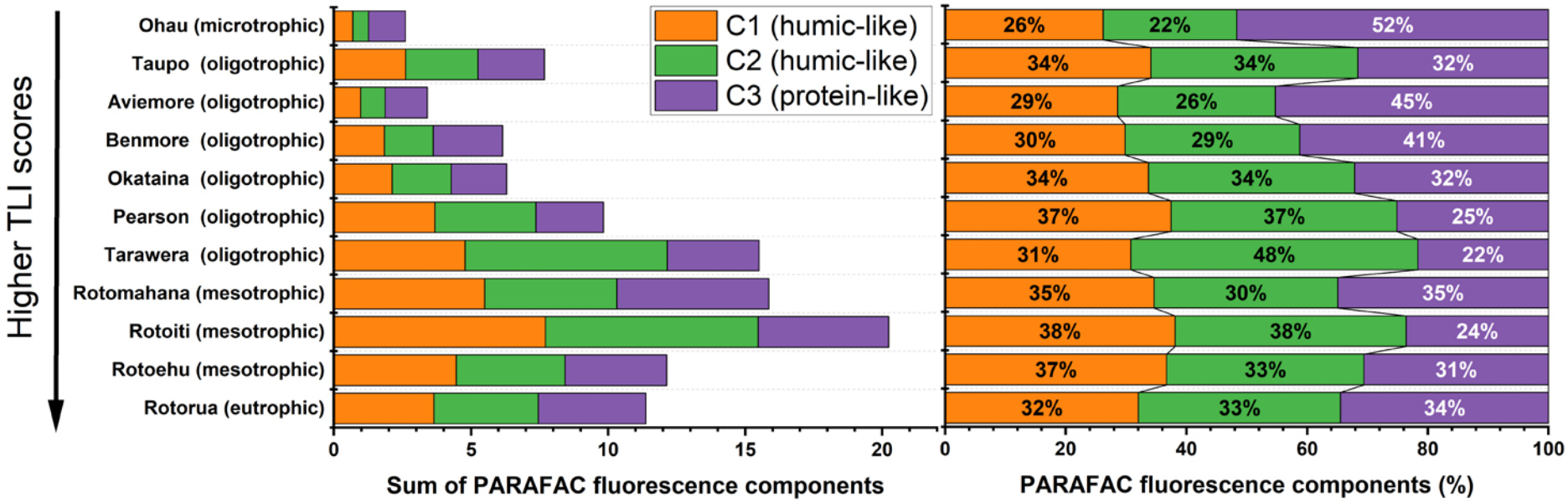


**Figure 3.A1- (a.)** Sum of PARAFAC components for each lake **(b.)** PARAFAC component (%) for each lake.

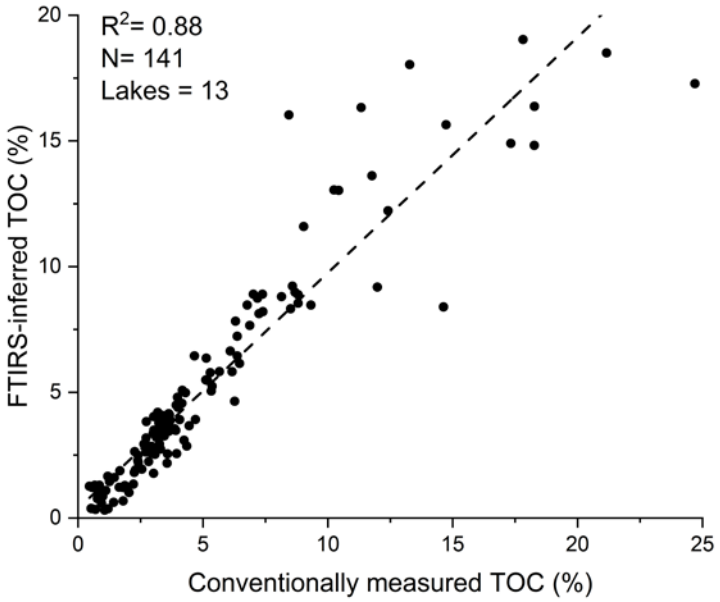


**Figure 3.A2**- FTIRS-TOC calibration.

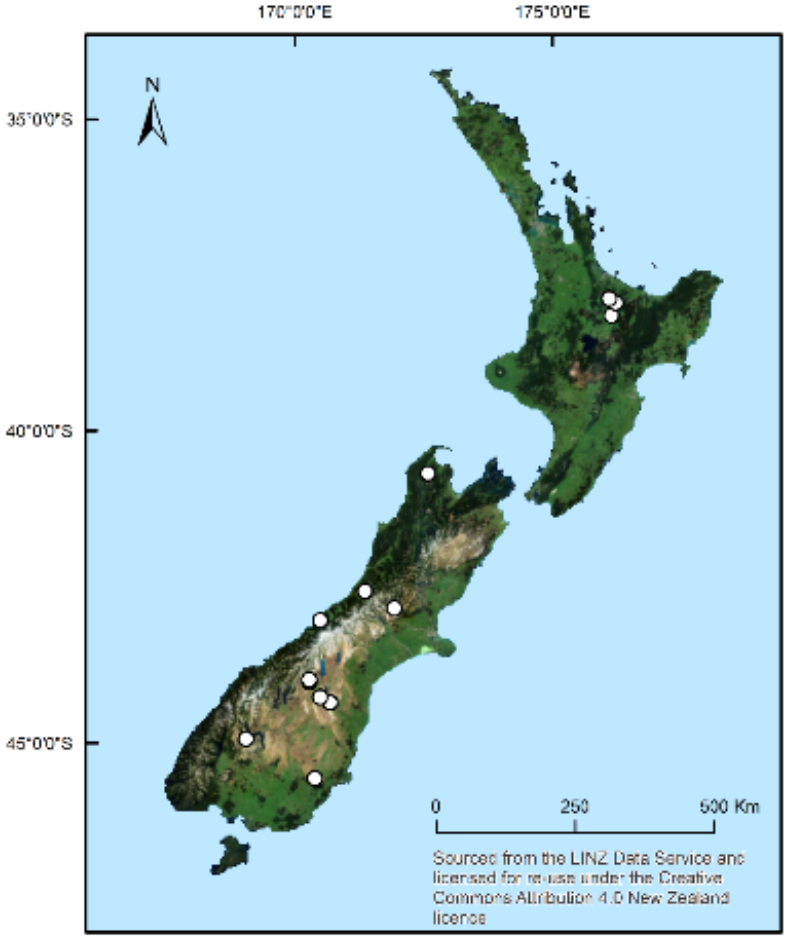


**Figure 3.A3-** Location (white circles) of FTIRS-TOC calibration lakes.

**Table 3.A2-** Information on lakes used in the FTIRS-TOC calibration.

| Lake | Mean FTIR-TOC (%) (range) | Mean NPOC measurement (%) (range) | Lake size (ha.) | Max. depth (m) | N. of modern samples | Region | Altitude (m) | Co-ordinates | Geomorphic type | Dominant land cover |
|---|---|---|---|---|---|---|---|---|---|---|
| Aviemore | 0.9 (0.5–1.1) | 0.9 | 2900 | unknown | 4 | Canterbury, S. Island. | 268 | Lat: -44.619; Long: 170.305 | reservoir | pasture |
| Adelaide Tarn | 10 (6.0–14.9) | 9.6 (5.8–13.6) | 6 | 7.6 | 10 | Tasman, S. Island | 1250 | Lat: -40.941; Long: 172.544 | glacial | native |
| Alpine Lake/ Ata Puai | 23.6 (10.1–29.8) | 24 (6.8–29.6) | 61.5 | 20 | 8 | West Coast, S. Island | 101 | Lat: -43.286; Long: 170.137 | glacial | native |
| Benmore | 0.9 (0.5–1.1) | 1.1 (0.6–1.2) | 7585 | 120 | 13 | Canterbury, S. Island | 361 | Lat: -44.525; Long: 170.076 | reservoir | pasture |
| Kaniere | 4.4 (3.3–5.2) | 3.1 (2.6–3.9) | 2200 | 195 | 3 | West Coast, S. Island | 72 | Lat: -42.830; Long: 171.145 | glacial | native |

| Lake | Mean FTIR-TOC (%) (range) | Mean NPOC measurement (%) (range) | Lake size (ha.) | Max. depth (m) | N. of modern samples | Region | Altitude (m) | Co-ordinates | Geomorphic type | Dominant land cover |
|---|---|---|---|---|---|---|---|---|---|---|
| Middleton | 8.7 (7.8–9.0) | 8.6 (6.2–8.7) | 118 | unknown | 5 | Canterbury, S. Island | 523 | Lat: -44.277; Long: 169.849 | glacial | native |
| Ngapouri | 5.8 (4.8–6.2) | 6.2 (5.2–7.8) | 991 | 24.5 | 8 | Waikato, N. Island | 475 | Lat: -38.338; Long: 176.334 | volcanic | native |
| Ohau | 0.6 (0.4–0.9) | 0.4 (0.3–0.4) | 5927 | 129 | 5 | Canterbury, S. Island | 410 | Lat: -44.235; Long: 169.850 | glacial | native |
| Okataina | 3.3 (1.1–7.1) | 3.0 (1.2–5.8) | 1080 | 78.5 | 55 | Bay of Plenty, N. Island | 284 | Lat: -38.134; Long: 176.407 | volcanic | native |
| Pearson | 3.6 (2.6–6) | 4.2 (3.2–6.4) | 202 | 17 | 12 | Canterbury, S. Island | 616 | Lat: -43.116; Long: 171.781 | glacial | native |
| Rotorua | 3.9 (3.2–4.1) | 5 (4.8–5.1) | 17980 | 45 | 3 | Bay of Plenty, N. Island | 386 | Lat: -38.068; Long: 176.273 | volcanic | pasture |
| Von | 12.7 (10.4–15.7) | 15.6 (9.2–19) | 0.87 | 15 | 10 | Otago, S. Island | 303 | Lat: -45.13926; Long: 168.35755 | glacial | native |

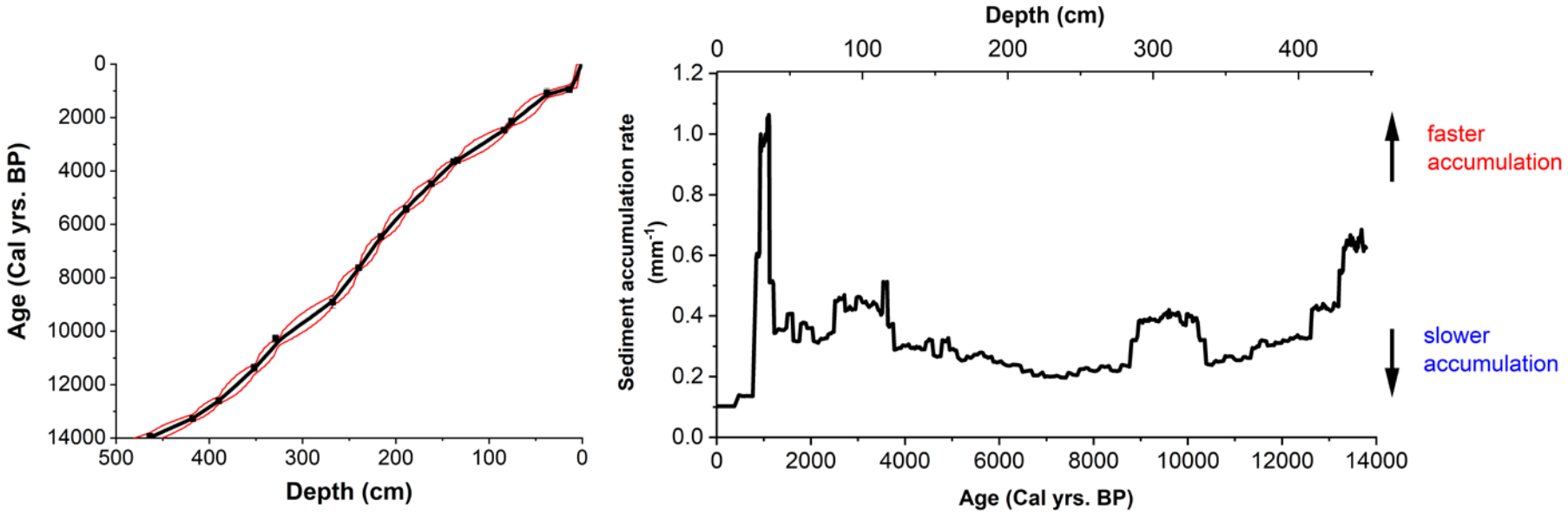


**Figure 3.A4- (a.)** Bayesian age model based on AMS radiocarbon dates from Adelaide Tarn reproduced (Jara *et al.*, 2015). The model was developed using BACON (Blaauw & Christen, 2011) in R software calibration was based on the SHCal13 calibration curve (Hogg *et al.*, 2013) with a calibration created using CALIB 6.01 (Stuiver & Reimer, 1993). The image shows a modelled weighted mean age (black line) and the 95% confidence intervals (red lines). **(b.)** Sediment accumulation rate based on the age-depth model, given as $mm^{-1}$ of accumulation per year.

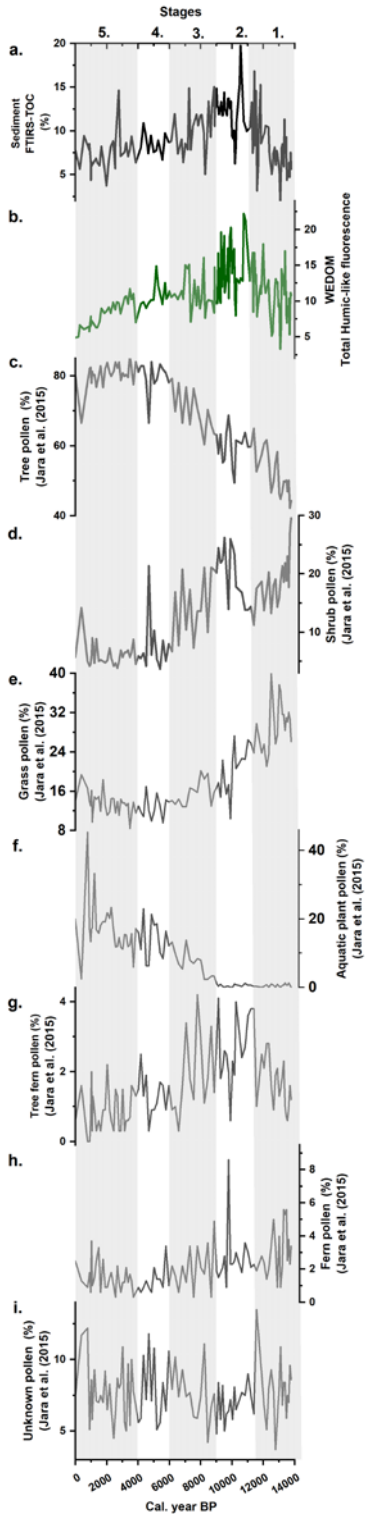


**Figure 3.A5- (a.)** FTIR-TOC %; **(b.)** Total Humic-like fluorescence; **(c.)** Tree pollen (%); **(d.)** Shrub pollen (%); **(e.)** Grass pollen (%); **(f.)** Grass pollen (%); **(g.)** Tree-fern pollen (%); **(h.)** Fern pollen (%); **(i.)** Unknown pollen (%). All pollen data from Jara *et al.*, (2015).

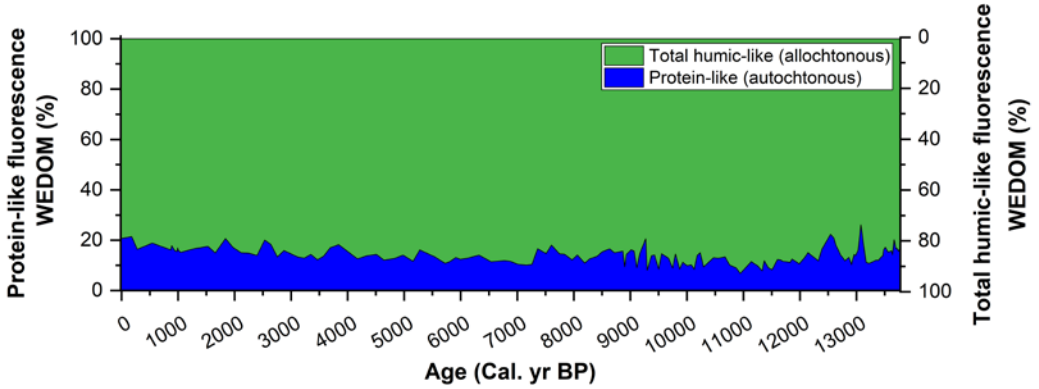


**Figure 3.A6 -** Total humic-like fluorescence and protein-like fluorescence as percentages of total WEDOM fluorescence through the sedimentary record of Adelaide Tarn.

**Table 3.A3-** TLI classification descriptions in New Zealand (LAWA, 2014)**.**

| Trophic level index score | Lake water quality |
|---|---|
| <2 | Microtrophic (very good water quality) |
| 2–3 | Oligotrophic (good water quality) |
| 3–4 | Mesotrophic (average water quality) |
| 4–5 | Eutrophic (poor water quality) |
| 5–7 | Supertrophic (very poor water quality) |

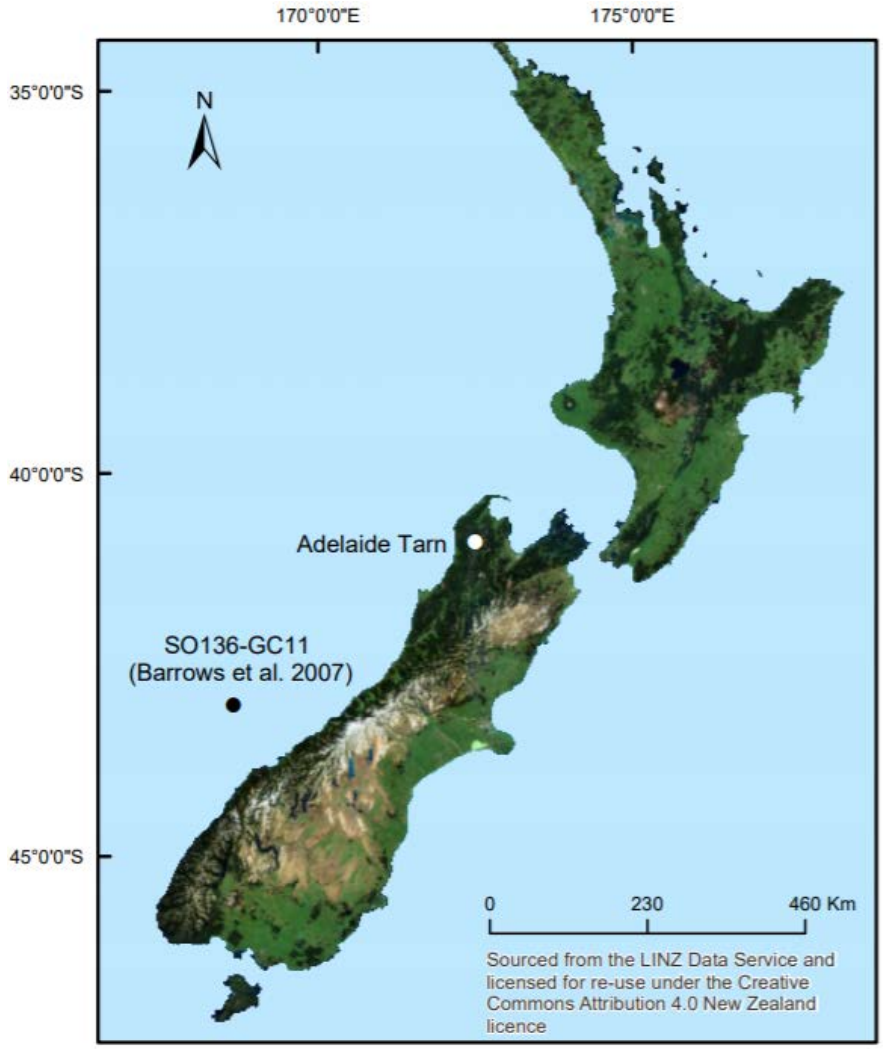


**Figure 3.A8-** Location of marine sediment core SO136-GC11 in location in the Tasman Sea, to the west of New Zealand's South Island, and the southwest of Adelaide Tarn. The alkenone-based SST reconstruction from this core was used in Figure 3.10 g.

# 4 Chapter 4

# Formation of calcite in the presence of dissolved organic matter: partitioning, fabrics and fluorescence

Andrew R. Pearson[1*], Adam Hartland[1], Silvia Frisia[2], Bethany R.S. Fox[3,1].

[1] Environmental Research Institute, School of Science, Faculty of Science and Engineering, University of Waikato, Hamilton, 3216, New Zealand.

[2] School of Environmental and Life Sciences, The University of Newcastle, Callaghan, New South Wales, 2308, Australia.

[3] Department of Biological and Geographical Sciences, University of Huddersfield, Huddersfield, HD1 3DH, United Kingdom.

Chemical Geology 539 (2020) 119492

Contents lists available at ScienceDirect

Chemical Geology

journal homepage: www.elsevier.com/locate/chemgeo

# Formation of calcite in the presence of dissolved organic matter: Partitioning, fabrics and fluorescence

Andrew R. Pearson[a,*], Adam Hartland[a], Silvia Frisia[b], Bethany R.S. Fox[c,a]

[a] Environmental Research Institute, School of Science, Faculty of Science and Engineering, University of Waikato, Hamilton 3216, New Zealand
[b] School of Environmental and Life Sciences, The University of Newcastle, Callaghan, New South Wales 2308, Australia
[c] Department of Biological and Geographical Sciences, University of Huddersfield, Huddersfield HD1 3DH, United Kingdom

ARTICLE INFO

Editor: Michael E. Boettcher

*Keywords:*
Dissolved organic matter (DOM)
Calcite
Calcite fabric
Carbonate
Flowstone
3D EEM (excitation emission matrix) fluorescence

ABSTRACT

Dissolved organic matter (DOM) is omnipresent in natural waters and is commonly incorporated into carbonates. Records of DOM from speleothems (secondary carbonates found in caves) have often been interpreted to reflect groundwater DOM concentrations. However, the fidelity of these records is largely untested. An understanding of the relationship between dripwater and speleothem DOM is thus required to allow speleothems to be reliably used as archives of DOM concentration.

We precipitated calcite ($CaCO_3$) crystals from weak solutions of $(NH_4)_2CO_3$, $CaCl_2$ and $NH_4Cl$. These solutions also contained peat DOM (from 0 to 15 mgC/L). Fluorescence 3D excitation-emission matrix (3D EEM) analysis showed a strong, positive correlation between [DOM] in the parent-solution, and [DOM] in the calcite. Calcite precipitation was reduced at high DOM concentrations, potentially indicating inhibition of crystallisation. Partition coefficient values showed that $DOM_{aq}$ was subtly preferentially incorporated into calcite.

Scanning electron microscope images indicated that the crystal structures were heavily influenced by DOM adsorption with finer, smooth-faced, rhombohedral crystals forming in growth solutions with low aqueous [DOM] (0–5 mgC/L), and prismatic, 'impure' crystals produced at high aqueous [DOM] (10 and 15 mgC/L).

Overall, our results indicate that authigenic carbonates are likely to faithfully record variations in aqueous [DOM] within the natural range of DOM concentrations in representative freshwater systems (caves, soil water), and that crystal habits are altered by aqueous [DOM] within their growth solutions.

We also applied our findings to three flowstones collected from three New Zealand caves which vary in climatic, vegetation and hydrological regimes. We conclude that differences in initial aqueous [DOM] do indeed control incorporation of DOM into calcite, and thus 3D EEM fluorescence can be used to reconstruct original aqueous [DOM] from authigenic carbonates.

## 1. Introduction

The organic matter (OM) components in soil contain more than three times as much carbon as either the Earth's atmosphere or terrestrial vegetation and are sensitive to climatic and environmental changes (Schmidt et al., 2011). Soil organic matter (SOM) is a heterogenous assortment of organic compounds ranging from intact plant materials to highly oxidised carbon in carboxylic acids at different degradation stages (Lehmann and Kleber, 2015), and also includes microbial biomass. Soil organic matter can adhere to and be strongly mixed with soil minerals, and therefore the number of compounds that may constitute soil organic matter is effectively limitless, and no single chemical description can be given (Evans et al., 2005). A fraction of soil organic matter is soluble and can be transported in dissolved or colloidal form into groundwater (Hartland et al., 2012). Dissolved organic matter is ubiquitous in natural environments and is arbitrarily defined as organic matter with particle sizes below 0.45 μm. "Dissolved" organic matter is therefore a misnomer, as colloidal particles can exist down to 1 nm (Lead and Wilkinson, 2006). However, since it is the conventional term for this class of organic matter, we will be using it throughout this paper.

DOM is highly complex and includes a diverse range of aromatic and aliphatic hydrocarbon structures that may have attached functional groups (Leenheer and Croué, 2003). In terrestrial waterbodies, DOM can affect biodiversity and ecological processes (Rae et al., 2001), contribute to global climate change via degassing as $CO_2$ and $CH_4$ (following degradation reactions (Cole et al., 1994; Cole et al., 2007; Mayorga et al., 2005)), and act as a vector for trace metal transport

* Corresponding author.
*E-mail address:* arp21@students.waikato.ac.nz (A.R. Pearson).

https://doi.org/10.1016/j.chemgeo.2020.119492
Received 14 October 2019; Received in revised form 27 January 2020; Accepted 2 February 2020
Available online 04 February 2020
0009-2541/ 

(Hartland et al., 2012; Sauve et al., 2000). DOM can precipitate out of waterbodies in mineral phases (e.g. in biogenic or abiogenic carbonate precipitates) or be deposited in sediments. Herein, $[DOM]_{aq}$ and $[DOM]_s$ refer to the aqueous (i.e. in solution) and solid phase (i.e. incorporated in calcite, the rhombohedral phase of $CaCO_3$) dissolved organic matter concentration, respectively. Little is known about DOM trends prior to the onset of widespread dissolved organic carbon (DOC) monitoring, which became routine in several countries the mid-late 20th century (e.g. the Acid Monitoring Network, UK (Monteith et al., 2014)). An ongoing debate surrounds the causes of recent (late 20th century to present) DOM increases in terrestrial waterbodies in mid/high-latitudes of the Northern Hemisphere (Evans et al., 2006; Monteith et al., 2007) (the Southern Hemisphere is comparatively understudied). Proposed contributing factors include increasing temperatures (Freeman et al., 2001), changes in soil water acidity due to declining atmospheric sulphur deposition (Evans et al., 2006; Monteith et al., 2007) elevated atmospheric $CO_2$ concentrations (causing stimulation of primary productivity) (Freeman et al., 2004), and changes in land-use (Stanley et al., 2012). This debate may be resolved using long-term (centennial to millennial-scale) records of DOM variability encoded in natural sedimentary or mineralogical archives, which may allow the isolation and assessment of individual potential contributing factors.

One of the most promising environmental archives is that of speleothems, secondary calcium carbonate deposits typically found in caves (e.g. flowstones and stalagmites) (Hill et al., 1997). Inorganic geochemical properties (isotopic and trace element data) (Affolter et al., 2019; Nagra et al., 2017; Scroxton et al., 2018; Williams et al., 1999) and physical properties (e.g. nano-crystal aggregation, open vs. compact columnar fabrics, defect-ridden fabrics) of natural calcium carbonate minerals have been routinely used to determine environmental parameters at their time of formation (Frisia et al., 2000; Nielsen et al., 2014). Speleothems can preserve organic molecules from overlying allochtonous vegetation, soil and microbial communities within the cave (Blyth et al., 2016). The precision and reliability of speleothem dating means that palaeo-environmental records containing seasonal/monthly resolutions can be produced, extending to hundreds of thousands of years (Borsato et al., 2007). Speleothems thus have the potential to record DOM trends prior to anthropogenic land-use impacts and anthropogenically induced fluctuations in atmospheric S deposition, two factors that have been proposed as contributing drivers of recent increases in DOM export from soil.

Slightly acidic groundwater dissolves limestone bedrock and thus transport both soil organic matter and calcium ($Ca^{2+}$) and carbonate ($CO_3^{2-}$) ions into cave systems. There, ions are reprecipitated as solid calcium carbonate, forming speleothems. During this process, soil-derived organic matter (including DOM) may be incorporated into the speleothem $CaCO_3$ (Baker et al., 1999; Genty et al., 2001). Organic matter has long been known to alter speleothem colour (Caldwell et al., 1982): dark coloured speleothems are known to contain greater amounts of particulate organic matter (POM), fulvic acid (FA) and humic acid (HA) compared to light-coloured speleothems (Van Beynen et al., 2001). Several studies (Chalmin et al., 2012; Quiers et al., 2015) have observed that humic acid fluoresces more strongly after incorporation into calcite, which suggests an interaction between humic acid molecules and the crystal lattice (fluorescence yields increase when molecules adopt more rigid conformations) (Sulatskaya et al., 2010), such as surface adsorption of organic molecules, and bonding between organic functional groups (e.g. carboxyl ($COO^-$) and cations ($Ca^{2+}$) (Fairchild and Baker, 2012; Hartland et al., 2014). It has also been suggested that organic matter may be incorporated into speleothems as fluid inclusions (Ramseyer et al., 1997). Blyth et al. (2016) reviewed the origin, transport and transformation of OM in speleothems and suggested that speleothem OM is primarily derived from vegetation or soil overlying the cave. An important consideration is that dripwater OM can be altered during transport, prior to being preserved in a speleothem. For example, speleothems fed by water with a long-residence time are likely to contain OM that has been heavily altered (e.g. by microbial activity) along the flow-path. It has been proposed that DOM may interfere with the calcium carbonate precipitation process by chelating calcium ions in solution (Falini et al., 2009). However, this is unlikely to be significant because of the limited number of cation exchange sites in DOM compared to the large number of $Ca^{2+}_{(aq)}$ ions, as well as competition from transition metals which preferentially occupy binding sites in DOM (Hartland and Zitoun, 2018). Frisia et al. (2018) investigated the role of DOM in $CaCO_3$ precipitation using transmission electron microscopy of both marine, non-bio-precipitated carbonates and natural precipitates from cave waters and fossil speleothems. They found that organic substances can act as either catalysts or inhibitors of crystal nucleation and growth and diagenesis, strongly influencing the preservation of original structures (Frisia et al., 2018). They proposed that, regardless of origin, the simple presence of organic molecules catalyses the precipitation of a carbonate from aqueous solution and allows its preservation. Thus, the interaction between $[DOM]_{aq}$ and the process of calcium carbonate precipitation may complicate the picture of $DOM_s$ as a faithful recorder of $[DOM]_{aq}$ and requires further investigation. Further, the presence of DOM in growth-solution has also been shown to alter crystal structure in experimental studies (Hoch et al., 2000). Yet, in cave environments, speleothem crystal habit has typically been related to dripwater supersaturation and flowrate (Frisia et al., 2000; Gonzalez et al., 1992).

A small fraction of DOM is fluorescent and is typically described as fluorescent dissolved organic matter (FDOM). Three-dimensional excitation emission matrix (3D EEM) fluorescence can be used to quantify and characterise FDOM properties (Coble, 1996; Stedmon and Bro, 2008). When fluorescence conforms to the Beer–Lambert law (i.e. the amount of light absorbed by a solution is proportional to the solution's molar absorptivity and the concentration of solute), mathematical identification (i.e. PARAFAC- parallel factor analysis of components) can be used to quantify and characterise analytes (Murphy et al., 2013), including DOM concentration and constituent molecules, by assessing fluorophore intensity and the wavelengths at which excitation and emission occur. Fluorescence methods (but not necessarily 3D EEMs) have been applied to assess DOM quantity and quality in speleothems and cave drip-waters in a diverse range of environmental and palaeo-environmental studies. Examples include studies of DOM loss and processes in the overlying soil (Genty et al., 2001; Perrette et al., 2015), land-use change (Blyth et al., 2007) and vegetation change (Baker et al., 1996). Several studies have also focused on the relationship between trace-metal-DOM complexation in cave dripwaters and speleothems (Hartland et al., 2012; Rutlidge et al., 2014).

Here, we aim to test (a) whether secondary calcium carbonate is a faithful recorder of $[DOM]_{aq}$ and (b) the effect of $[DOM]_{aq}$ on calcium carbonate crystal morphology and lattice defects. We test this by precipitating calcium carbonate in solutions containing varying concentrations of DOM (approximately 0, 5, 10, 15 mgC/L). Our calcite crystals were synthesised using an adapted Gruzensky protocol (Gruzensky, 1967), in which $NH_3$ and $CO_2$ gases are sublimed from ammonium carbonate and diffuse into an aqueous solution of calcium and ammonium chloride, causing supersaturation and precipitation of $CaCO_3$. Laboratory experiments exclude the complexities of changes in water chemistry, DOM characteristics, interactions with trace elements and potential microbial activity that may influence crystallisation pathways in the cave environment, therefore enabling us to simply test the effects of natural [DOM] on crystallisation processes and the relationship between $[DOM]_{aq}$ and $[DOM]_s$.

Most laboratory studies that focus on incorporation of organic impurities in calcite have relied on laboratory grade humic acids (Chalmin et al., 2012; Falini et al., 2009) or isolation of individual organic ligands (Mavromatis et al., 2017). However, carbonate precipitation in natural environments occurs with a range of organic molecules that may be altered by natural processes (e.g. microbial degradation,

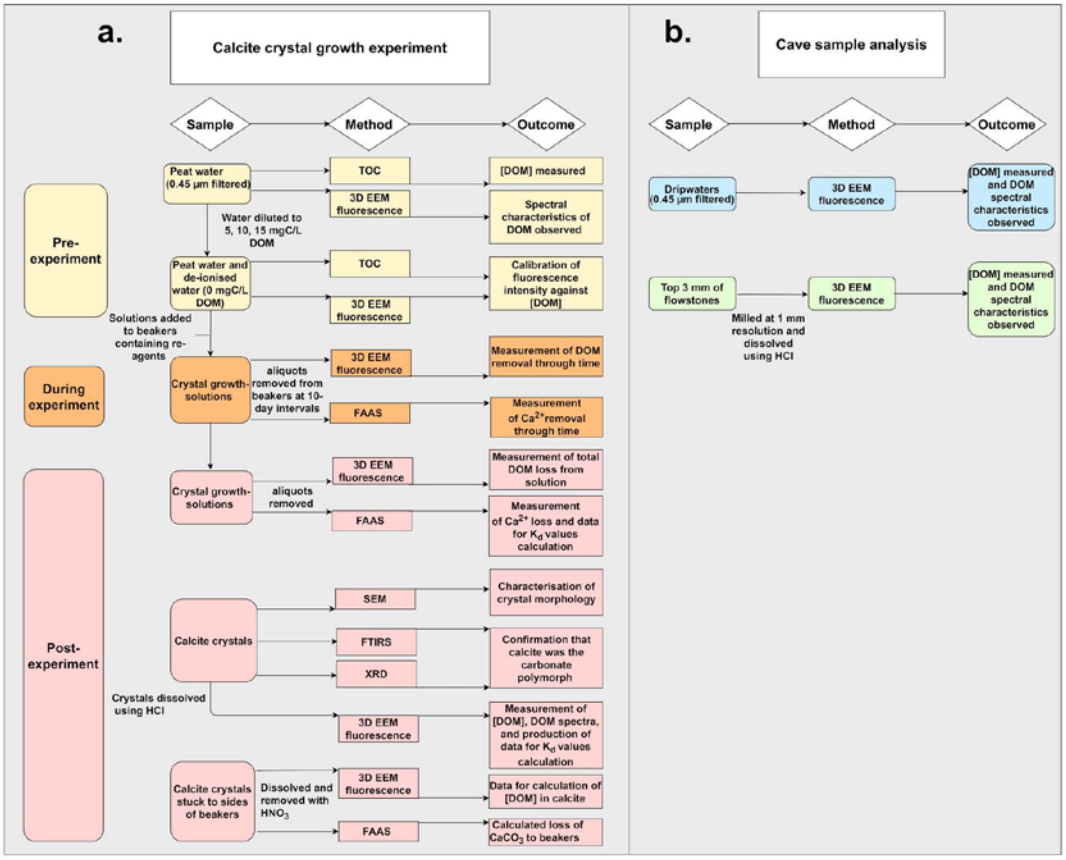


**Fig. 1.** (a.) Flowchart showing the experimental plan for the calcite crystal growth experiment. (b.) Flowchart showing the experimental plan for analysis of the dripwaters and flowstones from the cave sites.

decomposition). In this study, we aimed to address this issue by using natural DOM sourced from Kopuatai peat dome, a raised bog in central North Island, New Zealand. We also used the same fluorescence methods to test the reliability of three flowstones to record DOM concentrations from their parent dripwaters at three different cave sites in New Zealand.

## 2. Materials and methods

### 2.1. Experimental design

The carbonate precipitation experiment applied a range of methods to analyse the growth-solutions and the carbonate produced under the different experimental conditions (Fig. 1a).

Flame atomic absorption spectroscopy (FAAS) was used to determine the loss of calcium ions from the growth solution through time, whilst 3D EEM spectroscopy was used to measure removal of DOM through time. Post-experiment, 3D EEM spectroscopy was used to quantify [DOM] from the dissolved crystals, the morphology of the crystal habits was assessed using scanning electron microscopy (SEM), whilst the polymorph of the crystals was determined using Fourier transform infrared spectroscopy (FTIRS) and X-ray diffraction (XRD) (Fig. 1a). To assess the relevance of the experimental findings in a natural environment, [DOM] in dripwaters and flowstones from three caves were measured and compared using 3D EEM spectroscopy (Fig. 1b).

Peat water was chosen as the growth solution for our experiment because it contains high concentrations of DOM (enabling dilution to the concentrations required in our experiment). Peat-derived DOM is also relevant to cave research: several studies have analysed the fluorescence of dripwaters and speleothems in caves located beneath peat bogs (Baker et al., 1999; Charman et al., 2001).Water was pumped from a depth of approximately 20 m from Kopuatai, a raised bog (10,000 ha.) located in the Hauraki Plains, a lowland, temperate zone in the Waikato region, central North Island, New Zealand (Ratcliffe et al., 2019). After collection, the water was stored in the dark at 4 °C.

The Kopuatai water was filtered through 0.45 µm cellulose-acetate syringe filters (Microanalytix Pty Ltd., Australia), and analysed for total organic carbon (TOC). Prior to the experiment, the dissolved organic carbon (DOC) concentration of the filtered peat-solution was analysed using an O–I Analytical Aurora 1030 W TOC analyser, using the standard heated persulfate wet-oxidation method, whereby organic compounds are oxidised by high-temperature $Na_2S_2O_8$ to measure non-purgable organic carbon (NPOC) as TOC. Sample measurements were calibrated against standards of dilute potassium hydrogen phthalate (KHP) prepared using 18.2 MΩ water. Because the solution was filtered at 0.45 µm (and therefore classified as "dissolved"), TOC values will henceforth be referred to as DOM values. The peat-water was found to have a DOM concentration of 30 mgC/L, which is higher by a factor of ~2 than typically found in cave dripwaters. The peat water was diluted with deionised water to produce solutions containing ~5 mgC/L, ~10 mgC/L, and ~15 mgC/L DOM (Table 1; henceforth referred to as low, medium and high [DOM] treatments respectively). Two experimental blanks (~0 mgC/L DOM) were prepared from 18.2 MΩ water.

**Table 1**
$DOM_{aq}$ properties of day 10 and day 40 solutions, and $DOM_s$ incorporation in resulting $CaCO_3$ crystals.

| DOM Treatment (A and B are replicates) | $DOM_{aq}$ (mgC/L) (day 10) | $DOM_{aq}$ (mgC/L) (day 40) | $DOM_{aq}$ loss (mg) (day 10–40) | PC1[a] (day 10) | PC1[a] (day 40) | $Ca^{2+}$ (mg/L) (day 0) | $Ca^{2+}$ (mg/L) (day 40) | $DOM_s$ (in $CaCO_3$) (mgC/L) (day 40) | Total $CaCO_3$ yield (mg) (day 40) | $DOM_s$ (in $CaCO_3$) (mg) (day 40) | Log $K_d$ values (day 40) | Fractional difference[b] | pH (day 40) |
|---|---|---|---|---|---|---|---|---|---|---|---|---|---|
| Control A | 0.29 | 0.07 | 0.10 | 0.16 | 0.04 | 962.3 | 9 | 319 | 537 | 0.17 | −0.43 | 1.74 | 8.45 |
| Control B | 0.17 | 0 | 0.10 | 0.09 | −0.04 | 962.3 | 53.0 | 89 | 627 | 0.06 | −0.11 | 0.55 | 8.17 |
| Low A | 5.46 | 4.79 | 0.30 | 3.07 | 2.7 | 962.3 | 264 | 529 | 493 | 0.26 | 0.63 | 0.87 | 7.27 |
| Low B | 4.93 | 4.70 | 0.20 | 2.77 | 2.64 | 962.3 | 68.1 | 543 | 824 | 0.45 | 0.58 | 2.22 | 7.96 |
| Med A | 9.28 | 7.52 | 0.79 | 5.22 | 4.23 | 962.3 | 37.2 | 1415 | 805 | 1.14 | 0.44 | 1.44 | 8.29 |
| Med B | 9.37 | 8.06 | 0.69 | 5.27 | 4.53 | 962.3 | 21 | 1429 | 916 | 1.31 | 0.44 | 1.90 | 8.35 |
| High A | 15.70 | 13.26 | 1.10 | 8.83 | 7.46 | 962.3 | 102 | 1849 | 464 | 0.86 | 0.55 | 0.78 | 7.70 |
| High B | 15.53 | 12.85 | 1.21 | 8.73 | 7.22 | 962.3 | 48.2 | 1737 | 396 | 0.69 | 0.57 | 0.57 | 7.88 |

[a] PC1 = *PARAFAC* Component 1 fluorescence intensity score.
[b] Fractional difference = $DOM_s$ in $CaCO_3$ (mg)/$DOM_{aq}$ loss (mg).

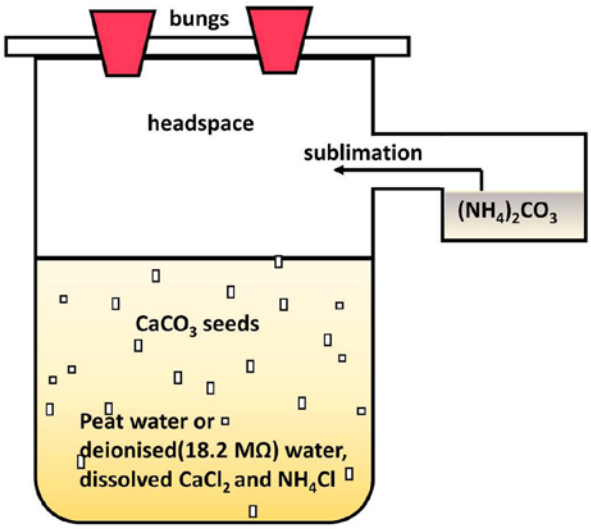


Fig. 2. Experimental design for the carbonate precipitation experiment.

$CaCl_2$ (284.44 g/L) and $NH_4Cl$ (2.66 g/L) were added to the growth solutions. 100 mg of reagent grade calcite (BDH laboratories Ltd.) was added to each solution to act as seed crystals. Each 450 mL growth solution was sealed in a 1000 mL acid-washed Pyrex beaker. Acid-washing involved soaking in 10% HCl for 24 h, followed by 24 h in de-ionised water. Solid ammonium carbonate $(NH_4)_2CO_3$ was added to glass vials, which were attached and sealed to the side of each Pyrex beaker (thus keeping the ammonium carbonate in contact with the headspace). The top of the beaker was sealed gas-tight with lubricating grease (Glisseal), a glass plate, and rubber bungs (Fig. 2). Calcium carbonate crystals were precipitated via sublimation of $CO_2$ and $NH_3$ from $(NH_4)_2CO_3$ (55.5 g/L).

The presence of a headspace enabled supersaturation with respect to $CaCO_3$. The experiment was undertaken at a constant temperature of 21 °C in darkness. Upon completion of the experiment, suspended crystals were removed, rinsed with 18.2 M Ω water, oven dried at 40 °C overnight, and weighed. Crystals that were adsorbed to the beaker were removed via dissolution using known volumes of 5% $HNO_3$.

### 2.2. FAAS (flame atomic absorption spectroscopy) of growth solutions

Every 10 days throughout the experiment, 1 mL of solution was removed, diluted 100 times with 18.2 M Ω water and acidified to 2% $HNO_3$ prior to measurement of $Ca^{2+}$ concentration by flame atomic absorption spectroscopy (FAAS) using a GBC Avanta flame atomic absorption spectrometer. These measurements were used to determine the loss of calcium ions from the solution over time and thus precipitation rates of $CaCO_3$. FAAS was also used to determine the loss of $CaCO_3$ by adsorption to beaker walls (via analysis of $HNO_3$ rinse solutions).

### 2.3. Fourier transform infrared spectroscopy (FTIRS) of crystals

Crystals from each experimental treatment were ground into a fine powder and homogenised using a pestle and mortar. Aliquots of 2 mg (±2.5%) of each sub-sample were extracted, mixed and homogenised with 400 mg of oven-dried (100 °C) KBr, before being compressed under 10,000 kg of pressure, forming translucent discs. Following the method of Ni and Ratner (2008), FTIR spectra were collected at a resolution of 1 $cm^{-1}$ with eight scans ranging between 600 and 1200 wavenumbers ($cm^{-1}$) using a Perkin-Elmer Spectrum 100 spectrometer. Background measurements of a blank KBr disc were taken.

### 2.4. X-ray diffraction (XRD) of crystals

Following the method of Ni and Ratner (2008), crystals from each treatment were ground into a fine powder prior to analysis on a Panalytical Empyrean XRD. Cu Kα radiation energy at 40 kV and 20 mA was used and the XRD patterns were collected at a scanning rate of 0.02°/s in 2θ with diffraction angles ranging from 20 θ to 60 θ.

### 2.5. Scanning electron microscopy (SEM) of crystals

Aliquots of crystals collected from each beaker and a sample of the seed crystals (reagent grade calcium carbonate, 98%, Sigma Aldrich) were sputter coated in an ultra-thin layer of platinum and palladium to ensure sample conductivity. The coated crystals were attached to aluminium stubs using double-sided adhesive tape. Observations were carried out in scanning mode using a voltage of 5 kV on a Hitachi S-4700 cold field emission microscope, with the aim of analysing and describing any potential effects of [DOM] on calcite crystal structure. Working at low voltage (5 Kv) minimises sample damage by the beam and allows production of detailed surface images.

### 2.6. Fluorescence analysis of experimental growth solutions and calcite samples

Prior to the experiment, DOM solutions were measured for 3D excitation emission matrix fluorescence (3D EEM) using a Horiba Jobin Yvon Aqualog spectrometer with a 0.5 s integration time, step-size of 3 nm, a measurement range of 240–600 nm excitation and 245–800 nm emission, and a CCD (charge-coupled device) detector. To correct for instrument specific biases (Stedmon and Bro, 2008), each matrix was corrected for inner-filter effects, scatter lines were Rayleigh masked,

and spectra were then normalised to the mean Raman intensity of distilled deionised water (using the Aqualog's in-situ data processing software and protocols (Gilmore and Cohen, 2013)). EEM data were processed with MATLAB using parallel factor analysis (PARAFAC) as implemented in the N-way toolbox (Andersson and Bro, 2000), and the drEEM toolbox (Murphy et al., 2013). PARAFAC provides multi-way data analysis in which the underlying phenomena of fluorescence can be distinguished and separated into statistically valid components (Fellman et al., 2010; Ishii and Boyer, 2012).

During the experiment, 3D EEM analysis was used to measure quantitative DOM loss from solution at 10-day intervals, from day 10 onwards. 1 mL samples were removed from the growth solution and diluted by a factor of ten prior to analysis (approximately four mL of solution is required for 3D EEM analysis). At the end of the experiment, three 2 mg aliquots of the calcite crystals (from each beaker) were dissolved in 4.5 mL of 0.025 M HCl and analysed via the same 3D EEM fluorescence method as the solutions. This resulted in calcite digests with a final pH of ~5.6. The concentration of HCl used was selected to provide sufficient $H^+$ ions to dissolve the calcite whilst minimising the acidity of the final solutions for fluorescence analysis.

The experimental samples (i.e. growth solutions and calcite) and the cave samples (i.e. dripwaters and flowstones) were measured using the same fluorescence method and data processing techniques. A one component PARAFAC model was found to be most suitable for the peat-solutions and the dissolved experimental crystal solutions, because only one meaningful fluorescence component (humic-like) was produced. The fluorescence signal of the growth solution was dominated by humic-like fluorescence peaks 'A' (ex 250–260; em 380–480) and 'C' (ex 330–350 nm; em 420–480) (Coble, 1996) (Fig. 3a, b). This two peak pattern is common in humic material from terrestrial environments (Coble et al., 1998) including cave dripwaters (Hartland et al., 2010; Rutlidge et al., 2014). The humic-like fluorescence intensity (PARAFAC Component 1 score) measurements were regressed against DOM measurements, producing a strong, positive correlation ($R^2$ = 0.99) (Fig. 3c).

### 2.7. New Zealand flowstones

To assess how reliably cave calcite incorporates representative concentrations of DOM from their parent waters, three flowstones (Fig. A3) and their associated drip-waters obtained at three New Zealand cave sites were analysed using 3D EEM fluorescence. Flowstones are deposited from flowing films of water, and such films generally have a larger catchment area of contributing drips than is typical of stalagmites (Fairchild and Baker, 2012). Thus, flowstones are likely to provide a more representative archive of soil carbon leaching from above the cave than other types of cave deposit (Lechleitner et al., 2017). Further, Blyth et al. (2016) claimed that speleothems with a rapid-flow component (e.g. flowstones) are expected to have higher amounts of allochtonous OM than other speleothem types. The three studies sites (Fig. A4) span approximately seven degrees of latitude with accompanying changes in surface vegetative cover and surface temperature. From north to south: 38 °S sub-tropical podocarp forests (Waipuna Cave, Waitomo, N. Island); 40 °S temperate beech forest (Hodges Creek, Mt. Arthur Tablelands, Kahurangi National Park, S. Island) and 45 °S alpine tussock grassland (Dave's Cave, Mt. Luxmore, Fiordland, Southland, S. Island).

### 2.8. Determination of the partition coefficient of $[DOM]_{aq}$ to $[DOM]_s$

We used the fluorescence measurements from the growth solutions ($[DOM]_{aq}$) and corresponding dissolved calcite ($[DOM]_s$) to calculate the partition coefficient (i.e. efficiency of incorporation) of DOM from solution into calcite in each experimental treatment and also from dripwaters to speleothems. We used the following formula:

$$K_d = (DOM_s/Ca_s)/(DOM_{aq}/Ca_{aq}) \quad (1)$$

where $K_d$ = partition coefficient, $_s$ = within calcite, and $_{aq}$ = within solution. All units are molar.

## 3. Results

### 3.1. Determining the calcium carbonate polymorph

FTIRS (Fig. 4a) of the precipitated carbonate crystals displayed the characteristic $_{v2}$ band of calcite at 874 $cm^{-1}$ and the characteristic $_{v4}$ band of calcite at 713 $cm^{-1}$. These observations were in agreement with spectra obtained from pure calcite crystals (Ni and Ratner, 2008). XRD (Fig. 4b) analysis displayed diffraction patterns that are consistent with calcite x-ray diffraction standards (Ni and Ratner, 2008).

### 3.2. DOM incorporation into calcite crystals

Table 1 gives the fluorescence-inferred DOM and FAAS-inferred $Ca^{2+}$ concentrations measured from growth solutions at day 10 and day 40 of the experiments, as well as the total mass of DOM incorporated into the calcite. PARAFAC component scores at day 10 were higher than those at day 0 for a number of the solutions, which at first glance suggests an increase in the organic carbon concentration. This was likely due to the addition of reagents as part of the experiment, resulting in an inner-filtering effect in the fluorescence measurements (thereby impacting fluorescence intensity values). To avoid confusion, initial fluorescence intensities presented correspond to experimental solutions at day 10 rather than day 0.

$DOM_s$ calculated as the sum of calcite removed by filtration and dissolution of residual crystals on vessel walls. Including Ca dissolution

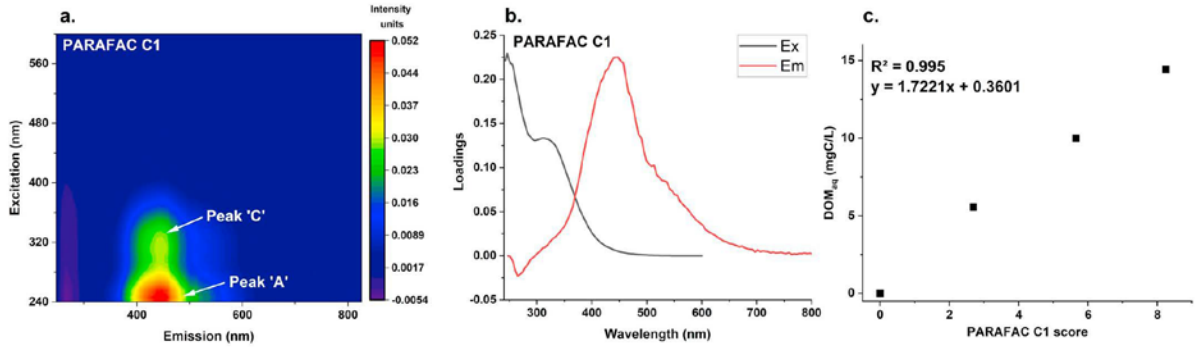


Fig. 3. (a.) 3D excitation-emission matrix of PARAFAC component 1 (C1) (b.) Excitation and emission loadings of PARAFAC component 1. (c.) Correlation between PARAFAC C1 score and DOM (mgC/L). The equation was applied to C1 scores to calculate [DOM] throughout this experiment.

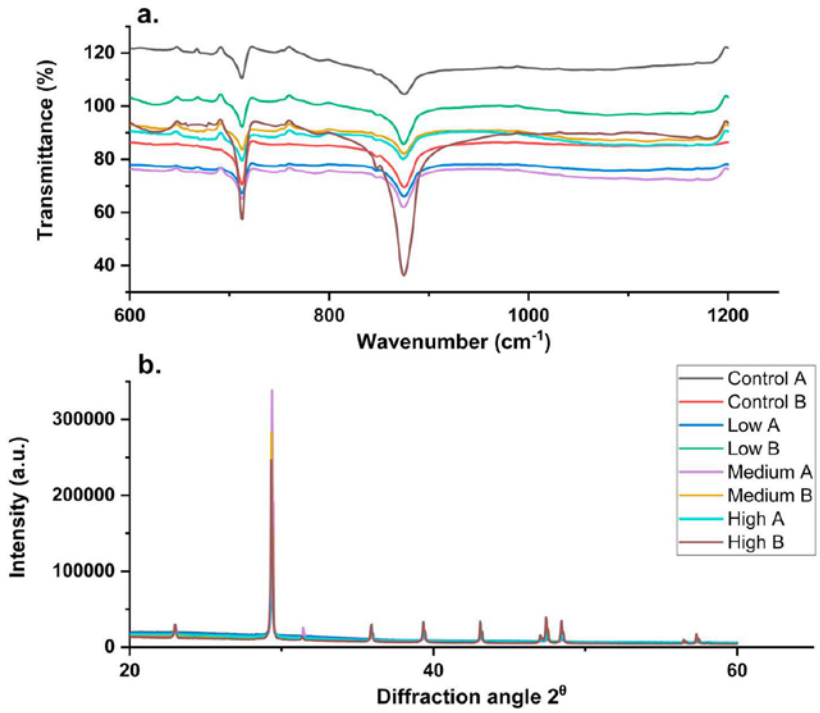


**Fig. 4.** (a) FTIRS spectra of the carbonate crystals (KBr pellets) and (b) XRD analysis of crystal aliquots from each [DOM] treatment.

over-estimates $DOM_s$ yield. $DOM_s$ based on filtration slightly under-estimates DOM yield.

Growth solution fluorescence measurements were conducted every 10 days in order to monitor $[DOM]_{aq}$ (as represented by PARAFAC component 1) throughout the experimental period (Fig. 5a). $[DOM]_{aq}$ in the growth solution continuously declined in each beaker (Fig. 5a). After day 30, the rate of removal of DOM decreased in four of the treatments (low B, med A, med B and high A) and increased in two (low A and high B).

Calcium ion concentrations in the growth solutions dropped throughout the experimental period for every treatment, indicating precipitation of calcium carbonate onto seeds (Fig. 5b). Fig. 5b shows consistent changes in the rates of calcium ion loss across treatments, except for the low [DOM] treatments, in which the removal rate of $Ca^{2+}_{aq}$ was slower in the earlier parts of the experimental period. After day 30, $Ca^{2+}$ removal from growth solution slowed in all solutions except Low A and High A. This reduction in growth rate corresponds to the reduction in the rate of $DOM_{aq}$ removal from day 30 to day 40 in most treatments, noted above. In most cases, changes in rate of DOM loss broadly resemble changes in rate of calcium ion loss; however, for

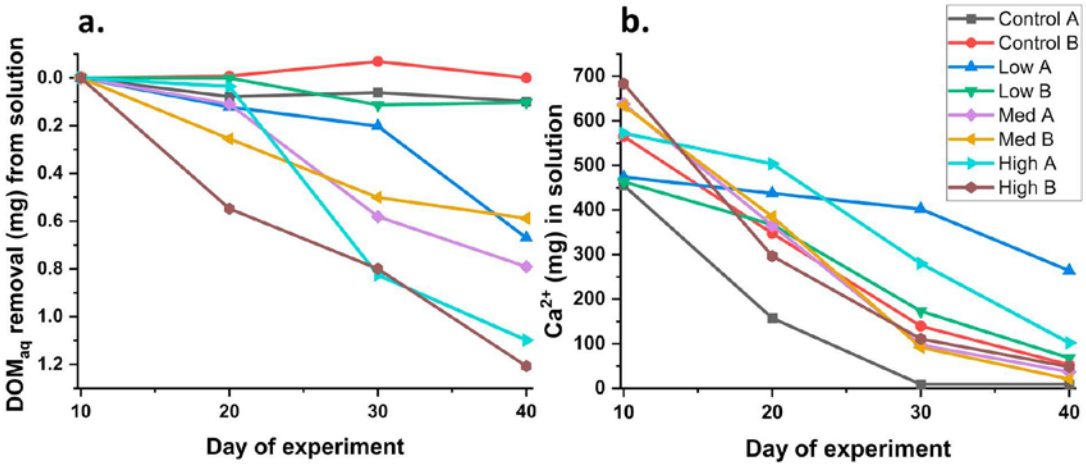


**Fig. 5.** (a.) Fluorescence-inferred cumulative mass of DOM removal from the growth solutions, measured at 10-day intervals. Note reversed scale on the y-axis for ease of comparison with b. (b.) FAAS-inferred $Ca^{2+}$ measured at 10-day intervals within the growth-solution.

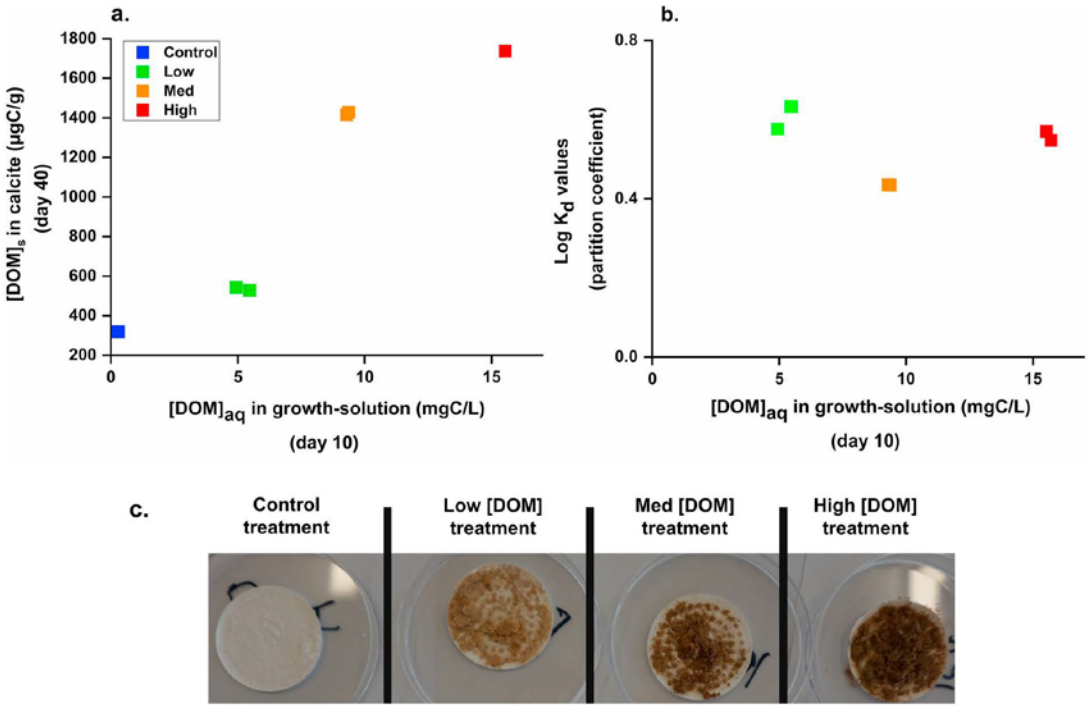


**Fig. 6.** Results of duplicated calcite growth experiments using peatland DOM. (a.) $[DOM]_{aq}$ in the growth solution (day 10) is positively correlated with $[DOM]_s$ in the experimental calcite crystals. (b.) Log $K_d$ (partition coefficient as a function of DOM incorporation) in the experimental calcite crystals (Log $K_d$ values cannot be produced for the control treatment). (c.) The crystals removed from the beakers upon completion of the experiment.

the high B treatment DOM loss accelerates after day 30 whilst calcium ion loss decelerates.

Notably, more $DOM_{aq}$ (by mass) was removed overall from the medium [DOM] treatments than the high [DOM] treatments. However, the organic carbon concentration was higher in crystals formed from the high [DOM] treatments (Fig. 6a; Table 1). There was a notable colour transition from white crystals synthesised in deionised water growth solution (Fig. 6c) through to very dark-brown crystals in the high [DOM] precipitates, indicating that [DOM] in the parent solution has a significant impact on calcite colour. Log $K_d$ values (Fig. 6b) are similar for all treatments.

Fig. 7 shows final calcite yields for each [DOM] treatment. The calcite produced from the control treatment contained the lowest [DOM] of any of the samples. The final calcite yields for the low [DOM] treatments are variable, with low A producing a similar yield to the control treatments. Notably, the low A treatment also showed unusual behaviour in terms of the rate of reduction of calcium ions in solution (Fig. 5b). The low B treatment produced a similar yield to the medium [DOM] treatments. Medium [DOM] treatments show significantly higher final calcite yields than control treatments. The high [DOM] treatments are characterised by a reduction in final yield in comparison with the medium [DOM] treatments.

Fig. 8 shows the 3D EEMs of the dissolved crystals. The fluorescence signal was dominated by humic-like peak C (ex 330–350 nm; em 420–480) (Coble, 1996), which increased as a function of higher DOM in the original growth solution. There was a notable lack of peak A (ex 250–260; em 380–480) compared to the fluorescence spectrum of the original growth solutions (Fig. A1; see Section 4.5 for discussion).

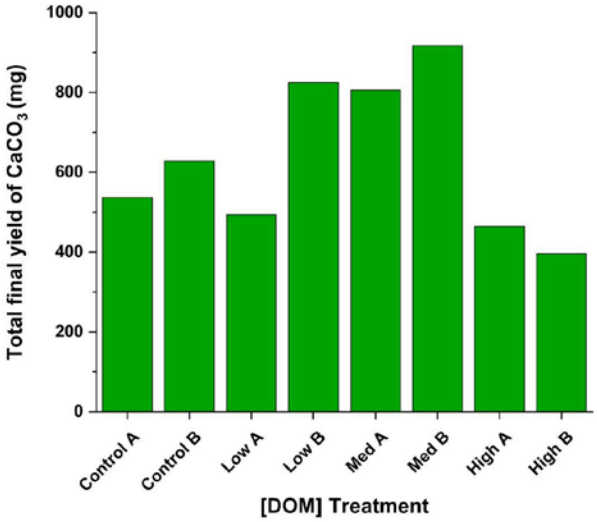


**Fig. 7.** Total final calcite yield of each [DOM] treatment.

### 3.3. Comparison to New Zealand dripwaters and flowstones

The upper 3 mm of each natural cave flowstone was sampled at 1 mm resolution (Table A1), each sample (5 mg calcite to 4 mL solution) was dissolved using the same method as the experimentally produced calcite. The fluorescence analysis indicates a positive relationship between DOM in the dripwaters and the flowstones (Fig. 9a), which complements the results from our laboratory-based experiment. Fig. 9b shows the empirical partition coefficients for these samples (based on modern dripwater measurements). These partition

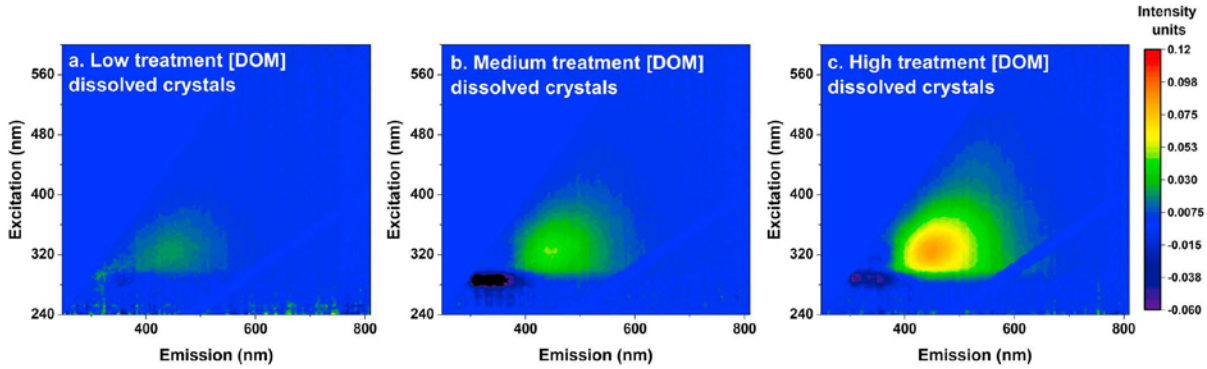


**Fig. 8.** Composite 3D EEM spectra of dissolved crystals (mean EEM of crystals from replicates A and B).

coefficients are higher and more variable than those for the experimental treatments (Fig. 6b). However, the absolute variability in $K_d$ as a function of $[DOM]_{aq}$ across all measurements (speleothem and experimental) is small and does not display any correlation with $[DOM]_{aq}$.

The 3D EEM spectra shown in Fig. 9c to h. show variability between each cave site, as well as between flowstones and their parent dripwaters. Waipuna Cave's dripwaters contained relatively low [DOM] (Fig. 9a) with a weak fluorescence signal consistent with aromatic organic acids (humic-like), whilst the Waipuna Cave flowstone also contained a protein-like fluorescence signal, which is typically indicative of microbial activity. Hodges Creek Cave's flowstone and dripwaters contained much higher [DOM] than the other sites (Fig. 9a) and this is shown in the 3D EEM spectra (Fig. 9e, f). The dripwaters in Hodges Creek are predominantly humic-like (i.e. from the soil), yet the strongest fluorescence signal in the flowstones is protein-like, suggesting that microbial activity was an important contributor to the carbonate DOM signal. Dave's Cave flowstone and dripwaters have low [DOM] (Fig. 9a), the humic-like signal was visible in the dripwater (Fig. 9g), but weaker within the flowstone (Fig. 9h).

### 3.4. Calcite crystal morphology and DOM incorporation

#### 3.4.1. Seed crystal morphology

The seed crystals (Fig. 10a, b, c) show rhombohedral morphology, well-developed flat-faces and clearly defined edges and corners. There was some aggregation of the crystals, which were relatively uniform in size (<10 μm diameter; Fig. 10a, b, c) and were notably smaller than the crystals that were synthesised during the experiment.

#### 3.4.2. Control treatment crystal morphology

The control treatment yielded almost exclusively rhombohedral crystals (Fig. 10d, e, f) which were symmetrical along the c-axis. The rhombohedra are characterised by well-defined flat faces with some macro-steps (Fig. 10d, e). Aggregation of crystals occurred across a distribution of crystal sizes (Fig. 10f). The most common size class had a width of 150–200 μm. The crystals produced in the control experiment solution were generally larger in size than those produced in the solutions containing DOM and strikingly similar to those obtained during abiotically mediated synthesis of calcium carbonate in the absence of exopolysaccharides and amino acids (Braissant et al., 2003).

#### 3.4.3. Low [DOM] treatment crystal morphology

The crystals formed under low [DOM] conditions show generally rhombohedral morphology and rounded corners (Fig. 10g, h). These crystals resemble the control [DOM] treatment crystals, apart from having rounded corners, which is symptomatic of the presence of organic matter (Frisia et al., 2018). Notably, there was a high density of sub-micron scale kinks on the crystal faces. The kinks could not have been produced during nucleation, as we seeded the experiments with rhombohedral calcite crystals prior to the experiment. They must therefore have been produced during the calcite growth process in the presence of DOM additives. In the calcite/DOM additive system, at low [DOM], there is clear evidence of habit modification and, based on purely morphological (SEM) observations, this seems to mostly affect the calcite (10–14) faces. This is similar to the effects of amino-acid additives (Orme et al., 2001). Furthermore, this experiment produced a clear range in crystal size. Fig. 10i shows several aggregations of rhombohedral crystals with individual crystal diameters below 10 μm attached to much larger >50 μm prismatic crystals with morphological relief on their faces.

#### 3.4.4. Medium [DOM] treatment crystal morphology

Fig. 10k displays a point of aggregation between two crystals, which have very clear topographical relief. The crystals were of mixed sizes, and the larger crystals were prismatic, with less well-defined corners than crystals formed in the low [DOM] treatment.

#### 3.4.5. High [DOM] treatment crystal morphology

Crystals formed from solution with high [DOM] were geometrically pyramidic and may have yielded both positive and negative rhombohedra (Fig. 10m, n, o). The crystals also have chiral morphologies due to step-effects. The crystals appear to have formed via aggregation with polymeric humic substances, incorporated as additives during nucleation and crystallisation. There was a diverse range of crystal orientations and sizes, but there was an upper size limit of 100 μm along the longest axis of individual crystals.

## 4. Discussion

### 4.1. Assessing the potential effects of [DOM] on $CaCO_3$ polymorph

Our experiment also allows us to assess the effect of [DOM] on the $CaCO_3$ polymorph. XRD and FTIRS analysis has determined that the synthesised crystals were calcite in each treatment. These data suggest that [DOM] up to ~15 mgC/L does not produce changes in $CaCO_3$ polymorphs during crystal growth, but rather drives calcite crystal morphogenesis (Cölfen and Antonietti, 2005). This finding may be consistent with a previous study, in which solutions containing 40 mgC/L humic acids were shown to precipitate 25% vaterite (*w*/w) alongside calcite in synthetic seawater solutions (Falini et al., 2009).

### 4.2. The effect of [DOM] on crystal structure and growth

Based on the atomic absorption measurements of $Ca^{2+}_{aq}$ at 10-day

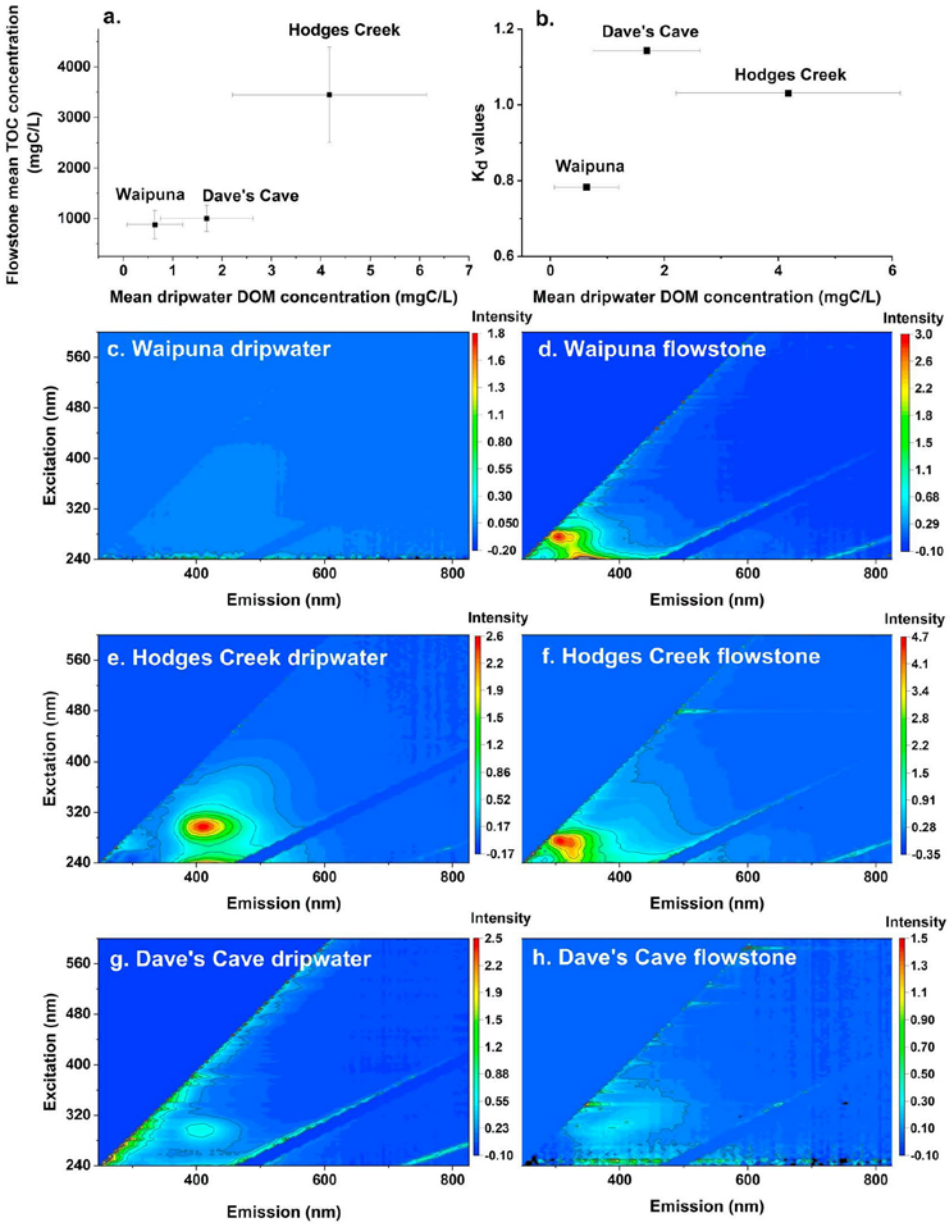


**Fig. 9.** (a.) Mean DOM concentrations (inferred by 3D EEM component 1 intensity score) in the cave dripwater vs mean DOM values (inferred by 3D EEM component 1 intensity score) incorporated into the upper 3 mm of the flowstone calcite. Error bars represent standard deviation. (b.) Dripwater DOM vs log $K_d$ values. Error bars represent standard deviation. Fig. 9. (c.) to (h.) shows the mean 3D EEM spectra from the dripwaters and flowstones from each site; (c.) Waipuna Cave dripwaters; (d.) Waipuna Cave flowstone; (e.) Hodges Creek Cave dripwaters (f.) Hodges Creek Cave flowstone; (g.) Dave's Cave dripwater; (h.) Dave's Cave flowstone.

intervals through the experiment, the rate of crystallisation was relatively consistent across treatments (Fig. 5b), with crystallisation rates in most samples decreasing after day 30. It is reasonable to infer that this growth limitation was caused by the reduction of available calcium cations.

SEM images show a clear morphological variability between the crystals that were precipitated in low [DOM] growth solutions, and the crystals grown in high-concentration DOM growth solutions (Fig. 10). In the low [DOM] treatment, aggregation of crystals is common. However, the fact that aggregation occurs across a range of crystal sizes

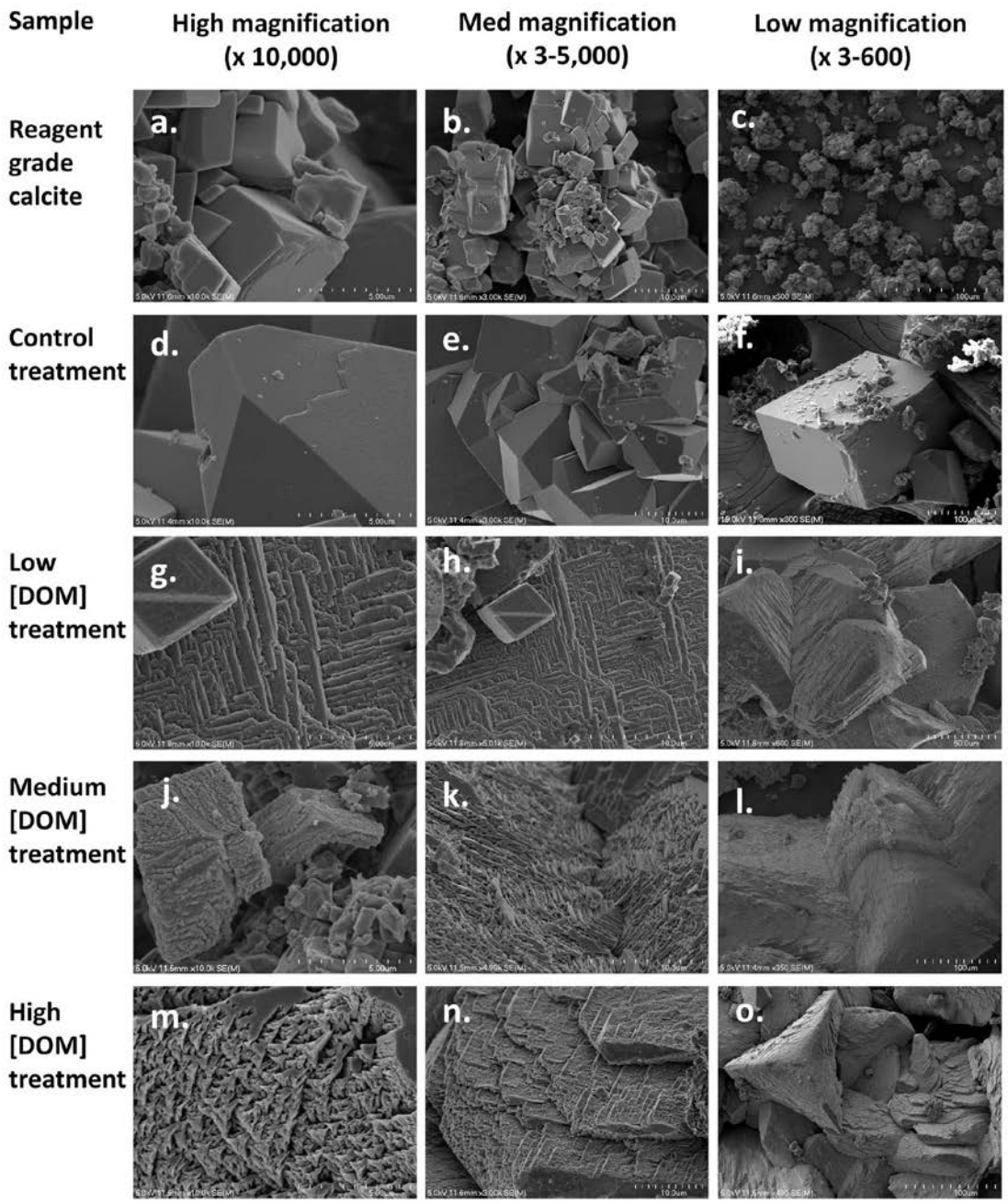


**Fig. 10.** Representative SEM micrographs of seed crystals, control treatment crystals and crystals from low, medium and high [DOM] treatments.

indicates that aggregation is not associated with the presence of DOM but must have been promoted by physical or electrostatic interactions. Low [DOM] treatments show some kinks and steps in the morphology of the crystal faces, which, as noted above, must have formed during crystal growth from seeds. These may represent active growth sites where DOM may have been adsorbed. High [DOM] treatments showed a diverse range of orientations, perhaps due to sporadic nucleation events around DOM colloids in the crystal-growth solution, as opposed to more controlled nucleation surrounding the seed-crystals in the control and low [DOM] treatments (Fig. 10).

Defects can occur in crystal habits due to the presence of impurities (Frisia et al., 2000), which, in turn, can affect the thermodynamics and

kinetics of growth (Frisia et al., 2000; Sangwal, 1996). An impurity is defined as a foreign substance other than the crystallising compound (Sangwal, 1996). DOM is adsorbed to $CaCO_3$ via electrostatic bonding at the mineral-growth solution interface (Chalmin et al., 2012) through interacting anionic functional groups ($COO^-$, $OH^-$, and $Ca^{2+}$). SEM images imply that the presence of organic matter increases micron to sub-micron scale morphological steps and kinks on individual crystal unit faces. Such irregularities were not present in the precipitates from the control treatments, within which rhombohedral flat-faced crystallites were synthesised, with both the positive and negative forms. Crystallites formed in the low [DOM] treatment were almost exclusively rhombohedral, with rounder corners than those produced in the control solution. The medium and high [DOM] treatment produced crystals with positive and negative rhombohedra with chiral morphologies, and clear disruptions within the crystal lattice. These crystals were increasingly elongated compared to the low-concentration DOM crystal morphologies, with corners and pits and a high-step density.

### 4.3. DOM incorporation mechanisms and partition coefficients

There was a marked colour transition from white crystals synthesised in deionised water growth solution through to very dark-brown crystals in the high [DOM] precipitates (Fig.6c, A2). The implication that the change in colour was related to incorporation of DOM was supported by the fluorescence-derived measurements of the $[DOM]_s$ in the dissolved calcite. There was a positive, linear relationship between the [DOM] incorporated into the calcite and the [DOM] of the original growth solution (Fig. 6a). Furthermore, fluorescence measurements of the growth solution throughout the experiment showed that DOM was progressively removed through time (presumably via incorporation into/between the crystals).

Our results indicate that, during growth, the $CaCO_3$ crystals reliably incorporated a representative concentration of DOM from the parent solutions. These findings are consistent with those of Chalmin et al. (2012), in which a crystal growth experiment tested the incorporation of reagent grade humic acids into calcite. They aimed to use sulphur as a trace element for entrapped humic acids and found that humic acid incorporation into $CaCO_3$ was directly proportional to the amount of humic acid in the precipitating solution. This result is also consistent with the claim that dark colouring of speleothems is related to the incorporation of organic matter (Gázquez et al., 2012; Van Beynen et al., 2001).

Organic matter in speleothems can be accommodated either in extra-lattice positions at crystal boundaries or within defects of a single crystal. DOM may also be incorporated as fluid inclusions (Ramseyer et al., 1997) and has been documented in 30–150 nm-wide pores in organically precipitated carbonate crystals between crystal subunits, as well as between individual crystals (Ramseyer et al., 1997). Ramseyer et al. (1997) suggested that, in the case of their study, DOM was incorporated during calcite growth but not within the lattice of carbonates. They were unable to firmly distinguish whether DOM was adsorbed onto the crystal surface or incorporated as aqueous fluid inclusions, though they suggested that a preferential adsorption onto crystal surfaces was the dominant mechanism (Ramseyer et al., 1997). An experimental study demonstrated that fulvic acids bind to calcite surfaces (Lee et al., 2005). Carboxyl groups ($COOH^-$) are common in natural DOM, and can readily be adsorbed onto calcite, which has a net positive charge (via $Ca^{2+}$). By contrast, an NMR (Nuclear Magnetic Resonance) spectroscopy study revealed that small organic (P containing) molecules can be incorporated in the calcite structure, thus supporting the notion that speleothems may provide a resilient record of organic matter present during crystallisation (Phillips et al., 2016). These results implied that calcite precipitated under natural conditions can accommodate organic molecules as structural defects.

SEM images of the crystals grown under increasing concentrations of DOM suggest a role for organic molecules in the morphogenesis of speleothem calcite. Increasing [DOM] results in increased density of observable steps and kinks at crystal surfaces, which may theoretically cause a positive feedback- loop of DOM incorporation in the form of fluid inclusions in the large number of pores visible in the crystals formed at high DOM concentrations (Fig. 10m–o). Morphologies shown in Fig. 10. for the medium and high DOM experiments are like those illustrated in Cölfen and Antonietti's (2005) seminal publication on mesocrystal (a superstructure of crystalline nanoparticles) formation, which sheds some light on the influence of DOM on the morphogenesis processes. In cave systems, nanocrystals and DOM form nanoparticles of approximately 3–4 nm (Fig. A5), which can assemble to form a mesoscale assemblage (i.e. a mesocrystal). Mesocrystals are characterised by voids between single nanoparticles, which may host organic matter. After completion of crystallographic fusion is reached (and a single crystal is formed) the organic matter can remain trapped at the boundaries between the former nanocrystals. High [DOM] may promote nano-inclusion in the amorphous phase, thus accommodating possible mismatches in nanocrystal lattices. Therefore, in the beakers containing [DOM] (but not in the blanks), there may have been a switch from a growth mechanism dominated by monomer-to-monomer attachment to a mechanism dominated by nano-particle attachment during the growth phase. Indeed, as there appears to be a linear relationship between DOM incorporation into the crystals and the quantity of the DOM in the original growth solution, we can confidently infer that DOM in cave waters influences the mechanisms of crystal growth, possibly including the formation of mesocrystals at the growth stage.

The determinant of morphological changes in our results appears to be [DOM]. Wynn et al. (2018) found that high crystal growth rates encouraged higher partition coefficients of sulphur into calcite due to increased defect sites on crystal surfaces (Wynn et al., 2018). This phenomenon was not clear in our experiment; however, positive Log $K_d$ values (Fig. 6b) showed that $DOM_{aq}$ favours incorporation into calcite. The subtle preference for DOM inclusion in calcite seen through positive log $K_d$ values may also be related to a selective bias towards incorporation of more aromatic hydrophobic DOM fractions into the calcite (Fig. 8). A strong positive relationship between DOM hydrophilicity and peak A fluorescence intensity has previously been observed (Baker et al., 2008), and peak A fluorescence was notably absent in the precipitates. The fluorescence spectra of calcite dissolutions could be altered by acid dissolution of the calcite, because at low pH values (final pH of 5.6 in crystal digests) the protonation of acidic groups (including $-COO^-$) can cause reductions in fluorescence or result in other conformational changes (Hartland et al., 2010). However, such artefacts did not account for the total absence of the peak A fluorophore (Fig. A6), implying that the fluorescence moieties underlying this peak were not incorporated into/between the crystals.

Clearly, more work examining the partitioning of specific DOM molecules/fractions is required. However, whilst qualitative differences are apparent, calcite appears to faithfully record DOM solution concentrations. Further, these findings are important for interpreting trace metal signals in carbonates. Certain metal ions that are carried by aqueous DOM complexes are non-exchangeable on the timescale of typical thin-film residence times (Hartland et al., 2011). Therefore, DOM contained in speleothems may be tracked by the metals in these inert complexes where these can be shown to be irreversibly bound (Hartland et al., 2014).

### 4.4. [DOM] potential for growth inhibition at high concentrations

This study demonstrates that crystal growth may be inhibited when the crystallising fluids contain between 10 mgC/Land 15 mgC/L of [DOM], although the reliability of this interpretation is limited by only having two experimental replicates. Nevertheless, evidence for this occurrence has been demonstrated in other studies. An experimental calcite precipitation study (Inskeep and Bloom, 1986) demonstrated that 0.03–0.14 mM $L^{-1}$ (0.36–1.68 mg/L as C) of carbon water-soluble soil organic ligands (fulvic acids or soil extracts) can inhibit calcite growth. Complete inhibition of $CaCO_3$ precipitation has also been observed in an experimental study using growth solutions containing 80 mg/L of humic acids in synthetic sea water solutions (Falini et al., 2009), whilst the same study showed that 40 mg/L of humic acids reduced the amount of $CaCO_3$ precipitate by around 50% in synthetic sea water solutions (Falini et al., 2009) (although this phenomenon was also influenced by the presence of seawater ions). Hydrophobic acids from higher plants (filtered at 0.1 μM) in the Florida Everglades have been shown to inhibit calcite growth rates by 50% in concentrations as low as 0.5 mg/L (Hoch et al., 2000). The same study demonstrated that DOM molecular weight and aromaticity correlated strongly with growth inhibition, which was attributed to enhanced stereochemical effects on blocking active crystal growth sites.

In our study, the final yield of calcite crystals was significantly higher for the medium [DOM] treatment (805 mg (replicate A) and 916 mg (replicate B)) than for the control treatment (537 mg and 627 mg). However, the low [DOM] treatment showed significant variability, with replicate A producing 494 mg whilst replicate B produced 824 mg. The low A treatment also showed unusual behaviour compared to the other treatments in terms of the rates of loss of calcium ions from solution (Fig. 5b). This may indicate an unforeseen problem with this treatment. However, given this variability in the low [DOM] treatment yields, at present we do not have enough data to clearly state the relationship between relatively low ( < 10 mgC/L) concentrations of organic carbon in solution and calcite precipitation.

The high [DOM] treatment replicates produced 464 mg (replicate A) and 396 mg (replicate B) of calcite. This is significantly lower than the medium [DOM] treatments and similar to the control treatments. This may indicate that concentrations of organic carbon >10 mgC/L tend to inhibit calcite precipitation. Additional replicates and treatments with even higher organic carbon concentrations would shed further light on this relationship.

### 4.5. Speleothems as archives of [DOM] and molecular characteristics

Speleothems exhibit different colours, and these changes have been predominantly attributed to organic matter content (Van Beynen et al., 2001; White, 1981). This was reinforced by our experiment, which showed a clear correlation between crystal colour and $[DOM]_s$ (Fig.6c, A2). Fluorescence analysis of dripwater and speleothems also indicated a strong positive relationship between dripwater fluorescence and fluorescence of the upper 3 mm of speleothem sample, consistent with the findings in our experiment. This indicates that speleothems are a reliable recorder of [DOM] in cave waters, opening the possibility of using speleothems to reconstruct soil carbon leaching rates. However, there is a notable lack of a fluorescent peak A (hydrophilic DOM) in our 3D EEM spectrum of $DOM_s$ from the dissolved experimental calcite (Fig. 8). More research is required to understand the causes of this and how it may affect the interpretation of DOM measurements from speleothem calcite. There is also a lack of hydrophilic DOM fluorescence in the flowstones at each site (Fig. 9d, f, h). Hodge's Creek was the only site at which dripwater contained fluorescent hydrophilic and hydrophobic DOM (Fig. 9e), yet the DOM contained in the flowstone is dominated by protein-like (e.g. amino acid) fluorescence (Fig. 9f), indicating microbial/bacterial input of DOM or microbial/bacterial degradation of DOM. The Waipuna flowstone also shows a strong protein-like fluorescence signal (Fig. 9d). Dave's Cave dripwater (Fig. 9g) and flowstone (Fig. 9h) both had relatively weak fluorescence signals which were dominantly hydrophobic in nature. The differences in dripwater fluorescence properties between sites may be explained by vegetation and soil type overlying the caves, whilst microbial activity (leading to increased protein-like fluorescence) is likely to be heavily influenced by temperature, however further research is required to confirm these hypotheses.

The results of this experiment are consistent with previous studies (Chalmin et al., 2012; Falini et al., 2009), which have shown that organic matter captured by calcite precipitates in analogue experiments can be representative of the growth solution. However, our study expands on these results by assessing the effects of natural DOM, rather than those of laboratory-grade humic acids. The experiments have also revealed the effects that natural DOM concentrations have on calcite crystallite morphology.

The most important piece of evidence for speleothem $[DOM]_s$ as a reliable proxy for cave water $[DOM]_{aq}$ is the positive, broadly linear relationship between $[DOM]_{aq}$ and $[DOM]_s$ in our experiment (Fig. 6a). The partition coefficients are similar for all treatments, indicating that $[DOM]_s$ of calcite is a reliable proxy for the $[DOM]_{aq}$ of the original growth solution. However, there is a difference in the partition coefficients found for natural speleothems (Fig. 9b) and our experimentally grown crystals (Fig. 6b), with the natural speleothems being characterised by higher and more variable partition coefficients. Given the range of factors (e.g., calcite precipitation rate, DOM compositional changes, supersaturation, pH, microbial activity) potentially influencing this process within a cave environment, it is beyond the scope of the current study to ascertain the cause of this difference. Further, the $K_d$ values calculated from the dripwater and flowstone samples (Fig. 9b) are likely to be relatively unreliable, given that the dripwater monitoring programme commenced potentially decades/hundreds of years after the precipitation of the flowstone sub-samples. However, the differences in log $K_d$ values both between different speleothem samples and between the speleothems and the experimental treatments are small and do not display any correlation with [DOM]. Thus, it is reasonable to interpret speleothem DOM records as reflecting DOM concentrations in karst groundwater within the range of typical karst DOM concentrations (0–10 mgC/L).

### 4.6. Crystal habits influenced by $DOM_{aq}$

Speleothem crystal habits have been used as proxies for drip-water supersaturation, presence of impurities and flow rates (Frisia et al., 2000), and to document diagenesis (Frisia et al., 2018). Indeed, calcite morphology in caves may be extremely complex, even when elements that are known to affect calcite morphology (such as Mg) are absent. Our study shows that crystal habits can be affected by [DOM] in the parent solution. Our results further suggest that the morphological relief (steps and kinks) in crystals formed at higher [DOM] may enable the formation of fluid-inclusions (Fairchild and Baker, 2012), thus potentially increasing DOM incorporation (Ramseyer et al., 1997). Fluid inclusions of DOM may also have occurred in our experiments within the large pores and topographical relief visible in the crystals produced in the medium and high [DOM] growth solutions.

Our experiments provide evidence for growth inhibition of calcite crystals at DOM concentrations above 10 mgC/L (see above). The presence of impurities has long been known to inhibit calcite

precipitation via adsorption of elemental impurities at crystal kinks (growth sites) (Meyer, 1984), whilst aqueous soil extracts and humic acid solutions have been found to inhibit calcite growth (Inskeep and Bloom, 1986).

The crystal morphologies in our controlled experiment were strongly influenced by [DOM]. Speleothem crystal habit has been related to a combination of supersaturation and flowrate (Gonzalez et al., 1992), the degree of saturation in our experiments was relatively consistent, so supersaturation is unlikely to have influenced differences in crystal habit between our samples. However, our experiment excluded many of the alternative factors (e.g. presence of Mg or Sr variation in supersaturation rate of the solution, drip rate variability) that are known to influence crystal habit in natural cave environments. Nevertheless, this is the first experimental work that unequivocally ties natural DOM concentration variability in cave-like waters to calcite crystal morphologies for conditions where the supersaturation state of the parent water may not vary considerably throughout the year and Mg concentration is negligible. The results of our experiments have wide implications for the interpretation of cave crystal morphologies in terms of parent water DOM concentrations.

### 4.7. Implications for carbonate sample selection

Our findings show further evidence that calcite fabric and colour can be strongly related to [DOM] incorporation. Researchers aiming to measure [DOM] in carbonates should undertake visual and petrographic observations when selecting samples. Owing to the relationship between high [DOM] and topographical relief between crystals and crystal subunits, this approach to sample selection may be of value to fluid-inclusion-based research.

### 4.8. Experiment limitations

Our experiment has several limitations that do not reflect natural cave environments. Notably, reagent grade calcite seed crystals that do not contain any DOM and are perfectly rhombohedral are extremely unlikely to occur in natural caves. The use of seed crystals may have somewhat altered the nature and characteristics of the encapsulating calcite crystals themselves. Our use of seed crystals also limits our ability to understand the nucleation processes of calcite crystals, and the effects that [DOM] may have on these processes. The experiment also excludes a range of natural occurrences in caves, such as microbial processes, changes in partial pressure, cave ventilation, temperature shifts and the presence of elements such as Mg and Sr. However, exclusion of these aforementioned factors was crucial in solely testing the effects of $[DOM]_{aq}$ on $[DOM]_s$ incorporation, calcite crystal morphology, and growth inhibition.

The $K_d$ values that were calculated based on the flowstones and dripwaters are likely to be somewhat unreliable because the flowstone had precipitated prior (potentially decades to hundreds of years) to the collection of the feeding dripwaters. A future study could better measure $K_d$ values in a natural environment by collecting dripwater [DOM] and sampling flowstones with faster growth rates than the flowstones used in this study.

Systematic controlled experiments could resolve many of the limitations of this study. For example; microbial organisms could be added to the growth-solutions, or growth-solutions with different DOM fractions (e.g. more protein-like, differing degrees of hydrophobicity), or growth-solutions from different sources (e.g. from a forest soil or a tundra soil) could be used. Growth-solutions could also be spiked with trace elements that are relevant to speleothem palaeo-climate reconstructions (e.g. Sr, Mg), to test the relationship between [DOM] and trace element incorporation into calcite.

## 5. Conclusions

Calcite crystals precipitated from solutions containing variable initial [DOM] showed consistent variability in organic carbon content and crystal habit, as well as less consistent variability in final crystal yield. We observed a positive, linear correlation between initial organic carbon concentration in solution and final organic carbon concentration in calcite, with log $K_d$ values of around 0.5. Crystals produced in 0 mgC/L DOM solutions were rhombohedral, white in colour and had very low fluorescence when dissolved in dilute HCl. In the low DOM treatment, small (<10 μm) rhombohedral crystallites with rounded corners were produced in aggregates, yet there were also much larger, prismatic crystals. Crystals that were synthesised in the medium and high DOM treatments were also prismatic with many steps and kinks. This may have important implications for interpreting the causes behind variability in crystal habit and fabric in speleothems, which have been previously utilised as proxies of hydrology and hydro-climatology.

Further calcite crystal growth experiments from parent solutions containing organic matter with different molecular characteristics should be undertaken to test preferential adsorption of different molecular constituents of DOM and the potential associated effects on crystal habit. For example, our study shows an absence of fluorescence peak A in the dissolved calcite. More research focusing on isolated DOM fractions should be undertaken to determine the reliability of calcite incorporation.

## Funding

This study was made possible by the Royal Society of New Zealand Marsden Fund Grant UOW1403 and Rutherford Discovery Fellowship award RDF-UOW1601 (AH) and the Australian Research Council (grant DP160101058) (SF).

## Declaration of competing interest

The authors declare that they have no known competing financial interests or personal relationships that could have appeared to influence the work reported in this paper.

## Acknowledgements

We would like to acknowledge Joshua L. Ratcliffe and Associate Professor David Campbell (University of Waikato) for assistance in collecting the peat water from Kopuatai bog, Dr. John C. Hellstrom (University of Melbourne) and Travis Cross (University of Auckland) for assistance in flowstone sample collection. Thanks to the Department of Conservation for allowing us to access and sample from Dave's Cave and Hodges Creek Cave (Research and Collection Permit 37934-GEO), and Pete and Libby Chandler for allowing us to access and sample from dripwaters and flowstones within Waipuna Cave and supporting our ongoing monitoring campaigns. Thanks to Helen Turner for assistance in using the SEM, Kirsty Vincent for help using the XRD and Steven Newcombe (all based at the University of Waikato) for producing the alterations to the glassware used in the experiment. Thanks to two anonymous reviewers for greatly improving the quality of this manuscript.

## Appendix A

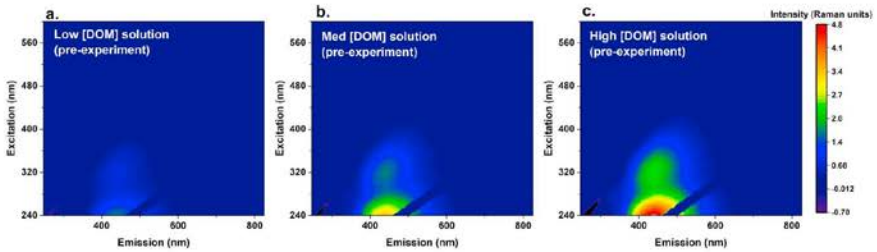


**Fig. A1.** 3D excitation-emission matrices of diluted peat-water solutions prior to crystal growth experiment.

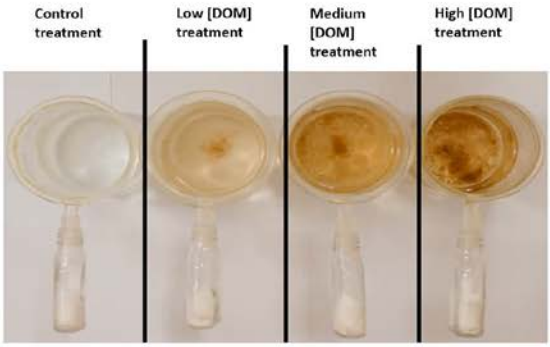


**Fig. A2.** Birds-eye view of beaker 'A' of Control, Low, Medium, High DOM treatments shortly after completion of the experiment on day 40.

Table A1
Cave dripwater samples and dissolved speleothem subsamples used in the composite 3D EEMs.

| Field-site locations of flowstones | N of dripwater samples | N of dissolved $CaCO_3$ fluorescence-inferred DOM measurements |
|---|---|---|
| Dave's Cave (Fiordland, South Island, New Zealand). | 2 | 3 (upper 3 mm) |
| Hodges Creek (Kahurangi National Park, South Island, New Zealand). | 5 | 3 (1,3,4 mm (no 2 mm subsample available)) |
| Waipuna (Waitomo region, North Island, New Zealand). | 32 | 3 (upper 3 mm) |

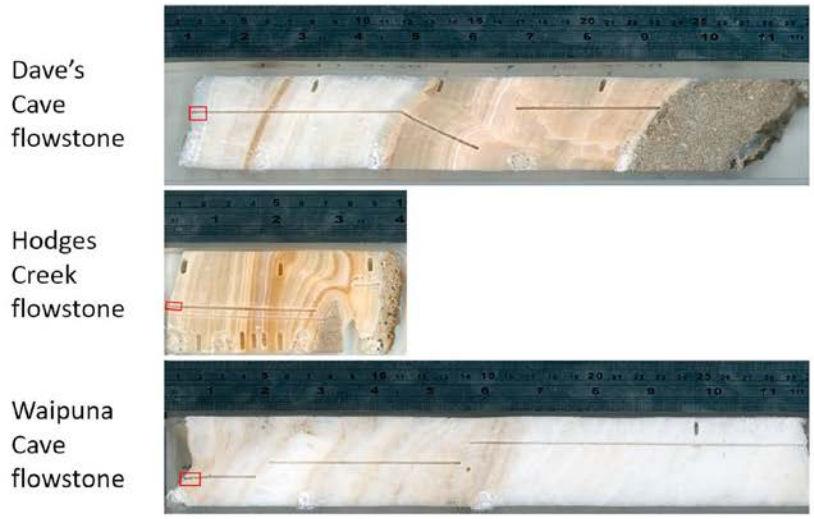


**Fig. A3.** Three flowstones from New Zealand displaying different colours that may be reflective of DOM incorporation. The red square marks the upper 3 mm from which fluorescence comparisons were made against dripwaters. (For interpretation of the references to colour in this figure legend, the reader is referred to the web version of this article.)

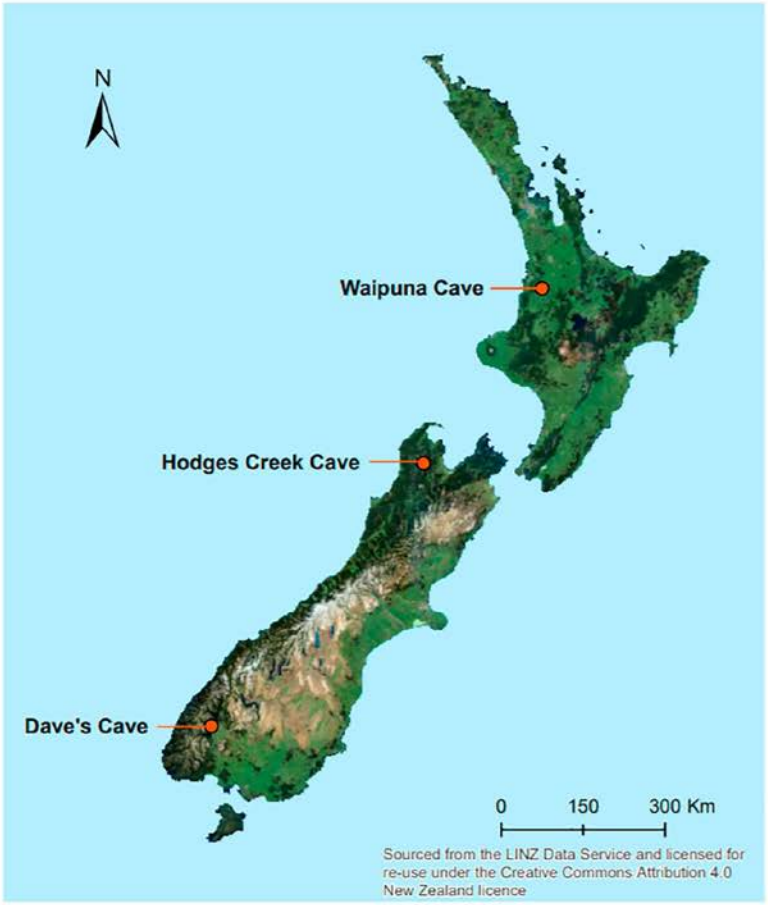


**Fig. A4.** Location of the cave sites within New Zealand.

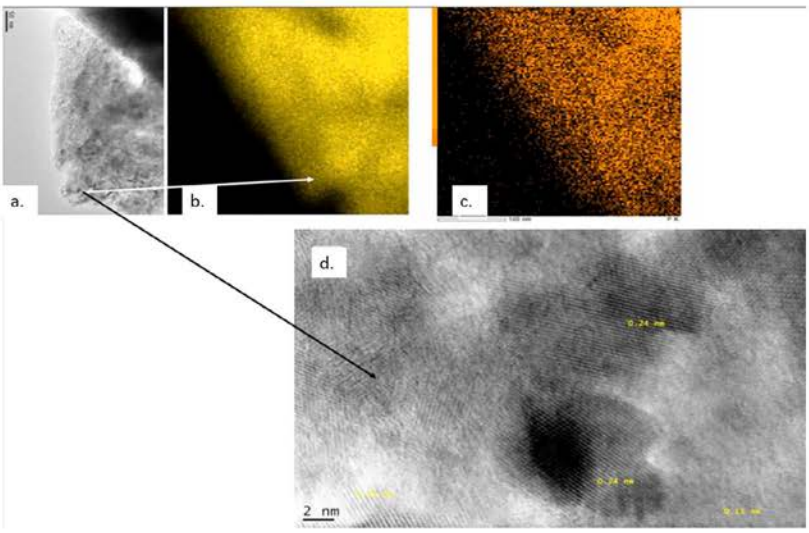


**Fig. A5.** TEM images of a precipitate from Rumbling Gut cave, Waitomo, N. Island, New Zealand. (a.) is the whole particle; (b.) a Ca map of the particle; (c.) a P map of the particle; and (d.) nanocrystal aggregation. The particle formed on a TEM grid where a drop of cave dripwater was left overnight to degas in a plastic vial. The particle was produced under a low drip-rate, which is common under low recharge conditions. The medium onto which the calcite (as determined by d-spacing of 2.4 Angstrom (d), the Ca composition (insert b)) precipitated is a C film on a copper grid. The result is an array of nanocrystals with lattices mismatched, bridged by amorphous material, which appears to consist of C and P, as well as Si. A reasonable interpretation is that colloidal particulate (Si, Al, C, P) was adsorbed onto the C grid and then the nanocrystal nucleation was favoured by the presence of colloids. These bridged the nanocrystals, which have a random orientation, most likely given by the amorphous C substrate. In the case of speleothems, where the substrate is already CaCO3 crystals, or our experiments (calcite seeds), it is more likely that the aggregates of nanocrystal found a suitable, active crystalline substrate that favoured their orientation. The colloidal particulate remained trapped between the nanocrystals.

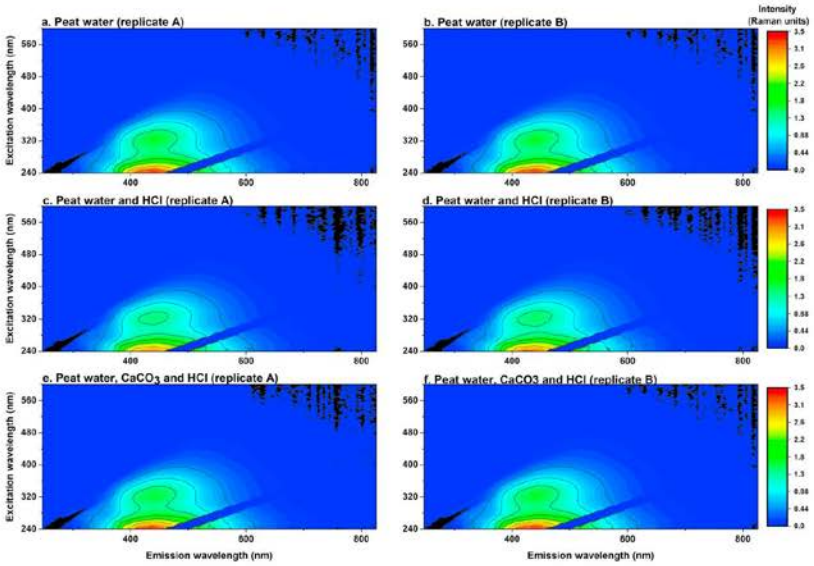


**Fig. A6.** 3D EEM spectra of Peat water (a., b.); Peat water and HCl (c., d.); and Peat water, dissolved $CaCO_3$ and HCl (e., f.).

## References

Affolter, S., et al., 2019. Central Europe temperature constrained by speleothem fluid inclusion water isotopes over the past 14,000 years. Sci. Adv. 5 (6), eaav3809.
Andersson, C.A., Bro, R., 2000. The N-way toolbox for MATLAB. Chemometrics and Intelligent Laboratory Systems 52 (1), 1–4.
Baker, A., Barnes, W., Smart, P.L., 1996. Speleothem luminescence intensity and spectral characteristics: signal calibration and a record of palaeovegetation change. Chem. Geol. 130 (1–2), 65–76.
Baker, A., et al., 1999. Stalagmite luminescence and peat humification records of palaeomoisture for the last 2500 years. Earth Planet. Sci. Lett. 165 (1), 157–162.
Baker, A., Tipping, E., Thacker, S.A., Gondar, D., 2008. Relating dissolved organic matter fluorescence and functional properties. Chemosphere 73 (11), 1765–1772.
Blyth, A.J., Asrat, A., Baker, A., Gulliver, P., Leng, M.J., Genty, D., 2007. A new approach to detecting vegetation and land-use change using high-resolution lipid biomarker

records in stalagmites. Quatern. Res. 68 (3), 314–324.
Blyth, A.J., Hartland, A., Baker, A., 2016. Organic proxies in speleothems – New developments, advantages and limitations. Quat. Sci. Rev. 149, 1–17.
Borsato, A., Frisia, S., Fairchild, I.J., Somogyi, A., Susini, J., 2007. Trace element distribution in annual stalagmite laminae mapped by micrometer-resolution X-ray fluorescence: implications for incorporation of environmentally significant species. Geochim. Cosmochim. Acta 71 (6), 1494–1512.
Braissant, O., Cailleau, G., Dupraz, C., Verrecchia, E.P., 2003. Bacterially induced mineralization of calcium carbonate in terrestrial environments: the role of exopolysaccharides and amino acids. J. Sediment. Res. 73 (3), 485–490.
Caldwell, J., Davey, A.G., Jennings, G.N., Spate, A.P., 1982. Colour in some Nullarbor Plain speleothems. Helictite 20 (1), 3–10.
Chalmin, E., Perrette, Y., Fanget, B., Susini, J., 2012. Investigation of organic matter entrapped in synthetic carbonates - a multimethod approach. Microsc. Microanal. 19, 132–144.
Charman, D.J., et al., 2001. Paleohydrological records from peat profiles and speleothems in Sutherland, northwest Scotland. Quat. Res. 55 (2), 223–234.
Coble, P.G., 1996. Characterization of marine and terrestrial DOM in seawater using excitation-emission matrix spectroscopy. Mar. Chem. 51 (4), 325–346.
Coble, P.G., Del Castillo, C.E., Avril, B., 1998. Distribution and optical properties of CDOM in the Arabian Sea during the 1995 Southwest Monsoon. Deep-Sea Res. II Top. Stud. Oceanogr. 45 (10), 2195–2223.
Cole, J.J., Caraco, N.F., Kling, G.W., Kratz, T.K., 1994. Carbon dioxide supersaturation in the surface waters of lakes. Science 265 (5178), 1568–1570.
Cole, J.J., et al., 2007. Plumbing the global carbon cycle: integrating inland waters into the terrestrial carbon budget. Ecosystems 10 (1), 172–185.
Cölfen, H., Antonietti, M., 2005. Mesocrystals: inorganic superstructures made by highly parallel crystallization and controlled alignment. Angew. Chem. Int. Ed. 44 (35), 5576–5591.
Evans, C.D., Monteith, D.T., Cooper, D.M., 2005. Long-term increases in surface water dissolved organic carbon: observations, possible causes and environmental impacts. Environ. Pollut. 137 (1), 55–71.
Evans, C.D., Chapman, P.J., Clark, J.M., Monteith, D.T., Cresser, M.S., 2006. Alternative explanations for rising dissolved organic carbon export from organic soils. Glob. Chang. Biol. 12 (11), 2044–2053.
Fairchild, I.J., Baker, A., 2012. Speleothem Science: From Process to Past Environments. John Wiley, Chichester, U.K.
Falini, G., Fermani, S., Tosi, G., Dinelli, E., 2009. Calcium carbonate morphology and structure in the presence of seawater ions and humic acids. Crystal Growth and Design 9 (5), 2065–2072.
Fellman, J.B., Hood, E., Spencer, R.G.M., 2010. Fluorescence spectroscopy opens new windows into dissolved organic matter dynamics in freshwater ecosystems: a review. Limnol. Oceanogr. 55 (6), 2452–2462.
Freeman, C., Evans, C.D., Monteith, D.T., Reynolds, B., Fenner, N., 2001. Export of organic carbon from peat soils. Nature 412, 785.
Freeman, C., et al., 2004. Export of dissolved organic carbon from peatlands under elevated carbon dioxide levels. Nature 430 (6996), 195.
Frisia, S., Borsato, A., Fairchild, I.J., McDermott, F., 2000. Calcite fabrics, growth mechanisms, and environments of formation in speleothems from the Italian Alps and southwestern Ireland. J. Sediment. Res. 70 (5), 1183–1196.
Frisia, S., Borsato, A., Hellstrom, J., 2018. High spatial resolution investigation of nucleation, growth and early diagenesis in speleothems as exemplar for sedimentary carbonates. Earth Sci. Rev. 178, 68–91.
Gázquez, F., Calaforra, J.M., Rull, F., Forti, P., García-Casco, A., 2012. Organic matter of fossil origin in the amberine speleothems from El Soplao Cave (Cantabria, Northern Spain). Int. J. Speleol. 41 (1), 113–123.
Genty, D., et al., 2001. Dead carbon in stalagmites: Carbonate bedrock paleodissolution vs. ageing of soil organic matter. Implications for $^{13}C$ variations in speleothems. Geochim. Cosmochim. Acta 65 (20), 3443–3457.
Gilmore, A.M., Cohen, S.M., 2013. Analysis of the chromophoric dissolved organic matter in water by EEMs with Horiba-Jobin Yvon fluorescence instrument called. Aqualog. Readout 41, 19–24.
Gonzalez, L.A., Carpenter, S.J., Lohmann, K.C., 1992. Inorganic calcite morphology: roles of fluid chemistry and fluid flow. J. Sediment. Res. 62 (3), 382–399.
Gruzensky, P., 1967. Growth of calcite crystals. Cryst. Growth 365–367.
Hartland, A., Zitoun, R., 2018. Transition metal availability to speleothems controlled by organic binding ligands. Geochemical Perspectives: Letters 8, 22–25.
Hartland, A., Fairchild, I.J., Lead, J.R., Baker, A., 2010. Fluorescent properties of organic carbon in cave dripwaters: effects of filtration, temperature and pH. Sci. Total Environ. 408 (23), 5940–5950.
Hartland, A., Fairchild, I.J., Lead, J.R., Zhang, H., Baalousha, M., 2011. Size, speciation and lability of NOM–metal complexes in hyperalkaline cave dripwater. Geochim. Cosmochim. Acta 75 (23), 7533–7551.
Hartland, A., et al., 2012. From soil to cave: transport of trace metals by natural organic matter in karst dripwaters. Chem. Geol. 304, 68–82.
Hartland, A., Fairchild, I.J., Müller, W., Dominguez-Villar, D., 2014. Preservation of NOM-metal complexes in a modern hyperalkaline stalagmite: implications for speleothem trace element geochemistry. Geochim. Cosmochim. Acta 128, 29–43.
Hill, C.A., Forti, P., Shaw, T.R., 1997. Cave Minerals of the World. National Speleological Society, Huntsville, AL.
Hoch, A.R., Reddy, M.M., Aiken, G.R., 2000. Calcite crystal growth inhibition by humic substances with emphasis on hydrophobic acids from the Florida Everglades. Geochim. Cosmochim. Acta 64 (1), 61–72.
Inskeep, W.P., Bloom, P.R., 1986. Kinetics of calcite precipitation in the presence of water soluble organic ligands. Soil Sci. Soc. Am. J. 50, 1167–1172.
Ishii, S.K.L., Boyer, T.H., 2012. Behavior of reoccurring PARAFAC components in fluorescent dissolved organic matter in natural and engineered systems: a critical review. Environ. Sci. Technol. 46 (4), 2006–2017.
Lead, J.R., Wilkinson, K.J., 2006. Aquatic colloids and nanoparticles: current knowledge and future trends. Environ. Chem. 3 (3), 159–171.
Lechleitner, F.A., Dittmar, T., Baldini, J.U.L., Prufer, K.M., Eglinton, T.I., 2017. Molecular signatures of dissolved organic matter in a tropical karst system. Org. Geochem. 113, 141–149.
Lee, Y.J., Elzinga, E.J., Reeder, R.J., 2005. Cu (II) adsorption at the calcite–water interface in the presence of natural organic matter: kinetic studies and molecular-scale characterization. Geochim. Cosmochim. Acta 69 (1), 49–61.
Leenheer, J.A., Croué, J.-P., 2003. Characterizing aquatic dissolved organic matter. Environ. Sci. Technol. 37, 18A–26A.
Lehmann, J., Kleber, M., 2015. The contentious nature of soil organic matter. Nature 528 (7580), 60–68.
Mavromatis, V., et al., 2017. Effect of organic ligands on Mg partitioning and Mg isotope fractionation during low-temperature precipitation of calcite in the absence of growth rate effects. Geochim. Cosmochim. Acta 207, 139–153.
Mayorga, E., et al., 2005. Young organic matter as a source of carbon dioxide outgassing from Amazonian rivers. Nature 436, 538.
Meyer, H.J., 1984. The influence of impurities on the growth rate of calcite. J. Cryst. Growth 66 (3), 639–646.
Monteith, D.T., et al., 2007. Dissolved organic carbon trends resulting from changes in atmospheric deposition chemistry. Nature 450 (7169), 537–540.
Monteith, D.T., Evans, C.D., Henrys, P.A., Simpson, G.L., Malcolm, I.A., 2014. Trends in the hydrochemistry of acid-sensitive surface waters in the UK 1988–2008. Ecol. Indic. 37, 287–303.
Murphy, K.R., Stedmon, C.A., Graeber, D., Bro, R., 2013. Fluorescence spectroscopy and multi-way techniques. PARAFAC. Anal. Methods 5 (23), 6557–6566.
Nagra, G., et al., 2017. Dating stalagmites in Mediterranean climates using annual trace element cycles. Sci. Rep. 7 (1), 621.
Ni, M., Ratner, B.D., 2008. Differentiating calcium carbonate polymorphs by surface analysis techniques—an XPS and TOF-SIMS study. Surf. Interface Anal. 40 (10), 1356–1361.
Nielsen, M.H., Aloni, S., De Yoreo, J.J., 2014. In situ TEM imaging of $CaCO_3$ nucleation reveals coexistence of direct and indirect pathways. Science 345 (6201), 1158–1162.
Orme, C.A., et al., 2001. Formation of chiral morphologies through selective binding of amino acids to calcite surface steps. Nature 411 (6839), 775.
Perrette, Y., et al., 2015. Determining soil sources by organic matter EPR fingerprints in two modern speleothems. Org. Geochem. 88, 59–68.
Phillips, B.L., Zhang, Z., Kubista, L., Frisia, S., Borsato, A., 2016. NMR spectroscopic study of organic phosphate esters coprecipitated with calcite. Geochim. Cosmochim. Acta 183, 46–62.
Quiers, M., Perrette, Y., Chalmin, E., Fanget, B., Poulenard, J., 2015. Geochemical mapping of organic carbon in stalagmites using liquid-phase and solid-phase fluorescence. Chem. Geol. 411, 240–247.
Rae, R., Howard-Williams, C., Hawes, I., Schwarz, A.-M., Vincent, W.F., 2001. Penetration of solar ultraviolet radiation into New Zealand lakes: influence of dissolved organic carbon and catchment vegetation. Limnology 2 (2), 79–89.
Ramseyer, K., et al., 1997. Nature and origin of organic matter in carbonates from speleothems, marine cements and coral skeletons. Org. Geochem. 26 (5–6), 361–378.
Ratcliffe, J.L., Campbell, D.I., Clarkson, B.R., Wall, A.M., Schipper, L.A., 2019. Water table fluctuations control $CO_2$ exchange in wet and dry bogs through different mechanisms. Sci. Total Environ. 655, 1037–1046.
Rutlidge, H., et al., 2014. Dripwater organic matter and trace element geochemistry in a semi-arid karst environment: implications for speleothem paleoclimatology. Geochim. Cosmochim. Acta 135, 217–230.
Sangwal, K., 1996. Effects of impurities on crystal growth processes. Prog. Cryst. Growth Charact. Mater. 32 (1), 3–43.
Sauve, S., Hendershot, W., Allen, H.E., 2000. Solid-solution partitioning of metals in contaminated soils: dependence on pH, total metal burden, and organic matter. Environ. Sci. Technol. 34 (7), 1125–1131.
Schmidt, M.W.I., et al., 2011. Persistence of soil organic matter as an ecosystem property. Nature 478, 49.
Scroxton, N., et al., 2018. Rapid measurement of strontium in speleothems using core-scanning micro X-ray fluorescence. Chem. Geol. 487, 12–22.
Stanley, E.H., Powers, S.M., Lottig, N.R., Buffam, I., Crawford, J.T., 2012. Contemporary changes in dissolved organic carbon (DOC) in human-dominated rivers: is there a role for DOC management? Freshw. Biol. 57, 26–42.
Stedmon, C.A., Bro, R., 2008. Characterizing dissolved organic matter fluorescence with parallel factor analysis: a tutorial. Limnol. Oceanogr. Methods 6 (11), 572–579.
Sulatskaya, A.I., Maskevich, A.A., Kuznetsova, I.M., Uversky, V.N., Turoverov, K.K., 2010. Fluorescence quantum yield of thioflavin T in rigid isotropic solution and incorporated into the amyloid fibrils. PLoS One 5 (10), e15385.
Van Beynen, P., Bourbonniere, R., Ford, D., Schwarcz, H., 2001. Causes of colour and fluorescence in speleothems. Chem. Geol. 175 (3–4), 319–341.
White, W.B., 1981. Reflectance spectra and colour in speleothems. National Speleological Society Bulletin 43 (1), 20–26.
Williams, P.W., Marshall, A., Ford, D.C., Jenkinson, A.V., 1999. Palaeoclimatic interpretation of stable isotope data from Holocene speleothems of the Waitomo district, North Island, New Zealand. The Holocene 9 (6), 649–657.
Wynn, P.M., et al., 2018. Sulphate partitioning into calcite: Experimental verification of pH control and application to seasonality in speleothems. Geochim. Cosmochim. Acta 226, 69–83.

# 5 Chapter 5

# Climate controls soil DOC export in the absence of human impacts

Andrew R. Pearson[a*]; Adam Hartland[a]; John C. Hellstrom[b]; Marcus J. Vandergoes[c]; Bethany R.S. Fox[d]; Sebastian F.M. Breitenbach[e]; Russell N. Drysdale[f,g].

[a]Environmental Research Institute, School of Science, Faculty of Science and Engineering, University of Waikato, Hamilton ,3126, New Zealand.

[b]School of Earth Sciences, The University of Melbourne, Victoria 3010, Australia.

[c]GNS Science, PO Box 30-368, Lower Hutt 5040, New Zealand.

[d]Department of Biological and Geographical Sciences, University of Huddersfield, Huddersfield, HD1 3DH, United Kingdom.

[e] Institute for Geology, Mineralogy & Geophysics, Ruhr-University Bochum, Bochum, Germany.

[f] School of Geography, University of Melbourne, Parkville, VIC, 3010, Australia.

[g]Environnements, Dynamiques et Territoires de la Montagne, UMR CNRS, Université de Savoie-Mont Blanc, 73376, Le Bourget du Lac, France.

*Corresponding author: apearson181@gmail.com

## 5.1 Abstract

Soils store a greater mass of carbon than terrestrial vegetation and the atmosphere combined, meaning that changes in soil carbon export can heavily impact the global carbon budget. The global average temperature is set to increase by >2 °C by 2100, yet, the impacts of climate change on dissolved organic carbon (DOC) export from soil are poorly understood. Using palaeo-environmental records of DOC may enable us reconstruct DOC concentrations over centennial/millennial timescales, and under varying climatic conditions, thus enabling us to assess the impact of climatic shifts.

This project focuses on New Zealand, a geographically isolated archipelago located in the Pacific Ocean. New Zealand had no human inhabitants until the 13$^{th}$ century and was not subject to 20$^{th}$ century industrial-scale atmospheric sulphate deposition. However, New Zealand has undergone notable climatic and environmental changes through the past 14,000 years BP.

In this study, 3D EEM fluorescence was used to measure humic-like DOC concentrations in modern dripwaters and within three flowstones (secondary carbonate deposits) from three caves distributed along a 7° latitudinal gradient. Flowstones capture DOC from dripwaters via co-precipitation, providing an authentic record of aquatic DOC trends. At each site, heightened humic-like DOC concentrations corresponded with periods of known temperature increases and often at times of reduced rainfall. The findings of this study imply that climate-driven landscape responses play an important role in soil C export and that speleothems are reliable recorders of such changes.

## 5.2 Background & Introduction

Soil organic carbon (SOC) stocks contain more carbon than vegetation and the atmosphere combined (Batjes, 1996). Soil can release organic carbon as DOC into aquatic environments, leading to several environmental impacts. For example, heightened DOC concentrations in terrestrial water bodies can reduce drinking water quality (Lavonen *et al.*, 2015), reduce aquatic biomass production (Karlsson *et al.*, 2015), and facilitate the release of $CO_2$ to the atmosphere (Lehmann & Kleber, 2015). Further, average global temperature is predicted to rise by > 2.0 °C by the year 2100 (Raftery *et al.*, 2017), with unknown consequences for the SOC pool and DOC export.

This study aimed to assess the impact of climate (temperature and precipitation) on soil DOC export over the past 14,000 years using speleothem and lake archives in New Zealand.

### 5.2.1 New Zealand's pre-human landscape can enable us to assess the impact of climate

New Zealand is a geographically isolated archipelago, located in the southern mid-latitudes (ca. 34.4 to 46.6 °S). New Zealand provides a unique opportunity to test the impacts of climate on soil carbon export because it was completely free of humans until the 13$^{th}$ century (McWethy *et al.*, 2014). Indeed, New Zealand's natural 'reference state' was in all practical terms, prior to the 18th century CE (Abell *et al.*, 2019), when European colonisers began to use land on an industrial scale.

New Zealand has undergone several climatic shifts and associated landscape responses through the past ~14,000 years BP (Jara *et al.*, 2015). New Zealand's isolation and relative lack of (pre 18th century CE) human influence on its

environment therefore provides a unique opportunity to assess the causes of soil DOC export in a pre-human continent. In the absence of instrumental data, paleo-environmental archives, such as speleothems and lake sediments, can enhance our understanding of long-term environmental change.

Testing the impact of climate on soil DOC export was undertaken by reconstructing humic-like DOC concentrations in cave dripwaters through the past ~14,000 years at three cave sites spanning a 7-degree latitudinal gradient. Our study analysed speleothems (secondary carbonate deposits found in caves) which accumulate through time, incorporating dissolved organic carbon (from their parent dripwaters) (Figure 5.1) as they grow.

New Zealand's climate has been heavily influenced by westerly winds throughout the Holocene, the strength and position of which have waxed and waned through time (Shulmeister *et al.*, 2004). Therefore, we compared our humic-like DOC concentration reconstructions against an alkenone-based sea surface temperature record from the Tasman Sea (Barrows *et al.*, 2007) off the west coast of New Zealand's South Island (Figure 5.2).

This study primarily aimed to test the impact of temperature on soil DOC export. However, it is also pertinent to understand the effect of meteoric precipitation, which can alter biodegradability, leaching and potentially alter transport of DOC from soil (Kalbitz *et al.*, 2000; Kaiser & Kalbitz, 2012). Ratios of Mg to Ca in speleothems are well-established as a proxy for effective meteoric precipitation overlying caves (Cruz *et al.*, 2007; Warken *et al.*, 2018), and were utilised in each flowstone record to qualitatively reconstruct rainfall through the past ~14,000 years BP.

### 5.2.2 Extending the record of aqueous DOC using fluorescence and speleothem archives

Speleothems have long been established as archives of environmental change via their geochemical and biogeochemical signatures. Speleothems are formed when water that is charged with $CO_2$ (carbonic acid, $H_2CO_3$) dissolves small amounts of limestone ($CaCO_3$) bedrock (Figure 5.1). Once these seepage waters enter a cave system, the lower $pCO_2$ within the cave atmosphere causes $CO_2$ to degas from solution, leading to the re-precipitation of $CaCO_3$ as a speleothem (Fairchild & Treble, 2009) via the equation:

$$\mathbf{Ca^{2+} + 2HCO_3^- \rightarrow CaCO_3 + H_2O + CO_2} \quad (5\text{-}1)$$

Speleothems accumulate through time, are not typically subject to post-depositional disturbance (unlike other archives such as lake sediments), and can also be precisely dated, enabling reconstructions of environmental conditions spanning hundreds of millennia (Li *et al.*, 1989). Speleothems have long been known to incorporate organic material during their growth (Baker *et al.*, 1998; Genty & Massault, 1999; Genty *et al.*, 2001; Blyth *et al.*, 2007; Blyth *et al.*, 2008; Perrette *et al.*, 2015; Quiers *et al.*, 2015), including pollen grains (Brook *et al.*, 1990; McGarry & Caseldine, 2004; Sniderman *et al.*, 2019), lipid biomarkers (Xie *et al.*, 2003; Rushdi *et al.*, 2011; Blyth *et al.*, 2016), lignin (Blyth *et al.*, 2016) and amino acids (James *et al.*, 1994). Experimental studies have also demonstrated that carbonates can be reliable recorders of DOC concentration (Pearson *et al.*, 2020). In most speleothems, DOC is predominantly derived from the overlying environment (soil, vegetation), or from microbial communities within the cave (Blyth *et al.*, 2016). DOC is incorporated into speleothems as they grow due to surface adsorption of organic molecules and bonding between organic functional groups (e.g. carboxyl ($COO^-$) and cations

($Ca^{2+}$) (Fairchild & Baker, 2012; Hartland *et al.*, 2014)). DOC can also be incorporated as fluid inclusions in the inter-crystalline pore spaces (Ramseyer *et al.*, 1997). This study utilised flowstones, which accrete when calcium carbonate precipitates from thin sheets of water on cave walls and floors (Fairchild & Baker, 2012), and can accumulate to be several metres thick. Flowstones can be fed by several drip-points (as opposed to stalagmites which are typically fed by one) (Figure 5.1), and therefore provide a more general cave record that is not reliant on one single drip point

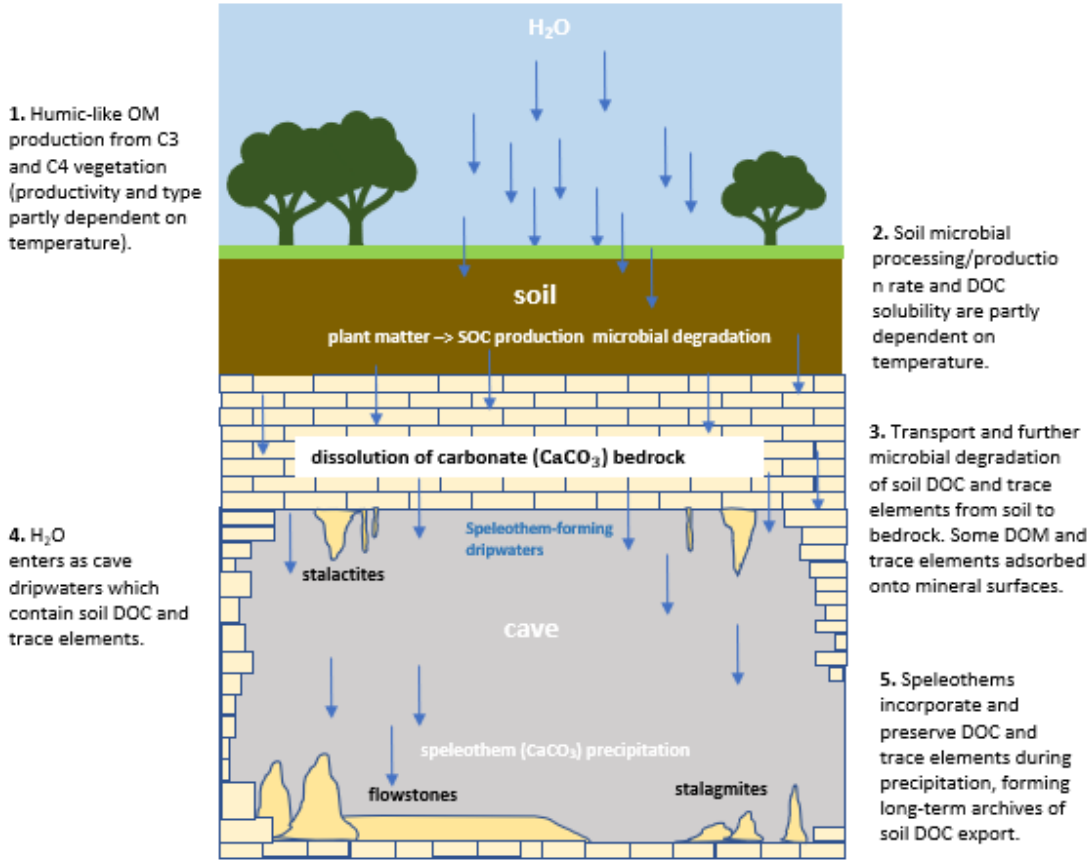


**Figure 5.1**-Summary of DOC transport from soil to speleothem. Important processes are numbered and briefly described.

Early studies of organic material in speleothems focused on the context of being a determinate of speleothem colour (Caldwell *et al.*, 1982; Van Beynen *et al.*, 2001). Baker *et al.*, (1993) and Shopov *et al.*, (1994) highlighted that speleothems display

luminescence caused by the presence of humic-like and fulvic-like material incorporated within. DOC quality can reflect source, biogeochemical reactions, the hydrologic regime and land-cover (Jaffé *et al.*, 2008), and can be assessed by fluorescence methods, which have been employed in a range of environmental settings (Coble *et al.*, 1990; Parlanti *et al.*, 2000; Baker, 2001; Baker & Inverarity, 2004; Baker & Spencer, 2004; Burdige *et al.*, 2004; Fellman *et al.*, 2010; Ziegelgruber *et al.*, 2013). Organic material fluoresces when the loosely bound electrons of molecules are excited by light energy (i.e. a photon) (Senesi *et al.*, 1989; Senesi *et al.*, 1991). The intensity of the re-emitted light (fluorescence) can be used to measure concentrations, whilst the wavelengths at which excitation and emission occur can be used to distinguish DOC molecular characteristics.

This study utilised 3D EEMs (excitation-emission matrices) to assess humic-like DOC concentrations (a function of DOC export from soil) in flowstones using the same methodological approach as Chapter 4 (Pearson *et al.*, 2020). From the concentrations of flowstone DOC through time, dripwater humic-like DOC concentrations (a function of soil DOC export) were reconstructed (using modern dripwater measurements as an analogue) at three cave sites (Figure 5.2). 3D EEMs (excitation-emission matrices) present fluorescence intensity data as a function of excitation and emission (Ishii & Boyer, 2012), the wavelengths at which excitation and emission occur can inform characterisation of the organic molecules present in the sample, whilst the intensity of the fluorescence can provide a quantitative measurement of humic-like DOC concentration. Numerous studies have applied fluorescence methods to assess DOC in cave dripwaters and speleothems (Baker *et al.*, 1996; Baker *et al.*, 1998; Hartland *et al.*, 2012; Rutlidge *et al.*, 2014; Perrette *et al.*, 2015; Quiers *et al.*, 2015; Rutlidge *et al.*, 2015).

## 5.3 Methods

### 5.3.1 Location and field site characteristics

Preference for site selection was given to relatively high-altitude (and therefore more climatically sensitive) areas that have been relatively undisturbed by humans. The three cave sites span a latitudinal gradient of ca. 7-degrees (or around 1,000 km). Waipuna Cave (38.3° S, approx. 80 m above sea level) is situated within the Waitomo region, western North Island (Figure 5.2 a) and is overlain by dense native forest, with organic-rich brown soils (Figure 5.A1). The limestone that makes up this region was deposited during the Oligocene, when the area was a shallow seafloor.

Hodges Creek (41° S, approx. 940 m above sea-level) is located on Mount Arthur tablelands, Kahurangi National Park, Nelson region, South Island (Figure 5.2 a). The cave is overlain by dense forest, dominated by silver beech with ferns and mosses in the lower canopy, producing a dark, organic-rich soil (5.A2). Mount Arthur tablelands are within New Zealand's temperate zone, with prevailing westerlies and a maritime climate. This region receives > 2,000 mm rainfall per year. The DOC reconstruction from Hodges Creek was compared against a sedimentary TOC record from Adelaide Tarn. Adelaide Tarn (described in detail in Chapter 3) is a sub-alpine lake also located in a glacial cirque in the Douglas Range of Kahurangi National Park (Figure 5.2 a). The proximity to Hodges Creek and its high-altitude setting means that Adelaide Tarn is a suitable record for comparison against Hodges Creek Cave. Both Adelaide Tarn and Hodge's Creek were covered by ice during the last glacial period. The ice had completely evacuated from the area by 14,000 years BP (Shulmeister *et al.*, 2005).

Dave's Cave (45° S, approx. 1450 m elevation above sea-level) is located close to the summit of Mount Luxmore, Fiordland, Southland, South West South Island. Fiordland is characterised by u-shaped valleys and glacial-carved lakes, which were formed during the last ice age (Hancox & Perrin, 2009). Above the cave, there are numerous tarns located on the mountainside, which overlooks lake Te Anau and South Fiord to the north. The summit of Mount Luxmore is positioned above the treeline, which is dominated by silver beech. Vegetation overlying Dave's Cave is relatively sparse, consisting of alpine shrubs and tussocks (Figure 5.2 d). The soil directly above the cave is highly organic and water-logged (Figure 5.A3), as the region receives up to 6,000 mm of rainfall per annum.

Each record of DOC was compared against an alkenone-based sea-surface temperature (SST) reconstruction from the Tasman Sea (Figure 5.2 a) (Barrows *et al.*, 2007). The SST record was selected for its location off the west coast, as westerly winds are the dominant wind-direction in New Zealand (Hodgson & Sime, 2010).

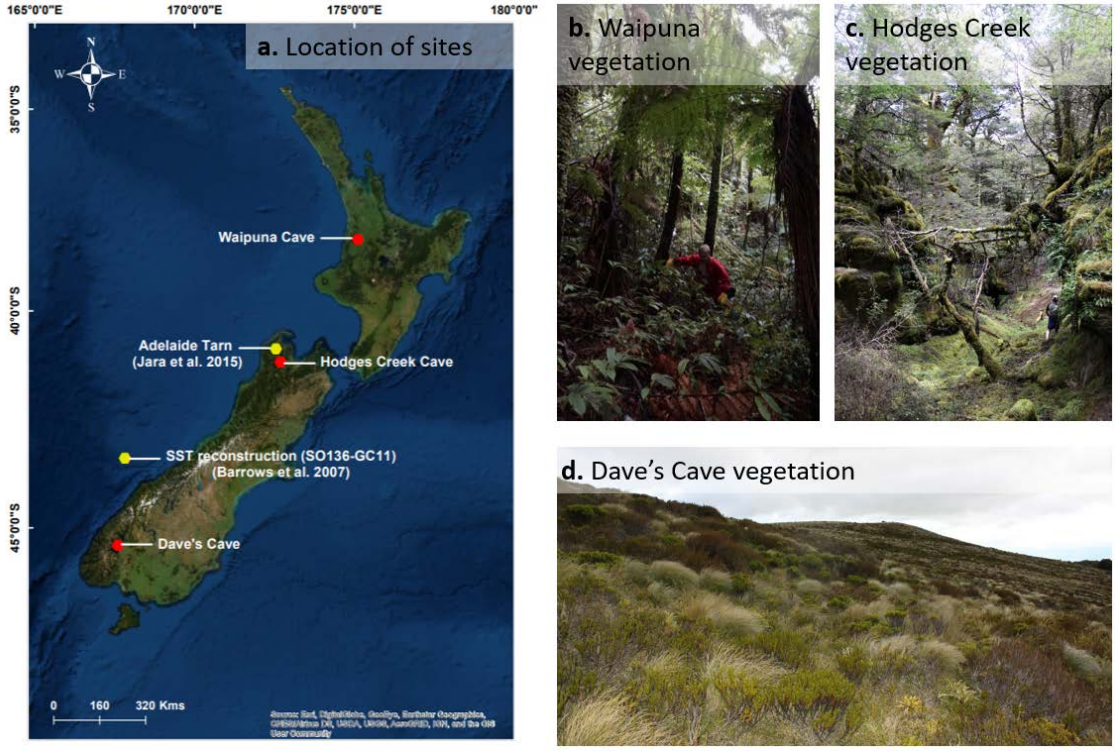


**Figure 5.2 (a.)** Location of cave sites (red circles) spanning ~7 ° of latitude across New Zealand, and Adelaide Tarn (TOC record) (yellow circle) and marine sediment core SO136-GC11 (SST reconstruction) (yellow circle); **(b.)** Vegetation overlying Waipuna Cave (Waitomo region, western North Island); **(c.)** Vegetation overlying Hodges Creek (Mt. Arthur, north-west South Island) **(d.)** Vegetation overlying Dave's Cave (Mt. Luxmore, south-west South Island).

**Table 5.1-** Above-cave environmental characteristics. Soils described using the New Zealand Soil Classification (Hewitt, 2010).

| Cave site | Location | Local Climate | Local vegetation | Local soil description | Modern cave dripwater humic-like DOC concentrations (ppm) |
|---|---|---|---|---|---|
| **Waipuna Cave** | **Lat:** 38.26 °S. **Long:** 175.10. **Altitude**: 80 m Waitomo, Waikato, western North Island. | **Surface MAT:** ~13 °C. **Annual Precipitation:** 1,473 mm (Waitomo region). | Podocarp conifer forest, dense sub-canopy consisting of shrubs, ferns, tree ferns. Some fungus. | Deep (> 1m) soils, typic orthic allophanic (LO) being developed on North Island rhyolitic volcanic ash deposits. Soils are exceptionally well drained; water typically reaches the cave within days/weeks following rainfall events (Nava *et al.,* in prep). | **Mean value:** 0.7 **Range:** 0.4–1.6 **Sample N:** 28 |
| ***Adelaide Tarn** | **Lat:** 40.56 °S. **Long:** 172.32. **Altitude:** 1250 | **Surface MAT:** ~6 °C **Annual Precipitation:** >2,500 mm | Located above the treeline. *Chionochloa* tussock grassland dominates within the cirque. | Thin soils. | N/A |

| | | | | | |
|---|---|---|---|---|---|
| **Hodges Creek Cave** | **Lat:** 41.19 °S. **Long:** 172.72. **Altitude**: 940 m. Kahurangi NP, Nelson, NW South Island. | **Surface MAT:** ~10 °C. **Annual Precipitation:** 2,500 mm | Mature beech forest, mosses. | Heavily weathered Oligocene limestone, incised by deep grykes filled with litter organic (LO) soils, which transition to orthic gley (GO) due to waterlogging (Fe reduction). | **Mean value:** 4.2 **Range:** 2.9–5.2 **Sample N:** 6 |
| **Dave's Cave** | **Lat:** 45.39 °S. **Long:** 167.59. **Altitude:** 1,450 m. Fiordland NP, Southland, SW South Island. | **Surface MAT:** ~6 °C **Annual Precipitation:** Up to 6,000 mm | Located above the treeline (beech). Thick tussock, grasses, native alpine plants. | Water-logged, organic rich. Soils had light brown A horizons at 20 cm. Characteristic Fe staining indicating Fe reduction and oxidation. | **Mean value:** 1.7 **Range:** 1.1–2.3 **Sample N:** 2 |

*TOC record from Adelaide Tarn's sedimentary archive. Methodology and findings described in detail in Chapter 3.

### 5.3.2 Flowstone sample recovery

Prior to sample recovery, overlying vegetation was photographed and described. Soil type was described (following the New Zealand Soil classification system (Hewitt, 2010)) to a depth of 1 m (Table 5.1) at each site (Figure 5.A 1 (Waipuna Cave), 5.A2 (Hodges Creek Cave), and 5.A3 (Dave's Cave)).

Within the cave, flowstone samples that were away from the cave entrance were visually inspected for the likelihood of good preservation, lateral laminations and for being under current growth-conditions. Core samples were extracted (Department of Conservation research and collection permit 37934-GEO) using a diamond-tipped steel coring-bit using a Makita drill (18 V). A flow of water was used for flushing cuttings from the borehole throughout the coring process. Holes created by coring were plugged with calcite. Scanned images of the cores are in Figure 5.A4 (WP15-1.1- Waipuna), Figure 5.A5 (HC15-2- Hodges Creek) and Figure 5.A6 (DC15-1- Dave's Cave).

### 5.3.3 Cave monitoring and dripwater sampling

Dripwaters were sampled monthly from numerous drips from 2015 to 2018 in Waipuna Cave, and in summer 2015 in Dave's Cave and Hodges Creek Cave. Dripwater electric conductivity and pH were measured on site. Dripwater trace element concentrations, total organic carbon concentrations, and 3D EEM fluorescence were analysed in the laboratory (see relevant method sub-section for each method).

### 5.3.4 Preparation of speleothems for analysis

Flowstones were placed into polyester casting and encapsulating resin and mixed with an MEKP (methyl ethyl ketone peroxide) catalyst. After the solidification of the resin, the slabs were sliced with a diamond-tipped circular saw, so that the

internal surface of the flowstones were exposed. The sample surfaces were then ground flat using diamond-tipped polishing belts and polished using fine cork-belts.

### 5.3.5 Flowstone sub-sample milling and 3D EEM fluorescence analysis

Samples and equipment were cleaned thoroughly with 95 % ethanol, before the upper 0.2 mm of sample was milled and discarded to reduce the possibility of contamination. Sub-sample powders were milled at 1 mm resolution along the growth-axis of each flowstone. Milling was undertaken using a tungsten carbide drill-bit on a Sherline 5410 deluxe vertical milling machine. Powdered calcite (5 mg) was dissolved in 4.5 ml of 0.025 M HCl (18 MΩ water) in acid-washed (2 % $HNO_3$) polypropylene tubes and then centrifuged at 3600 rpm for 20 minutes. The solutions (pH ~5.6) were placed in quartz cuvettes (4 ml volume, 1 cm width) and measured for fluorescence using a charge-coupled device (CCD) detector in a Horiba Jobin Yvon Aqualog® fluorescence spectrometer. The fluorescence protocol used a 0.5 second integration time, a step-size of 3 nm, and a measurement range of 600–240 nm excitation and 800–245 nm emission wavelengths. To correct for instrument specific biases (Stedmon & Bro, 2008), each matrix was corrected for inner-filter effects, scatter lines were Rayleigh masked, and spectra were then Raman normalised to the mean Raman intensity of Milli-Q water (*18.*0 MΩ) using the instruments in-built software programme.

3D EEMs data were processed using parallel factor analysis (PARAFAC) using the N-way toolbox (Andersson & Bro, 2000), a multivariate modelling technique developed in MATLAB®. PARAFAC provides multi-way data analysis in which the underlying phenomena of the fluorescence can be distinguished and separated into statistically valid independent components, thus providing estimates of the relative contribution of each component to the total fluorescence signal. PARAFAC is a more advanced method than manual peak identification and enables the

quantification of common fluorophores present in natural organic matter samples (i.e. humic-like, fulvic-like and protein-like peaks) as statistical components (Fellman *et al.*, 2010; Ishii & Boyer, 2012).

### 5.3.6 Calibration of humic-like DOC concentrations using natural DOC standards

Water was pumped from approximately 20 m depth from Kopuatai bog, central North Island, New Zealand. The water was filtered through 0.45 μm cellulose-acetate syringe filters (Microanalytix Pty Ltd, Australia), and analysed for TOC (total organic carbon) using a wet-oxidation method, producing a value of 16.3 ppm. The peat-water was diluted with deionised water to produce solutions containing 5.6 ppm, 10.0 ppm, and 14.4 ppm TOC, and calibrated against PARAFAC component scores, producing a calibration of 0.99 $R^2$. The peat water contained one, simple humic-like component (with no protein-like fluorescence discernible using PARAFAC analysis).

3D EEMs data from each cave site (speleothems and dripwaters) were analysed separately in PARAFAC. However, each PARAFAC model included 3D EEMs of Kopuatai peat water (which were previously analysed for TOC concentrations) to create a bespoke calibration for each site (as humic-like fluorescence characteristics were slightly variable between cave sites). The equations from each calibration (Kopuatai humic-like DOC vs TOC concentrations) were then used to calculate humic-like DOC concentrations in the individual carbonate digests and then in the cave dripwaters (using the appropriate Kd value [see Chapter 4]).

### 5.3.7 Reconstructing humic-like DOC concentrations in palaeo-dripwaters

After calculation of the equivalent humic-like DOC concentration in each carbonate sample (mol/g), the efficiency of incorporation of DOC from solution (i.e.

dripwaters) to the upper 1 mm of speleothem was calculated as a partitioning coefficient, where $_{(s)}$ = within calcite, and $_{(aq)}$ = within solution, and concentrations are in moles, using the formula:

$$\mathbf{K_d = (DOC_{(s)}/Ca_{(s)}) / (DOC_{(aq)}/Ca_{(aq)})} \quad (5\text{-}2)$$

The $K_d$ values produced from the humic-like DOC PARAFAC scores of the modern dripwaters (mean PARAFAC score) and top 1mm of each speleothem sample were then used to back-calculate dripwater concentrations through the past ~14,000 years BP at each cave site, based on humic-like DOC concentrations of the speleothems (which were calculated using a calibration against humic-like fluorescence intensity from the Kopuatai peat water solutions). The $K_d$ values thus derived were consistent with experimental values from a laboratory partitioning experiment (Chapter 4).

### 5.3.8 Speleothem sub-sampling for dating

Speleothem sub-samples were milled for dating. Flowstones and equipment were cleaned thoroughly with 95 % ethanol, before and after a 'cleaning' traverse (in which the upper 0.2 mm of calcite from each trench was milled to a powder and then discarded). Sub-sample trenches were of different sizes, as trenches followed visible growth laminae. Milling was undertaken using a tungsten carbide drill-bit and a Sherline 5410 deluxe milling machine. Ratios of $^{230}Th/^{234}U$ were determined using a Nu Instruments multi-collector inductively coupled plasma mass-spectrometer (MC-ICP-MS) at the University of Melbourne (Hellstrom, 2003).

Age-depth modelling was undertaken using the Constructing Proxy Records from Age Models (COPRA) algorithm (Breitenbach *et al.*, 2012) in MATLAB. COPRA was used to generate 2000 Monte-Carlo simulations of each age-model, whilst

Piecewise cubic Hermite interpolation (PCHIP) was applied to interpolate the ages and produce median proxy values with 95 % confidence intervals.

### 5.3.9 Elemental analysis using LA-ICPMS

Trace element measurements were collected at 100 µm spatial resolution using a RESOlution-SE Compact 193 nm excimer laser ablation (LA) system in tandem with an Agilent 8900 Inductively Coupled Plasma- Mass Spectrometer (ICP-MS). Analyses of the speleothem surface were conducted by pulsing the laser at 10 Hz with a 100 µm spot size and energy density of 5.0 J/cm$^2$ with a scan speed of 27.855 µm/s. Ultra-high purity helium was used as the carrier gas to deliver the ablated sample from the LA system to the ICP-MS. The ICP-MS was optimized to maximum sensitivity daily (Table 5.1). Background counts (gas background, measured with the laser off) were collected for 30 seconds between samples. National institute of standards and Technology (NIST) glass standards (610, 612) were analysed after every sample line to account for any instrument drift.

Data processing was performed using Iolite (v3.32 (Paton *et al.*, 2011)). Background counts were subtracted from the raw data, and all data were standardised to NIST 612 glass. NIST 610 glass was utilised as a secondary standard. GeoReM database (Jochum *et al.*, 2005) was utilised for NIST glass values.

## 5.4 Results and discussion

### 5.4.1 Flowstone age-depth models

The details of the dates of the flowstone samples for WP15-1-1 are given in Table 5.2. Figure 5.3 presents the resulting age-depth model. WP15-1-1 represents the upper section of a larger flowstone core (which contains two other, lower sections not featured in this study). The flowstone was actively accumulating calcite when

it was removed from the cave in 2015, and therefore the top of the core was taken to be -65 years BP. Prior to the Holocene, the growth rate is relatively fast but then appears to have been roughly constant from 13,000 years BP. The age uncertainty increases near the top because of the large 2 σ error of sample UA.

#### 5.4.1.1 WP15-1-1 (Waipuna Cave) age-depth model

**Table 5.2**- U/Th ages for flowstone core WP15-1-1.

| U/Th Sample ID | Depth (mm) | Age (years BP) | 2 σ (years) |
|---|---|---|---|
| WP15- 1.1 UA | 3.88 | 468 | 2026 |
| WP15 1.1 UB | 65.8 | 4770 | 594 |
| WP15 1.1 UC | 147.95 | 9405 | 452 |
| WP15 1.1 UC_2 | 209 | 12606 | 134 |
| WP15 1.1 UC_3 | 255 | 12751 | 222 |
| WP15 1.1 UC_4 | 283 | 13212 | 244 |

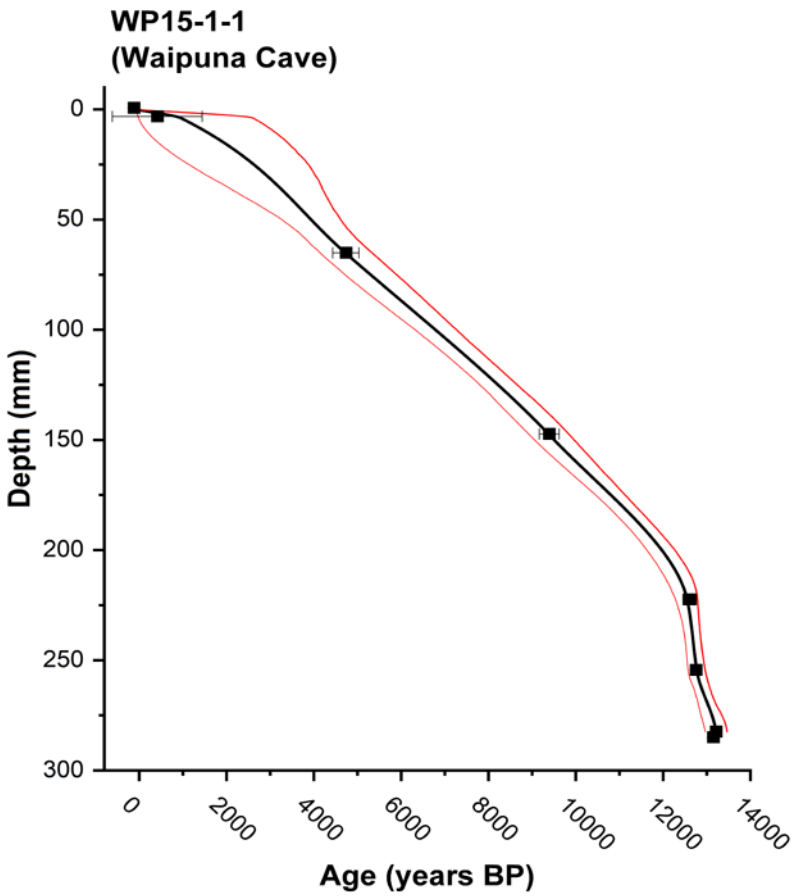


**Figure 5.3-** Age-depth model for WP15-1-1. The thick black line represents the median age, whilst the thin red lines represent the 95 % confidence ranges.

### 5.4.1.2 HC15-2 (Hodges Creek) age-depth model

The age-depth model for HC15-2 displayed in Figure 5.4, and details of the flowstone dating samples are given in Table 5.3. A total of ten U/Th dates were used to construct the model. HC15-2 has a basal age of 13,470 years BP and is the smallest of the three flowstone cores, with the slowest growth rate. The flowstone was actively accumulating calcite when it was removed from the cave in 2015, and therefore the top of the core was taken to be -65 years BP.

**Table 5.3-** U/Th ages for flowstone core HC15-2.

| U/Th Sample ID | Depth (mm) | Age (years BP) | 2 σ (years) |
|---|---|---|---|
| HC15-2_UA_XX_A | 2 | 2480 | 220 |
| HC15-2 UA1 | 12.4 | 3946 | 131 |
| HC15-2UB_XX_A | 20.9 | 5310 | 110 |
| HC15-2UB_XX_B | 27.85 | 6990 | 143 |
| HC152 UB 1 | 30.75 | 7906 | 260 |
| HC152 UB 2 | 35.05 | 8697 | 174 |
| HC152 UB 3 | 38.7 | 9147 | 104 |
| HC152 UB 4 | 45.85 | 10096 | 55 |
| HC15-2UC | 55.7 | 11540 | 112 |
| HC15_2UD XX_A | 64.95 | 13470 | 136 |

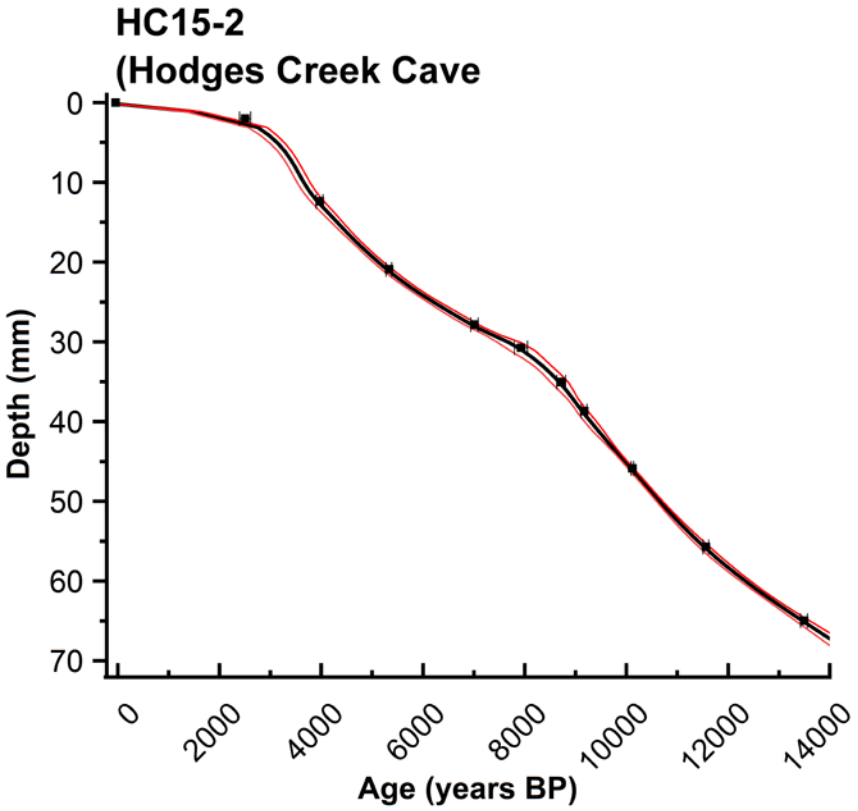


**Figure 5.4-** Age-depth model for HC15-2.The thick black line represents the median age, whilst the thin red lines represent the 95 % confidence ranges.

#### 5.4.1.3 DC15-1 (Dave's Cave) age-depth model

The age-depth model for DC15-1 displayed in Figure 5.5 and details of the flowstone dating samples given in Table 5.4. A total of sixteen U/Th dates were used to construct the model. DC15-1 has a basal age of 13,480 years BP. The flowstone growth rate has clearly varied throughout the record. Notably, there was a growth-hiatus from 5,500 years BP to 1,525 years BP. The flowstone was actively accumulating calcite when it was removed from the cave in 2015, and therefore the top of the core was taken to be -65 years BP.

**Table 5.4-**U/Th ages for flowstone core DC15-1.

| U/Th Sample ID | Depth (mm) | Age (years BP) | 2 σ (years) |
|---|---|---|---|
| DC15 1.1A | 3 | 65 | 94 |
| DC15 1.1AA | 16.5 | 642 | 32 |
| DC151.1AU1 | 24.8 | 1499 | 126 |
| DC15 1.1 B_XX_A | 28.45 | 5563 | 106 |
| DC15 1.1 B_XX_B | 33.85 | 5618 | 108 |
| DC15 1.1 B_A | 49.85 | 6068 | 50 |
| DC15 1.1BU1 | 62.75 | 6220 | 52 |
| DC15 1.1C | 85.6 | 6531 | 54 |
| DC15 1.1CU1_AA | 90.9 | 7592 | 74 |
| DC15 1.1CU1B | 105.7 | 8439 | 98 |
| DC15 1.1CU2 | 125.7 | 10518 | 190 |
| DC15 1.1CU3 | 134.2 | 10780 | 200 |
| DC15 1.1D | 142.8 | 12004 | 152 |
| DC15-1.1DU1 | 172.45 | 12696 | 178 |
| DC15-1.1DU2 | 189.7 | 13430 | 230 |
| DC151.1EXX_A | 196.1 | 13480 | 1450 |

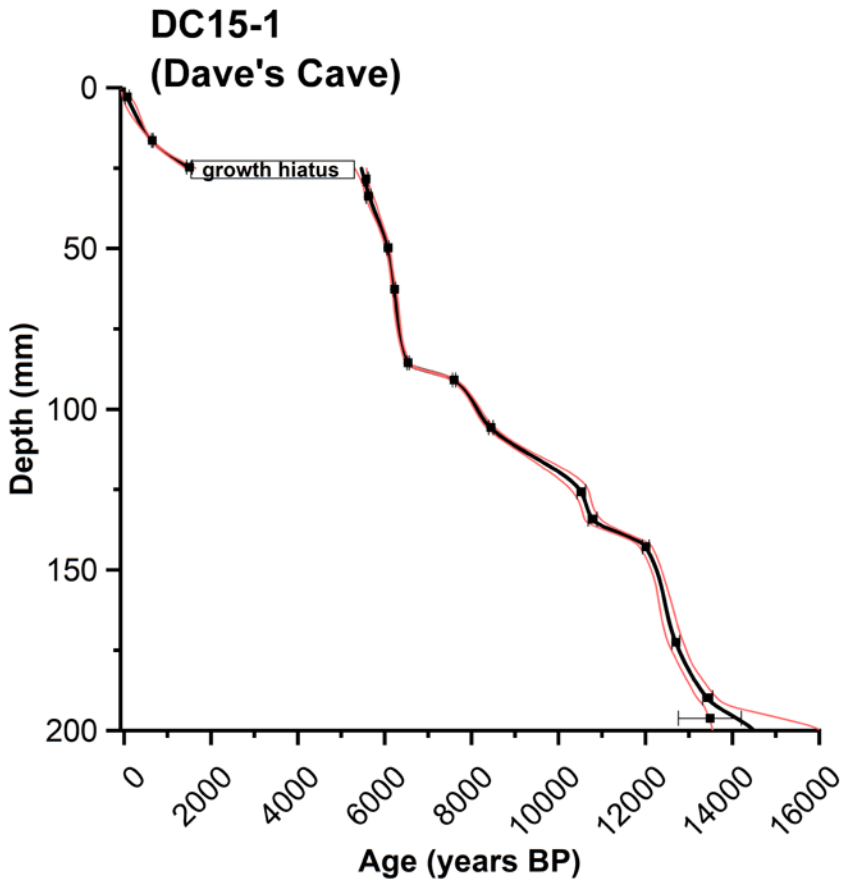


**Figure 5.5-** Age-depth model for DC15-1. The thick black line represents the median age, whilst the thin red lines represent the 95 % confidence ranges.

### 5.4.2 Optical characteristics of speleothem and dripwater humic-like DOC

Humic-like DOC (albeit with variable optical properties) is present within each speleothem. Figure 5.6 shows the predominant humic-like PARAFAC component from the studied speleothem samples. The humic-like fluorescence signals of Waipuna Cave (Figure 5.6 a) and Hodges Creek Cave (Figure 5.6 b) are similar, and both are dominated by excitation-emission peak A (Ex: 240–260; Em: 400–470) (as described in Coble *et al.*, 1996). The Humic-like fluorescence signal in Dave's Cave is dominated by peak C (Ex: 300–340; Em: 400–480 nm), although a peak A signal is also present. (Figure 5.6 c).

Notably, PARAFAC models of Dave's Cave did not produce a protein-like fluorescence component (Figure 5.A9), indicating that microbial activity was low at the site, perhaps owing to the relatively low temperature and wetter (and likely anoxic) soil conditions (Figure 5.A9) compared to the other sites.

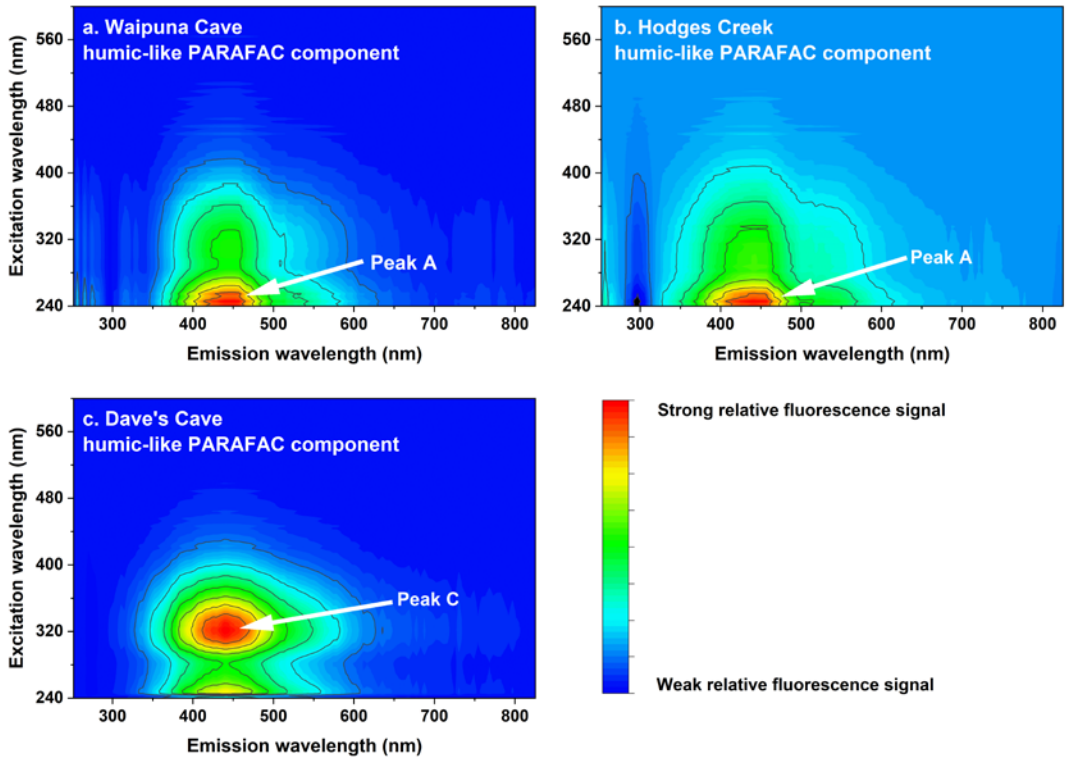


**Figure 5.6**- Humic-like PARAFAC components from each cave (speleothems and dripwaters were used in the same model), **(a.)** Waipuna Cave; **(b.)** Hodges Creek; **(c.)** Dave's Cave.

### 5.4.3 A ~14,000-year history of soil DOC export in relation to pre-human environmental change

In our speleothem records, four stages of deposition can be distinguished based on the fluorescence values and temperature shifts from an alkenone-based sea-surface temperature record from the Tasman Sea (Barrows *et al.*, 2007). Each of the stages as defined from the fluorescence and temperature data are discussed individually below. The discussion then compares the reconstructed humic-like DOC concentrations against modern measurements of humic-like DOC concentrations from dripwaters collected during the cave monitoring campaign.

#### 5.4.3.1 Stage 1- 14,000–12,000 years BP

Waipuna Cave is relatively low latitude (and therefore higher mean annual temperature than at the other sites), has a low altitude and is overlain by dense vegetation. Therefore, it is surprising that it had the lowest humic-like DOC concentrations of the cave sites. The low humic-like DOC concentrations at Waipuna may be suggestive of a precipitation of DOC from percolating waters in the vadose zone, prior to entering the cave. Dripwater humic-like DOC concentrations were relatively low (~0.5 ppm), with little variability during this stage. Based on the Mg/Ca results, from 13,200 years BP until 10,000 years BP there was a continuous, steady drying trend, although this period was the wettest in the entire record.

From 14,700–12,000 years BP New Zealand was undergoing its late glacial transition (Pedro *et al.*, 2015). Sea surface temperature increased by over 1 °C from 14,000 to 12,000 years BP (Barrows *et al.*, 2007) (Figure 5.7 g) in the Tasman Sea, showing strong correspondence with increases in TOC concentration from 6 % to 11 % at Adelaide Tarn, and a dramatic increase in dripwater humic-like DOC concentration at Hodges Creek from 4 ppm to 12 ppm. Notably, Adelaide Tarn and Hodges Creek are located at similar altitudes and near each other in Kahurangi National park, north-west South Island. Analysis of pollen grains from Adelaide Tarn's sedimentary record indicated that during the HCO, terrestrial plant species that are typically found at lower altitudes were present in Adelaide Tarn's sub-alpine catchment (Jara *et al.*, 2015), suggesting an increase in biomass and productivity occurred during this period of relatively high temperature and high humic-like DOC concentrations. This interpretation is consistent with the interpretation of increased biogenic C (or, biomass effect) causing a large negative

excursion in $\delta^{13}C$ in speleothems from Mt. Arthur (a high-altitude cave-site in north-west Nelson) from 11,000–10,000 years BP (Hellstrom *et al.*, 1998).

Dave's Cave showed a marked decline in dripwater DOC from 4 ppm to 2 ppm between 14,000–12,000 years BP. However, Dave's Cave is the most southerly site in this study and is therefore subject to greater influence from the Antarctic. The discrepancy between sites may therefore be explained by other temperature records, which indicate that a period of cooling known as the Antarctic cold reversal (ACR) (14,500–12,800 years BP) (Blunier *et al.*, 1997) occurred during New Zealand's late glacial transition (Alloway *et al.*, 2007; Pedro *et al.*, 2015). Humic-like DOC concentrations at Dave's Cave also appear to be strongly anti-correlated with rainfall overlying the cave (as inferred from Mg/Ca values) (Fig 5.7 f.) during this period.

#### 5.4.3.2 Stage 2- The Holocene climatic optimum 11,500–9,000 years BP

The Holocene climatic optimum (HCO) was characterised by mean annual temperatures of between 1.5–3 °C warmer than today (Wilmshurst *et al.*, 2007). A sea surface temperature reconstruction off the west coast of New Zealand in the Tasman Sea (Figure 5.7 g) (Barrows *et al.*, 2007) shows a peak of 17.3 °C at 11,220 years BP, the highest temperature observed through the entire record, for comparison, at 50 years BP, Tasman Sea surface temperature was 15 °C (Barrows *et al.*, 2007).

For much of the HCO, the relationship between temperature and dripwater humic-like DOC concentration is less clear at Waipuna Cave than at the other sites. From 11,500 years BP to 10,200 years BP the humic-like DOC concentrations were relatively low (~0.5 ppm). However, a very rapid increase in humic-like DOC concentration occurred from 10,000 years BP (shortly prior to the end of the HCO), culminating in a maximum value of 1.0 ppm at 9,700 years BP. An environmental

reconstruction from Lake Pupuke (a volcanic crater lake in Auckland, northern. North Island (37 °S) showed the onset of a warm period with limited seasonality at 10,200 years BP (Stephens *et al.,* 2012), approximately 500 years prior to the large increase in humic-like DOC concentrations (Figure 5.7 a) and the large shift to drier conditions (Figure 5.7 b) at Waipuna Cave. Stephens *et al.,* (2012) described an early Holocene warm period from 10,200 to 7,600 years BP, a period that would coincide with humic-like DOC concentration increase at Waipuna.

During the HCO, humic-like DOC concentrations fluctuated at Hodges Creek, but were relatively high compared to later, cooler stages. After the peak of 12 ppm DOC at 12,000 years BP, there was a rapid decline to 4 ppm at 11,200 years BP, followed by a peak of 8.2 ppm at 11,000 years BP and a peak of 11.6 at 9,500 years BP, followed by a further rapid decline immediately after the climax of the HCO. According to the Mg/Ca results, the HCO was very dry at Hodges Creek (Figure 5.7 c) but rapidly became wetter from 10,000 to 9,000 years BP.

Dave's Cave dripwater humic-like DOC concentrations slightly increased from 2.2 ppm at 12,000 years BP, before increasing to a notable but relatively short-lived peak of 4 ppm DOC at 10,500 years BP (the highest concentration throughout the entire record). Dave's Cave was relatively wet during the HCO and steadily became wetter until 9,500 years BP, before the onset of a drier phase (Figure 5.7 e).

#### 5.4.3.3 Stage 3- Cooling and DOC decrease (9,000–6,000 years BP)

At Waipuna Cave, the Mg/Ca record provides evidence for a dry period between 9,000–8,000 years BP, followed by an increase in effective precipitation which steadily continued through this stage until reaching a peak at 4,200 years BP. Through this stage, humic-like DOC concentrations appear to anti-correlate with precipitation. Dripwater humic-like DOC concentrations decreased from 1.1 ppm at 8,700 years BP, to 0.8 ppm at 8,000 years BP, before declining further to 0.55

ppm at 6,250 years BP (Figure 5.7 a). This decrease in dripwater DOC appears to correspond with climate cooling (Figure 5.7 g). Stephens *et al.,* (2012) noted an increase in seasonality from 7,600 years BP at Lake Pupuke, which coincided with a marked reduction in humic-like DOC concentration at Waipuna, and a large increase in wetness (Figure 5.7 a, b). Lake Pupuke also showed a broad peak in TOC, total nitrogen and total silica (a proxy for within-lake productivity) between 10,200–7,600 years BP, followed by a marked decline between 7,600 to 5,700 years BP (Stephens *et al.*, 2012). The same study described an early Holocene warm period that lasted from 10,200–7,600 years BP, which implies that the HCO may have occurred slightly earlier on the South Island than on the North Island, thus explaining the relatively late peak in humic-like DOC concentrations at Waipuna compared to Hodges Creek and Dave's Cave.

Nevertheless, the three cave records show some notable similarity. Overall, between 9,000–6,000 years BP, humic-like DOC concentrations greatly decreased (albeit with some variability) at each cave site and is consistent with the TOC reconstruction from Adelaide Tarn (Figure 5.7 c). The decrease in humic-like DOC concentrations is strongly consistent with a reduction in sea surface temperature of approximately 0.3 °C from 9,000–6,000 years BP (Barrows *et al.*, 2007) in the Tasman Sea. At Hodges Creek, humic-like DOC concentrations decreased markedly from 10 ppm (at 8,700 years BP) to 4.2 ppm by 6,000 years BP. This decrease coincides with a notable decrease in TOC and vegetation composition changes in the catchment surrounding Adelaide Tarn (Jara *et al.*, 2015) (located close to Hodges Creek). Humic-like DOC concentrations continued to decrease further until reaching a concentration of 2.5 ppm at 3,900 years BP (coinciding with a continued downwards SST trend, reaching 15.5 °C by 3,000 years BP). The decrease in DOC at Adelaide Tarn and Hodges Creek during this period is

indicative of temperature driven vegetation changes (Jara *et al.*, 2015) coinciding with a reduction in aquatic DOC in the area.

At Dave's Cave, there was a substantial reduction from 2.5 ppm humic-like DOC concentration at 9,000 years BP, down to 0 ppm at 6,000 years BP (Figure 5.7 e). From 9,000–8,000 years BP, humic-like DOC concentrations and wetness declined in tandem, however from 8,000–6,000 years BP a large increase in precipitation occurred, coinciding with a continued reduction in humic-like DOC concentrations (Figure 5.7 e), which indicates that the extent of which humic-like DOC concentration in Dave's Cave was influenced by precipitation has varied through time.

#### 5.4.3.4 Stage 4- Late Holocene cooling (4,000 years BP to present)

Sea surface temperature declined from 15.6 °C at 4,000 years BP to 14.4 °C at 1,000 years BP (Figure 5.10 g). A notable drying trend was observed at Waipuna Cave (Figure 5.10 b) through this period, which coincided with a dramatic increase in humic-like DOC concentrations. The increase in humic-like DOC concentrations corresponds with temperature cooling in the Tasman Sea SST record, indicating that humic-like DOC export was primarily controlled by rainfall at Waipuna Cave during this stage.

The temperature decline (Figure 5.7 g) corresponds with a reduction in TOC concentration at Adelaide Tarn (albeit with some variability), and from 4,000–3,000 years BP at Hodges Creek. However, at Hodges Creek, there was a sharp increase in humic-like DOC concentrations to a peak at 2,000 years BP, followed by a further decline to present day conditions. From 4,000 years BP to present, the Mg/Ca data indicates that there was a general drying trend up to present at Hodges Creek, an interpretation that is consistent with $\delta^{18}O$ records from a speleothem in Nettlebed cave (also in north-west Nelson) which indicate a drying trend from 3,000 years BP

onwards (Hellstrom *et al.*, 1998). At Dave's Cave, there was a growth-hiatus from 5,500 years BP to 1,525 years BP. Dave's Cave was relatively wet during this period, with low humic-like DOC concentrations up to 1,000 years BP, followed by a sharp increase.

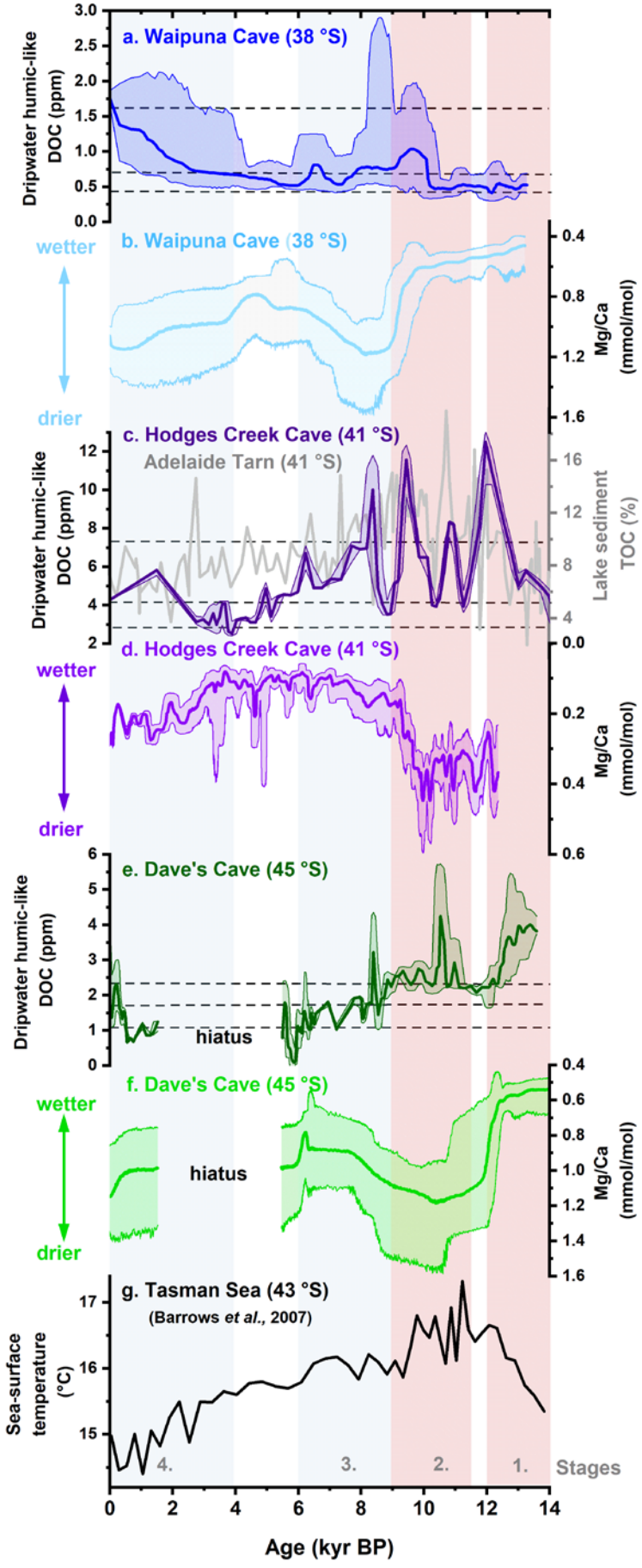
a. Waipuna Cave (38 °S)
Dripwater humic-like DOC (ppm)
b. Waipuna Cave (38 °S)
wetter
drier
Mg/Ca (mmol/mol)
c. Hodges Creek Cave (41 °S)
Adelaide Tarn (41 °S)
Lake sediment TOC (%)
d. Hodges Creek Cave (41 °S)
e. Dave's Cave (45 °S)
hiatus
f. Dave's Cave (45 °S)
g. Tasman Sea (43 °S)
(Barrows et al., 2007)
Sea-surface temperature (°C)
4.
3.
2.
1.
Stages
Age (kyr BP)

**Figure 5.7** Comparison of reconstructions of humic-like DOC concentrations in dripwaters and Mg to Ca ratios from flowstones each cave site with regional TOC and SST records. 95% confidence intervals as estimated using COPRA (Breitenbach *et al.*, 2012).

### 5.4.4 Possible mechanisms underlying climate DOC causality

Climate has demonstrably altered vegetation throughout the Holocene in New Zealand (Jara *et al.*, 2015). Temperature and precipitation are both important determinants of vegetation density over long timescales (Larsen *et al.*, 2011). Indeed, concentrations of dissolved organic carbon are thought to be highly sensitive to environmental drivers that impact net primary productivity (Freeman *et al.*, 2004). However, several variables other than vegetation density (changes in seasonality (Neff *et al.*, 2006; Ågren *et al.*, 2007), soil productivity, or increased soil OC solubility and biodegradability (Marschner & Kalbitz, 2003)) may overlap with each other and can influence the concentration of DOC exported from soils.

Precipitation is another important and complex control on soil DOC export. In our study, drier conditions appear to be associated with increased levels of dripwater humic-like DOC concentration. The relationship between precipitation and DOC is highly complex (Zhang *et al.*, 2010), and may influence DOC export through several indirect mechanisms (Hudson *et al.*, 2003). An increase in precipitation would initially be associated with the export of DOC from soil, however this is not always the case because high rainfall density may dilute the concentrations of exported DOC (Zhang *et al.*, 2010), thus decoupling the relationship between high levels of DOC loss from soils and high humic-like DOC concentrations in inland waters. Indeed, high levels of precipitation may cause high levels of initial DOC export, thus depleting the organic carbon available to be exported from the soil. As an example of the complexity involved, a study of Canadian boreal lakes (over 21 years) demonstrated a strong anti-correlation between summer precipitation and humic-like DOC concentrations, but a strong positive relationship between winter precipitation and humic-like DOC concentrations (Hudson *et al.*, 2003).

At our cave sites, contemporary precipitation is relatively high, and the Mg/Ca ratios suggest that precipitation has been higher during earlier stages of the Holocene. It is plausible that the observed relationship between drier conditions (or a reduced number of dense precipitation events) and higher concentrations of DOC at each site may simply be caused by less dilution (of DOC), and less depletion of soil porewater DOC available for flushing into the caves.

### 5.4.5 Contemporary monitoring data in comparison to the palaeo-environmental reconstructions

From 2015 to 2017, modern dripwater humic-like DOC concentrations in Waipuna Cave ranged from 0.4–1.6 ppm, with a mean value of 0.7 (n=28 Table 5.1). The reconstructed Waipuna data has a humic-like DOC concentration range of 0.4 to 1.85 ppm. Of each of the study sites, Waipuna could be expected to be the least temperature sensitive, owing to its low-altitude, low-latitude location, well-below the current treeline.

At Hodges Creek, modern dripwater humic-like DOC concentrations ranged from 2.9–5.2 ppm, with a mean value of 4.2 ppm (n=6 Table 5.1). The highest concentration of humic-like DOC occurred at 12,000 years BP (12.5 ppm). At Hodges Creek, there is strong evidence for temperature-induced DOC concentration increases. For example, the median value of humic-like DOC concentration through the whole record was 4.7 ppm, yet during the HCO the median humic-like DOC concentration value was 6.5 ppm. Following the HCO, there was a SST decrease from 16.1 to 15.8 °C (from 9,000–6,000 years BP), resulting in a median humic-like DOC concentration of 5.1 ppm. Another important cooling stage was 4,000 years BP to 290 years BP (during which temperature decreased from 15.6 at 4,000 years BP to 14.5 °C at 290 years BP). This period of

cooling included the coolest temperatures observed in the entire temperature record and had a relatively low median humic-like DOC value of 3.3 ppm.

At Dave's Cave, monitoring data shows that contemporary dripwater DOC values range between 1.1–2.3 ppm (n=2). The reconstructed humic-like DOC concentrations rarely increased beyond this range, apart from notable peaks during the HCO and from 12,500–13,500 years BP. As with Hodges Creek, humic-like DOC concentration values were much higher than average during the HCO, with a median value of 2.5 ppm, whilst the median concentration of humic-like DOC almost declined by half from 9,000–6,000 years BP (1.3 ppm). Although there was a growth-hiatus from 5,500 years BP to 1,400 years BP, from 1,400 years BP to present the values were also relatively low, with a median value of 1.4 ppm.

Our data indicate that organic carbon export (particularly at high-altitude sites such as Hodges Creek and Dave's Cave) may be expected to increase under future warming and drying conditions. The HCO was > 1.5 °C warmer than present conditions (Wilmshurst *et al.*, 2007), and humic-like DOC concentrations were much higher at Dave's Cave and Hodges Creek during periods of anomalous warmth in the palaeo-record. However, the relationship between temperature and soil DOC export was not clear at Waipuna Cave (the lowest altitude site), yet high DOC concentrations corresponded with drier conditions.

### 5.4.6 Limitations of the study and potential future research

This study assessed the changes in soil DOC export in relation to climatic shifts over centennial/millennial time scales, with an emphasis on the impacts of temperature. However, the driving mechanisms behind the relationship between temperature and soil DOC export are difficult to disentangle with our dataset. For example, atmospheric and soil temperature increases can drive vegetation and soil

productivity and microbial decomposition of soil OC. Increased microbial activity causes increased respiration, thus heightening soil $CO_2$ partial pressure (Hicks Pries *et al.*, 2017). Increased soil $CO_2$ partial pressure should increase rates of bedrock weathering and cave dripwater saturation.

This study interpreted Mg/Ca as a prior calcite precipitation (PCP) in the vadose zone, and is, therefore, a proxy for palaeohydrology and effective precipitation in the environment overlying each cave, an approach used elsewhere (Cruz *et al.*, 2007; Warken *et al.*, 2018). Proxy calibration at Waipuna Cave supports this interpretation (Nava *et al.*, in prep) and the three caves all developed in Oligocene shallow marine limestones and are similarly shallow. However, our conclusions are limited by only using one flowstone per cave. Further, the collection of monitoring and drip-water collection was relatively limited at Dave's Cave and Hodges Creek Cave.

## 5.5 Conclusions and implications

This study used flowstone archives to assess the impacts of climate on the aquatic carbon cycle in the absence of human interference (until the 13$^{th}$ century). Several studies have demonstrated that speleothems encapsulate organic material as they grow; however, this study was the first to use 3D EEM fluorescence methods to calculate aquatic humic-like DOC concentrations in the distant past. Because speleothems provide reliable, well-dated archives that are not typically subject to post-depositional disturbance, speleothem archives of DOC concentration may be complimentary to other archives such as lake sediments. Indeed, speleothems represent the only terrestrial archive that forms from groundwater and captures soil DOC without further diagenesis or post-depositional mobility (after becoming a closed system). That said, the correspondence between the Hodges Creek and

Adelaide Tarn records also strengthens the argument for the use of lake sediments as archives of the aquatic carbon cycle.

The humic-like DOC concentration reconstructions from the flowstone records indicate that soil carbon export had a strong, positive relationship with temperature over the past ~14,000 years BP in New Zealand. At Hodges Creek and Dave's Cave dripwater humic-like DOC concentrations were higher during warmer periods, such as the HCO, and reduced during cooler periods, such as the mid-late Holocene. Waipuna also demonstrated a notable peak shortly before the cessation of the HCO. The relationship between temperature and TOC was also clear from Adelaide Tarn's sedimentary record, which showed similar trends to the Hodges Creek DOC record. Adelaide Tarn and Hodges Creek are both located at relatively high-altitudes and in relative proximity; therefore, these findings suggest that climate impacts soil DOC export on regional scales.

A further notable finding from this study was that rainfall amount negatively corresponded with dripwater humic-like DOC concentrations. Dripwater humic-like DOC concentrations increased dramatically during drier periods at each cave site. This could be explained by i) a concentration effect during arid periods, and conversely a dilution effect during periods of high rainfall, ii) a depletion of available soil organic carbon during periods of increased rainfall, or iii) differing soil microbial behaviour due to the changing temperature regimes between each site.

The findings from this study indicate that aquatic humic-like DOC concentrations have been higher in the past, particularly during periods of warmer climate, and that soil DOC export can vary dynamically on a range of timescales in response to climate forcing. Therefore, it may be that humic-like DOC export from soil may increase under future warming conditions at high-altitude sites. Nevertheless,

understanding the mechanisms that link climate change and carbon cycling remains a great challenge. Further palaeo-environmental records of soil DOC export may provide opportunities to isolate and test the impact of temperature on soil DOC export elsewhere. Global mean annual temperature is expected to increase by up to 2 °C by 2100 CE, yet the impacts of temperature on soil DOC export remain relatively unexplored.

## 5.6 Funding sources

This study was made possible by Marsden Fund Grant UOW1403 and public research funding from the Government of New Zealand via contract C05X1702 to GNS Science. AH was also supported by a Rutherford Discovery Fellowship award (RDF-UOW1601).

## 5.7 Acknowledgements

We would like to thank Steven Newcombe (University of Waikato) for assistance in cutting and polishing the speleothem slabs, the Department of Conservation for allowing us to access and sample from Dave's Cave, Hodges Creek Cave, and Waipuna Cave (Research and Collection Permit 37934-GEO). Thanks to Pete and Libby Chandler for allowing us to access and sample from dripwaters and flowstones within Waipuna Cave and supporting our ongoing monitoring campaigns. We would also like to thank Travis Cross for assistance in field and flowstone coring support. Thanks to Amanda French for LA-ICPMS analysis of samples.

## 5.8 References


Abell, J. M., Özkundakci, D., Hamilton, D. P., van Dam-Bates, P., & McDowell, R. W. (2019). Quantifying the Extent of Anthropogenic Eutrophication of Lakes at a National Scale in New Zealand. *Environmental Science & Technology, 53,* 16, 9439-9452.

Ågren, A., Buffam, I., Jansson, M., & Laudon, H. (2007). Importance of seasonality and small streams for the landscape regulation of dissolved organic carbon export. *Journal of Geophysical Research: Biogeosciences, 112*(G3).

Alloway, B. V., Lowe, D. J., Barrell, D. J. A., Newnham, R. M., Almond, P. C., Augustinus, P. C., Bertler, N. A. N., Carter, L., Litchfield, N. J., McGlone, M. S., Shulmeister, J., Vandergoes, M. J., Williams, P. W., & members, N.-I. (2007). Towards a climate event stratigraphy for New Zealand over the past 30 000 years (NZ-INTIMATE project). *Journal of Quaternary Science, 22*(1), 9-35.

Andersson, C. A., & Bro, R. (2000). The N-way toolbox for MATLAB. *Chemometrics and Intelligent Laboratory Systems, 52*(1), 1-4.

Baker, A. (2001). Fluorescence excitation− emission matrix characterization of some sewage-impacted rivers. *Environmental Science & Technology, 35*(5), 948-953.

Baker, A., Barnes, W., & Smart, P. L. (1996). Speleothern luminescence intensity and spectral characteristics: Signal calibration and a record of palaeovegetation change. *Chemical Geology, 130*(1-2), 65-76.

Baker, A., Genty, D., & Smart, P. L. (1998). High-resolution records of soil humification and paleoclimate change from variations in speleothem luminescence excitation and emission wavelengths. *Geology, 26*(10), 903-906.

Baker, A., & Inverarity, R. (2004). Protein-like fluorescence intensity as a possible tool for determining river water quality. *Hydrological Processes, 18*(15), 2927-2945.

Baker, A., & Spencer, R. G. (2004). Characterization of dissolved organic matter from source to sea using fluorescence and absorbance spectroscopy. *Science of the Total Environment, 333*(1-3), 217-232.

Barrows, T. T., Lehman, S. J., Fifield, L. K., & De Deckker, P. (2007). Absence of cooling in New Zealand and the adjacent ocean during the Younger Dryas chronozone. *Science, 318*(5847), 86-89.

Batjes, N. H. (1996). Total carbon and nitrogen in the soils of the world. *European journal of soil science, 47*(2), 151-163.

Blunier, T., Schwander, J., Stauffer, B., Stocker, T., Dällenbach, A., Indermühle, A., Tschumi, J., Chappellaz, J., Raynaud, D., & Barnola, J. M. (1997). Timing of the Antarctic Cold Reversal and the atmospheric $CO_2$ increase

with respect to the Younger Dryas event. *Geophysical Research Letters, 24*(21), 2683-2686.

Blyth, A. J., Asrat, A., Baker, A., Gulliver, P., Leng, M. J., & Genty, D. (2007). A new approach to detecting vegetation and land-use change using high-resolution lipid biomarker records in stalagmites. *Quaternary Research, 68*(3), 314-324.

Blyth, A., Baker, A., Collins, M., Penkman, K., Gilmour, M., S. Moss, J., Genty, D., & Drysdale, R. (2008). Molecular organic matter in speleothems and its potential as an environmental proxy. *Quaternary Science Reviews, 27*(9-10), 905-921.

Blyth, A. J., Hartland, A., & Baker, A. (2016). Organic proxies in speleothems – New developments, advantages and limitations. *Quaternary Science Reviews, 149*, 1-17.

Breitenbach, S. F., Rehfeld, K., Goswami, B., Baldini, J., Ridley, H., Kennett, D., Prufer, K., Aquino, V., Asmerom, Y., & Polyak, V. (2012). COnstructing Proxy-Record Age models (COPRA). *Climate of the Past., 8*(5), 1765-1779.

Brook, G. A., Burney, D. A., & Cowart, J. B. (1990). Desert paleoenvironmental data from cave speleothems with examples from the Chihuahuan, Somali-Chalbi, and Kalahari deserts. *Palaeogeography, Palaeoclimatology, Palaeoecology, 76*(3-4), 311-329.

Burdige, D. J., Kline, S. W., & Chen, W. (2004). Fluorescent dissolved organic matter in marine sediment pore waters. *Marine Chemistry, 89*(1), 289-311.

Caldwell, J., Davey, A., Jennings, G., & Spate, A. (1982). Colour in some Nullarbor Plain speleothems. *Helictite, 20*(1), 3-10.

Coble, P. G., Green, S. A., Blough, N. V., & Gagosian, R. B. (1990). Characterization of dissolved organic matter in the Black Sea by fluorescence spectroscopy. *Nature, 348*, 432.

Cruz, F. W., Burns, S. J., Jercinovic, M., Karmann, I., Sharp, W. D., & Vuille, M. (2007). Evidence of rainfall variations in Southern Brazil from trace element ratios (Mg/Ca and Sr/Ca) in a Late Pleistocene stalagmite. *Geochimica et Cosmochimica Acta, 71*(9), 2250-2263.

Evans, C. D., Chapman, P. J., Clark, J. M., Monteith, D. T., & Cresser, M. S. (2006). Alternative explanations for rising dissolved organic carbon export from organic soils. *Global change biology, 12*(11), 2044-2053.

Fairchild, I. J., & Baker, A. (2012). *Speleothem science: from process to past environments*. (Vol. 3). John Wiley & Sons.

Fairchild, I. J., & Treble, P. C. (2009). Trace elements in speleothems as recorders of environmental change. *Quaternary Science Reviews, 28*(5-6), 449-468.

Fellman, J. B., Hood, E., & Spencer, R. G. M. (2010). Fluorescence spectroscopy opens new windows into dissolved organic matter dynamics in freshwater ecosystems: A review. *Limnology and Oceanography, 55*(6), 2452-2462.

Freeman, C., Fenner, N., Ostle, N., Kang, H., Dowrick, D., Reynolds, B., Lock, M., Sleep, D., Hughes, S., & Hudson, J. (2004). Export of dissolved organic carbon from peatlands under elevated carbon dioxide levels. *Nature, 430*(6996), 195.

Genty, D., Baker, A., Massault, M., Proctor, C., Gilmour, M., Pons-Branchu, E., & Hamelin, B. (2001). Dead carbon in stalagmites: carbonate bedrock paleodissolution vs. ageing of soil organic matter. Implications for 13C variations in speleothems. *Geochimica et Cosmochimica Acta, 65*(20), 3443-3457.

Genty, D., & Massault, M. (1999). Carbon transfer dynamics from bomb-14C and δ13C time series of a laminated stalagmite from SW France—modelling and comparison with other stalagmite records. *Geochimica et Cosmochimica Acta, 63*(10), 1537-1548.

Hancox, G. T., & Perrin, N. D. (2009). Green Lake Landslide and other giant and very large postglacial landslides in Fiordland, New Zealand. *Quaternary Science Reviews*, 28(11), 1020-1036.

Hartland, A., Fairchild, I. J., Lead, J. R., Borsato, A., Baker, A., Frisia, S., & Baalousha, M. (2012). From soil to cave: transport of trace metals by natural organic matter in karst dripwaters. *Chemical Geology, 304*, 68-82.

Hartland, A., Fairchild, I. J., Müller, W., & Dominguez-Villar, D. (2014). Preservation of NOM-metal complexes in a modern hyperalkaline stalagmite: implications for speleothem trace element geochemistry. *Geochimica et Cosmochimica Acta, 128*, 29-43.

Hellstrom, J. (2003). Rapid and accurate U/Th dating using parallel ion-counting multi-collector ICP-MS. *Journal of Analytical Atomic Spectrometry, 18*(11), 1346-1351.

Hellstrom, J., McCulloch, M., & Stone, J. (1998). A detailed 31,000-year record of climate and vegetation change, from the isotope geochemistry of two New Zealand speleothems. *Quaternary research, 50*(2), 167-178.

Hewitt, A. E. (2010). New Zealand soil classification. *Landcare research science series*(1), Manaaki Whenua—Landcare Research New Zealand Ltd.

Hicks Pries, C. E., Castanha, C., Porras, R. C., & Torn, M. S. (2017). The whole-soil carbon flux in response to warming. *Science, 355*(6332), 1420-1423.

Hodgson, D. A., & Sime, L. C. (2010). Southern westerlies and $CO_2$. *Nature Geoscience, 3*, 666.

Hudson, J. J., Dillon, P. J., & Somers, K. M. (2003). Long-term patterns in dissolved organic carbon in boreal lakes: the role of incident radiation, precipitation, air temperature, southern oscillation and acid deposition. *Hydrology and Earth System Sciences Discussions, 7*(3), 390-398.

Ishii, S. K. L., & Boyer, T. H. (2012). Behavior of reoccurring PARAFAC components in fluorescent dissolved organic matter in natural and engineered systems: A critical review. *Environmental Science & Technology, 46*(4), 2006-2017.

Jaffé, R., McKnight, D., Maie, N., Cory, R., McDowell, W. H., & Campbell, J. L. (2008). Spatial and temporal variations in DOM composition in ecosystems: The importance of long-term monitoring of optical properties. *Journal of Geophysical Research: Biogeosciences, 113*(G4).

James, J. M., Patsalides, E., & Cox, G. (1994). Amino acid composition of stromatolitic stalagmites. *Geomicrobiology Journal, 12*(3), 183-194.

Jara, I. A., Newnham, R. M., Vandergoes, M. J., Foster, C. R., Lowe, D. J., Wilmshurst, J. M., Moreno, P. I., Renwick, J. A., & Homes, A. M. (2015). Pollen–climate reconstruction from northern South Island, New Zealand (41°S), reveals varying high- and low-latitude teleconnections over the last 16 000 years. *Journal of Quaternary Science, 30*(8), 817-829.

Jochum, K. P., Nohl, U., Herwig, K., Lammel, E., Stoll, B., & Hofmann, A. W. (2005). GeoReM: a new geochemical database for reference materials and isotopic standards. *Geostandards and Geoanalytical Research, 29*(3), 333-338.

Kaiser, K., & Kalbitz, K. (2012). Cycling downwards – dissolved organic matter in soils. *Soil Biology and Biochemistry, 52*, 29-32.

Kalbitz, K., Solinger, S., Park, J.-H., Michalzik, B., & Matzner, E. (2000). Controls on the dynamics of dissolved organic matter in soils: a review. *Soil science, 165*(4), 277-304.

Karlsson, J., Bergström, A.-K., Byström, P., Gudasz, C., Rodríguez, P., & Hein, C. (2015). Terrestrial organic matter input suppresses biomass production in lake ecosystems. *Ecology*, 96(11), 2870-2876.

Larsen, S., Andersen, T., & Hessen, D. O. (2011). Climate change predicted to cause severe increase of organic carbon in lakes. *Global Change Biology, 17*(2), 1186-1192.

Lauritzen, S.-E., & Lundberg, J. (1999). Speleothems and climate: a special issue of The Holocene. *The Holocene, 9*(6), 643-647.

Lavonen, E. E., Kothawala, D. N., Tranvik, L. J., Gonsior, M., Schmitt-Kopplin, P., & Köhler, S. J. (2015). Tracking changes in the optical properties and molecular composition of dissolved organic matter during drinking water production. *Water Research*, 85, 286-294.

Lehmann, J., & Kleber, M. (2015). The contentious nature of soil organic matter. *Nature*, 528(7580), 60-68.

Li, W.-X., Lundberg, J., Dickin, A., Ford, D., Schwarcz, H., McNutt, R., & Williams, D. (1989). High-precision mass-spectrometric uranium-series dating of cave deposits and implications for palaeoclimate studies. *Nature, 339*(6225), 534-536.

Marschner, B., & Kalbitz, K. (2003). Controls of bioavailability and biodegradability of dissolved organic matter in soils. *Geoderma, 113*(3), 211-235.

McGarry, S. F., & Caseldine, C. (2004). Speleothem palynology: an undervalued tool in Quaternary studies. *Quaternary Science Reviews, 23*(23-24), 2389-2404.

McGlone, M. S., Turney, C. S. M., Wilmshurst, J. M., Renwick, J., & Pahnke, K. (2010). Divergent trends in land and ocean temperature in the Southern Ocean over the past 18,000 years. *Nature Geoscience, 3*(9), 622-626.

McWethy, D. B., Wilmshurst, J. M., Whitlock, C., Wood, J. R., & McGlone, M. S. (2014). A high-resolution chronology of rapid forest transitions following Polynesian arrival in New Zealand. *PLoS One, 9*(11), e111328.

Neff, J., Finlay, J. C., Zimov, S., Davydov, S., Carrasco, J., Schuur, E., & Davydova, A. (2006). Seasonal changes in the age and structure of dissolved organic carbon in Siberian rivers and streams. *Geophysical Research Letters, 33*(23).

Parlanti, E., Wörz, K., Geoffroy, L., & Lamotte, M. (2000). Dissolved organic matter fluorescence spectroscopy as a tool to estimate biological activity in a coastal zone submitted to anthropogenic inputs. *Organic Geochemistry, 31*(12), 1765-1781.

Paton, C., Hellstrom, J., Paul, B., Woodhead, J., & Hergt, J. (2011). Iolite: Freeware for the visualisation and processing of mass spectrometric data. *Journal of Analytical Atomic Spectrometry, 26*(12), 2508-2518.

Pearson, A. R., Hartland, A., Frisia, S., & Fox, B. R. (2020). Formation of calcite in the presence of dissolved organic matter: Partitioning, fabrics and fluorescence. *Chemical Geology, 539*, 119492.

Pedro, J. B., Bostock, H. C., Bitz, C. M., He, F., Vandergoes, M. J., Steig, E. J., Chase, B. M., Krause, C. E., Rasmussen, S. O., Markle, B. R., & Cortese, G. (2015). The spatial extent and dynamics of the Antarctic Cold Reversal. *Nature Geoscience, 9*, 51.

Perrette, Y., Poulenard, J., Protière, M., Fanget, B., Lombard, C., Miège, C., Quiers, M., Nafferchoux, E., & Pépin-Donat, B. (2015). Determining soil sources by organic matter EPR fingerprints in two modern speleothems. *Organic Geochemistry, 88*, 59-68.

Quiers, M., Perrette, Y., Chalmin, E., Fanget, B., & Poulenard, J. (2015). Geochemical mapping of organic carbon in stalagmites using liquid-phase and solid-phase fluorescence. *Chemical Geology, 411*, 240-247.

Raftery, A. E., Zimmer, A., Frierson, D. M. W., Startz, R., & Liu, P. (2017). Less than 2 °C warming by 2100 unlikely. *Nature Climate Change, 7*, 637.

Ramseyer, K., Miano, T. M., D'orazio, V., Wildberger, A., Wagner, T., & Geister, J. (1997). Nature and origin of organic matter in carbonates from

speleothems, marine cements and coral skeletons. *Organic Geochemistry*, *26*(5-6), 361-378.

Rushdi, A. I., Clark, P. U., Mix, A. C., Ersek, V., Simoneit, B. R., Cheng, H., & Edwards, R. L. (2011). Composition and sources of lipid compounds in speleothem calcite from southwestern Oregon and their paleoenvironmental implications. *Environmental Earth Sciences*, *62*(6), 1245-1261.

Rutlidge, H., Andersen, M. S., Baker, A., Chinu, K. J., Cuthbert, M. O., Jex, C. N., Marjo, C. E., Markowska, M., & Rau, G. C. (2015). Organic characterisation of cave drip water by LC-OCD and fluorescence analysis. *Geochimica et Cosmochimica Acta*, *166*, 15-28.

Rutlidge, H., Baker, A., Marjo, C. E., Andersen, M. S., Graham, P. W., Cuthbert, M. O., Rau, G. C., Roshan, H., Markowska, M., Mariethoz, G., & Jex, C. N. (2014). Dripwater organic matter and trace element geochemistry in a semi-arid karst environment: Implications for speleothem paleoclimatology. *Geochimica et Cosmochimica Acta*, *135*, 217-230.

Senesi, N., Miano, T., Provenzano, M., & Brunetti, G. (1989). Spectroscopic and compositional comparative characterization of IHSS reference and standard fulvic and humic acids of various origin. *Science of the Total Environment*, *81*, 143-156.

Senesi, N., Miano, T. M., Provenzano, M. R., & Brunetti, G. (1991). Characterization, differentiation, and classification of humic substances by fluorescence spectroscopy. *Soil Science*, *152*(4), 259-271.

Shulmeister, J., Fink, D., & Augustinus, P. C. (2005). A cosmogenic nuclide chronology of the last glacial transition in North-West Nelson, New Zealand—new insights in Southern Hemisphere climate forcing during the last deglaciation. *Earth and Planetary Science Letters*, 233(3-4), 455-466.

Shulmeister, J., Goodwin, I., Renwick, J., Harle, K., Armand, L., McGlone, M. S., Cook, E., Dodson, J., Hesse, P. P., Mayewski, P., & Curran, M. (2004). The Southern Hemisphere westerlies in the Australasian sector over the last glacial cycle: a synthesis. *Quaternary International*, *118-119*, 23-53.

Sniderman, J., Hellstrom, J., Woodhead, J., Drysdale, R., Bajo, P., Archer, M., & Hatcher, L. (2019). Vegetation and climate change in southwestern Australia during the Last Glacial Maximum. *Geophysical Research Letters*, *46*(3), 1709-1720.

Stedmon, C. A., & Bro, R. (2008). Characterizing dissolved organic matter fluorescence with parallel factor analysis: a tutorial. *Limnology and Oceanography: Methods*, *6*(11), 572-579.

Stephens, T., Atkin, D., Augustinus, P., Shane, P., Lorrey, A., Street-Perrott, A., Nilsson, A., & Snowball, I. (2012). A late glacial Antarctic climate teleconnection and variable Holocene seasonality at Lake Pupuke, Auckland, New Zealand. *Journal of Paleolimnology*, *48*(4), 785-800.

Van Beynen, P., Bourbonniere, R., Ford, D., & Schwarcz, H. (2001). Causes of colour and fluorescence in speleothems. *Chemical Geology, 175*(3-4), 319-341.

Warken, S. F., Fohlmeister, J., Schröder-Ritzrau, A., Constantin, S., Spötl, C., Gerdes, A., Esper, J., Frank, N., Arps, J., & Terente, M. (2018). Reconstruction of late Holocene autumn/winter precipitation variability in SW Romania from a high-resolution speleothem trace element record. *Earth and Planetary Science Letters, 499*, 122-133.

Wilmshurst, J. M., McGlone, M. S., Leathwick, J. R., & Newnham, R. M. (2007). A pre-deforestation pollen-climate calibration model for New Zealand and quantitative temperature reconstructions for the past 18,000 years BP. *Journal of Quaternary Science, 22*(5), 535-547.

Xie, S., Yi, Y., Huang, J., Hu, C., Cai, Y., Collins, M., & Baker, A. (2003). Lipid distribution in a subtropical southern China stalagmite as a record of soil ecosystem response to paleoclimate change. *Quaternary Research, 60*(3), 340-347.

Zhang, J., Hudson, J., Neal, R., Sereda, J., Clair, T., Turner, M., Jeffries, D., Dillon, P., Molot, L., Somers, K., & Hesslein, R. (2010). Long-term patterns of dissolved organic carbon in lakes across eastern Canada: Evidence of a pronounced climate effect. *Limnology and Oceanography, 55*(1), 30-42.

Ziegelgruber, K. L., Zeng, T., Arnold, W. A., & Chin, Y.-P. (2013). Sources and composition of sediment pore-water dissolved organic matter in prairie pothole lakes. *Limnology and Oceanography, 58*(3), 1136-1146.

## 5.9 Appendix


**Figure 5.A1-** Vegetation and soil horizons above Waipuna Cave.

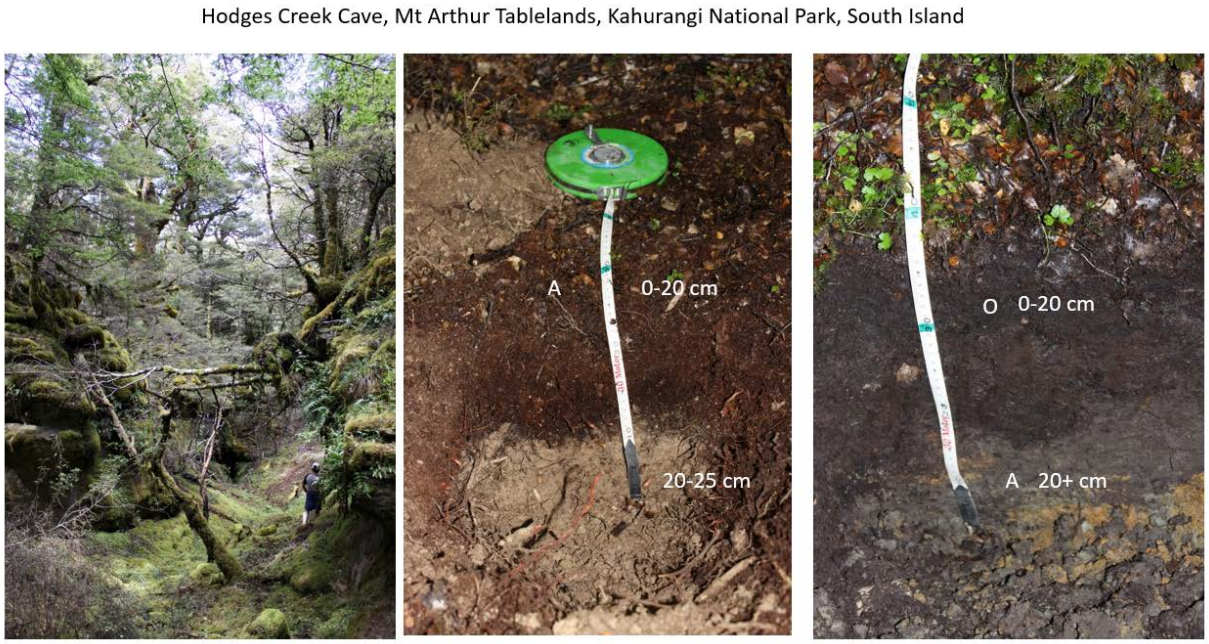


**Figure 5.A2-** Vegetation and soil horizons above Hodges Creek Cave.

Dave's Cave, Mt Luxmore, Fiordland National Park, South Island

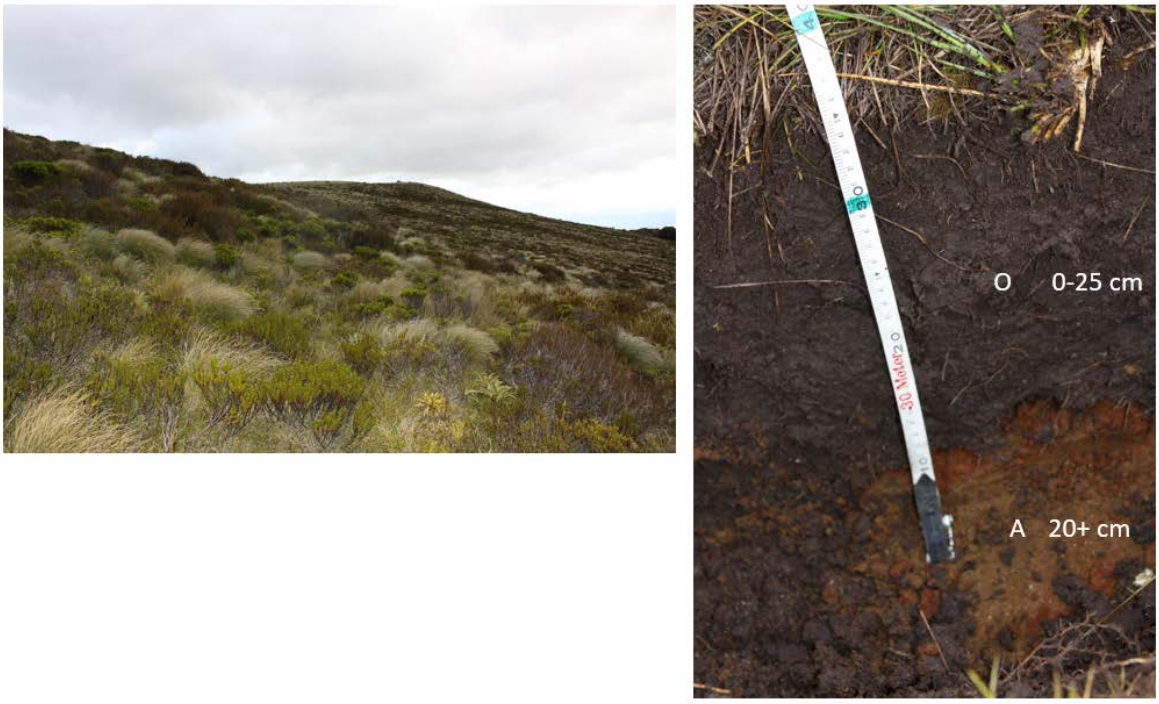


**Figure 5.A3-** Vegetation above and soil horizons above Dave's Cave.

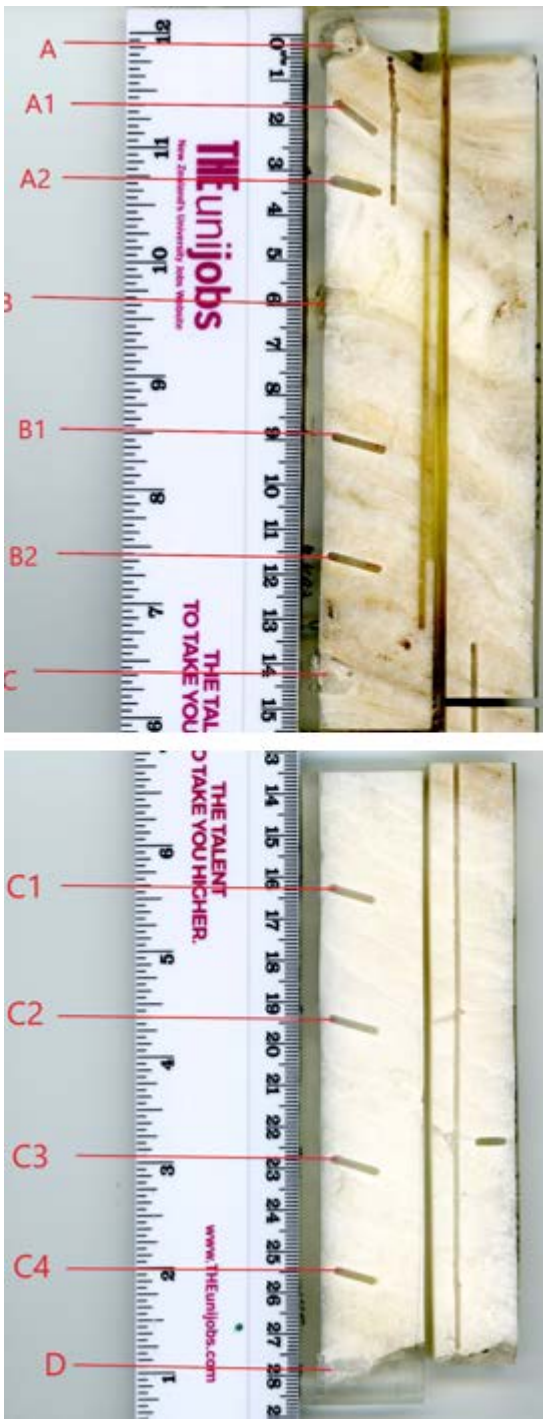


**Figure 5.A4**- WP15-1.1 (Waipuna) flowstone core. Red labels refer to U/Th sample depths (Table 5.2). The sample depths not included in the tables were not used in the age–depth model due to contamination. Sample was split to fit into LA-ICPMS cell.

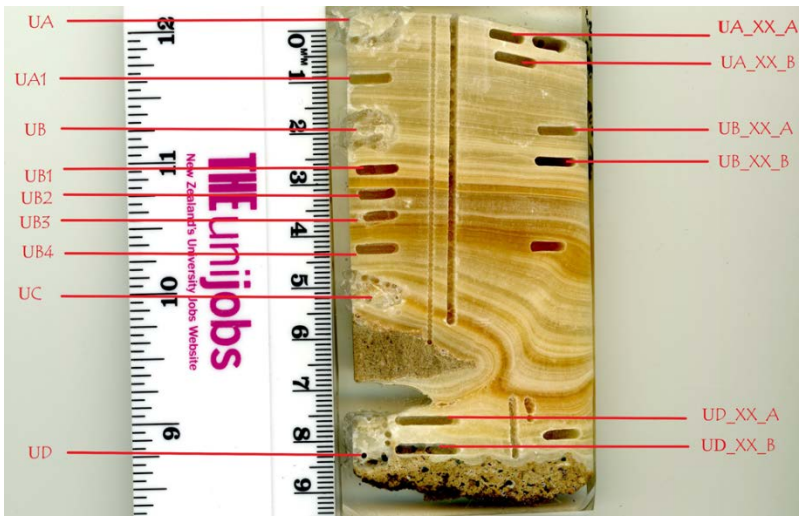


**Figure 5.A5-** HC15-2(Hodges Creek) flowstone core. Red labels refer to U/Th sample depths (Table 5.3). The sample depths not included in the tables were not used in the age–depth model due to contamination.

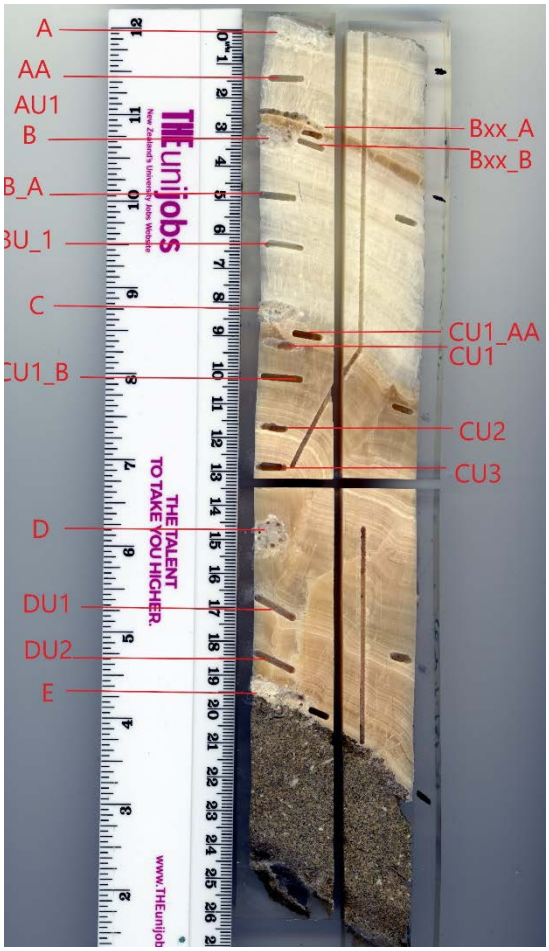


**Figure 5.A6-** DC15 (Dave's Cave**)** flowstone core. Red labels refer to U/Th sample depths (Table 5.4). The sample depths not included in the tables were not used in the age–depth model due to contamination. Sample was split to fit into LA-ICPMS cell.

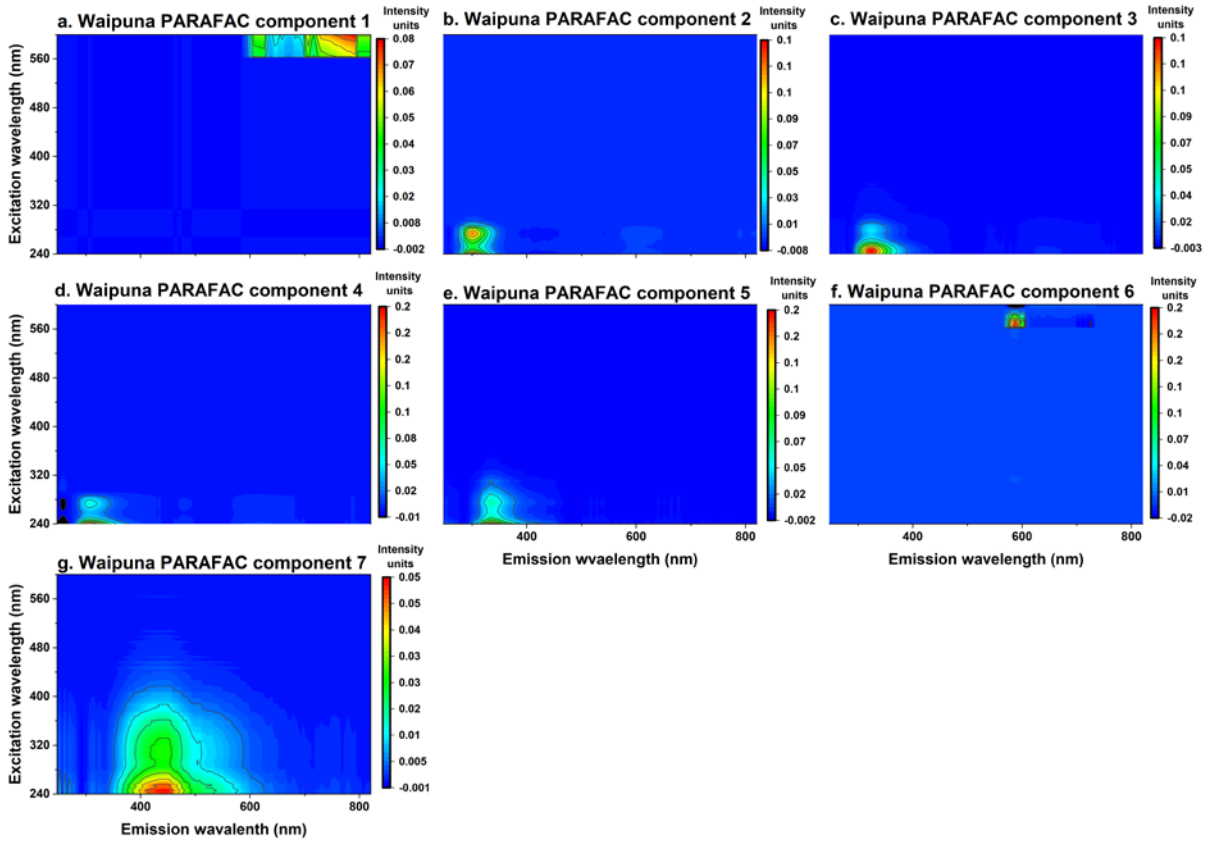


**Figure 5.A7**- PARAFAC components 1 to 7 of DOC from Waipuna Cave from a seven-component model. (**a.)** scatter (C1); (**b.)** protein-like (C2); (**c.)** protein-like (C3); (**d.)** protein-like (C4); (**e.)** protein-like (C5); (**f.)** scatter (C6); (**g.)** humic-like (C7).

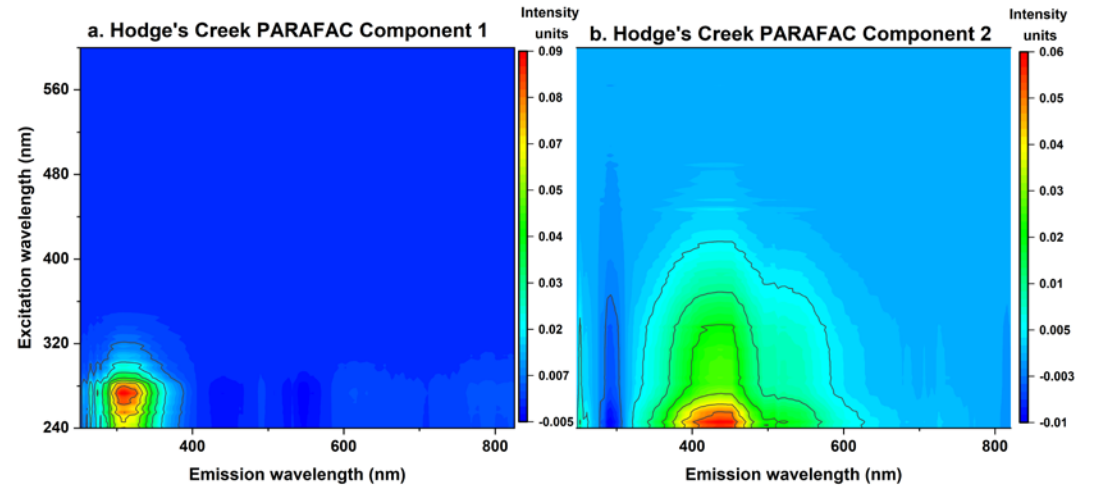


**Figure 5.A8 (a.)** PARAFAC component 1 (protein-like); **(b.)** PARAFAC component 2 (humic-like) of DOC from Hodges Creek Cave from a two-component model.

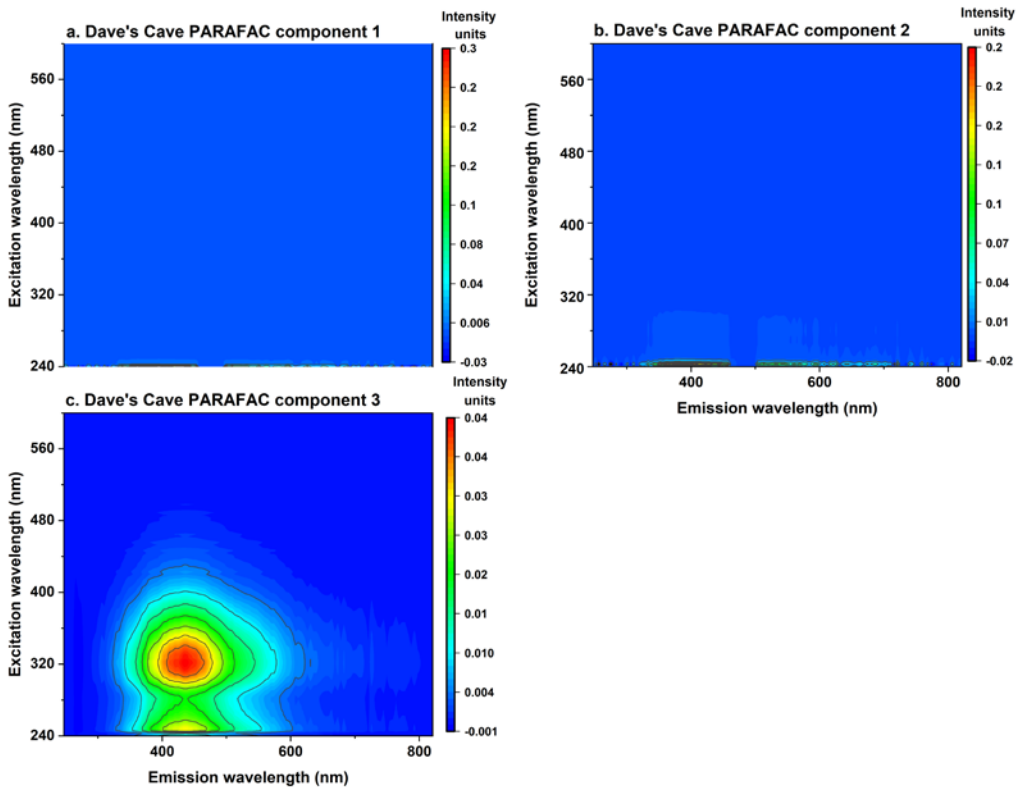


**Figure 5.A9** PARAFAC components 1, 2 and 3 from Dave's Cave from a three-component model.

# 6 Chapter 6

# Conclusions

The research presented in this thesis aimed to assess the impacts of climate on dissolved organic carbon (DOC) in aquatic environments. DOC concentrations in terrestrial waterbodies are thought to be positively related to DOC export from soil organic carbon (SOC) stocks. This project sought to contextualise this understanding.

This research utilised 3D excitation-emission matrix (EEM) fluorescence of DOC contained in palaeo-environmental archives (lake sediment and flowstones) which extend well beyond human arrival (13$^{th}$ century (McWethy *et al.*, 2014)) in New Zealand. This approach enabled the segregation of natural drivers from potential anthropogenic drivers, and solely test the impacts of climatic shifts on aquatic DOC concentrations on centennial-to-millennial timescales for the past ~14,000 years BP.

## 6.1 Assessing the impact of climate on water quality and total organic carbon in a pristine lacustrine sedimentary record

One aim of Chapter 3 was to establish a relationship between water extractable dissolved organic carbon (WEDOM) 3D EEM fluorescence properties and water column quality (trophic level index) parameters from New Zealand's freshwater monitoring programme. The study then aimed to apply this relationship to a 13,770-year sedimentary record from a pristine, sub-alpine, climatically sensitive lake (Adelaide Tarn) (Jara *et al.*, 2015), located in the north west of the South Island. The rationale was to enable the separation of humic-like DOC fluxes from protein-

like DOM production to evaluate past soil carbon fluxes, and additionally, inform contemporary water quality assessments in New Zealand.

The comparison of WEDOM fluorescence properties and trophic level index (TLI) values yielded positive correlations between protein-like fluorescence and mean TLI parameters from each lake (chlorophyll a $R^2$= 0.44; total nitrogen $R^2$= 0.50; total phosphorus $R^2$= 0.81; overall TLI score $R^2$= 0.74). This study indicates that protein-like fluorescence in sedimentary WEDOM can be used as an indicator of lake water column trophic status. The equation produced from the relationship between the water column TLI score and sedimentary WEDOM protein-like fluorescence was used to reconstruct TLI scores from Adelaide Tarn's sedimentary archive, demonstrating that the lake was oligotrophic or microtrophic throughout the entire record.

A further aim of the study was to assess the influence of temperature on sedimentary TOC (total organic carbon) concentrations and humic-like fluorescence intensity of WEDOM through the past 13,770 years at Adelaide Tarn. A partial least square relationship (PLSR) was established between Fourier transform infrared spectroscopy (FTIRS) and conventional (combustion) TOC measurements of sediments from thirteen lakes (N of sediments= 141, $R^2$= 0.88). The calibration was then applied to Adelaide Tarn's sediment, building a record of TOC through the past 13,770 years BP.

At Adelaide Tarn, humic-like fluorescence intensity and FTIRS inferred-TOC concentrations both showed a strong correspondence with a sea-surface temperature reconstruction from the Tasman Sea (Barrows *et al.*, 2007). Humic-like fluorescence intensity and TOC concentrations were higher during warm periods (such as the Holocene climatic optimum) and reduced during cooler periods (from 9,000–6,000 years BP). The findings from Adelaide Tarn also showed some

correspondence with climatically induced vegetation change in the glacial cirque surrounding Adelaide Tarn (Jara *et al.*, 2015).

## 6.2 Testing the ability of calcite to record DOC

One of the overriding aims of the research project was to utilise speleothems as archives of DOC. Although the focus on speleothem organic matter has developed over recent years (Blyth *et al.*, 2016), little attention has been paid to testing the relationship between dripwater dissolved organic carbon and speleothem organic carbon. This study utilised a calcium carbonate precipitation experiment (Gruzensky, 1967) to test the relationship between parent growth-water $[DOC]_{aq}$ and final $[DOC]_s$ concentrations contained in the calcium carbonate.

The study precipitated calcium carbonate crystals in growth solutions containing varying concentrations of DOC (measured using conventional wet-oxidation TOC analysis, which was then calibrated against 3D EEM humic-like fluorescence intensity). The experimental growth solutions consisted of a control (0 ppm; 18 MΩ water), and peat water (collected at a depth of 30 m from Kopuatai bog, central North Island) diluted to 5 ppm, 10 ppm and 15 ppm DOC concentrations. Post experiment, the crystals were dissolved using dilute HCl, and their DOC concentrations were then measured via a calibration between TOC and humic-like fluorescence intensity (produced using parallel factor analysis of components (PARAFAC) (Murphy *et al.*, 2013)). The study demonstrated a positive, linear correlation between initial organic carbon concentration in solution and final organic carbon concentration in calcite, with log $K_d$ values of around 0.5. This experiment shows that speleothems are likely to reliably record DOC concentrations from their parent solutions and that 3D EEM fluorescence can be used to measure DOC concentrations from dissolved carbonates.

The study also tested DOC concentrations in flowstone dripwaters versus flowstone DOC (from recently deposited calcite) concentrations from three cave sites in New Zealand. This case study reaffirmed our experimental findings, i.e. that DOC concentrations in speleothems appear to reliably record $[DOC]_{aq}$ from parent solutions.

Another important finding was that DOC concentrations have an important effect on crystal habit. From the control (0 ppm), carbonate crystals were white and rhombohedral with clean faces. From 5 ppm to 15 ppm, the carbonate crystals were progressively darker in colour, prismatic and had very clear unconformities, particularly in the crystals precipitated in 10 ppm and 15 ppm DOC solutions.

## 6.3 Testing the impact of climate on DOC on a pre-human landmass using speleothem archives

This study utilised flowstones from three caves spanning a range of 7 degrees of latitude. Waipuna Cave is in the western North Island, whilst Hodge's Creek is in the north west of the South Island, and Dave's Cave is located on the south west of the South Island. A cave monitoring programme was undertaken at each cave, in which soil descriptions were made, and dripwaters assessed for pH, electric conductivity and DOC concentrations. Each flowstone was dated using the U/Th disequilibrium method via multi-collector inductively coupled plasma mass spectrometry (MC ICPMS) (Hellstrom, 2006). This study utilised the same measurement approach as in the carbonate precipitation experiment (i.e. dissolution of calcite in dilute HCl, followed by analysis of [DOC] and DOC characteristics using 3D EEM fluorescence. The study utilised the monitoring data and most recently deposited calcite to produce DOC $K_d$ values, which were then applied to

the measurements of flowstone DOC in each setting, thus enabling the reproduction of dripwater humic-like DOC concentrations through time.

Dripwater concentrations from Waipuna Cave showed a marked peak in concentration shortly after the Holocene climatic optimum, and a large increase from 4,000 years BP to present, coinciding with increasingly drier climatic conditions. Dripwater humic-like DOC concentrations from the more elevated Hodge's Creek Cave and Dave's Cave showed a strong correspondence with sea surface temperatures (Tasman Sea) (Barrows *et al.*, 2007) and dryness through the past 14,000 years BP. DOC concentrations were relatively high during the Holocene climatic optimum (which was 1.5–3 °C warmer than today (Wilmshurst *et al.*, 2007)) and declined through the period of climatic cooling which followed. Notably, [DOC] from Hodge's Creek and [TOC] from Adelaide Tarn (both sub-alpine sites located within Kahurangi National Park at 41 °S) showed extremely similar shifts through their records, implying that there was coherent regional variability, which was strongly influenced by temperature changes.

Rainfall reconstructions (from ratios of Mg/Ca) showed a clear correspondence between drier conditions and higher DOC concentrations at each site, again indicating that climate has a very important role in the terrestrial carbon cycle (in the absence of human interference). The influence of drier conditions appears to confirm experimental findings that suggest DOC is mobilised to a greater extent by cycles of wetting and drying.

## 6.4 Suggestions for further research

### 6.4.1 Further research of 3D EEM fluorescence in relation to water quality parameters and C cycling

The relationship between 3D EEM fluorescence in contemporary water samples and in recently deposited sediments and/or suspended sediments should be tested further. Microbial reworking of sedimentary organic carbon may diminish the total DOC concentration and alter DOC composition. Therefore, the organic carbon contained in sediment may be degraded compared to organic carbon contained in surface waters (Meyers & Ishiwatari, 1993). A systematic evaluation of this diagenetic process is needed.

Our study focused on lake water quality in a pristine lake (Adelaide Tarn) that has undergone no human interference. A further study should focus on testing test protein-like fluorescence intensity of sedimentary WEDOM in a New Zealand lake which has been subjected to human impacts (e.g. land-use change, high levels of nutrient input), and has thus transformed from a pristine lake into a heavily impacted lake. Such a study would be an important validation of the approach taken here.

### 6.4.2 Incorporation of DOC in carbonates

Additional calcite crystal growth experiments from parent solutions containing organic matter with different molecular characteristics should be undertaken to test preferential adsorption of different molecular constituents of dissolved organic carbon. The calcite precipitation carried out in this thesis showed an absence of fluorescence peak A in the dissolved calcite, despite being present in the initial growth-solution. Therefore, further research on the incorporation of varying DOC isolates (e.g. fulvic-like, protein-like) should be undertaken.

Further, DOC has been shown to bind to trace metals in dripwaters (Hartland *et al.*, 2011).

### 6.4.3 Speleothem records of DOC concentration

This study focused on the relationship between DOC concentrations and climatic shifts. A further study could take the opposite approach and utilise speleothem records to assess changes in DOC concentrations and molecular characteristics under heavily impacted sites (e.g. under farmland, heavily polluted sites or sites that have been heavily affected by atmospheric sulphate deposition).

The findings of our study demonstrate a relationship between climate and DOC export, particularly at the high-altitude sites. Future research could expand upon this by utilising sites in other climatic regimes and at different altitudinal gradients, to determine whether this relationship is observable elsewhere.

## 6.5 Thesis summary

This thesis addresses the impact of climate on terrestrial dissolved organic carbon concentrations on centennial-to-millennial timescales in the absence of human impacts. The research tested the viability of 3D EEM fluorescence methods in lake sediments and speleothems, and then applied these methods to these palaeo-environmental archives. The main outcomes are that DOC concentrations are heavily influenced by climate (either directly or indirectly) in the absence of anthropogenic impacts, as exemplified through the past ~14,000 years BP in Aotearoa New Zealand. This research demonstrates that DOC concentrations can indeed be influenced by climate and that DOC concentrations in New Zealand appear to have been higher (than present) during warmer periods in the past.

## 6.6 References


Barrows, T. T., Lehman, S. J., Fifield, L. K., & De Deckker, P. (2007). Absence of cooling in New Zealand and the adjacent ocean during the Younger Dryas chronozone. *Science, 318*(5847), 86-89.

Blyth, A. J., Hartland, A., & Baker, A. (2016). Organic proxies in speleothems – New developments, advantages and limitations. *Quaternary Science Reviews, 149*, 1-17.

Gruzensky, P. (1967). Growth of calcite crystals. *Crystal growth*, 365-367.

Hartland, A., Fairchild, I. J., Lead, J. R., Zhang, H., & Baalousha, M. (2011). Size, speciation and lability of NOM–metal complexes in hyperalkaline cave dripwater. *Geochimica et Cosmochimica Acta, 75*(23), 7533-7551.

Hellstrom, J. (2006). U–Th dating of speleothems with high initial 230Th using stratigraphical constraint. *Quaternary Geochronology, 1*(4), 289-295.

Jara, I. A., Newnham, R. M., Vandergoes, M. J., Foster, C. R., Lowe, D. J., Wilmshurst, J. M., Moreno, P. I., Renwick, J. A., & Homes, A. M. (2015). Pollen–climate reconstruction from northern South Island, New Zealand (41°S), reveals varying high- and low-latitude teleconnections over the last 16 000 years. *Journal of Quaternary Science, 30*(8), 817-829.

McWethy, D. B., Wilmshurst, J. M., Whitlock, C., Wood, J. R., & McGlone, M. S. (2014). A high-resolution chronology of rapid forest transitions following Polynesian arrival in New Zealand. *PLoS One, 9*(11), e111328.

Meyers, P. A., & Ishiwatari, R. (1993). Lacustrine organic geochemistry—an overview of indicators of organic matter sources and diagenesis in lake sediments. *Organic Geochemistry, 20*(7), 867-900.

Murphy, K. R., Stedmon, C. A., Graeber, D., & Bro, R. (2013). Fluorescence spectroscopy and multi-way techniques. PARAFAC. *Analytical Methods, 5*(23), 6557-6566.

Wilmshurst, J. M., McGlone, M. S., Leathwick, J. R., & Newnham, R. M. (2007). A pre-deforestation pollen-climate calibration model for New Zealand and quantitative temperature reconstructions for the past 18 000 years BP. *Journal of Quaternary Science, 22*(5), 535-547.